8-28-2012

The impact of dams, droughts, and tributary drainages on channel form and process : Rio Grande and Rio Chama, NM

Benjamin Swanson

Benjamin J. Swanson
Candidate

Earth and Planetary Sciences
Department

This dissertation is approved, and it is acceptable in quality and form for publication:

Approved by the Dissertation Committee:

Grant A. Meyer, Chairperson

Julie Coonrod

Thomas Turner

John Pitlick

THE IMPACT OF DAMS, DROUGHTS, AND TRIBUTARY DRAINAGES ON CHANNEL FORM AND PROCESS: RIO GRANDE AND RIO CHAMA, NM

By

Benjamin J. Swanson

B.S., Geology, University of Montana, 1996
M.S., Geology, University of Montana, 2002

DISSERTATION

Submitted in Partial Fulfillment of the
Requirements for the Degree of

Doctor of Philosophy
Earth and Planetary Sciences

The University of New Mexico
Albuquerque, New Mexico

July 2012

Acknowledgements

This dissertation would not have been accomplished without the help of a number of people. First, I would like to thank my committee and the Earth and Planetary Sciences Department for all the encouragement and support, especially Cindy and Mabel. I would also like to thank the U.S. Army Corps of Engineers for providing the bulk of the funding for the work, and Dr. Julie Coonrod for getting me involved with the Corps' Urban Flood Demonstration Project and supporting me throughout. I'd also like to acknowledge Mark Tyra, Amy Ellwein, Bekah Levine, Leah Roberts, Travis Naibert, and Jessi Meyer for helping me measure rocks. My mother also braved thunderstorms, heat, rattlesnakes, and a lack of shower facilities to help me in the field for long stretches. And thank you, Jessi, for tolerating me when I was at home. Also at home, I am grateful to Amy Ellwein ,Tim Wawrzyniec , and Mark Tyra for moral support. Finally, I'd like to express my gratitude to Jessica Meyer, my wife, and Dr. Grant Meyer, my primary advisor, for providing ladders to bring me down when needed and a tow truck to drag me to the end.

THE IMPACT OF DAMS, DROUGHTS, AND TRIBUTARY DRAINAGES ON CHANNEL FORM AND PROCESS: RIO GRANDE AND RIO CHAMA, NM

By

BENJAMIN J. SWANSON

B.S., Geology, University of Montana, 1996
M.S., Geology, University of Montana, 2002
Ph.D., Earth and Planetary Sciences, University of New Mexico, 2012

ABSTRACT

A guiding principle in river science maintains that channel systems evolve to convey the sediment loads and water discharges imposed upon them. Changes in sediment and water inputs may result in adjustments to channel geometry, bed texture, and related parameters. Over the last century, geomorphic processes along the Middle Rio Grande and one of its major tributaries, the Rio Chama, NM, have been altered by intensified land and water management and climate change. Using a GIS, channel characteristics were digitized from georeferenced photographs and analyzed, with particular attention to quantifying measurement error. Along the Rio Grande, average channel widths decreased from 516±67m to 176±7m between 1918 and 1963, mostly due to decreasing peak flows and the implementation of flood control and other engineering measures. From 1985 to 2008, widths decreased from 176 ± 23 m to 146 ± 5 m, primarily over periods of low peak flow. The Rio Chama, downstream of El Vado Dam, narrowed from an average width of 58 m to 44 m, with most of the adjustment occurring after dam closure in 1935.

Along both rivers, evidence suggested that the spatial patterns of planform change were partly controlled by tributaries confluences. To examine tributary controls along the Rio Chama, elevation and bed sediment data were collected at 200 cross sections situated up and downstream of 26 tributary confluences along a 17 km reach situated just upstream of Abiquiu Reservoir. Compared to reaches between junctions, confluences reduced gradients and bed sediment size upstream of confluences and increased them downstream. These shifts in gradient and bed texture appear to drive variations in sediment entrainment and transport capacity and the relative storage of sand along the channel bed, as well. Although the larger clasts downstream of junctions are harder to move and slow transport, the steeper slopes at these location likely help pass smaller gravel and sands delivered by the tributaries. However, channel form and process are highly variable along the study reach, reflecting variations in the sediment inputs related to watershed geology, mainstem morphology, and past depositional events.

Table of Contents

List of Figures

Chapter 1:

Chapter 2:

Chapter 3:

List of Tables

Chapter 1:

Chapter 2:

Chapter 1

Magnitude and Uncertainty of Airphoto-based Measurements of Channel Narrowing in Response to Historical River Engineering and Reductions in Peak Discharge: Rio Grande Near Albuquerque, New Mexico

Authors:
Benjamin J. Swanson[1], Grant Meyer[1], and Julie Coonrod[2]

[1]Department of Earth and Planetary Sciences, MSCO3-2040, University of New Mexico Albuquerque, New Mexico, USA, 87131
(505) 277-2661, (505) 277-8843 (fax), swanson@unm.edu

[2]Department of Civil Engineering, MSC01-1070, University of New Mexico, Albuquerque, NM 87131

Keywords:
aerial photographs, measurement error, channel narrowing, droughts, flood control, Rio Grande

Abstract

Over the last century, geomorphic processes along the Middle Rio Grande have been altered by flood control and bank stabilization projects, intensified land and water use, and climate change. In response to potential risks to infrastructure and ecological integrity, we investigated recent (1985-2008) adjustment and reviewed historic (1918-1985) changes in Rio Grande channel planform through the Albuquerque, New Mexico, area, especially in relation to changes in annual peak discharge and river engineering measures. Using a GIS, channel characteristics were digitized from georeferenced photographs and analyzed with particular attention to quantifying potential measurement error and its propagation. Error associated with average channel widths and channel area ranged between 4 and 13%. For smaller polygons, e.g. islands, error was higher (11 to 40% for width and >200% for area) because width error is large relative to polygon width. Between 1918 and 1963, average

channel widths decreased 8 m/yr, from 516 ± 67 m to 176 ± 7 m, mostly due to decreasing peak flows and the implementation of flood control and other engineering measures. From 1985 to 2008, widths decreased 0.7 m/yr, from 176 ± 23 m to 146 ± 5 m, accompanied by an increase in vegetated island area which largely coincided with low flow periods. Narrowing was concentrated at tributary inputs and in the upstream part of the reach, where bedload trapping by Cochiti Dam has caused degradation. Bank protection structures and dense vegetation limit bank erosion in the reach, but erosion is significant where expanding islands, incision, and increased meandering force water against banks.

Introduction

A guiding principle in river science maintains that channel systems evolve to convey the sediment loads and water discharges imposed upon them. Changes in sediment and water inputs often result in adjustments to channel slope, depth, width, sinuosity, roughness, and related parameters (Mackin, 1948; Lane, 1955; Leopold and Bull, 1979). For example, channels may widen in response to increases in bedload sediment supply where higher water stages and flow deflection around new bars help destabilize banks (Knighton, 1988; Madej and Ozaki, 1998). Widening may also occur in degrading systems, where higher banks and steeper bank slopes lead to instability (Thorne, 1982; Pizzuto 1994). Alternatively, rivers may narrow through the in-channel berm formation, bar stalling, and abandonment of secondary channels in braided or wandering systems. Vegetation encroachment often stabilizes sediment in these areas and (or) promotes further aggradation until bars and islands attach to former banks and floodplain surfaces, often becoming part of the floodplain (e.g., Schumm and Lichty, 1963; Johnson, 1994; Pizzuto, 1994; Allred and Schmidt, 1999). Thus, channel width adjustment occurs in numerous circumstances and typically accompanies

changes in other channel parameters. Depending on pre-disturbance conditions such as bedload size, channel confinement, and climate, each river system may experience a different style, magnitude, and (or) rate of adjustment (Brewer and Lewin, 1998; Grant et al., 2003). Therefore, determining how individual rivers react to altered sediment loads and hydrology is of primary interest to river managers and engineers.

River adjustments to local and regional sediment delivery and hydrology are especially important along major rivers, which often provide transportation, agricultural and municipal water supplies, recreation, and other services that support adjacent population centers, and are also heavily managed to control risks to infrastructure and the local economy. These rivers experience numerous perturbations to the timing and magnitude of water and sediment delivery related to land use and river-related engineering projects, as well as from climate change. For example, agricultural activities have been implicated in increasing surface runoff and sediment delivery to rivers, often leading to periods of prolonged aggradation (e.g., Trimble and Mendel, 1995; Knox 2006). Increased runoff and decreases in sediment supply related to urbanization have resulted in channel expansion and incision (e.g., Wolman, 1967; Booth, 1990; Chin and Gregory, 2001). Also, levee construction and other channel stabilization methods can force aggradation in the restricted channel and floodplain and increase stage levels for equivalent flows, leading to increases in flood risks (Brookes, 1988; Landwehr and Rhoads, 2003). Flood control and hydroelectric dams, which are often built explicitly to impede flood and bedload sediment passage, have repeatedly been shown to alter downstream channel and floodplain dynamics (e.g., Petts, 1979; Williams and Wolman, 1984; Andrews, 1986; Brandt, 2000; Schmidt and Wilcock, 2008).

In New Mexico, human settlement has centered on the Rio Grande for centuries (Kelley, 1955; Scurlock, 1998; Table 1). Since the 1200s, Native American pueblos along the river relied on its water to support crops, and in the 16th and 17th centuries, Spanish colonists established irrigation and grazing economies. In the 1700s, the middle Rio Grande between Cochiti and Elephant Butte Reservoirs was described as a wide, braided, sand-bedded channel that supported numerous wetlands and the largest cottonwood forest in North America (Crawford et al., 1993; Scurlock, 1998). Major modifications to the river began in the late 1800s, when climate variability, drought, extreme floods, and (or) poor land use practices led to tributary arroyo incision and increased sediment delivery to the middle Rio Grande (Bryan, 1925; Cooke and Reeves, 1979; Balling and Wells, 1990). Accompanying changes in channel form and elevated water table levels, as well as likely damage to irrigation infrastructure, resulted in the collapse of agriculture in the valley (Scurlock, 1998). In response, hundreds of kilometers of irrigation diversions, drainage ditches, and levees were constructed during the 1920s and 1930s, followed by channelization via dredging, continued levee construction, and the installation of over 100,000 Kellner jetty jacks to stabilize banks in the 1940s-1960s (Woodson and Martin, 1962). Additionally, water and sediment supplies were impacted by rapid urban development in the late 20th century and the construction of dams and irrigation diversions along the mainstem and major upstream tributaries (Lagasse, 1981; Williams and Wolman, 1984; Mussetter Engineering (MEI), 2003), notably Cochiti Dam (Rio Grande-1973), Jemez Canyon Dam (Rio Jemez-1953), Galisteo Dam (Galisteo Creek-1970), and El Vado and Abiquiu Dams (Rio Chama-1935 and 1963). Average annual peak flows over the 20 years after Cochiti Dam was completed

declined by 10% compared to the 20 years prior to closure, and according to Lagasse (1981), the dam also reduces downstream bedload transport by 80%.

These historical impacts resulted in numerous channel adjustments along the entire middle Rio Grande since the early 1900s, including aggradation-degradation cycles, narrowing, loss of heterogeneity, increased sinuosity, vegetation encroachment, and an increase in stable islands (MEI, 2003; 2006; Richard and Julien, 2003; Ortiz, 2004; Makar et al., 2006; Massong et al., 2006; Table 1). Along the Rio Grande upstream of Albuquerque, NM, reduced sediment loads and peak discharge magnitudes from operation of Cochiti Dam led to channel incision and armoring, as well as an increase in sinuosity and bank erosion that threatens the levee system (Lagasse, 1981; Leon, 1998; Bauer, 2000; Massong, 2005). In the reach we are focusing on, centered on Albuquerque, an expanding population continues to impact the river, with associated concerns over floodplain infrastructure and ecology.

Previous studies have documented major alterations to the Rio Grande system, but have concentrated primarily on decadal-scale changes over relatively long reaches of the river. In this paper, we briefly review historical (1900-1985) channel change through Albuquerque, and provide new information on recent (1985-2008) planform channel and floodplain dynamics. First, we detail channel narrowing and local bank erosion along the Albuquerque reach using banklines digitized from sequential aerial photographs taken 1 to 7 years apart. We then relate these adjustments to changes in hydrology, especially drought and reduced stream flows. Additionally, estimates of uncertainty in channel width and area measurements are considered. Although useful in assessing the validity of results in channel change studies relying on historical images and maps, measurement errors are commonly disregarded (Downward et al., 1994).

Regional Setting and Study Reach

The Rio Grande above Albuquerque drains 37,555 km^2 of southern Colorado and northern New Mexico, including headwaters in the Sangre de Cristo, southern San Juan, and Jemez Mountains. The mainstem river flows through a series of rift grabens filled with sand and gravel associated with river and alluvial fan deposition (Connell, 1998; Dethier, 1999). Vegetation can be broadly characterized as desert scrub to grasslands at lower elevations, piñon-juniper and scrub oak woodlands at middle elevations, and conifer forests dominating the highest areas. Land use includes ranching, till agriculture, and urban-suburban activities in the valleys, with some forestry at higher elevations (Finch and Tainter, 2004).

Climate varies widely with elevation in the Rio Grande Basin upstream of Albuquerque. Average maximum and minimum temperatures at Albuquerque are 21° and 6°C (Western Regional Climate Center; wrcc.dri.edu; site 290234, elevation 1618 m), and between 15° and 3°C at sites situated at higher elevations and further north, e.g. Chama, New Mexico (site 291664, elevation 2393 m), and San Luis, Colorado (site 057430, elevation 2452 m). Precipitation at Albuquerque is between 20 and 25 cm/yr, with maximum precipitation occurring in the summer. However, high elevations in the San Juan Mountains receive over 100 cm/yr of precipitation, mostly as winter snowfall. Thus, snowmelt runoff from the northern mountain regions provides the majority of flow in the Rio Grande, and produces sustained peak flows in the Albuquerque study reach, primarily in mid-spring (water.usgs.gov; site 08330000). Peak flows are also generated in late summer by heavy rainfall from monsoon-season convective storms or dissipating tropical cyclones. Although these summer peaks can be large, they are generally much shorter in duration than the snowmelt peaks (Bullard and Wells, 1992).

The study reach includes approximately 29 km of the Rio Grande in Bernalillo County and the Albuquerque metropolitan area (Figure 1). Four tributaries enter the river from the west in this reach: Cabezon Arroyo, Calabacillas Arroyo, San Antonio Arroyo, and an unnamed tributary. Although flows in these highly engineered channels are ephemeral, the west-side arroyos can transport large volumes of sand and gravel into the river during floods related to summer storm events, which sometimes exceed 200 m^3/s (e.g., Leopold, 1946). On the east, the North and South Albuquerque Metropolitan Arroyo Flood Control Authority (AMAFCA) floodways drain Albuquerque and the western front of the Sandia Mountains, and include numerous detention basins and other water and sediment management features. The AMAFCA channels likely supply lesser, but significant, amounts of sediment to the river (Ortiz, 2004). The river channel and relatively small parts of its predevelopment floodplain lie between levees intended to protect adjacent urban and suburban areas from inundation. Just above the study reach, the river channel undergoes a downstream transition from a gravelly, mostly single-thread system that is largely a product of sediment trapping by Cochiti Dam usptream, to a wandering system characterized by multiple sand bars and vegetated islands (Ortiz, 2004; Meyer and Hepler, 2007). Vegetation on the floodplain and stable islands includes native cottonwood *(Populus deltoides)* and willow *(Salix elugia)*, and non-native Russian olive (*Elaeagnus augustifolia.*), Siberian elm (*Ulnus pumila*), and salt cedar (*Tamarix chinensis*).

Methods and Materials

Aerial photography. Interpretation of temporal sequences of aerial photographs and images can provide essential qualitative and quantitative two-dimensional data describing river system dynamics, including channel widths, vegetation cover, sinuosity, braiding index,

and others (e.g., Brice 1964, 1975; Lewin and Manton, 1975; Gilvear et al., 1999; Winterbottom, 2000). Aerial photography of the Rio Grande through Albuquerque has been conducted at least 19 times between 1935 and 2008 (Table 2), including annual to biannual image sets obtained since 1999, providing an excellent opportunity to examine historical adjustments and recent, short-term changes in the Rio Grande system.

The images used in this study were obtained in a spatially rectified format from multiple government sources and span from 1985 to 2008 (Table 2). Photograph quality varies between and within photographic sets. The scale and water level at which each image was obtained also differs from set to set. Most of the images are of good quality and produced relatively low Root Mean Square errors (RMSE < 3 m) in coregistration of photographs. The 1985 and 1992 photographs were often difficult to interpret due to poor resolution and contrast. Bankline data produced from pre-1985 photographs and a 1918 map were obtained from the US Bureau of Reclamation (Oliver, 2004). The source images for these data likely varied in quality and resolution as well.

Bankline and vegetated island digitization. The senior author used the 1985-2008 photographs to conduct on-screen digitization of channel banks and stable islands for each photographic year. Digitization was conducted within a geographic information system (GIS; ArcInfo 9.2) at a set scale of 1:2500. Besides the pre-1985 bankline data, the USBR Rio Grande Planform Project database (Oliver, 2004) also includes banklines from 1985, 1992, 2001, and 2002, but to maintain consistency, channel features from these photo years were re-digitized from Bernalillo County photographs.

Breaks in slope and changes in vegetation at channel margins often demarcated the boundary between channel and floodplain in the study reach. Vertical bank tops were

generally easy to locate on the air photos; however, shadows, gradual slope changes where bars join the floodplain, and especially overhanging trees complicated bank delineations. Photo interpretation and field observations suggested that, over the recent study period, long subreaches (>100m) where banks are obscured by vegetation are relatively stable. Assuming little or no bank adjustment, a 1999 LIDAR-based digital elevation model (http//:www.bernco.gov/gis) and unpublished USBR cross-section data were used as guides, along with the bank vegetation on the 1999 photos, to delineate banks along these locations on each photo set. If the vegetation on the 1999 photos and the working photo set were the same, the bank positions were assumed to be the same as well. Banks were drawn separately for each photo set, however. This protocol was employed along less than 6,500 m of the approximately 59,000 m of bank (11%).

On most of the photographs, vegetation was the primary feature used to delineate stable island and bar positions in the study reach. Mussetter Engineering, Inc.'s (2006) study suggests that with the present hydrology and channel configuration, the river cannot produce enough shear stress to remove riparian vegetation from emergent bars and islands. Therefore, persistent bars with established vegetation were considered stable and classified as islands or new floodplain (and no longer part of the channel). Vegetated islands were considered to be attached to the bank and no longer within the main channel when the remaining side channels were less than 10 m wide and appeared choked with vegetation, especially at the downstream end. In most cases, the digitized banklines demarcate islands and floodplains that are emergent and stable at moderate flows, but may be submerged during floods greater than estimated bankfull flow (>150 m^3/s; MEI, 2006).

Channel measurements. Channel planform and vegetated island areas for each year were measured directly within the GIS from the digitized polygons, and "total" widths and areas for each year were calculated by subtracting the island measurements from the channel measurements. Widths were assessed along lines drawn perpendicular to the 1996 channel position at 60 m intervals, equivalent to the minimum widths measured on the first photo sets obtained for the study (1996, 2001). Average width was calculated as the mean of the channel widths measured on each photo set (n=477). Bank erosion areas were identified by comparing the positions of the bank lines and differences in width between each set of photographs. Before being designated as an erosion area, the banklines had to meet two criteria: (1) Banks must be clearly retreating from the oldest banks to the youngest (eroded vegetation, decreasing distances to nearby floodplain structures, etc.), and (2) the maximum distance between the 1992 and 2008 bank lines must exceed the estimated measurement error. Once designated, then a polygon representing the eroded area was digitized in relation to the 2008 bank line (n=34). The digitization was completed at a scale of 1:1000. Total erosion over a photo period is the sum of the eroded area at each polygon over that period.

Finally, changes in channel width or area were calculated by subtracting data measured from the newer photographs from the measurement associated with the older photograph (+ values indicate widening; - values indicate narrowing), and rates were determined by dividing the given magnitude of change by the time elapsed between photographs (days / 365.25 days/yr).

Uncertainty in Photo Set Measurements

Aerial photos always contain distortions related to study area relief and pitch and yaw of the aircraft. Georectification reduces these distortions, but some warping inevitably

remains. Additionally, operator error is associated with locating features and performing measurements. Photographic quality, resolution, color, scale, and other attributes affect operator errors, as do interpretive skill and the scale at which delineations are conducted. Most river scientists have ignored these measurement uncertainties or focused primarily on RMSE calculated during photograph co-registration. Exceptions include Mount et al. (2003), Mount and Lewis (2005), and Hughes et al. (2006), however, error estimates are still rarely considered in air photo measurements, hindering evaluation of the reliability of results (Downward et al., 1994).

Methods. For this study, channel width measurement errors were estimated using the Mount et al. (2003) method, which comprises two independent error estimates. The first estimate represents the operator error associated with bankline digitization. It was calculated by multiplying the pixel resolution (R) by the mean of the maximum number of pixels (p) between repeat left and right bankline delineations. These delineations for each photo set were conducted at 20 sites located roughly equidistant along the channel. Although not equal at each site, the mean left and right bank errors were within 0.2 m of each other for all photo sets, so the offset data for each set was lumped into one average pixel error value (p). The second error estimate represents distortions within the air photos. It was measured by finding the difference in distance between 26 floodplain locations that could be identified accurately on all photograph sets (e.g., fence posts, telephone poles, and building corners), and those same locations identified on the highest quality photo set, the 2008 images. The mean difference in distance between the points represented the image distortion error (θ) for each photo set. The mean of all of the 1996 to 2006 distortion differences was used for the 2008 distortion error (instead of 0). The total width error (E_w) was calculated as:

(1) $E_w = 2^{1/2}pR + 2\theta$. (Mount et al., 2003)

For the pre-1985 photographs, where banklines were digitized by USBR, width error was estimated at 13% based on the error for the lowest quality images used in this study (1985) and unknown digitization parameters (e.g., scale, interpretive ability of digitizer, photograph distortions, etc.) over a wider channel.

For error associated with polygon area (channel, island, erosion), two assumptions were made: (1) the length of the channel, vegetated island, or eroding bank segment was constant (no error) and (2) the polygons representing these areas are rectangular. Therefore, the measurement error associated with area equaled the length of the polygon multiplied by the error in width. For erosion area, the measurement error was based on the lengths of the 1992-2008 erosion polygons.

Error associated with differences between photograph sets, largely for propagation of error in estimating rates of change, were calculated following procedures outlined in Mount et al. (2003) and Taylor (1982):

(2) $E_{dif} = (E_{photo1}^2 + E_{photo2}^2)^{1/2}$

where E_{dif} is the error of uncertainty associated with the comparison to subsequent photos, E_{photo1} is the measurement error associated with the first image set and E_{photo2} is the measurement error associated with the comparison photograph set. To find the uncertainty in estimates of channel change rate, E_{dif} was divided by the time elapsed between photograph dates, as per Mount et al., 2003).

Channel measurements made by the USBR on the 1992, 2001, and 2002 photographs (Oliver, 2004), and an original set of measurements made without the 1999 LIDAR and

cross-section data were reserved for comparison with final measurements made by the senior author on photo sets of the same years.

Error results. The error in average channel width measurements ranged from 5 m for the 2008 photographs to 23 m for the 1985 photographs. For differences in widths between sequential photo sets, the average error was 8 m for 2002-2004 and 30 m for 1985-1992. For the post-1985 photographs, average measurement error for channel width is 8 m, which is 6% of the average width and 16% of the narrowest width on the 2008 photographs. Additionally, from 1992, there is less than a 3 m difference between subsequent channel widths in 88% of the cross-sections. Air photo assessment at random sites where subsequent width differences where greater than 3 m revealed observable changes in channel form (e.g., island expansion, anabranch abandonment, etc.).

Compared to results from Oliver's (2004) bankline data for 1992, 2001, and 2002, channel areas measured in this study were 2%, 4%, and 6% greater, respectively. Average widths for the three photo sets differed by 4, 8, and 9 m. When compared to a preliminary set of banklines digitized by the senior author, the final differences in channel area ranged between 2 and 6% for the 1992 to 2006 data sets, and average widths increased by an average of 6 m. Differences in stable bar and island delineation and re-evaluation of subreaches with overhanging trees accounted for most differences between the older data and the final data sets. Using the LIDAR and cross-section data for reference reduced the range in variability between repeat bankline delineations, thereby decreasing error in width measurements by up to 5 m.

Uncertainty in channel area measurements ranged from 0.15 to 0.65 km^2 (3 to12 %) for the 2008 and 1985 image sets, respectively (Table 3), comparable to the width errors.

Relative errors in island and erosion polygon area were much greater because of the large error in channel width compared to polygon width. Island areas had relative errors of 11% for 1999, 2002, 2004, and 2008 photos and 40% for 1986 photographs. The erosion areas possess relative errors of over 1000% percent in periods where little erosion occurred (2001-2004, 2005-2006), and even the lowest relative error is over 200% (e.g., 2004-2005).

Overall, the error analysis for change detection revealed few differences in average channel width and rates of change between photographs exceeded the average measurement error during the 1985-2008 study period. The only statistically significant change in average width between subsequent image sets occurred between 1985 and 1992 (paired t-test, $\alpha = 0.10$), although differences between image sets obtained further apart in time are also statistically significant (e.g., 1999 and 2002, 2001 and 2004, 2004 and 2006, 1999 and 2008).

Discussion of error results. Using similar methods, width errors estimated by Mount et al. (2003) for the River Trannon ranged from ±1.4 to 5.4 m, clearly lower than in this study. This difference likely stems in significant part from different processes in these contrasting fluvial systems. The River Trannon is widening due to an influx of sediment due to landuse change (Mount et al., 2003), whereas the Rio Grande is narrowing (this study). Eroding banks can usually be accurately delineated by abrupt breaks between the channel and floodplain or terrace surfaces. In contrast, rivers tend to decrease width by depositing sediment on bars and along channel margins. Determining when and where sediment accumulation and plant cover has formed a new stable floodplain surface is more difficult. In this study, photo shading and texture were sometimes difficult to interpret in this respect, especially on bars where deposited gravel, vegetation, wood, and even wet sand appear similar. Large increments of narrowing are associated with abandonment of side channels,

but determining just when a side channel is no longer active is also problematic. In addition, differences in discharge between photographs also complicated bank line placement. Discharge and stage relations are not necessarily linear and discharge should not be used as evidence for comparable wetted areas in each image. Along steep, eroding banks, planform flow margin may not change much as flow changes, but even small adjustments in discharge on shallow bar slopes may inundate or expose large areas of channel floor.

Measurement errors are large relative to the magnitude of channel differences between subsequent photographs because of the additive nature of error propagation (Taylor, 1982). For instance, if the channel areas for year A and B are 30,050 ± 400 m^2 and 30,000 ± 300 m^2, respectively, then the difference is 50 m^2, but the error for this change in channel area is 500 m^2 (= $\sqrt{300^2 + 400^2}$). This example also indicates that relatively small percent errors (10%) can amount to large error magnitudes. These large errors are also propagated through the erosion or deposition rate calculations, where over small time periods they result in very large errors relative to low rates of change.

Assuming that residual error associated with photographic distortions is isotropic, or that an average maximum value of bankline offset represents the location error, will not hold for all photographs (Mount and Louis, 2005). In the current study, estimates of error in polygon area are typically oversimplified and overpredicted, although it seems reasonable that the relative error associated with channel areas are similar to those associated with average width for each photo set. However, while in all cases uncertainty in erosion area indicates the possibility of no erosion, in most cases bank retreat was clearly indicated by failed bank material or eroded vegetation. Erosion areas were evaluated and digitized at a larger scale and the banks were commonly better defined on the photos, therefore, they likely

have less than the estimated error. Finally, assuming that all uncertainty in polygon area is normal to the channel obviously ignores errors in other directions. If air photo error is non-isotropic, the magnitude and direction of the error relative to the shape of the polygon, as well as the polygon shape itself (i.e., elongation), will determine the error associated with area measurements and its significance. A method based more on probability distributions of error in repeat measurements would likely provide more realistic error estimates, but is beyond the scope of this paper. Further development of methods is needed for estimating uncertainty in airphoto-based channel change analyses, but the methods herein provides a reasonable first approximation of maximum error bounds.

Errors in air photo measurement of channel adjustments are relatively small for larger rivers and over longer timespans. For the Rio Grande, the 2008 width error was only 4% of the average width and 11% of the narrowest subreach. Error becomes more problematic on narrower rivers; for example, along the Rio Chama, a Rio Grande tributary, similar absolute error magnitudes to the Rio Grande resulted in 2005 width errors equaling 12% of the average width (41 m) and 28% of the narrowest reach. Similarly, greater areas of erosion associated with longer time periods between photographs or faster retreat rates generally have less proportional error (Mount et al., 2003). For example, at the fastest erosion rate for the Rio Grande, 0.3 m/yr between 1985 and 1992, 10 to 15 years between photographs would be required to exceed measurement error. At the average rate for 1985-2008, 30 years between photos are needed.

Although changes in average channel width between subsequent photo periods on the Rio Grande do not exceed measurement errors, real change is qualitatively evident on the air photos. Most of these adjustments are concentrated in a few subreaches where width

differences are significantly greater than the error, often by a factor of two or more. Average changes are insignificant because little planform adjustment has occurred along most of the study reach length. Based on this investigation, analyzing photographs over shorter time intervals is probably unnecessary for a generalized assessment of channel change, but is still important in identifying local areas where rapid change is occurring.

Results and Analysis

Discharge changes. Annual peak discharges at Albuquerque exhibit a strong declining trend since the late 1800s ($P < 0.001$; Figure 2). From 1884 to 1920, eight large floods of over 550 m^3/s surged through the study reach, with some projected well over 850 m^3/s (30,000 ft^3/s), (Kelley, 1982). As estimated by regression with the Otowi Bridge gage (R^2=0.76; USGS site 8279500), annual peak floods in Albuquerque from 1895-1918 averaged around 420 m^3/s (14,900 ft^3/s). However, from 1920 to 1942, the average decreased to 354 m^3/s (12,500 ft^3/s), and from 1949 to 1964, the average was only 200 m^3/s (7,000 ft^3/s). By the recent study period (1985-2008), average peak flows had declined to 144 m^3/s (5,100 ft^3/s), with the largest peak flows just under 270 m^3/s (9,540 ft^3/s).

Reductions in discharge through the reach can be attributed to both short-term climate fluctuations (Woodhouse and Lukas, 2006) and dam construction upstream of Albuquerque (Legasse, 1981; MEI, 2003). Peak flows at the Albuquerque gage decreased by 64% when comparing the first 25 years of discharge estimates (1895-1920) to the most recent 25 years (1983-2008). Over these same periods, peak flows along the Rio Grande decreased by 44% at the Embudo gage (USGS site 8313000) upstream of all major Rio Grande dams; they also decreased by 49% at the Otowi Bridge gage upstream of Cochiti Dam (closed in 1973) and downstream of the confluence with the Rio Chama, which is regulated by El Vado and

Abuqiu Dams (closed in 1935 and 1963). The drop at all three stations, which largely occurred prior to 1950 and major flow regulation, likely reflects a climatic shift toward lower snowpacks (Woodhouse and Lukas, 2006).

A similar comparison can be done for peak flow data for the three gages before Cochiti Dam (1942-1973) and post-Cochiti Dam (1974-2008). At Embudo and Otowi Bridge, average peak flow over these periods decreased 1 and 13 m^3/s (1% and 7%), respectively, whereas at the Albuquerque gage, the average peak flow decreased by 73 m^3/s (33%), showing the large impact of flow regulation by the dam.

Channel change. Like most of the middle Rio Grande (Makar et al., 2006), channel widths in the Albuquerque study reach decreased over the last century (Figure 3), from 516 m (± 103 m) to 145 m (± 5m). The channel narrowed rapidly between 1918 and 1962 (8 m/yr ± 2 m/yr), but from 1962 to 2008 channel widths largely stabilized and the narrowing rate fell to 0.7 m/yr (± 1 m/yr). The only apparent increase in average channel width occurred between 1962 and 1973. The standard deviation in channel width, a measure of channel heterogeneity, also declined from 183 m to 40 m between 1918 and 2008. Although the magnitude of change in average channel width diminished after 1962, the river continued to adjust to old and new impacts over the remainder of the study period (Figure 4). From 1985 to 2008, the channel narrowed by 30 m and the standard deviation in width measurements fell from 49 m to 38 m. Over that time, narrowing rates between photograph sets ranged from 0.3 m/yr (± 3.6 m/yr) for 1996-1999 to 3.0 m/yr (± 10 m/yr) for 2005-2006.

Channel area and vegetated island. As channel widths dropped between 1985 and 2008, total channel area decreased from 5.3 km^2 (± 0.7 km^2) to 4.9 km^2 (± 0.2 km^2; Table 4). Much of this shrinking was associated with vegetated island initiation and expansion.

Stabilized islands area increased from 0.1 km^2 (± 0.04 km^2) to 0.6 km^2 (± 0.07 km^2) between 1972 and 2008. During this period, a number of vegetated islands became attached to the floodplain and were no longer classified as islands, otherwise the increase in island are would have been larger. Figure 5 illustrates the change in channel area (without subtracting the islands) and vegetated island area over time. Stratigraphic and photographic evidence (Meyer and Hepler, 2007; this study) suggests that stable islands were rare prior to 1985, but began to form and grow at a steady rate between 1985 and 1999. Channel area including islands remained fairly stable over that same time, indicating a period of vegetated island growth and reduction of the effective channel area. From 1999 to 2004, channel area decreased while vegetated island area continued to grow, signifying that islands were still developing, but beginning to attach to channel banks. Bank attachment of a number of large islands caused the drop in both vegetated bar and channel area between the 2004 and 2005 photographs, followed by continued island formation, expansion, and attachment from 2005-2006. During the last photo period, both island area and channel area increased, largely due to construction and mechanical maintenance of a number of side channels and mechanical lowering of some bar surfaces.

Although island edges experienced some erosion, extensive protection measures and densely vegetated banks limited bank retreat along most of the study reach. Since 1985, only 5,200 m (~9%) of the banks have experienced substantial erosion, resulting in 98,000 m^2 of removed material. Since 1996, only 2,800 m of the banks show noticeable retreat (~5%). Erosion rates decreased from 0.3 $m^2/m/yr$ (7,600 ± 16,800 m^2/yr) over the 1985-1992 photo period to 0.02 $m^2/m/yr$ (650 ± 8,800 m^2/yr) by the 2002-2004 period (Figure 6). The flood of 2005 over the 2004-2005 photo period led to erosion rates of 0.2 $m^2/m/yr$(5,400 ± 17,400

m^2/yr), followed by a return to 0.1 m^2/m/yr (2,000 ± 10,200 m^2/yr) between 2006 and 2008. The 2006-2008 rate is artificially elevated due to restoration activities. Although some bank erosion occurs in the Albuquerque reach, over the recent study period, narrowing outpaces erosion at almost all cross sections.

Discussion

Over the last century, several factors have combined to reduce the width of the Rio Grande in the study reach. Rapid channel narrowing prior to 1962 was followed by a period of more gradual change that continues today. Reductions in peak discharge, changes in sediment delivery, river engineering, and vegetation encroachment played varying roles over these periods. The channel adjustments have also changed ecological processes in both the channel and floodplain, but over the last decade, efforts to preserve and restore ecologic integrity along the middle Rio Grande have increased (USBR, 2005, SWCA 2007). Understanding where these changes occur and the processes involved will help to guide management decisions related to maintaining the system, and adds to process knowledge that will help to understand other systems as well.

Causes of channel change.

1918-1962: Climate and channel control (Phase 1). Numerous investigations relate channel shape to the magnitude and frequency of flows that most effectively transport sediment over time (e.g., Wolman and Miller, 1960; Pickup, 1976; Emmett and Wolman, 2001). In arid regions, infrequent large floods are inferred to move the most sediment, and therefore control channel shape (Wolman and Gerson, 1978). Thus, changes in peak flow magnitudes and durations are effective in changing channel planform and cross-section form (e.g., Schumm and Lichty, 1963; Burkham, 1972; Pizzuto, 1994).

Burkham (1972) discussed widening on the similar Gila River, New Mexico between 1875 and 1917, where average channel widths increased from 55 m to 610 m and the channel shifted from a wandering, meandering type to braided. The change was attributed to an increase in large, fall and winter frontal storms occurring in adjacent mountains over that time. Flooding was also indicated in the six-fold increase in average channel width along the Cimarron River from 1914 to 1942 (Schumm and Lichty, 1963). In both cases, flooding destabilized banks and tributary junctions, increasing the amount of sediment left on the channel bed after flooding subsided. Similar processes were likely operating along the Rio Grande, along with increased bedload inputs from arroyos. Reconstructions of discharge based on tree ring data found discharge between 1900 and 1925 were the largest over the last 500 years (Woodhouse and Lukas, 2006) and large floods and increases in sediment delivered from arroyo incision (Cooke and Reeves, 1979) had likely shaped a relatively wide, shallow, sandy and braided channel.

Peak discharges decreased during the first phase of narrowing (1918 to 1962), limiting the transport of new deposits and likely leaving areas of the channel bed exposed, even during some spring flows. Areas of concentrated flow within the active channel (i.e., low flow channels) likely reworked sediment during moderate and low peak flows, depositing it in backwater areas, side channels, and on lower bar surfaces, leading to the abandonment of channel margins and anabranches. Friedman et al. (1996) documented similar behavior after a large flood on Plum Creek, CO, where a combination of channel abandonment, bed-level decrease, and vegetation establishment returned the widened, aggraded channel to conditions similar to the pre-flood state. Burkham (1972) described similar readjustment following early 20th century flooding along the Gila River. For initially

braided channels, Rinaldi (2003) observed that limited incision was sufficient to cause marked narrowing along numerous river reaches in Tuscany, Italy, leaving large areas of the former channel abandoned and exposed. Like along the Gila River as it re-narrowed after 1917 (Burkham, 1972), relatively high peak flows along the study reach, such as the 1908 or 1917 floods, likely continued to redistribute sediment across the channel, with some associated channel widening. However, narrowing was the dominant response to the general decrease in peak flow.

Diminishing annual flood magnitudes were not the only impact to the channel over this period. Most of the flood control and channel stabilization measures (with the exception of Cochiti Dam) were also implemented during the 1920s and 1930s. Relatively rapid periods of narrowing appear to be common after similar channel confinement. Reductions in channel width and braiding indices within the first two decades following flow regulation and embankment construction have been documented along the braided, sandy Platte River channel (Johnson, 1994), as well as the gravelly Piave River, Italy (Surian, 1999), and the Hunter River, Australia (Erskine, 1992).

The reduction in available sediment and higher flood stages created by channelization schemes along the Rio Grande likely contributed to incision and further narrowing, although few data exist to directly assess the effects of these activities. Irrigation and drainage ditches removed water from the system, and irrigation diversion dams trapped sediment and attenuated floods. Levees limited the area impacted by floods and the areal extent of sediment deposition, likely increasing the rate of vertical sediment accumulation and further concentrating flow in the active channel. Also levees and jetty jacks were often placed within the active channel, as well as the floodplain, directly contributing to channel

narrowing. With these new constraints on the channel, aggradation continued at a rate of 2.5 cm/yr between 1917 and 1936 (Happ, 1948). The study reach aggraded during normal peak flows, and larger peak flows, such as the 1941 and 1942 floods, likely scoured the narrower channel and aggraded floodplain terraces (Happ 1948), leaving a more entrenched, narrowed system by the end of the 1949 photo period.

In the 1950s and 1960s, further engineering began to reverse the aggradation trend. Jetty jacks were placed along banks and in bends and backwater areas to trap sediment and direct flow, furthering the decrease in channel width. Additionally, dredging produced narrower, deeper channels in many subreaches, and tributary dams cut off sediment to the main channel, beginning a period of channel incision directly upstream of the study reach.

1962-2008: Dams and droughts (Phase 2). The second, slower phase of narrowing, relates to limitations in peak flow imposed by upstream dams and multi-year droughts. Along rivers in the semi-arid western U.S., one of the most common adjustments to dam-related control of sediment and floods is channel narrowing (e.g., Willams and Wolman, 1984; Everitt, 1993; Grams and Schmidt, 2002). The Rio Grande downstream of Cochiti Dam has become sediment limited into the Albuquerque area (Schmidt and Wilcock, 2008). The channel bed has incised and coarsened, and the planform has shifted from primarily a braided channel to a more meandering, single-thread system (e.g., Lagasse, 1981; Ortiz, 2004; Massong et al., 2006). Incision from the dam to Bernalillo is typically over 2 m, and in much of the study reach, the vertical difference between the floodplain and narrowed channel is often greater than 1 m (Massong et al., 2006). The zone of bed coarsening appears to be slowly moving into the uppermost study reach (Ortiz, 2004). Additionally, evacuated bed sediment from upstream has likely been transported into the study reach where, due to

limited peak flows, it stalls in bars or is deposited on the floodplain and in areas of slack water. Lower average flood magnitudes have dramatically decreased the exceedance probability of the effective discharge. Mussetter Engineering, Inc (2003) calculated that the effective discharge of about 150 m^3/s at the Albuquerque gaging station is only equaled or exceeded 4% of the time since the closure of Cochiti Dam.

Along many western rivers, multiple-year periods of low discharge, whether anthropogenic or natural, have been observed to accelerate channel narrowing (Schumm and Lichty, 1963; Friedman et al., 1996; Allred and Schmidt, 1999). Within the study reach, comparison of channel change rates and average annual peak discharge over photo periods indicates that some of the more recent narrowing is related to drought periods (Figure 7). Extended periods of greater than average narrowing rates are associated with years of low spring runoff, such as 1988-1992, 1995-1997, and 1999-2005. These droughts are characterized by weak peak flows, usually under 120 m^3/s (~1.6 yr recurrence interval) and often below 60 m^3/s. During these low flow periods, sediment tends to deposit at channel and island margins and on stalled sand bars (MEI, 2006; Meyer and Hepler, 2007). Mussetter Engineering, Inc. (2006) found an average of 0.45 m of sand was deposited on emergent bar surfaces during the 2005 flood, reducing their duration of inundation from 20 to 4 days/yr and increasing the flood magnitude required for inundation from 42 m^3/s to 113 m^3/s.

Vegetation encroachment and island expansion (Phase 1 and 2). Narrowing of braided or wandering sand-bed channels associated with a decrease in morphologically significant floods is often accompanied by expansion of woody vegetation into the channel (Johnson, 1994; Friedman et al., 1996; 1998). Once the plants are established, roots provide

shear strength to cohesionless sands on bars and banks, and stems and leaves provide local flow resistance, reducing velocities and promoting deposition (Smith, 1976; Millar, 2000; Moody and Meade, 2008). Plants take advantage of exposed surfaces created by geomorphic adjustment, but by stabilizing bars and banks and trapping sediment during overbank flows, they may also help direct the trajectory and timing of channel change, often towards a more single-thread planform.

Prior to the construction of Cochiti Dam, channel constriction and bank stabilization by jetty jacks and levees limited the number of existing islands and island formation. However, width and area measurements indicate expansion and bank attachment of vegetated islands account for much of the channel narrowing along the study reach after 1985. During this time, incision upstream of and deposition within the study reach often resulted in exposure of channel surfaces, especially mid-channel sand bars. Willows and non-native species took hold on these emergent bars and other abandoned surfaces during drought periods. Once established, the plants tend to persist. Flows of 140 m^3/s often inundate newly stabilized islands, but photographs, field observations (Meyer and Hepler, 2007), and initial two-dimensional modeling adjacent to the AMAFCA South Diversion outlet suggests that the local roughness created by vegetation limits overtopping flow velocities, even at much higher discharges. Additionally, field evidence shows that instead of being removed at this discharge, established vegetation often traps sediment on island surfaces and in low velocity eddies and backwater areas downstream (MEI 2006). We infer that vegetation in the study reach helps build islands and floodplain via deposition on and around lower islands and bank-attached surfaces, further concentrating flow in single channels and likely exacerbating incision in the upper study reach.

Locations of channel change. Through Albuquerque, most of the measured channel change occurred in three main areas. Narrowing is concentrated in the upper third of the study reach, with smaller areas within 2 to 3 km up and downstream of the U.S. Interstate 40 Bridge and the confluence with the AMAFCA South Diversion Channel (Figure 8). In the upstream sub reach, these adjustments are primarily related to the downstream progression of channel degradation associated with Cochiti Dam (Ortiz, 2004; Massong et al., 2006). Deposition and island formation occur downstream of the transition from a narrow, incised channel with higher bed shear stresses to a wider channel with less transport capacity. Enhanced island formation, and hence, channel narrowing likely moves downstream ahead of the incision in the zone of transition (Meyer and Hepler, 2007).

In all three subreaches, tributary junctions and bridge crossings also factor into the narrowing (Figure 8). Some tributaries such as Cabezon and Calabacillas Arroyos may deliver more sediment than the Rio Grande can remove rapidly, especially considering that much of the tributary sediment is transported during summer storms, out of phase with the longer-duration spring runoff floods. In such situations, local aggradation is common, with deposition upstream due to backwater effects and downstream due to limited transport ability (Ferguson et al., 2006). This phenomenon is especially evident up and downstream of Calabacillas Arroyo, which has constricted the Rio Grande channel by constructing a large tributary fan and supplying sediment for downstream deposition in eddies, on bars, and in anabranches. The deposition and narrowing associated with Calabacillas Arroyo has steadily moved downstream over time as lower flow areas below the fan have filled with sediment. Narrowing at the outlet of the AMAFCA channels is likely exhibiting a similar pattern. Other researchers have documented tributary control of base level and channel adjustments at

confluences upstream of the study reach as well (Lagasse, 1981; Ortiz, 2004). Finally, in the upper half of the study reach, the river flows under three major bridges. One-dimensional hydraulic modeling indicates that the bridge piers create backwater upstream. This velocity reduction likely compounds the trend of deposition on bars and newly formed low floodplains, and in flow separation zones upstream of the bridges. Eddies formed below the bridge piers also appear to trap and store sediment.

Although narrowing is the primary mode of change along the Rio Grande through Albuquerque, there are a few subreaches that experience bank erosion. This erosion generally occurs in floodplain material deposited between the levees after 1949. Faster rates of erosion between1985 and 1992 are related to higher flows and possibly to rapid adjustment after the closure of Cochiti Dam. Much of the erosion after 1992 is coupled with vegetated island expansion where diminishing width constrains flows, focusing greater stress on opposing banks. The end result of island expansion and bank attachment appears to be a simpler, meandering river system that erodes at the outside of bends and deposits on the inside, at least where banks are less protected. Upstream of the study reach, the Rio Grande already exhibits these new characteristics, and the trend is evident at the north and south ends of the study reach. Figure 9 depicts how overall narrowing related to island expansion led to bank erosion near the South AMAFCA outlet over the study period.

Comparisons with other river systems. Semi-arid and arid rivers in the United States have undergone similar processes of narrowing over the last century. Although measured using a variety of methods and over varying time spans, the above rivers seem to exhibit the same general patterns. Along the Platte River, Nebraska, channels narrowed between 65 and 90% between 1938 and 1986 (~1.5%/yr), with most of the narrowing

completed by the mid-1960s. The Rio Grande below Elephant Butte Reservoir exhibited narrowing of 50-70 % between 1900 and 1970 (~1%/yr) (Everitt, 1993). Channel widths along the well-studied Green River decreased by an average of 27% at 18 sites in Canyonlands National Park, Utah, between the early 1900s and the 1970s (Graf, 1978). Allred and Schmidt (1999) showed a decrease in bankfull width measured on air photos of the Green River of about 30 m (19%) between 1930 and 1993 near Green River, Utah, including a 6% decrease in average width between 1938 and 1952, relative channel stability from 1952 to 1962, and an 11% decrease between 1962 and 1993. Other researchers report narrowing rates for the Green River between 9 and 20% over various time spans after the closure of Flaming Gorge Dam in 1962 (see Grams and Schmidt (2002) for details). Van Steeter and Pitlick (1998) reported 20% narrowing along the Colorado River near Grand Junction, Colorado, between 1937 and 1993; Hereford (1984) found narrowing of 50% of the Little Colorado, Arizona, between the 1930s and 1980s; and Burkham documented a 90% decrease in Gila River width, from 610 m to 60 m, between 1917 and 1964. In this study, the Rio Grande through Albuquerque narrowed by 58% of its 1918 width prior to 1965, after which narrowing slowed considerably. Between 1985 an 2008, it had narrowed another 7%.

Comparing these width adjustment measures and their rates is difficult due to the various techniques used, the number, magnitude, and timing of impacts to the channel, channel location, bed material, and many other factors, but it is significant that all these rivers have exhibited substantial narrowing over the last century. The most important factor implicated in these studies is a reduction in peak discharges, whether from dam construction and operation on the Green, Colorado, Rio Grande, and Platte Rivers, irrigation withdrawals on the Platte, and/or climate on the Little Colorado, Gila, and Rio Grande. If climate change

leads to a drier American West, and as demand rises, we can likely expect more reduction in flows in the future, which may result in continued narrowing on many regional waterways.

In addition, the processes involved in narrowing appear to be similar across these various rivers, except possibly canyon reaches on the Green River (Grams and Schmidt, 2002). Narrowing appears to follow the general pattern described by Schumm and Lichty (1963), Burkham (1972), and Johnson (1994), characterized by (1) stalled sediment on bars or in-channel berms, (2) vegetation establishment on abandoned bars during low flow years, (3) vertical aggradation on stabilized, vegetated bars, (4) abandonment and filling of anabranches, and (5) eventual attachment of bars to the old floodplain. In the process, possible ecological habitats, such as side channels and backwater areas, are filled (e.g., Van Steeter and Pitlick, 1998). Faster rates of change seem to be associated with drought periods (Johnson, 1994; Allred and Schmidt, 1999; Joeckel and Henebry, 2008; this study). In all cases except the Platte River, tamarisk is the main species encroaching onto the floodplain, although at least prior to Cochiti Dam closure, cottonwood recruitment occurred along the Albuquerque reach of the Rio Grande. It also appears that sandy channels, such as the Rio Grande, Gila, and Platte Rivers, have larger responses to perturbations, and narrowing rates may depend on the supply of fine material for channel reconstruction and vegetation regeneration, as well as the relative reduction in flows.

The role of tributaries in channel adjustments is addressed in the case of the Green River (in Dinosaur National Monument, CO; Grams and Schmidt, 2002), the Platte River (Joeckel and Henebry, 2008), and the Rio Grande (Everitt, 1993; this study). Larger tributaries on the Platte River attenuated downstream narrowing and increased bank erosion (Joeckel and Henebry, 2008). Along the Green River in Lodore Canyon, most of the

narrowing occurred on tributary debris fan-eddy complexes, with greater narrowing in reaches with the most post-dam decrease in stream power (Grams and Schmidt, 2002). Along the Rio Grande below Elephant Butte Reservoir, tributary sediment often choked the channel, forcing avulsion of the channel at the toe of resulting fans (Everitt, 1993). In our study reach, narrowing is greatest downstream of tributary sediment inputs, where fans impinge on the channel and deposition occurs on downstream bars and side channels. The varying responses of narrowing channels in reaches with tributary confluences is a function of the ratio of tributary to mainstem water flux, sediment flux, and sediment size (Ferguson et al., 2006), and possibly how fast vegetation can colonize exposed tributary deposits. For example, along the Platte River, there is likely enough stream power, to move sediment below confluences, whereas tributaries to the lower Rio Grande supplied excess sediment and insufficient water for the river to maintain its course.

Implications

Along river systems with limited human impacts, alluvial channels are usually free to adjust to local or regional perturbations in sediment and water flux, which often results in a variety of floodplain and lotic habitats within the system (Ward et al., 1999). These habitats generally support a diverse and productive biosystem adapted to the physical parameters imposed upon it. However, flood control and other river engineering methods tend to simplify rivers, often greatly altering associated ecosystems. Decreased frequency and intensity of flooding related to dam and irrigation operations have major effects on riparian ecosystems (Busch and Smith, 1995; Ward and Stanford, 1995; Friedman et al., 1998; Shafroth et al., 2002).

Human modification and reduced peak discharges have created a highly altered and simplified system along the Rio Grande, with decreased lateral mobility, loss of floodplain connectivity, reduced channel area, and a more single-thread planform. As a result, cottonwood forests are being replaced by non-native trees and aquatic habitats have been altered. Recent restoration activity has focused on these issues, especially restoration of breeding habitat for endangered silvery minnow (*Hybognathus amarus;* Bestgen and Platania, 1991). This effort includes removing jetty jacks and non-native vegetation, construction and maintenance of side channels and lowering of floodplain surfaces in small areas along the study reach. These measures have the added benefit of decreasing erosion risks where islands cause flow to impinge against banks adjacent to infrastructure.

Nonetheless, many of the processes responsible for narrowing are ongoing, and major impacts to the channel remain. Several climate forecasts predict a drier southwest and lowered streamflows in the Rio Grande over the next century (Hurd and Coonrod, 2008). The channel narrowing trend will likely continue, with sediment deposition in natural and restored side channels and on lower elevation, emergent surfaces. Current and future restoration projects will need to consider these channel adjustment processes and may require continued mechanical maintenance to avoid sedimentation in constructed anabranches and on lowered bars and floodplain areas.

Conclusions

This study utilizes sequential aerial photos to evaluate channel planform adjustment over the last century, focusing on the last 25 years. Short intervals between photograph sets allow for detailed temporal measurements of channel and island widths and areas, as well as areas of bank erosion. However, errors associated with measurement uncertainty indicate

that differences in channel width between such closely spaced photographs are not often significant, although they may be consistent with a trend in channel change.

Over the last 90 years, the Rio Grande has experienced major natural and anthropogenic perturbations to both its discharge and sediment load. Because of climate change and flood control dams, the channel through Albuquerque, New Mexico, has experienced a decline in spring flood magnitudes. Along with river engineering projects and droughts in the 1930s through the 1960s, this has led to decreased sediment transport and channel narrowing. More recently, narrowing has occurred with the growth and bank attachment of vegetated islands, especially during the drought in the late 1990s; and incision has stemmed from the encroachment of sediment-limited conditions from upstream dams, stabilized banks, and possibly positive feedback associated with increased velocity and shear stress in the narrower entrenched channel.

Overall, the channel through the study reach is shifting from a sandy, wide, braided system with a large active floodplain to a narrower, deeper, wandering or single-thread channel with a disconnected floodplain and limited lateral mobility. This situation will likely persist into the future as climate change and population growth continue to perturb the system in the study reach, and restoration and maintenance of ecological integrity will likely require continuous attention.

Acknowledgements

We would like to thank Tamara Massong and others at the U.S. Bureau of Reclamation, Albuquerque Office for supplying air photos and bank line data. We would also like to thank the Resource Geographic Information System Program at the University of New Mexico and the Bernalillo County GIS Department for providing online access to their

air photos and other GIS data. Funding for this project was provided by the U.S. Army Corps of Engineers, Engineer Research and Development Center, Urban Flood Damage Reduction and Channel Restoration Demonstration Program. We would also like to thank Dr. Gigi Richard and two anonymous reviewers for comments that helped to substantially improve this paper.

Tables

Time Period	*Activities*	*Impacts*	*Rio Grande Channel Changes*
late 1800s	intensified grazing	reduced vegetation, upland and gully erosion, increased sediment delivery (?)	aggradation, widening
1880s-1920s	large floods	tributary arroyo incision, increased sediment delivery	aggradation, widening
1920-1940	floodplain engineering	irrigation withdrawals, drainage ditches, levees, spread of exotic riparian vegetation	narrowing, degradation, vegetation encroachment
1940-1960	channel engineering	levees, dredging, bank stabilization	narrowing, degradation, vegetation encroachment
1935-1970	dam construction (major tributaries)	peak flow and sediment load reduction	narrowing, degradation
1940-2005	urban development	construction-related erosion, increased impervious area and runoff	increased urban runoff, sedimentation (especially at major stormwater drain confluences)
1973-2005	Cochiti Dam (Rio Grande) operations	major peak flow and sediment load reduction in study reach	narrowing, degradation downstream of dam
1980-2005	recent droughts	reduced flows	narrowing, vegetation encroachment

Table 1. Historical Impacts to the Rio Grande near Albuquerque, NM, and their potential effect on watershed and channel processes.

Photo Year	Date	Availability [a]	Quality	Resolution	Color [d]	Scale (1:X)	Discharge (m^3/s) [b]
1918	1918	USBR	MAP	NA	B/W	NA	NA
1935	1935	USBR	Poor Contrast	0.92	B/W	8000	NA
1949	1949	USBR	Adequate	0.3	B/W	5000	NA
1962	3/15/62	USBR	Poor	0.3	B/W	4800	18
1972	*March-72*	USBR	Poor Contrast	1.22	B/W	4800	*33 (11-43)* [c]
1985	3/13/85	USBR	Poor Contrast	2.4	B/W	4800	81
1992	2/24/92	USBR	Poor Resolution/Error	4	B/W	4800	9
1996	10/6/96	RGIS	Adequate	1	B/W	12000	18
1999	4/6/99	BERN	Good	0.3	Color	12000	20
2001	2/13/01	USBR	Good/High Error	0.6	B/W	4800	19
2001	*March-01*	BERN	Poor Contrast	0.3	B/W	12000	*20 (15-33)* [c]
2002	3/27/02	USGS/BERN	Good	0.3	Color	15000	13
2004	3/27/04	RGIS/BERN	Good	0.3	Color	19000	44
2005	6/21/05	USACE	Adequate	0.6	Color-QB	NA	120
2006	1/23/06	USBR	Good	0.5	Color IR	4800	18
2008	*3/23-4/24/09*	BERN	Good	0.15	Color	12000	*93 (70-113)* [c]

[a]Available from the following agencies

RGIS	*New Mexico Resource Geographic Information System (http://rgis.unm.edu)*
BERN	*Bernalillo County, NM GIS (http://www.bernco.gov)*
USBR	*US Bureau of Reclamation - Albuquerque Office (http://www.usbr.gov/uc/albuq/index.html)*
USACE	*US Army Corps of Engineers - Albuquerque District (http://www.spa.usace.army.mil/)*

[b]Discharge data from USGS Rio Grande at Albuquerque gage (site 08330000; waterdata.usgs.gov/nwis/uv?08330000)

[c]Discharge *100* (10-1000) represents *mean daily flow* (minimum daily flow - maximum daily flow) for given month

[d] B/W-Black and White, IR-Infrared, QB-Quickbird Satellite

Table 2. Aerial photography sets covering the Albuquerque Reach of the Rio Grande. Photographs are available for most decades since 1935, and imagery has been collected at least every other year since 1996. Images and maps used to create the USBR Bankline Project data (Oliver, 2004) utilized in this study (not digitized by the senior author) are indicated in grey.

Photo Year	Location Error (m)	Residual Error (m)	Width Error (m)	Width Diff Error (m)	Channel Area Error (km^2)	Island Area Error (km^2)	Erosion Area Error (m^2)	Width Error %	Width Diff Error %	Channel Error %	Island Error %	Erosion Error %
1985	13.6	1.2	23	29	0.65	0.04	117300	13%	241%	12%	40%	221%
1992	11.3	1.0	19	21	0.55	0.05	66300	12%	398%	11%	14%	310%
1996	4.2	1.1	9	11	0.27	0.09	27500	6%	1360%	5%	18%	610%
1999	2.5	0.8	6	10	0.17	0.06	17500	4%	246%	3%	11%	464%
2001	4.2	0.5	8	10	0.22	0.08	22600	5%	731%	4%	14%	1692%
2002	2.5	0.8	6	8	0.17	0.07	17600	4%	213%	3%	11%	1333%
2004	2.5	0.8	6	9	0.17	0.08	17400	4%	544%	3%	11%	260%
2005	3.4	0.9	7	10	0.21	0.08	21800	5%	547%	4%	14%	1465%
2006	2.8	1.0	7	9	0.20	0.08	20500	5%	4766%	4%	14%	507%
2008	1.9	0.9	5	-------	0.15	0.07	15600	4%	-------	3%	11%	-------
Mean	*4.9*	*0.9*	*9.5*	*13.0*	*0.28*	*0.07*	*34400*	*6%*	*1005%*	*5%*	*16%*	*762%*

Table 3. Error associated with channel parameter measurements from aerial photographs, Rio Grande through Bernalillo County (Albuquerque), New Mexico, 1985-2008. Location error = pR, Residual Error = θ, and Sequential Diff = error in the difference between sequential photograph sets.

Photo Year	Average Width (m)	Stand Dev (m)	% change from 1985	% change from 1918	Maximum Width (m)	Minimum Width (m)	Channel Area (km^2)	Island Area (km^2)	Erosion Area (m^2)
1985	176	49	0%	61%	319	51	5.3	0.09	53100
1992	164	44	7%	64%	294	58	5.1	0.35	21400
1996	159	42	10%	65%	290	58	5.1	0.50	4500
1999	158	42	10%	65%	292	58	5.1	0.54	3800
2001	154	40	12%	66%	257	58	5.1	0.58	1300
2002	153	40	13%	66%	259	58	5.1	0.62	1300
2004	149	40	15%	67%	253	58	5.0	0.69	6700
2005	147	40	16%	68%	242	47	4.9	0.57	1500
2006	146	41	17%	68%	242	46	4.8	0.58	4000
2008	146	38	17%	68%	244	46	4.9	0.66	--------
Mean	*155*	*42*	---	---	*269*	*54*	*5.0*	*0.52*	*10800*

Table 4. Rio Grande channel planform parameters measured from aerial photograph sets, Bernalillo County (Albuquerque), New Mexico, 1985-2008.

Figures

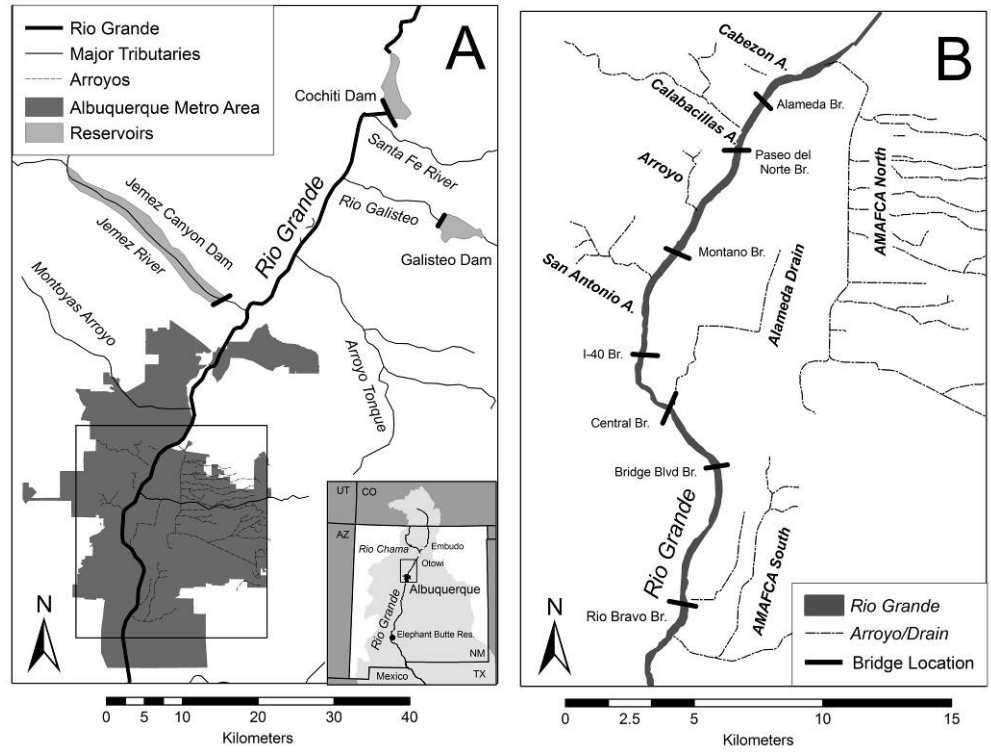

Figure 1. (A) Map of the study area depicting the Rio Grande from Cochiti Dam through Albuquerque. Inset map at bottom right shows the location of map A, with the Rio Grande basin in light gray, and locations of the Embudo and Otowi Bridge gaging stations and Elephant Butte Dam shown. (B) Study reach through metropolitan Albuquerque from the North to South AMAFCA Diversion Channel outlets. Abiquiu and El Vado Dams (not shown) lie on the middle Rio Chama.

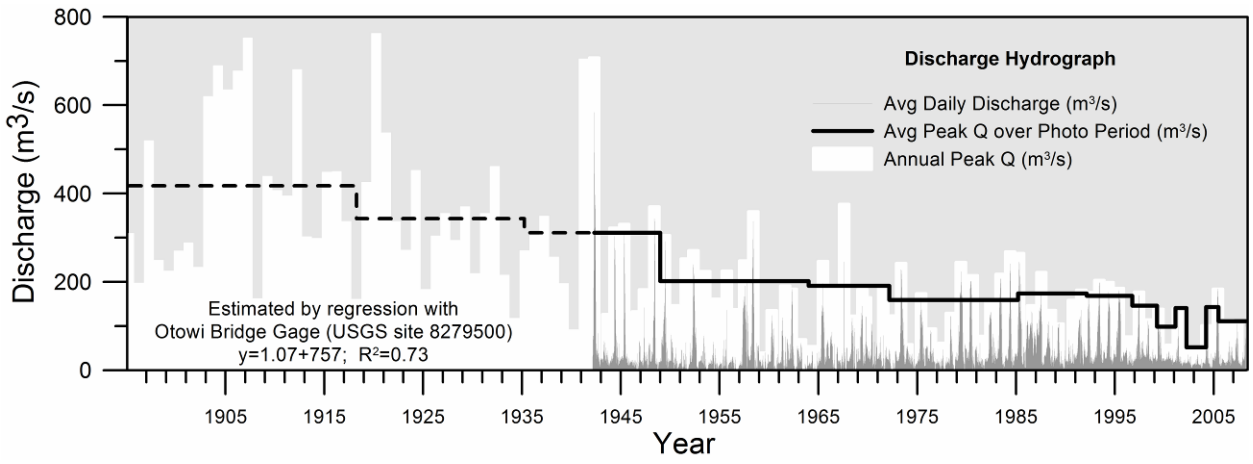

Figure 2. Hydrograph from the USGS Rio Grande at Albuquerque, New Mexico, gage (1942-2008; site 08330000). Pre-gage peak flows were estimated by regression with data from the USGS Rio Grande at Otowi Bridge, New Mexico, gage (1895-2008; site 08279500) for 1942-1973. Over the regression period, discharge at Otowi Bridge was partly controlled by El Vado Dam, and any pre-1942 floods generated downstream from Otowi Bridge in summer monsoon storms would not be represented, so flows may be underestimated. The step plot tread represents average annual peak discharge values between photo periods and the riser represents a photo date. Cochiti Dam closed in 1973.

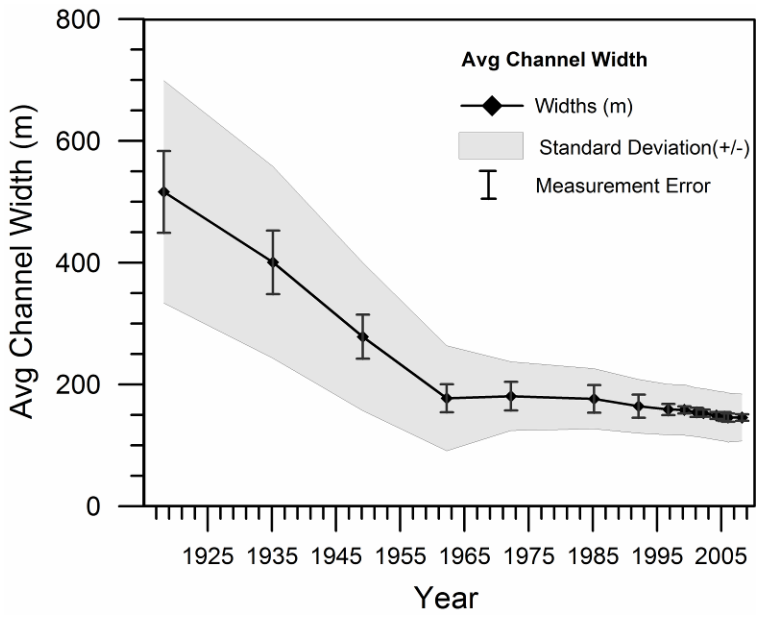

Figure 3. Change in Rio Grande average channel width through Bernalillo County (Albuquerque), New Mexico, 1918-2008. Channel widths decrease over the study period, but most of the adjustments are complete by 1962. Channel heterogeneity represented by the standard deviation in channel width (gray) also decreases.

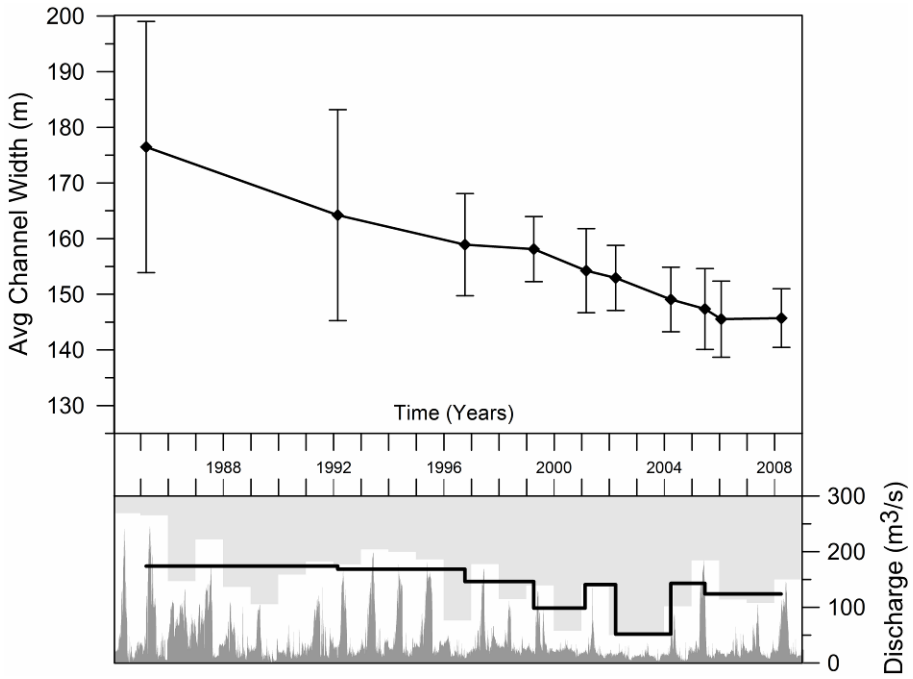

Figure 4. Change in average channel width along the Rio Grande through Bernalillo County (Albuquerque), New Mexico, from 1985 to 2008 compared to the hydrograph from the USGS Rio Grande at Albuquerque, New Mexico gage (site 08330000; waterdata.usgs.gov/nwis/ uv?08330000); discharge parameters are shown as in Figure 2. Measurement error, as represented by the error bars, is estimated using the method of Mount et al. (2003). The average channel widths decrease over the study period, but changes from photograph year to photograph year are within the measurement error.

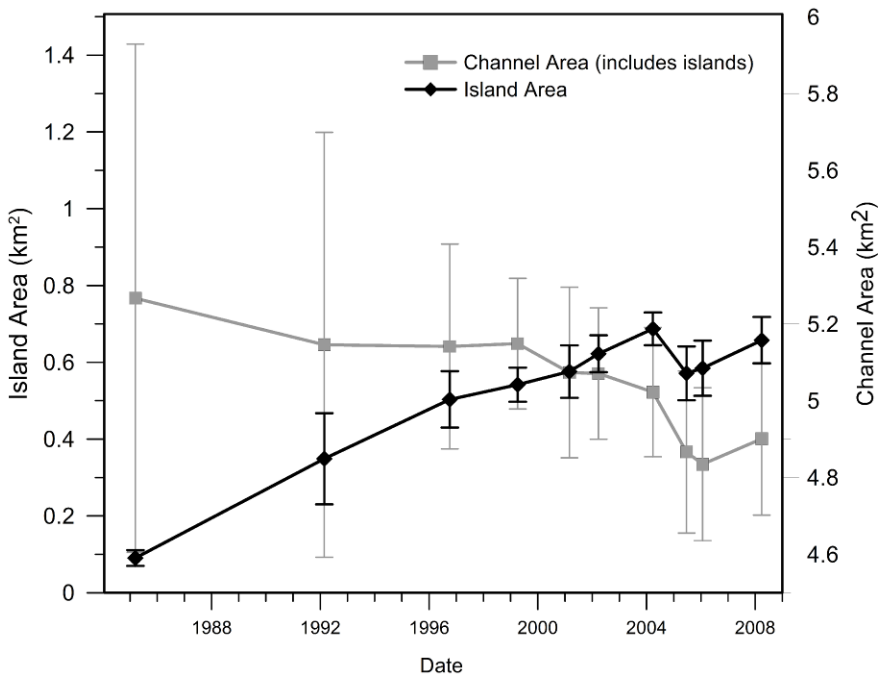

Figure 5. Change in vegetated island area and channel area along the Rio Grande, Bernalillo County (Albuquerque), New Mexico, 1985-2008. Vegetated island area increases over this time period; limited change since 2002 is in part because bank attachment of islands caused reductions in total area. Error bars represent measurement error estimated using method of Mount et al. (2003).

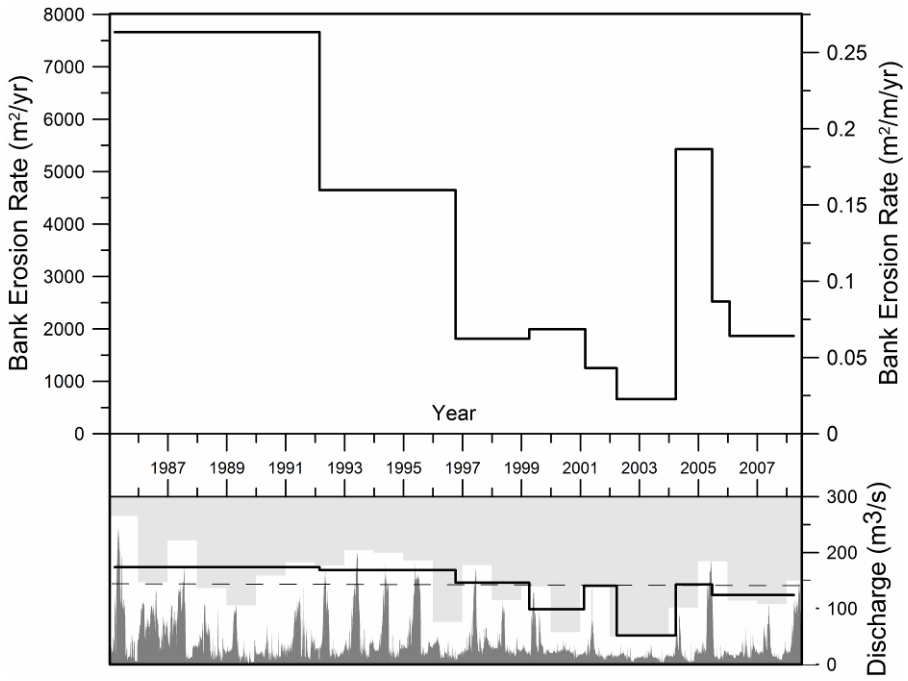

Figure 6. Bank erosion rates between photo periods along the Rio Grande through Bernalillo County (Albuquerque), New Mexico, 1985-2008. The step plot tread represents bank erosion rate over photo periods and the riser represents a photo date. All data is within the measurement error (see Table 1). Discharge parameters are shown as in Figure 2, with dashed line representing approximate bankfull discharge (defined at the level of the active floodplain before incision following Cochiti Dam closure). Measurements are calculated from the total area of erosion during a photo period digitized at the 34 active erosion sites within the study reach. Erosion rates decreased by a factor of 15 between 1985 and 2004, including low rates of bank retreat in the drought years between 1999 and 2004. The 2005 flood, which was just over bankfull flow, resulted in increased erosion, followed by relatively low rates despite mechanical intervention during the 2006-2008 photo period.

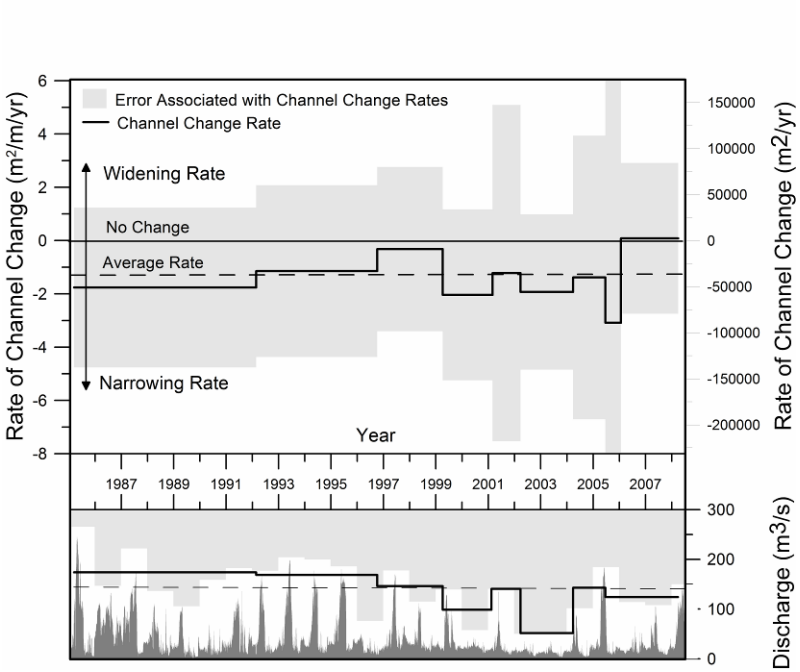

Figure 7. Comparison of recent channel narrowing rates and average annual peak discharge over photo periods, Bernalillo County (Albuquerque), New Mexico, 1985-2008. The step plot tread represents the channel change (narrowing) rate over photo periods and the riser represents a photo date. All data is within the measurement error (see Table 1). Discharge parameters are shown as in Figure 2, with dashed line representing approximate bankfull discharge. Extended periods of greater than average narrowing rates (< -1.3 m/yr) seem to be associated with years of weak spring runoffs, such as 1988- 1992, 1995-1997, and 1999-2005. Faster narrowing rate during 2005-2006 is vegetation established on new surfaces after the 2005 flood.

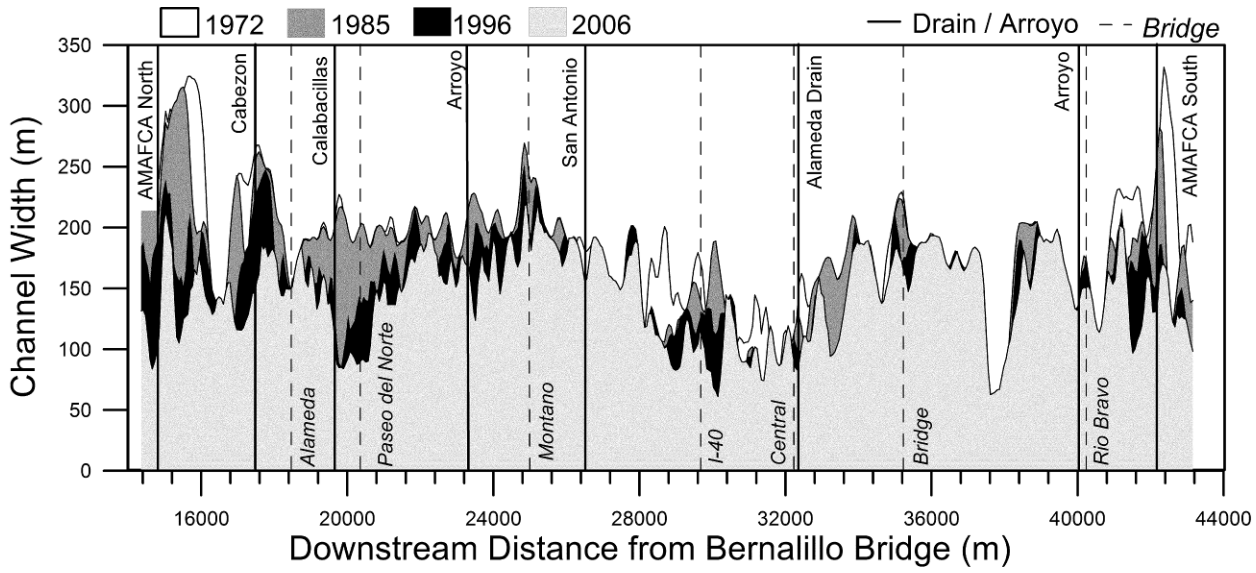

Figure 8. Change in channel width along the Rio Grande in Bernalillo County (Albuquerque), New Mexico, from 1972 to 2008. Narrowing is most prominent in the upper third of the channel (North AMAFCA Diversion Channel to Montano Ave. Bridge), within 2 km of the I-40 bridge, and 2 km up and downstream of the South AMAFCA Diversion Channel outlet.

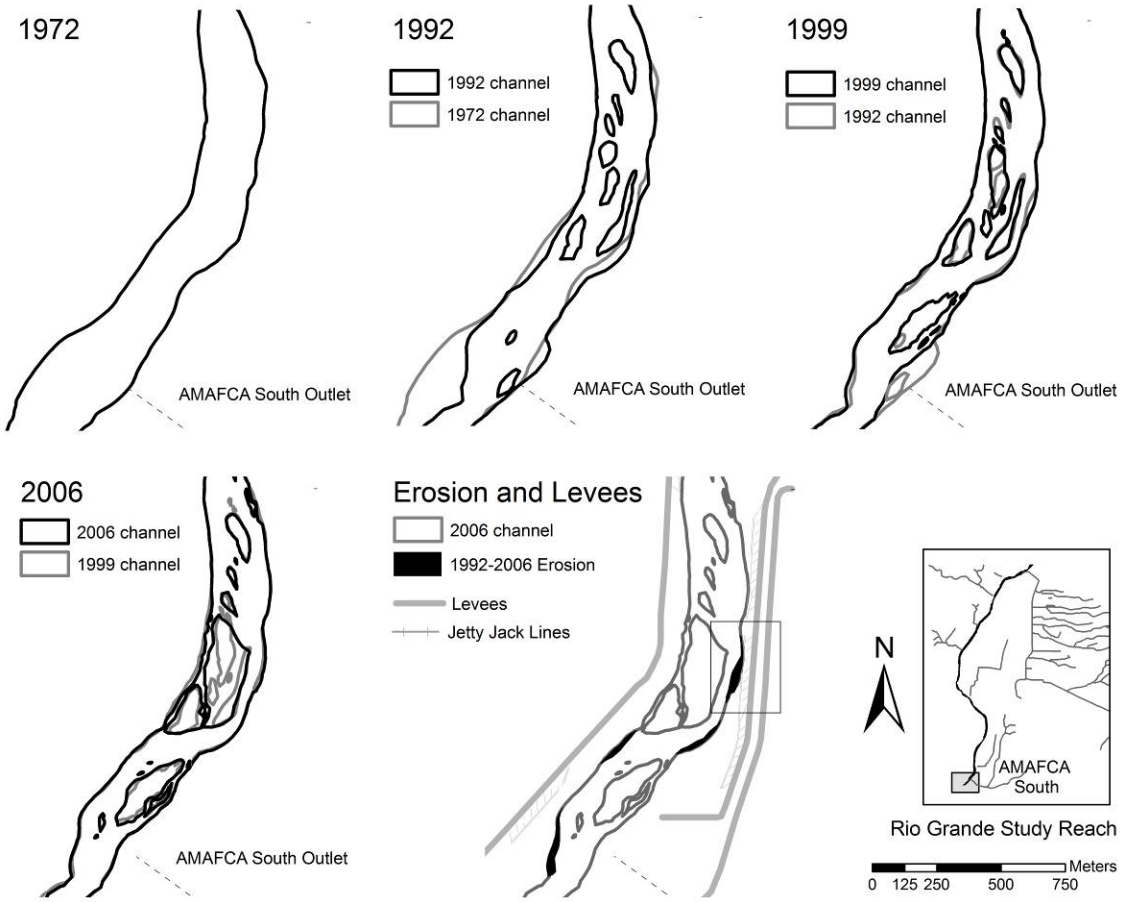

Figure 9. Channel narrowing via vegetated island expansion upstream of the AMAFCA South Diversion Floodway outlet, 1972-2006. Insert map shows location within the study reach. No islands existed in this subreach in 1972, but islands formed, expanded, and coalesced through the 1990s and early 2000s. The expanding islands force flow against banks, causing bank erosion that now threatens flood control infrastructure. The rate of bar formation and island expansion outpaces the rate of erosion, with a result of overall narrowing. Banks within the box (bottom, center) experienced 35 m of retreat from 1992 to 2006. This erosion is impacting adjacent jetty jack lines and the bank is now within 20 m of the levee.

References

Allred, TM, Schmidt, JC. 1999. Channel narrowing by vertical accretion along the Green River near Green River, Utah. *Geological Society of America Bulletin* 111: 1757-1772.

Andrews, ED. 1986. Downstream effects of Flaming Gorge Reservoir on the Green River, Colorado and Utah. *Geological Society of America Bulletin* 97: 1012-1023.

Bauer, TR. 2000. *Morphology of the Middle Rio Grande from Bernalillo Bridge to the San Acacia Diversion Dam, New Mexico*. Unpublished MSCE Thesis. Department of Civil Engineering, Colorado State University, Fort Collins, Colorado. Dr. P. Julien, advisor. 308p.

Balling, RC, Wells, SG. 1990. Historical rainfall patterns and arroyo activity within the Zuni River Drainage Basin, New Mexico. *Annals of the Association of American Geographers* 80: 603 – 617.

Bestgen, KR, Platania, SP. 1991. Status and Conservation of the Rio Grande Silvery Minnow, Hybognathus amarus. *Southwestern Naturalist* 36: 225-232.

Booth, DB. 1990. Steam-channel incision following drainage basin urbanization. *Water Resources Bulletin* 26: 407-417.

Brandt, SA. 2000. Classification of geomorphological effects downstream of dams. *Catena* 40: 375–401.

Brewer PA, Lewin, J. 1998. Planform cyclicity in an unstable reach: complex fluvial response to environmental change. *Earth Surface Processes and Landforms* 23: 989 – 1008.

Brice, JC. 1964. *Channel patterns and terraces of the Loup Rivers in Nebraska*. USGS Professional Paper 422-D. Department of the Interior, Washington, DC. 41p.

Brice, J.C., 1975. *Air Photo Interpretation of the Form and Behavior of Alluvial Rivers.* Final Report to the U.S. Army Research Office, Durham, North Carolina.

Brookes, A. 1988. *Channelized Rivers: Perspectives for Environmental Management*. Wiley: New York, NY.

Bryan, K. 1925. Date of channel trenching (arroyo cutting) in the arid southwest. *Science* 62: 339.

Bullard, TF, Wells, SA. 1992. *Hydrology of the Middle Rio Grande from Velarde to ElephantButte Reservoir, New Mexico*. USFWS Technical Report Series 179. Department of the Interior, Washington, DC. 51p.

Burkham, DE. 1972. *Channel changes of the Gila River in Safford Valley, AZ, 1846-1970*. USGS Professional Paper. Department of the Interior, Washington, DC. 24p.

Busch, DE, Smith, SD. 1995. Mechanisms associated with decline of woody species in riparian ecosystems of the Southwestern U.S. *Ecological Monographs* 65: 347-370.

Chin, A, Gregory, KJ. 2001. Urbanization and adjustment of ephemeral stream channels. *Annals of the Association of American Geographers*, Vol. 91, No. 4 (Dec., 2001), p. 595-608

Connell, SD. 1998. Geologic Map of the Bernalillo Quadrangle. New Mexico Bureau of Mines and Mineral Resources, OF-DM-16. Socorro, New Mexico.

Cooke RU, Reeves RW. 1976. Arroyos and Environmental Change in the American Southwest. Clarendon Press: Oxford, UK.

Crawford, CS, Culley, AC, Leutheuser, R, Sifuentes, MS, White, LH, Wilber, JP. 1993. *Middle Rio Grande Ecosystem: Bosque Biological Management Plan.* USFWS, Albuquerque, NM. 291p.

Dethier, DP. 1999. Quaternary evolution of the Rio Grande near Cochiti lake, northern Santo Domingo basin, New Mexico. *New Mexico Geological Society Guidebook*. 50th Field Conference, Albuquerque Geology: 371-378.

Downward, SR, Gurnell, AM, Brookes, A. 1994. A methodology for quantifying river channel change using GIS. In *Variability in Stream Erosion and Sediment Transport*. Publication 224. International Association of Hydrological Sciences: 449–456.

Emmett, WW, Wolman, MG. 2001. Effective discharge and gravel-bed rivers. *Earth Surface Processes and Landforms* 26: 1369-1380.

Erskine, WD. 1992. Channel response to large-scale river training works: Hunter River, Australia. *Regulated Rivers: Research & Management* 7: 261-278.

Everitt, BL. 1993. Channel responses to declining flow on the Rio Grande between Ft. Quitman and Presidio, Texas. *Geomorphology* 6: 225-242.

Finch, DM, Tainter, JA. 2004. *Ecology, Diversity and Sustainability of the Middle Rio Grande Basin.* Diane Publishing: Darby, PA. 186p.

Friedman, JM, Osterkamp, WR, Lewis, WM-Jr. 1996. The role of vegetation and bed-level fluctuations in the process of channel narrowing. *Geomorphology* 14: 341-351.

Friedman, JM, Osterkamp, WR, Scott, ML, Auble, GT. 1998. Downstream effects of dams on channel geometry and bottomland vegetation: regional patterns in the Great Plains. *Wetlands* 18: 619-633.

Ferguson, RI, Cudden, JR, Hoey, TB, and Rice, SP. 2006. River system discontinuities due to lateral inputs: generic styles and controls. *Earth Surface Processes and Landforms* 31: 1149–1166.

Gilvear, DJ, Winterbottom, SJ, Sichingbula, H. 1999. Character of meander planform change on the Luangwa River, Zambia. *Earth Surface Processes and Landforms* 16: 1-24.

Graf, WL. 1978. Fluvial adjustments to the spread of tamarisk in the Colorado Plateau region. *Geological Society of America Bulletin* 89: 1491–1501.

Grams, PE, Schmidt, JC. 2002. Streamflow regulation and multi-level flood plain formation: channel narrowing on the aggrading Green River in the eastern Uinta Mountains, Colorado and Utah. *Geomorphology* 44: 337-360.

Grant, G, Schmidt, JC, Lewis, SL. 2003. A geological framework for interpreting downstream effects of dams on rivers. *A Unique River. Water Science and Application 7*. American Geophysical Union: 209-225.

Happ, SC. 1948. Sedimentation in the Middle Rio Grande Valley, New Mexico. *Geological Society of America Bulletin* 59: 1191-1216.

Hereford, R. 1984. Climate and ephemeral-stream processes: Twentieth-century geomorphology and alluvial stratigraphy of the Little Colorado River, Arizona. *Geological Society of America Bulletin* 95: 654-668.

Hughes, ML, McDowell, PF, Marcus, WA. 2006. Accuracy assessment of georectified aerial photographs: Implications for measuring lateral channel movement in a GIS. *Geomorphology* 74: 1 –16.

Hurd, BH, Coonrod, J. 2008. Climate Change and Its Implications for New Mexico's Water Resources and Economic Opportunities. New Mexico State University, Agricultural Experiment Station, Technical Report 45. Las Cruces, NM. 28 p.

Joeckel, RM, Henebry, GM. 2008. Channel and island change in the lower Platte River, Eastern Nebraska, USA: 1855–2005. *Geomorphology* 102: 407-418.

Johnson, WC. 1994. Woodland expansion in the Platte River, Nebraska: Patterns and causes. *Ecological Monographs* 64: 45-84.

Kelley, VC. 1982. Albuquerque, its mountains, valley, water, and volcanoes. *NewMexico Bureau of Mines & Mineral Resources, Scenic Trips to the Geologic Past No. 9*. 106 p.

Kelley, WD. 1955. Settlement of the Middle Rio Grande Valley. *Journal of Geography* 54: 387-399.

Knighton, AD. 1988. River adjustment to changes in sediment load: The effects of tin mining on the Ringarooma River, Tasmania, 1875-1984. *Earth Surface Processes and Landforms* 14: 333-359.

Knox, JC. 2006. Floodplain sedimentation in the Upper Mississippi Valley: Natural versus human accelerated. *Geomorphology* 79: 286-310.

Lagasse, PF. 1981. Geomorphic response of the Rio Grande to dam construction. New Mexico Geological Society, Special Publication 10: 27–41.

Landwehr, K, Rhoads, BL. 2003. Depositional response of a headwater stream to channelization, East Central Illinois, USA. *River Research and Applications* 19: 77-100.

Lane, EW. 1955. The importance of fluvial morphology in hydraulic engineering. *Proceedings of the American Society of Civil Engineers* 81: 1–17.

Leon, C. 1998. *Morphology of the Middle Rio Grande from Cochiti Dam to Bernalillo Bridge, NM.* Unpublished MSCE thesis, Colorado State University, Ft. Collins, CO. Dr. P. Julien, advisor. 57p.

Leopold, LB. 1946. Two Intense Floods in New Mexico. *American Geophysics Union Transaction* 27: 535-540.

Leopold, LB, Bull, WB. 1979. Base level, aggradation, and grade. *American Philosophical Society Proceedings* 123: 168-202.

Lewin, J, Manton, MM. 1975. Welsh floodplain studies: the nature of floodplain geometry. *Journal of Hydrology* 25: 37-50.

Mackin, H. 1948. Concept of the graded river. *Geologic Society of America Bulletin* 59: 463-512.

Madej, MA, Ozaki, V. 1998. Channel response to sediment wave propagation and movement, Redwood Creek, California, USA. *Earth Surface Processes and Landforms* 21: 911-927.

Makar, P, Massong, T, Bauer, TR, Tashjian, P, and Oliver, KJ. 2006. Channel width and flow regime changes along the Middle Rio Grande, NM. Joint 8th Federal Interagency Sedimentation Conference and 3rd Federal Interagency Hydrologic Modeling Conference, Reno, Nevada.

Massong, T. 2005. Bank erosion Report – San Acacia Reach of the Rio Grande, NM. Unpublished report for the U.S. Bureau of Reclamation, Albuquerque, NM. December 2005. 13 p.

Massong, T, Tashjian, P, Makar, P. 2006. Recent Channel Incision and Floodplain Evolution within the Middle Rio Grande, NM. Joint 8th Federal Interagency Sedimentation Conference and 3rd Federal Interagency Hydrologic Modeling Conference, Reno, NV.

Meyer, GA, Hepler, C. 2007. *Vegetated Island Formation and Change in the Middle Rio Grande near Albuquerque, NM.* Unpublished report for the U.S. Bureau of Reclamation, Albuquerque, NM. Cooperation Agreement 01-FC-40-4670. April 9, 2007. 47p.

Millar, RG. 2000. Influence of bank vegetation on alluvial channel patterns. *Water Resources Research* 36: 1109-1118.

Moody, JA, Meade, RH. 2008. Terrace aggradation during the 1978 flood on Powder River, Montana, USA. *Geomorphology* 99: 387-403.

Mount, NJ, Louis, J, Teeuw, RM, Zukowski, PM, Stott, T. 2003. Estimation of error in bankfull width comparisons from temporally sequenced raw and corrected aerial photographs. *Geomorphology* 56: 65– 77.

Mount, NJ, Louis, J. 2005. Estimation and propagation of error in measurements of river channel movement from aerial imagery. *Earth Surface Processes and Landforms* 30: 635– 643.

Mussetter Engineering, Inc (MEI). 2003. *Geomorphic and Sedimentologic Investigations of the Middle Rio Grande between Cochiti Dam and Elephant Butte Reservoir.* Report prepared for New Mexico Interstate Stream Commission by Mussetter Engineering, Inc., Fort Collins, Colorado. 195 p.

Mussetter Engineering, Inc. (MEI). 2006. Evaluation *of Bar Morphology, Distribution and Dynamics as Indices of Fluvial Processes in the Middle Rio Grande, New Mexico.* Unpublished report for the New Mexico Interstate Stream Commission by Mussetter Engineering, Inc., Fort Collins, Colorado. 156p.

Oliver, KJ. 2004. Middle Rio Grande Project - 1918-2002 Geomorphology Study for the Rio Grande from Velarde to the Narrows of Elephant Butte, New Mexico. U. S. Department of the Interior, Bureau of Reclamation, Technical Service Center, Remote Sensing and GIS Group, Denver, CO.

Ortiz, R. 2004. *A River in Transition: Geomorphic and Bed Sediment Response to Cochiti Dam on the Middle Rio Grande, Bernalillo to Albuquerque, NM.* Unpublished MS thesis, Department of Earth and Planetary Science, University of New Mexico, Albuquerque, NM. Dr. Grant Meyer, advisor. 76p.

Petts, GE. 1979. Complex response of river channel morphology subsequent to reservoir construction. *Progress in Physical Geography* 3: 329-362.

Pickup, G. 1976. Adjustment of stream-channel shape to hydrologic regime. *Journal of Hydrology* 30: 365-373.

Pizzuto, JE. 1994. Channel adjustments to changing discharges, Powder River, Montana. *Geological Society of America Bulletin* 106: 1494-1501.

Richard, G, Julien, P. 2003. Dam impacts on and restoration of an alluvial river – Rio Grande, New Mexico. *International Journal of Sediment Research* 18: 89-96.

Rinaldi, M. 2003. Recent channel adjustments in alluvial rivers of Tuscany, central Italy. Earth Surface Processes and Landforms 28: 587-608.

Schmidt, JC, Wilcock, PR. 2008. Metrics for assessing the downstream effects of dams. *Water Resources Research* 44: W04404, doi:10.1029/2006WR005092.

Schumm, SA, Lichty, RW. 1963. Channel widening and floodplain construction along Cimarron River in southwestern Kansas. United States Geological Survey Professional Paper 352D.

Scurlock, D. 1998. From the Rio to the Sierra: An environmental history of the Middle Rio Grande Basin. General Technical Report RMRS-GTR-5. USDA, Forest Service, Rocky Mountain Research Station. Ft. Collins, CO. 440 p.

Shafroth, PB, Stromberg, JC, Patten, DT. 2002. Riparian vegetation response to altered disturbance and stress regimes. *Ecological Applications* 12: 107–123.

Smith, DG. 1976. Effect of vegetation on lateral migration of anastomosed channels of a glacier meltwater river. *Geological Society of America Bulletin* 87: 857-860.

Surian, N. 1999. Channel changes due to river regulation: The case of the Piave River, Italy. *Earth Surface Processes and Landforms* 24: 1135-1151.

SWCA Environmental Consultants. 2007. Middle Rio Grande Riverine Restoration Project Phase II Environmental Assessment. Prepared for the US Bureau of Reclamation, Albuquerque, NM, on behalf of the New Mexico Interstate Stream Commission, Albuquerque, NM. 76 pp. http://www.usbr.gov/uc/albuq/envdocs/

ea/mrg/rrph2/index.html, accessed May 4, 2009.

Taylor, JR. 1982. An Introduction to Error Analysis: the Study of Uncertainties in Physical Measurements. University Science Books: Mill Valley, CA. 270 p.

Thorne, C. 1982. Processes and mechanisms of river bank erosion. In J. Bathurst., R.D. Hey and C. Thorne, editors, *Gravel-bed Rivers*, Chichester, England, John, Wiley and Sons, 227-272.

Trimble, SW, Mendel, AC. 1995. The cow as a geomorphic agent—a critical review. *Geomorphology* 13: 233– 253.

U.S. Bureau of Reclamation. 2005. Middle Rio Grande Riverine Habitat Restoration Project Environmental Assessment. Albuquerque Area Office, Albuquerque. 76 pp.

Van Steeter, MM, Pitlick, J. 1998. Geomorphology and endangered fish habitats of the upper Colorado River, 1, Historic changes instreamflow, sediment load and channel morphology. *Water Resources Research 34*: 287–302.

Ward, JV, Stanford, JA. 1995. Ecological connectivity in alluvial river ecosystems and its disruption by flow regulation. *Regulated Rivers: Research & Management* 11 : 105 – 119.

Ward, JV, Tockner, K, Schiemer, F. 1999. Biodiversity of floodplain river ecosystems: ecotones and connectivity. *Regulated Rivers: Research & Management* 15: 125 – 139.

Williams, GP, Wolman, MG. 1984. Downstream Effects of Dams on Alluvial Rivers, USGS Professional Paper 1286. US Government Printing Office, Washington, DC.

Winterbottom, SJ. 2000. Medium and short-term channel planform changes on the Rivers Tayand Tummel, Scotland. *Geomorphology* 34: 195-208.

Wolman, MG. 1967. A cycle of sedimentation and erosion in urban river channels. *Geografiska Annaler. Series A, Physical Geography* 49: 385-395

Wolman, MG, Gerson, R. 1978. Relative scales of time and effectiveness of climate in watershed geomorphology. *Earth Surface Processes and Landforms* 3: 189 – 208.

Wolman, MG, Miller JP. 1960. Magnitude and frequency of forces in geomorphic processes. *Journal of Hydrology* 69: 54-74.

Woodson, RC, Martin, JT. 1962. The Rio Grande comprehensive plan in New Mexico and its effects on the river regime through the middle valley. In: Carlson, EJ, Dodge, EA, eds. Control of Alluvial Rivers by Steel Jetties. American Society of Civil Engineers Proceedings, Waterways and Harbors Division Journal 88. American Society of Civil Engineers, NY, NY, p. 53-81.

Woodhouse, CA, and Lukas, JJ. 2006. Drought, Tree Rings, and Water Resource Management in Colorado. *Canadian Water Resources Journal* 31: 1-14.

Chapter 2

Coupling of Hydrologic/Hydraulic Models and Aerial Photos through Time Fluvial Geomorphologic Changes along the Rio Chama, New Mexico 1935-2005

2010 Report to U.S. Army Corps of Engineers,
Urban Flood Demonstration Program

Authors:
Benjamin Swanson (swanson@unm.edu), **Grant Meyer** (gmeyer@unm.edu), Department of Earth and Planetary Sciences, University of New Mexico, Albuquerque, NM 87131

Julie Coonrod (jcoonrod@unm.edu), Department of Civil Engineering, University of New Mexico, Albuquerque, NM 87131

Acknowledgments

We thank the U.S. Army Corps of Engineers Urban Flood Demonstration Program for support of this work. We would also like to acknowledge Laura Gleasner of the University of New Mexico Earth Data Analysis Center for help in obtaining aerial photographs, and Darrel Eidson of the U.S. Army Corps of Engineers for review and suggestions.

Abstract

This study investigated the relation of average and peak flows in the Rio Chama to changes in channel planform measured on historical aerial photographs taken from 1935 to 2005. The study included two reaches of the Rio Chama: one upstream of El Vado Dam, from the Rio Brazos junction to the USGS stream gage near LaPuente, NM, and the other, between Rio the Gallinas confluence and the upstream end of Abiquiu Reservoir. Digitized and georeferenced photographs were analyzed using a GIS, with particular attention paid to quantifying potential measurement error and its propagation through estimates of channel areas and bank erosion rates. Average total channel widths along the upstream reach decreased from 51 m (±13 m) to 31 m (± 9 m) over the study period, and from 58 m (± 12 m)

to 38 m (± 6 m) downstream. Variability in channel widths also declined along both reaches. The main narrowing process includes bar establishment, stabilization, and vertical and horizontal growth, along with concurrent vegetation establishment, which is consistent with other narrowing channels in semi-arid areas of the United States. Relationships between planform change and discharge were not consistent, likely due to changing channel processes and changes in sediment flux to the channel. Channel stability and decreasing widths along the upstream Rio Chama study reach are likely associated with probable changes in precipitation and land use/ land cover related to grazing and logging. Early narrowing (pre-1963) along the reach downstream of El Vado Dam is likely linked to dam closure (1935) and low flow conditions. A return to high flow conditions in the 1960s and 1970s resulted in some erosion and stable channel widths (or some channel widening), but later wet years (1975-1996) seem to be correlated with a decrease in channel width along both reaches. The upstream channel appeared to be much more active (i.e., avulsions, erosion, bar formation), especially in the early part of the study period, than the downstream reach, and significant width changes occurred throughout the upper study reach above the Rito de Tierra Amarilla confluence. Along the downstream reach, width changes are concentrated between nodes, and appear to be controlled by valley confinement and debris flow inputs.

Introduction

A guiding principle in river science maintains that channel systems evolve to convey the sediment loads and water discharges imposed upon them. Alterations in hillslope and channel parameters within a drainage area, both human induced or natural, can have profound impacts on river channel and floodplain form and process, often resulting in adjustments to channel slope, depth, width, sinuosity, roughness, and (or) related parameters

(e.g., Mackin, 1948; Lane, 1955; Burkham, 1972; Leopold and Bull, 1979; Trimble, 1983; Meyer et al., 1985). Watershed and channel impacts can occur at a range of scales and over varying time spans within the catchment, and may work together or oppose each other to modify outcomes.

Because of their ability to impede and control the downstream passage of sediment and water in rivers, dams are often cited as major contributors to modern channel change (Williams and Wolman, 1984; Brandt, 2000; Petts and Gurnell, 2005). Williams and Wolman (1984) describe the impacts on river channels from dam construction and operation, depicting a wide range in the magnitude and timing of channel adjustments. Case studies conducted since 1984 have also documented a variety of downstream responses to dams, including little change below the Pelton-Round Butte Hydroelectric Dam on the Deschutes River (Fassnacht et al., 2003), to aggradation and narrowing along the Green River below Flaming Gorge Reservoir (Andrews, 1986; Allred and Schmidt, 1999; Grams and Schmidt, 2002), to bed degradation below the Elwha dams on the Olympic Coast of Washington (Pohl, 2004). In the Rio Grande drainage area, Cochiti Dam and other engineering structures (levees, diversion dams, canals, etc.) have lead to bed degradation and coarsening below the dam (Lagasse, 1981; Musseter Engineering, Inc (MEI), 2003; Richard and Julien, 2003) and channel narrowing and vegetation encroachment through Albuquerque (Swanson et al., 2007; 2010 (submitted)). Similar adjustments were observed below the Jemez Canyon Dam on the Jemez River (Williams and Wolman, 1984).

However, although dams may trap upstream sediment and control discharge, broader environmental controls, for example, large-scale land use, or short-term climate shifts such as droughts, may also impact the channel system. Changes in water and sediment fluxes from

the basin to the main channel, due to changes in land use, land cover, or climate, may increase or decrease the impact of the dam and dam operations. Most of the studies documenting channel change downstream of dams have not examined concurrent upstream channel changes, which may be a function of environmental controls that could also be contributing to change within the channel downstream of the dam.

In the past decade, there has been much research on the historical responses of the middle Rio Grande to climate and anthropogenic impacts (e.g., Mussetter Engineering Inc., 2003, 2006; Richard and Julien 2003; Makar et al. 2006), including UFDP research on recent (1972-2006) changes in channel width (Swanson et al. 2007, 2010). These investigations identified major trends in Rio Grande channel adjustment, such as channel narrowing, and major factors contributing to these trends, such as flow regulation and sediment trapping at dams, placement of levees and jetty jacks, non-native vegetation encroachment, and droughts. The effects of these and other disturbances along the Albuquerque reach of the river create interesting research problems; however, the sheer quantity and magnitude of these disturbances, often working in concert, also makes separating their effects a difficult problem in itself.

In the attempt to concentrate on particular disturbances and their impacts on southwestern rivers, continued research on linking hydrology to channel changes seen on aerial photographs was shifted to the Rio Chama, a major tributary to the Rio Grande, that has experienced fewer impacts. Unlike the Rio Grande, there has been very little work on channel geomorphology or hydrology along the Rio Chama despite its association with three dams (Abiquiu, El Vado, and Heron) and Albuquerque's San Juan - Chama Drinking Water Project.

As part of the UFDP research on linking channel width change to hydrology, Swanson et al. (2008) investigated channel planform changes along the Rio Chama between El Vado Dam and Abiquiu Reservoir from 1935-2005, documenting channel narrowing attributed to dam construction and operations. The overall purpose of this new work is to extend documentation of fluvial system changes to the Rio Chama system. We updated the previous work on the Chama below El Vado Dam by filling in gaps between aerial photograph years with additional measurements from newly acquired photograph sets. Additionally, we investigated the relation of average and peak flows to decadal changes in Rio Chama channel bank position upstream of the dams situated along the Rio Chama, as seen on historical aerial photographs. This analysis provides additional detail on the historical impact of land use, dam operations, and droughts along both the upper study reach and the study reach between El Vado and Abiquiu Reservoirs (Swanson et al., 2008).

Study Area

Considering its hydrologic, economic, and social importance within the Rio Grande system, there have been surprisingly few investigations covering Rio Chama channel and floodplain processes. Fogg et al. (1992) summarize many of the investigations involved with obtaining Wild and Scenic River status, including the impacts of dam management on riparian cover, fish habitat, sediment transport, and recreational opportunities, but the discussion does not incorporate geomorphic adjustment along the river. Research concerning the geomorphology within the Upper and Lower Rio Chama basin has primarily examined the relationships between terrace formation, climate, and tectonics (Gonzales and Dethier, 1991; Love and Connell, 2005) over much longer time periods than concerned with here. Love and Connell (2005) indicated that Holocene climate change had little effect on the

grade of the upper Rio Chama; however, a thick, fine-grained, late-Holocene fill along the middle river below El Vado Dam dates to about 500 years before present, and multiple younger fluvial terraces (Persico et al., 2005) reflect major channel adjustments in this river segment over the last several centuries. These deposits might be expected along an ephemeral arroyo system with relatively inconsistent flows, but they are unexpected along a relatively large perennial snowmelt-fed river with stream power presumably high enough during spring runoff to flush fine sediment downstream. The timing of these adjustments and the roles of climate change, sediment inputs, and dam operations remain unknown.

The Rio Chama is the largest tributary to the Rio Grande in New Mexico, draining 8,300 km^2 above its confluence with the Rio Grande near Española, NM. Its headwater streams drain the southern San Juan Mountains, characterized by conifer forests, snowmelt-dominated hydrology, and variable but relatively resistant bedrock. The watershed's lower elevations are characterized by the more erodible rocks, sparser shrubland vegetation, and summer monsoon-dominated storm hydrology of the Colorado Plateau and Rio Grande Rift (Fogg et al., 1992; Love and Connell, 2005). The river is roughly divided into three sections by two major dams. El Vado Dam was constructed in 1935 by the Middle Rio Grande Conservancy District to manage water for flood relief and irrigation in the Rio Grande Valley and is currently operated by the Bureau of Reclamation. It divides the Upper Rio Chama from the Middle Rio Chama, and is the focus of this study. Abiquiu Dam closed in 1963, disconnecting the Lower and Middle Rio Chama. A third dam, Heron Dam, lies on Willow Creek, a tributary of the Rio Chama situated upstream of El Vado Reservoir. It was constructed in 1971 to store water transferred from the adjacent San Juan River Basin for use

in Albuquerque, NM (San Juan-Chama Drinking Water Project: *http://www.abcwua.org/content/view/31/24/).*

This study focuses on two reaches of the Rio Chama: one study reach upstream of El Vado Dam and Reservoir and another downstream of the dam. The upper reach includes 17 km of river between the Rio Chama – Rio de la Brazos confluence to downstream of the U.S. Geological Survey stream gage near LaPuente, NM (Figure 1). The second study reach comprises 16 km of the Rio Chama flowing from just upstream of the Rio Chama – Rio Gallinas confluence to just downstream of the USGS Rio Chama above Abiquiu Reservoir stream gage (Figure 1).

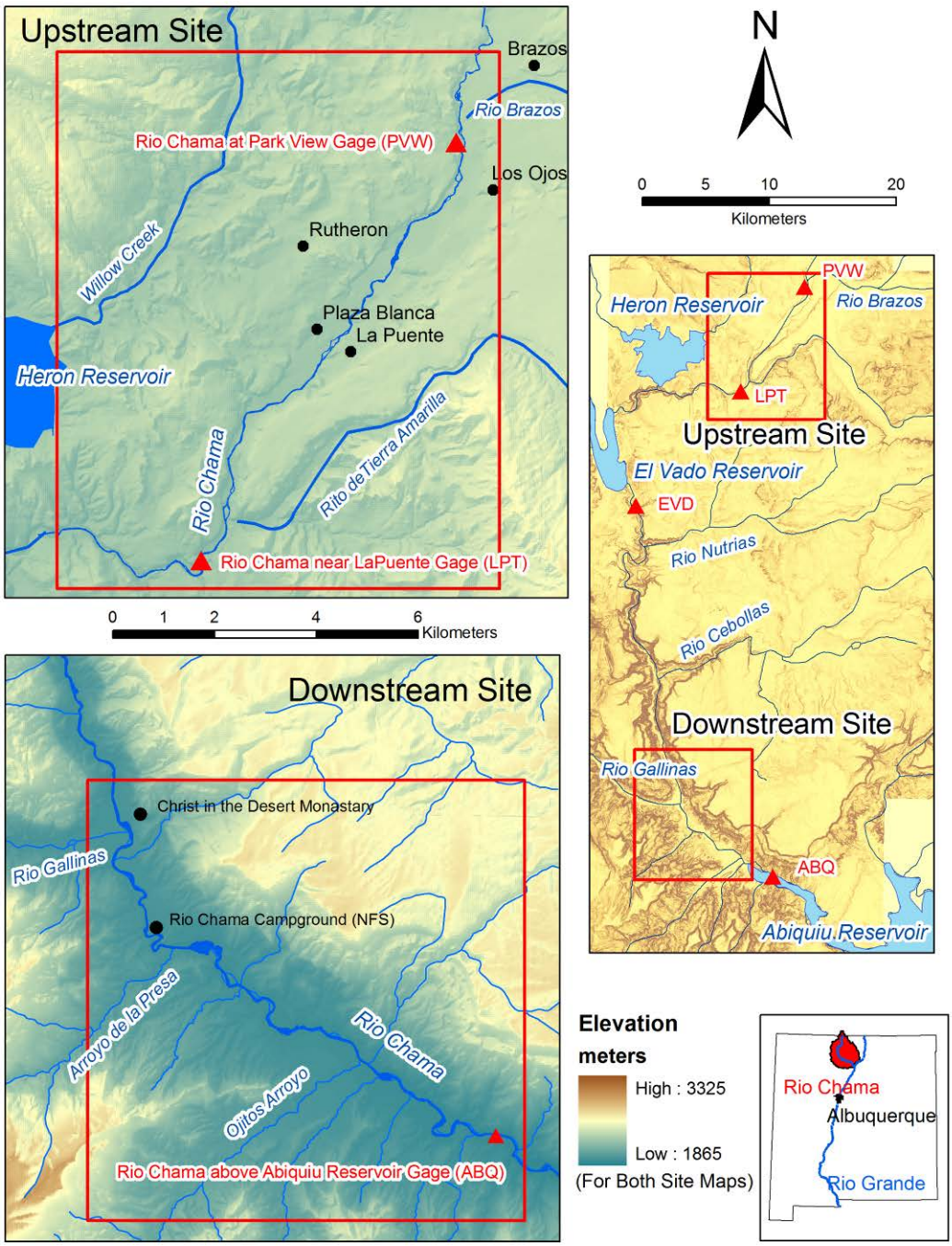

Figure 1. Study area, Rio Chama study reaches located up and downstream of El Vado Dam.

Upstream study reach. The main headwater streams for the system empty from the southern San Juan and Cumbres Mountains just north of the upstream study area, and major tributaries within the study area include the Rito de Tierra Amarilla and the Rio de la Brazos (Figure 1). The upper half of the reach flows through a relatively wide alluvial valley underlain by Cretaceous Mancos Group shales and Mesaverde Group sandstones, and flanked by Quaternary river and landslide deposits and basalt flows (Manley et al., 1987). The lower half of the reach is constrained by high terraces and a bedrock canyon cut through Cretaceous Dakota sandstone. Cretaceous sandstones, along with Triassic sedimentary rocks and the Precambrian metamorphic rocks of the Cumbres Mountains and Brazos Peak areas can be found at higher elevations. In part because of wide variations in rock types and strengths, particle sizes within the channel bed range from silt to boulders, but are primarily sand and gravel. Various grasses, junipers, pines, and sagebrush grow at middle elevations, with aspens and spruces populating the higher elevation regions. Floodplain vegetation is primarily cottonwoods and willows.

Prior to the mid-1800s, the valley was used by various Native American tribes (i.e., Utes, Apaches, Navajo) for hunting and as a trading route to downstream Spanish settlements. Multiple attacks on settlers, traders, and herders in the valley kept the Spanish from establishing a permanent presence upstream of the village of Abiquiu, downstream of both Rio Chama study reaches, until the mid-1800s (Poling-Kempes, 1997). Railroad construction in the 1880s brought a boom to the area, drastically increasing local lumber, ranching, and other industries in the upper Rio Chama Valley. Grazing continued until bad winters and the Great Depression drastically reduced the number of sheep and cattle in the 1930s, and large-scale forestry gradually declined until its end in the 1960s. The Upper Rio

Chama watershed is currently dominated by private land with the U.S. Forest service managing 5%, and the State of New Mexico managing approximately 15% (EPA, 2004). Today, primary land uses in the Upper Rio Chama watershed include ranching, forestry, agriculture, recreation and tourism, with very limited urban development. There are several active irrigation canals that divert surface water for agriculture, and several active and inactive gravel mines are located along the river and its tributaries (EPA, 2004).

Downstream study reach. Along the downstream study reach, the channel flows through a relatively wide canyon, where it is generally alluvial in character but often constrained by bedrock or alluvial fan and landslide deposits. Major tributaries entering the river downstream of El Vado Dam, but upstream of this study reach include the Rio Nutrias and the Rio Cebolla; within the study reach, the Rio Gallinas and Canada de la Presa enter the Rio Chama (Figure 1). The rock types within the watershed are primarily Cretaceous to Triassic sedimentary rock, varying in grain size and strength (Manley et al., 1987; Fogg et al., 1992). The rocks are often exposed along cliff faces throughout the lower watershed, where there is much more relief adjacent to the river than along the upstream reach (Figure 1). Weathering of the sedimentary rocks, especially the Chinle, Entrada, and Morrison Formations, produces a large amount of sand and fine-grained sediment, as indicated by the relatively large volume of sand deposited along the canyon and valley floor (Persico et al., 2005). Particle sizes within the channel of the Rio Chama vary considerably. At low flows ($Q < 400$ cfs), approximately 1/3 of the bed is sand (< 4 mm) and the remaining bed is primarily gravel (4-64 mm) and cobbles (64-256 mm; Swanson, unpublished data). Tributaries and channel migration into floodplain deposits and fans supply finer sediment to

the system, including large inputs of sand from the Rio Gallinas. Coarser material is delivered to the main channel via tributary debris flows, channel migration, and landslides.

Compared to the upper Rio Chama and the Rio Grande downstream of Cochiti Dam, the downstream Rio Chama reach has experienced few impacts. The primary, historical disturbances to the study reach are short-term climate shifts and land use changes such as roads and grazing. In most of the study area, the Rio Chama is designated as a Wild and Scenic River, and much of the adjacent catchment is managed by the U.S. Forest Service, Bureau of Land Management, and the Jicarilla Apache Reservation.

Methods and Data Acquisition

Aerial photography. Interpretation of temporal sequences of aerial photographs and images can provide essential qualitative and quantitative two-dimensional data describing river system dynamics, including channel widths, vegetation cover, sinuosity, braiding index, and others (e.g., Brice 1964, 1975; Lewin and Manton, 1975; Gilvear et al., 1999; Winterbottom, 2000). Systematic aerial photography of the Rio Chama study reaches has been conducted a number of times since 1991 (Tables 1 and 2), providing an opportunity to examine historical adjustments and recent, short-term changes in the Rio Chama system.

Various government agencies have obtained aerial photographs of the Rio Chama valley, primarily the U.S. Geological Survey (USGS), Bureau of Land Management (BLM), and Forest Service (USFS). This study includes six photograph sets covering the upstream study reach acquired in 1935, 1954, 1962, 1975, 1997, and 2005 (Table 1). The periods between these photo sets range from 8 years (1997-2005) to 22 years (1975-1997), with an average of 14 years. For the downstream reach, photographs utilized for the Swanson et al. (2008) UFDP report included sets obtained in 1935, 1954, 1963, 1975, 1997, and 2005. In

order to better constrain the timing of channel adjustment and possible associated hydrologic changes, additional photograph sets from 1969, 1985, and 1991 were included in this updated analysis (Table 2). Periods between the downstream photo sets ranged from 6 years (e.g., 1985-1991) to 19 years (1954-1935), with an average of 9 years. Major distortions associated with aircraft movement and abrupt changes in valley elevation (i.e., cliffs, arroyos, etc.) characterize all of the images, and the scale, contrast, and general quality of the photographs used for the upstream study reach are less than the photographs used for the downstream study reach (Swanson et al., 2008; this study) and the companion study on the Rio Grande through Albuquerque (Swanson et al., 2007; Swanson et al., 2010 (submitted)).

Photograph Set	Date Flown	Source	Scale (1:X)	Resolution (m)	Color	Quality	Discharge (m^3/s)
1935	*Aug-35*	EDAC	31680	1	B/W	Adequate	*2.4* (4.4)
1954	4/17/1954	EDAC	20000	1.6	B/W	Adequate	29.7
1962	9/10/1962	EDAC	20000	0.75	B/W	Adequate	1.0
1975	6/5/1975	EDAC	15840	0.55	B/W	Poor Contrast	64.3
1997	10/5/1997	RGIS	40000	1	B/W	Adequate	2.9
2005	7/28/2005	RGIS	40000	1	Color/IR	Good-shadows	2.0

Discharge-1935 and 1954 discharge from USGS RC at Parkview gage. All others from USGS RC near Lapuente gage
1935 Discharge - *avg daily* (max) over month of record
EDAC-Earth Data Analysis Center
RGIS-New Mexico Resource Geographic Information Systems

Table 1. Characteristics of the aerial photography sets covering the Rio Chama study area upstream of El Vado Dam. Photo quality is relatively poor compared to those used in the Rio Chama study reach located downstream of the dam and for the Rio Grande study reach flowing through Albuquerque.

Photograph Set	Date Flown	Source	Scale (1:X)	Resolution (m)	Color	Quality	Discharge (m^3/s)
1935	*Aug-35*	EDAC	31680	1.0	B/W	Adequate	*4.1* (11.6)
1951	5/28/1951	EDAC	15840	1.3	B/W	Adequate	15.6
1963	5/26/1963	EDAC	20000	0.6	B/W	Good	6.7
1969	5/19/1969	EDAC	12000	0.3	Color	Good	55.8
1975	6/3/1975	EDAC	15840	0.6	B/W	Good	18.2
1985	9/26/1985	EDAC	24000	0.7	Color	Good	2.9
1991	5/29/1991	EDAC	40000	1.0	Color	Good	37.9
1997	10/5/1997	RGIS	40000	1.0	B/W	Good	23.2
2005	7/28/05	RGIS	40000	1.0	Color/IR	Good-Shadows	9.9

Discharge - 1935 Discharge from USGS RC at Parkview gage, all others from USGS RC below El Vado gage
Discharge - *11* (111) - *avg daily* (max) over photograph month
EDAC - Earth Data Analysis Center
RGIS - New Mexico Resource Geographic Information System

Table 2. Characteristics of the aerial photography sets covering the Rio Chama study area *downstream* of El Vado Dam.

The 1997 and 2005 photograph sets for both study reaches are USGS Digital Orthophotos and are publicly available from the New Mexico Resource Geographic Information System (*rgis.unm.edu*). Although they match each other relatively well, they possess some localized distortion and in a few areas, alignment is off by as much as 50 m. In these areas, the 1997 photos were georectified with the other photographs. The 1935 through 1991 photographs were obtained as digitized prints (600 dpi) from the University of New Mexico Earth Data Analysis Center. These digital photos were then spatially referenced (georectified) to the 2005 orthophotographs using the image processing software provided with ESRI ArcInfo 9.2 (*www.esri.com*). This process was conducted at a set scale of 1:1500 by the primary author. The Delauney Triangulation Algorithm (*adjust*) in ArcInfo 9.2 was used to process local distortions remaining after initial rectification. Final RMSE values after coregistration were approximately 3.5 m for the downstream photographs and 5 m for the upstream photographs.

Channel digitization. Once georectified, the images were used to produce quantitative data characterizing the channel for each photographic year. This process involved air photo interpretation and on-screen digitization of channel banks and stable islands using a geographic information system (GIS; ArcInfo 9.2; *esri.com*). The banks and stable bars on the photographs were digitized at a set scale of 1:1,500, and to maintain consistency in the analysis, the primary author performed all of the digitization.

Obvious breaks in slope, water position, and the absence or presence of vegetation between subsequent photo sets allowed for relatively easy bank identification of channel margins along most of the study reaches; however, problems involving overhanging trees and shadows, resolution, and scale, as well as differences in photo shading and texture, were

common, especially on the poorer quality upstream photographs. Also, the upper Rio Chama channel is characterized by large, exposed bars on many of the photographs and the channel appears to have been much more active during the duration of the study period, especially in regards to avulsions across point bars and mid-channel bars/islands. These geomorphic factors often made distinguishing between active and inactive floodplain deposits extremely difficult. Relative bank, vegetation, scroll bar, and infrastructure positions on previous and subsequent photographs were referred to for help in determining bank line locations when necessary, but errors associated with photo interpretation for the upper study reach are high and may increase if compared to interpretations by others for the same reach.

As in the Rio Grande study (Swanson et al., 2007; 2010), vegetation played a major role in defining islands (stable bars) and "stabilized" floodplain in the Rio Chama study areas. Other researchers have used vegetation as the primary guide for channel delineation (e.g., Gurnell, 1998; Gilvear et al., 2000) and MEI's (2006) work on islands and bars showed that in-channel vegetation is not typically removed by higher flows under the present hydrology and channel configuration of the Rio Grande. Along the downstream Rio Chama study reach, this assumption was supported by the air photos, which showed established vegetation persisting from one photo set to another unless eroded away along cutbanks. Additionally, field observations suggest that the large 2009 flood release (>170 m^3/s; ~35 year recurrence interval) from El Vado Dam did not qualitatively alter the existing vegetated islands downstream. Therefore, bars with substantial new vegetation and little change from year to year were included as islands or new floodplain (no longer in the channel) for the Rio Chama study reaches. The upper Rio Chama, however, appears to be much more active over the study period, and vegetation does not always hold islands in place. Relying on vegetation

likely overestimates stable island area and underestimates overall active channel area, but the practice was continued to maintain consistency and for lack of a better method to differentiate seasonal, low flow deposition and more stable bars from aerial photographs.

Channel width measurement. Channel widths were measured at 100 ft (30 m) intervals by calculating the length of cross-section line segments lying within the channel and island areas in the GIS (*clip geoprocessing tool*). Cross-section lines used in the measurements were of equal length, spanned the entire meander belt and crossed the 1975 channel at 90° (± 7°). Due to the relatively large amount of channel activity (avulsions, erosion, deposition), many cross-sections along the study reaches spanned previous or subsequent channels at angles significantly different than 90 degrees. These cross-sections were removed from the analysis. To overcome this issue, average channel widths were also calculated by dividing the active channel area by the centerline length of the channel. The differences between average channel width measured at cross sections and measured by dividing area by length for the upstream reach Rio Chama study ranged between 0.5 (1935) and 1.7 (1975), with an average of 0.8 m.. For the downstream study reach, average widths measured by the two methods differed between 0.1 m (1963) and 2.2 m (1991), with an average decrease of 0.7 m (interpretations remain the same). Measurements were made directly within the GIS.

Finally, changes in channel width or area were calculated by subtracting data measured from the newer photographs from the measurement associated with the older photograph (positive values indicate widening; negative values indicate narrowing), and rates were determined by dividing the given magnitude of change by the time elapsed between photographs (days / 365.25 days/yr).

Erosion and depositional (stabilized) areas. In the UFDP Rio Grande aerial photograph study (Swanson et al., 2007), eroded floodplain area was hand-digitized from sequential photos. This method likely provided more accurate data, but was also time consuming and probably did not improve the error substantially. Managing these factors, as well as the greater amount of channel adjustment along the Rio Chama study reaches, required a more automated approach. For this study, the digitized channel for each photo set was laid over the previous digitized channel in the GIS. Areas occupied by the younger channel (water) but not by the older channel (land) were designated as "erosion" areas, and areas occupied by the older channel (water) and not by the younger channel (land) were labeled as "deposition" areas, or areas of newly developed floodplain (no longer part of the "active" channel). This "spatial overlay" was performed using the *union* tool in ArcToolbox in ArcInfo 9.2 and checked for accuracy on the air photos. Overall, the spatial overlay method required far less time to process, and as long as the banks were digitized carefully, the measurement error should not be much greater than with hand digitization; however, some control in the erosion delineation is lost.

Error Analysis

Aerial photos always contain distortions related to study area relief and pitch and yaw of the aircraft. Rectification reduces these distortions, but some warping inevitably remains. Additionally, operator error is associated with locating features and performing measurements. Photographic quality, resolution, color, scale, and other attributes affect operator errors, as do interpretive skill and the scale at which delineations are conducted. Most river scientists have ignored these measurement uncertainties or focused primarily on RMSE calculated during photograph co-registration. Exceptions include Mount et al. (2003),

Mount and Lewis (2005), Hughes et al. (2006), and Swanson et al. (2010 (submitted)); however, error estimates are still rarely considered in air photo measurements, hindering evaluation of the reliability of results (Downward et al., 1994).

Methods. For this study, channel width measurement errors were estimated using the Mount et al. (2003) method, which comprises two independent error estimates. The first estimate represents the operator error associated with bankline digitization. It was calculated by multiplying the pixel resolution (R) by the mean of the maximum number of pixels (p) between repeat left and right bankline delineations. Delineations of the channel margin were repeated at 10 sites located roughly equidistant along each study reach. The second error estimate represents distortions within the air photos. It was measured by finding the difference in distance between 20 floodplain locations that could be identified accurately on all photograph sets (e.g., fence posts, telephone poles, and building corners), and those same locations identified on the highest quality photo set, the 2005 images. The mean difference in distance between the points represented the image distortion error (θ) for each photo set. As the base for this error estimate, the distortion for the 2005 photographs should technically be 0 (no distortion), but for this study, the average of the error associated with the older photos was used instead. The total width error (E_w) was calculated as:

(3) $E_w = 2^{1/2} pR + 2\theta$. (Mount et al., 2003)

For error associated with polygon area (channel, island, erosion), two assumptions were made: (1) the length of the channel, vegetated island, or eroding bank segment was constant (no error) and (2) the polygons representing these areas are rectangular. Therefore, the measurement error associated with area equaled the length of the polygon multiplied by the error in width.

Error associated with differences between photograph sets, largely for propagation of error in estimating rates of change, were calculated following procedures outlined in Mount et al. (2003) and Taylor (1982):

$$(4)\ E_{dif} = (E_{photo1}^2 + E_{photo2}^2)^{1/2}$$

where E_{dif} is the error of uncertainty associated with the comparison to subsequent photos, E_{photo1} is the measurement error associated with the first image set and E_{photo2} is the measurement error associated with the comparison photograph set. To find the uncertainty in estimates of channel change rate, E_{dif} was divided by the time elapsed between photograph dates, as per Mount et al., 2003).

Error results. The error in average channel width measurements for the study reach upstream of El Vado Dam ranged from ±8.5 m for the 1996 photographs to ±13.1 m for the 1935 photographs (Table 3). Average measurement error for channel width is ±10.1 m, which is 32% of the average width and 91% of the narrowest width on the 2005 photographs. For the downstream reach, error ranged from ±5.1m for the 1969 photographs to ±11.8 for the 1935 photos (Table 4). The average error, ±7.1 m, is 18% of the average width and 85% of the narrowest width of the 2005 channel.

Uncertainty in channel area measurements along the upstream study reach ranged from ±0.15 to ±0.23 km^2 for the 1997 and 1935 image sets, respectively (Table 3), and relative errors ranged from 20% (1962) to 29% (2005), which are similar to relative width errors. Downstream, channel area error was between ±0.08 and ±0.18 km^2 (12 and 20%) for 1969 and 1975, respectfully (Table 4). Relative uncertainty in island area varied from 23-40% for the upstream reach (Table 3) and 12-19% for the downstream reach (Table 4).

Finally, areas of erosion and deposition possessed relative errors between 54% percent and 115% along the upstream reach, and 90 to 280% downstream.

Photo Year	Location Error (m)	Residual Error (m)	Width Error (m)	Sequential Error (m)	Channel Area Error (km^2)	Island Area Error (km^2)	Width Error (%)	Sequential Error (%)	Channel Error (%)	Island Error (%)
1935	5.7	3.7	13.1	17.1	0.23	0.043	26%	597%	26%	41%
1954	4.5	3.3	11.1	14.1	0.19	0.062	24%	416%	23%	31%
1962	3.2	2.8	8.7	12.5	0.15	0.057	20%	1086%	20%	25%
1975	3.1	2.9	8.9	12.3	0.15	0.042	20%	105%	20%	23%
1997	4.2	2.1	8.5	12.4	0.15	0.022	25%	542%	25%	32%
2005	2.8	3.1	9.0	12.4	0.16	0.022	28%	542%	29%	29%
Mean	*3.9*	*3.0*	*10.1*	*13.7*	*0.17*	*0.041*	*24%*	*549%*	*24%*	*30%*

Table 3. Error associated with channel parameter measurements from aerial photographs, Rio Chama, upstream of El Vado Dam, New Mexico, 1935-2005. Location error = pR, Residual Error = θ, and Sequential Diff = error in the difference between sequential photograph sets.

Photo Year	Location Error (m)	Residual Error (m)	Width Error (m)	Sequential Error (m)	Channel Area Error (km^2)	Island Area Error (km^2)	Width Error (%)	Sequential Error (%)	Channel Error (%)	Island Error (%)
1935	4.2	3.8	11.8	14.0	0.18	0.028	20%	191%	20%	16%
1951	3.7	1.9	7.5	10.4	0.11	0.025	15%	168%	15%	16%
1963	3.2	2.0	7.2	9.1	0.11	0.026	16%	3546%	16%	15%
1969	2.1	1.7	5.5	9.0	0.08	0.017	12%	592%	12%	13%
1975	3.1	2.0	7.1	9.7	0.11	0.024	16%	379%	15%	19%
1985	3.2	1.7	6.6	8.9	0.10	0.023	16%	1734%	15%	16%
1991	2.8	1.6	6.0	8.4	0.09	0.019	14%	252%	14%	14%
1997	2.8	1.5	5.8	8.7	0.09	0.016	15%	713%	14%	12%
2005	2.8	1.8	6.4	---	0.10	0.018	17%	---	16%	14%
Mean	*3.1*	*2.0*	*7.1*	*9.8*	*0.11*	*0.022*	*16%*	*947%*	*15%*	*15%*

Table 4. Error associated with channel parameter measurements from aerial photographs, Rio Chama, downstream of El Vado Dam, New Mexico, 1935-2005. Location error = pR, Residual Error = θ, and Sequential Diff = error in the difference between sequential photograph sets.

Overall, the error analysis for change detection revealed few significant differences in average channel width and rates of change between photographs exceeded the average measurement error during the study period. However, changes in width between subsequent image sets were *statistically* significant (paired t-test, $\alpha = 0.05$), except for the 1962-1975 upstream measurements and 1963-1969 and 1969-1975 downstream measurements (downstream exceptions were statistically significant at $\alpha = 0.1$).

Discussion of error results. Using similar methods, width errors estimated by Mount et al. (2003) for the River Trannon ranged from ±1.4 to 5.4 m, clearly lower than in this study. This difference likely stems in significant part from different processes in these contrasting fluvial systems. The River Trannon is widening due to an influx of sediment due to land use change (Mount et al., 2003), whereas the Rio Chama is narrowing (this study). Additionally, the River Trannon is primarily a single-thread channel, whereas the Rio Chama has wandering to braided sections with large, unvegetated bars exposed at low flows. Eroding banks in meandering systems can usually be accurately identified by locating abrupt breaks between the channel and floodplain or terrace surfaces. In contrast, rivers tend to decrease width by depositing sediment on bars and along channel margins. Determining when and where sediment accumulation and plant cover has formed a new stable floodplain surface is more difficult. In this study, photo shading and texture were sometimes difficult to interpret in this respect, especially on poorer quality photographs. Large increments of narrowing are associated with abandonment of side channels or avulsions, but determining just when a side channel is no longer active is also problematic. In addition, differences in discharge between photographs also complicated bank line placement. Along steep, eroding banks, the flow margin may not change much as discharge changes, but even small discharge changes on shallow bar slopes may inundate or expose large areas of channel floor.

Estimates of uncertainty in the width measurements along the Rio Grande through Albuquerque (1985-2008) range between ±23m and ±9 m, with an average of ±9.5 m (Swanson et al., 2010 (submitted)). These estimates compare well with the downstream Rio Chama width error estimates, and are lower than the estimates for the upstream Rio Chama reach. This difference is likely due to more accurate photographic processing in the case of

the Rio Grande and downstream Rio Chama reaches, and overall photographic quality and scale for all study areas. The *ortho*rectification process used for the Rio Grande photographs, which uses difficult to attain flight path data and digital elevation models, is more accurate than using the soft ground control points (i.e., shrubs) in the general *geo*rectification process used along the Rio Chama (Mount reference). Distortions, poor contrast, shadows, and other issues were also much greater for the aerial photographs used for the Rio Chama upstream of El Vado than those used in the previous investigations (Swanson et al., 2007; 2008, 2010), affecting both the georectification and delineation processes.

Relative width error also increases from an average of 6% along the Rio Grande study reach, to 16% for the downstream Rio Chama site, to 24% for the upstream Rio Chama site. The relative error is the ratio of the error linked to the channel width and the associated average channel width measurement. Therefore, reduced channel size and increased measurement errors from downstream to upstream accounts for most of the observed shift in relative error. Increases in relative error with decreasing channel size suggests that some channels are too narrow for air photo analysis to be practical, especially if relying on older, black and white photos not necessarily intended for this use.

Relative uncertainty associated with measurements of island area along the Rio Grande (mean = 15%) were also similar to those along the downstream Rio Chama study reach (mean = 16%). In contrast, relative error for the upstream Rio Chama reach was elevated (mean = 30%), largely reflecting the larger width error values. Finally, relative errors associated with channel change (erosion and deposition) were actually lower for the Rio Chama study reaches than the Rio Grande, which had erosion errors ranging from 221% to 1692% with an average of 762%. This difference is largely a factor of the time elapsed

between subsequent photo sets and the amount of change along the river (Mount et al., 2003; Swanson et al., 2010). Image sets used in the Rio Grande through Albuquerque, NM, study (1985-2008; Swanson et al., 2007; 2010) were acquired within 3 years of each other, often less, and the largest gap was 7 years. During that time, there was very little erosion within the study reach. The active erosion occurred along relatively long cutbanks, so when treated as a polygon, the error estimate (length multiplied by width error) was often larger than the erosion itself, especially in years with little to no erosion. In comparison, the Rio Chama channel is much more active (avulsions, bank and bar scour, etc), especially in the upstream study reach, and photographs were acquired 8 years apart for the upstream reach and 6 years apart for the downstream reach. The lowest relative erosion error is associated with the 1975-1997 measurements along the upstream Rio Chama, which includes major channel avulsions and a 22 year time span between photographs.

Finally, the error method used in this study produces an average maximum error bound, but actual error is likely much lower. Between the two most similar data sets, 1997 and 2005, 75% of the upstream width measurements are within 3 m and 63% are within 1 m. Along the downstream reach, 85% of the width measurements are within 1 m. Air photo assessment at random sites where subsequent width differences were greater than 3 m revealed observable changes in channel form (e.g., island expansion, anabranch abandonment, avulsions, etc.) at these locations. Additionally, the channel delineations were redone for the downstream Rio Chama channel with the addition of the new, better quality photographs, and area changes were within 5% over the shortened study reach. Island area was the exception, where errors were as high as 47% due to a processing error where bank-attached islands were included in the total area measurements. Compared to the corrected

data, the earlier island area measurements were within 8% of the final data. A method based more on probability distributions of error in repeat measurements would likely provide more realistic error estimates, but is beyond the scope of this report. Further development of methods is needed for estimating uncertainty in airphoto-based channel change analyses, but the methods herein provides a reasonable first approximation of maximum error bounds.

Although changes in average channel width between subsequent photo periods on the Rio Grande and the Rio Chama do not exceed measurement errors, real change is qualitatively evident on the air photos. Most of these adjustments are concentrated in a few subreaches where width differences are significantly greater than the error, often by a factor of two or more. Average changes are often insignificant because little planform adjustment has occurred along most of the study reach length. Based on these investigations (Swanson et al., 2007; 2010; this study), analyzing photographs over shorter time intervals is probably unnecessary and inappropriate for a generalized assessment of channel change, but is still important in identifying local areas where rapid change is occurring.

Channel Adjustment and Hydrology, Rio Chama, 1935-2005

Hydrology and discharge data. There are four USGS stream gages located along the Rio Chama (Figure 1). Flow data for the Rio Chama study reach upstream of El Vado Dam were obtained from the Rio Chama near Park View (PVW) gage (08283500; waterdata.usgs.gov) and the Rio Chama at La Puente (LPT) gage (08284100; waterdata.usgs.gov). At PVW, the annual peak discharge record spans from 1913 to 1915 and from 1925 through 1955, with continuous daily data from 1930 to 1955. The LPT gage replaced the PVW gage in 1955 and includes continuous data up to the present. The average daily flow at both the PVW and LPT gages is 9 m^3/s, and average peak flows are 123 m^3/s at

PVW and 124 m^3/s at LPT. These average peak discharges have a recurrence interval of about 3 years and the 2 year flood is approximately 110 m^3/s. The ten biggest discharges all exceed 200 m^3/s, with the largest ranging from 270 to 317 m^3/s (1926, 1973, 1979, 1984, 1985). Minimum peak flows are generally between 15 m^3/s and 30 m^3/s.

Figure 2 and Table 5 depict the variability in discharge at PVW and LPT over the 20th century, including the study period. Prior to the earliest photo set (1935), average peak flows were similar to the 1935-1954 photo period, with a few large estimated peak (>175 m^3/s) discharges between 1903 and 1912, as well as 1920 and 1921. Peak flows decrease over the 1935-1954 period, and from 1950 through 1956, a drought period in New Mexico, only one flow exceeds the two-year flood. Variability characterizes the annual maximum discharges between 1954 and 1975. Large peaks occur in 1957, 1965, 1968, and 1973, but two or three years of low peaks (<80 m^3/s) in the mid 1960 and early 1970s separate these higher flows. The average peak flows decrease from approximately 130 m^3/s during the 1935-1954 period to 110 m^3/s over the following two photograph periods (1954-1962; 1962-1975). The average peak flow between the 1975 and 1997 photo sets increases to 148 m^3/s, driven by a very wet interval between 1979 and 1985. Five of the top eight flows documented at the gage stations occur during this episode, which was followed by three years of low peak flows, and then a return to near-average flows by the mid-1990s. Finally, the 1997-2005 period was characterized by a drought affecting much of the region, and the average peak discharge fell to 88 m^3/s. Over this span, five of nine flows fall below 80 m^3/s, and eight fall below 100 m^3/s. The peak flow in 2002 was only 13 m^3/s, the lowest on record.

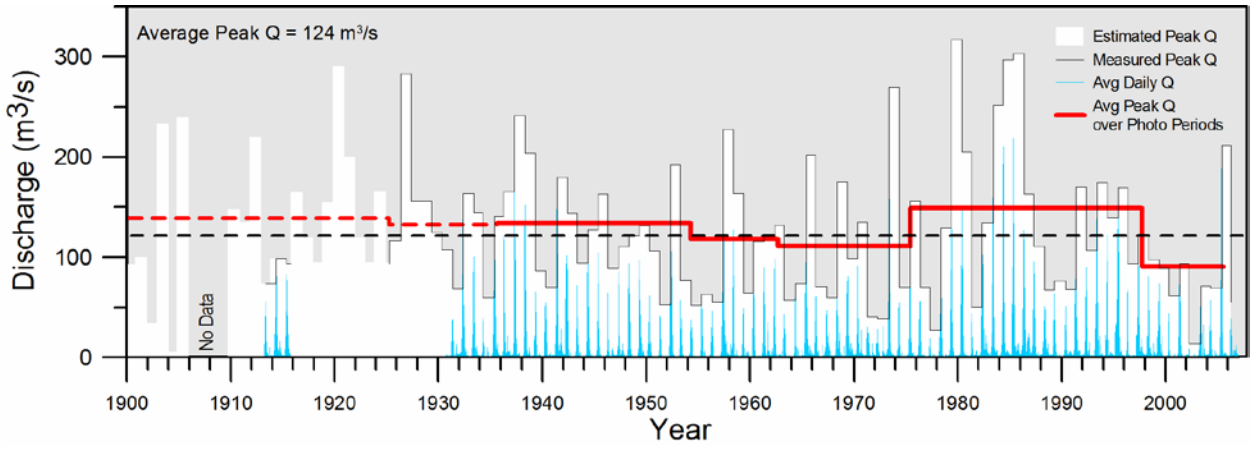

Figure 2. Water discharge for the Rio Chama upstream of El Vado Dam, New Mexico, 1900-2005. Histogram represents annual peak discharges and blue lines represent average daily discharge measured at the USGS Rio Chama near Park View stream flow gage (site 08283500; *waterdata.usgs.gov/usa/nwis/uv?site_no=08286500*) from 1925 to 1954 and at the Rio Chama at La Puente gage (site 08283500; *waterdata.usgs.gov/usa/nwis/uv?site_no=08284100*) from 1954 through 2005. Pre-1925 data were estimated by correlation with data from the Rio Grande at Otowi Bridge gage (site 08313000; *waterdata.usgs.gov/nwis/uv?08313000).* The tread of the red line step plot represents average peak flows over photo periods, and the riser represents breaks between those periods (dashed for estimated data and solid for measured data). Dashed black line is the average flow over the study period (1935-2005). Discharge is variable over the study period with 1 to 5 year periods of low flows followed by 1 to 2 years with higher than average floods. Drought periods include 1950-1957 and late 1996-2005, and prolonged periods of high flows include 1932-1938, 1978-198, and 1992-1996.

Photo Period	Avg Peak Q	Avg Daily Q	St Dev-Peak Q	St Dev - Daily Q	Max Peak Q	MinDaily Q
1900-1925	*139*	*3*	*72*	*12*	*291*	*0*
1925-1935	133	3	63	13	283	0
1935-1954	131	9	52	20	242	0
1954-1962	108	9	63	19	228	0
1962-1975	111	8	71	17	270	0
1975-1997	148	12	84	23	317	0
1997-2005	88	8	57	17	212	0

Q - Discharge (m^3/s)

1900-1925 Q estimated from Q data at USGS Rio Grande at Otowi Bridge stream gage (site 08313000) by correlation (R^2=0.78).

Table 5. Peak and daily discharge statistics for photograph periods, Rio Chama, *upstream* of El Vado Dam, New Mexico, 1900-2005.

Two USGS stream gages bracket the Rio Chama study reach located downstream of El Vado Dam (Figure 1). At the Rio Chama below El Vado Dam (EVD) gage (08285500; *waterdata.usgs.gov*), the record spans from 1914 through the present, with continuous daily data from 1935. The Rio Chama above Abiquiu Reservoir (AQR) gage (08286500; *waterdata.usgs.gov*) includes data from 1961 through the present. Over the study period, average daily flows at the EVD and AQR gages are 11 and 14 m^3/s, respectively. Average peak flows are 75 m^3/s at EVD and 96 m^3/s at AQR, with a maximum flood of 255 m^3/s occurring in 1920 (pre-dam, EVD). The largest peak flows range from 160 m^3/s to 190 m^3/s (1941, 1973, 1984, 1985), and minimum peak flows are generally between 25 m^3/s and 35 m^3/s. The hydrology in the downstream study reach is dominated by spring snowmelt and late summer/early fall convective storms. Peak flows at EVD are primarily associated with snowmelt, but the influence of summer storms is greater at AQR, primarily due to monsoon-related floods in the Rio Nutrias, Rio Cebolla, and Rio Gallinas tributaries. This monsoonal affect is indicated by the greater number of maximum annual flows occurring later than June at the AQR site (17) as opposed to the EVD site (4) since the AQR gage came online (1961, n=44). These summer floods are often of high magnitude, but are characterized by relatively short durations. Little evidence suggests summer rainfall is a major contributor to stream flow at the LPT and PVW gages along the upstream study reach, which is dominated by spring snowmelt runoff.

Historical flow data over the photo periods for the downstream Rio Chama study reach are presented in Figure 3 and Table 6. Prior to the dam, the river below El Vado likely had peak flows similar to those documented at PVW, with average peak discharge between 130 and 140 m^3/s, or greater. Over the 1935-1951 photo period, peak discharges are above

average for the post-dam period, especially in the early 1940s, but they diminish in the second half of the interval, resulting in an average peak flow of 76 m^3/s. Between 1951 and 1963, the study area is in a prolonged drought, with most peak flows falling below 40 m^3/s, and the average peak flow reaching only 53 m^3/s. Low flows in the river continue over into the 1963-1969 period, but peak flows return to near-average and moderate peak flows persist through 1975. The second largest peak flow on record, 170 m^3/s, occurs in 1973. The wettest photo period is from 1975 to 1985. It includes numerous peak flows at or above 120 m^3/s, including the largest discharge in the study period, 187 m^3/s (1985). The 1991-1997 photo period is a transition interval. It begins with large peak discharges, but ends as New Mexico begins another drought, which persists through the final photo period (1997-2005).

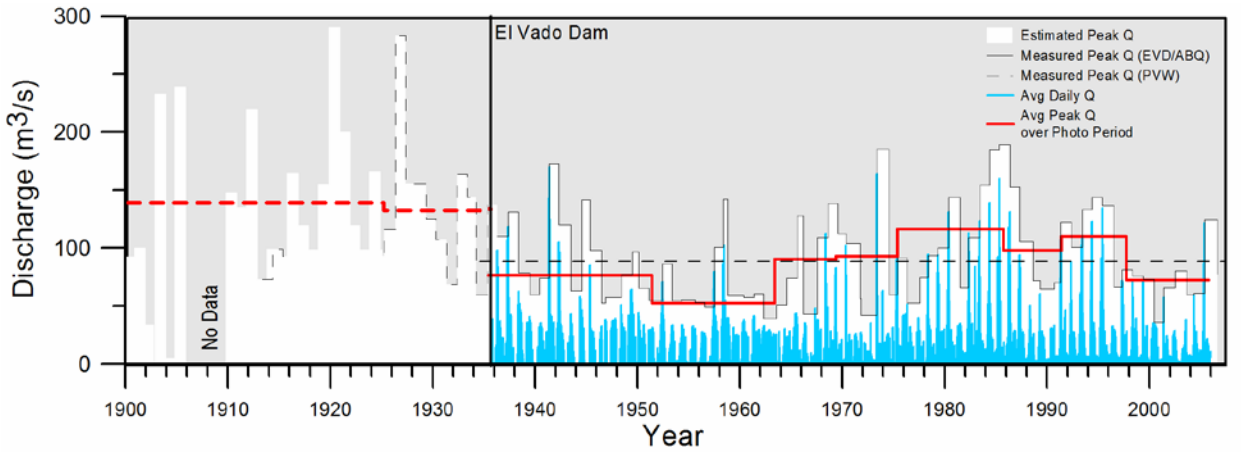

Figure 3. Water discharge for the Rio Chama downstream of El Vado Dam, New Mexico, 1900-2005. Histogram represents annual peak discharges and blue lines represent average daily discharge measured at the USGS Rio Chama upstream of Abiquiu Reservoir stream gage from 1962 to 2005, and estimated by correlation with data from the Rio Chama downstream of El Vado Reservoir gage (R^2=0.81) from 1935 to 1962. 1900 to 1935 data is the same as in Figure 2. The tread of the red line step plot represents average peak flows over photo periods, and the riser represents breaks between those periods (dashed for estimated data and solid for measured data). Dashed black line is the average flow over the study period (1935-2005). Discharge is less variable than upstream over the study period (1935-2005). Periods of prolonged low peak discharge include 1946-1966 and late 1996-2005, and prolonged periods of high flows include 1978-1986, and 1991-1996. Average peak flows decreased after completion of El Vado Dam (1935).

Photo Period	Avg Peak Q	Avg Daily Q	St Dev-Peak Q	St Dev - Daily Q	Max Peak Q	MinDaily Q
1935-1951	*76*	*13*	*41*	*20*	*170*	*0*
1951-1963	*53*	*10*	*33*	*14*	*135*	*0*
1963-1969	91	10	40	14	138	0
1969-1975	93	10	48	17	185	0
1975-1985	117	16	49	24	189	1
1985-1991	98	14	35	18	153	2
1991-1997	110	17	32	20	143	1
1997-2005	73	11	24	12	125	0

Q - Discharge (m^3/s)
1935-1961 Q measurements from EVD gage

Table 6. Peak and daily discharge statistics for photograph periods, Rio Chama, *downstream* of El Vado Dam, New Mexico, 1935-2005.

The hydrographs for the Rio Chama study reaches possess similar shapes, indicating the timing of large flows, droughts, and wet periods are also similar. They are somewhat comparable to the flows in the Rio Grande study reach as well, which also include high peak flows in the early 1940s and 1980s and low peaks in the late 1950s and the late 1990s into the 2000s (Swanson et al., 2007; 2010 (submitted)). The main difference between the Rio Chama data sets is flood magnitude, which is primarily due to flow regulation at El Vado Dam. The dam was constructed in 1935 by the Middle Rio Grande Conservancy District to manage water for flood relief and irrigation in the Rio Grande Valley. Analyses of the discharge records at all four gage sites used in this study reveal that management of El Vado Dam decreases peak flows (Figure 5). The 2 year flood recurrence interval for the upstream gages (PVW and LPT) is approximately 110 m^3/s and the 5 year flood is approximately 200 m^3/s. At ABQ, the 2 year flood recurrence interval is approximately 85 m^3/s and the 5 year flood is 120 m^3/s, reductions of 23% and 45% when compared to the upstream gages, respectfully. Additionally, the dam decreases the suspended sediment load (Langman and Anderholm, 2004), and likely catches most of the sand-sized and larger sediment coming

from the upper basin. This change in sediment and water flux into the system, should in turn, impact the channel geometry, substrate texture, planform, or some combination of the above in the downstream study reach (Lane, 1955; Williams and Wolman, 1984). Additionally, it seems likely that El Vado Dam operations also played a role in the reduction in peak flow magnitude experienced in Albuquerque after 1935. Differences between the Chama gage data and the Rio Grande gage data are due to a variety of factors, including multiple upstream dams and a larger, more varied watershed associated with the Rio Grande.

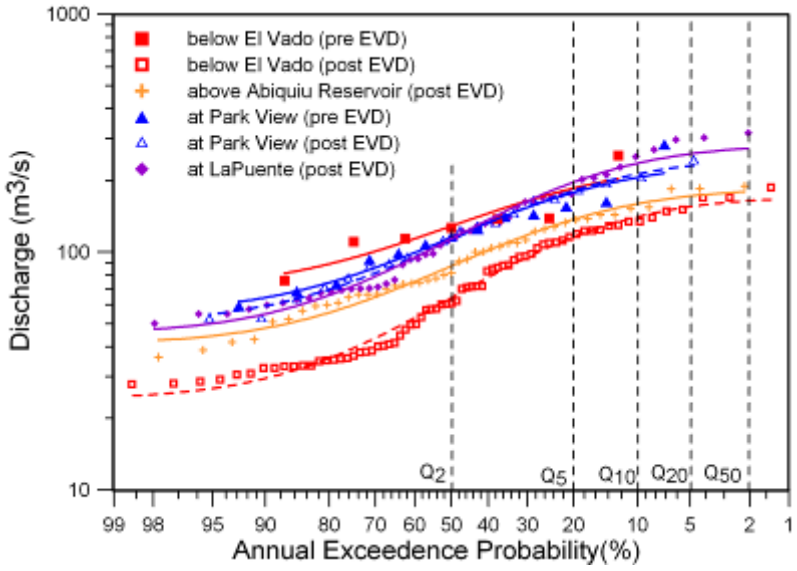

Figure 4. Exceedence probabilities for peak flows measured at stream gages in the Rio Chama study area (see Fig. 1 for locations). The post-dam flows below El Vado Dam (orange-AQR, open red-EVD) are lower than the pre-dam EVD peak flows and the upstream gages, both pre-dam and post-dam. Q_2 – 2-year recurrence interval flood, Q_5 – five-year recurrence interval flood, etc.

Channel adjustment. Analysis of the sequential air photos shows that channel width upstream of El Vado Dam decreased between 1935 and 2005, from an average channel width of 51 m (±13 m) to 31 m (± 9 m), a reduction of 38% (Table 7 and Figure 5). Over that time, active channel area decreased from 0.87 km^2 (± 0.23 km^2) to 0.56 km^2 (±0.16 km^2).

Downstream of El Vado Dam, channel widths also decrease over the study period (Table 8; Figure 6). The average width over the downstream study reach decreased from 58 m (± 12 m) in 1935 to 38 m (± 6 m) in 2005, a reduction of 32%. Channel area was reduced from 0.88 km^2 (± 0.18 km^2) to 0.63 km^2 (± 0.10 km^2) over the same interval in this reach. Additionally, standard deviations associated with channel width measurements also decrease for both study reaches, indicating diminished channel heterogeneity (Tables 7 and 8).

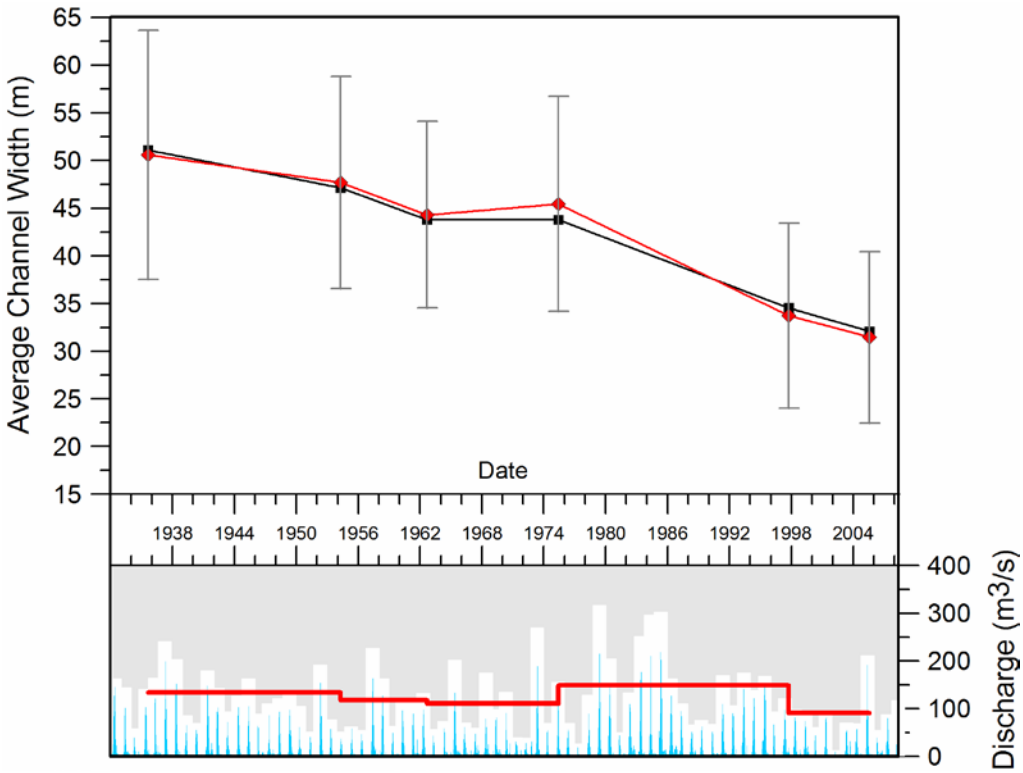

Figure 5. Change in average channel width along the Rio Chama upstream of El Vado Dam, New Mexico, 1935-2005 compared to the hydrograph for the same reach (Figure 2). Measurement error, as represented by the error bars, is estimated using the method of Mount et al. (2003). Red line is the average width measured at 574 cross sections along the study reach; black line is the average width measured by dividing channel area by the length of the study reach for each photograph set. The average channel widths decrease over the study period, especially after 1975, but changes from photograph year to photograph year are within the measurement error.

Photo Year	Average Width (m)	Stand Dev (m)	% change from 1935	Maximum Width (m)	Minimum Width (m)	Channel Area (km^2)	Island Area (km^2)	Erosion Area (km^2)	Stabilized Area (km^2)
1935	51	26	---	141	14	0.87	0.11	---	---
1951	48	22	6%	150	14	0.83	0.20	0.27	0.32
1962	44	19	12%	159	15	0.77	0.22	0.14	0.20
1975	45	21	10%	140	15	0.79	0.18	0.14	0.12
1997	34	14	33%	113	10	0.60	0.07	0.15	0.34
2005	31	12	38%	110	11	0.56	0.08	0.06	0.10
Mean	*42*	*19*	---	*136*	*13*	*0.74*	*0.14*	*0.15*	*0.22*

Table 7. Channel planform parameters measured from aerial photograph sets, Rio Chama *upstream* of El Vado Dam, New Mexico, 1935-2008.

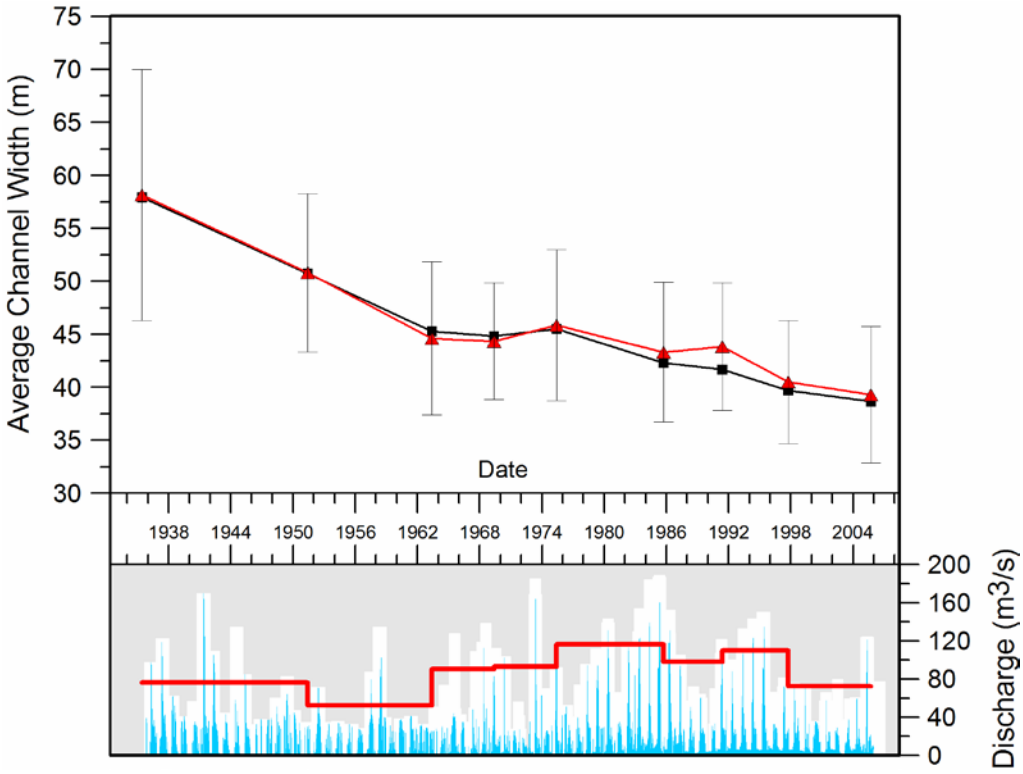

Figure 6. Change in average channel width along the Rio Chama downstream of El Vado Dam, New Mexico, 1935-2005 compared to the hydrograph for the same reach (Figure 2). Measurement error, as represented by the error bars, is estimated using the method of Mount et al. (2003). Red line is the average width measured at 440 cross sections along the study reach; black line is the average width measured by dividing channel area by the length of the study reach for each photograph set. The average channel widths decrease over the study period, especially prior to 1962, but changes from photograph year to photograph year are within the measurement error.

Photo Year	Average Width (m)	Stand Dev (m)	% change from 1935	Maximum Width (m)	Minimum Width (m)	Channel Area (km^2)	Island Area (km^2)	Erosion Area (km^2)	Stabilized Area (km^2)
1935	58	31	---	218	17	0.88	0.18	---	---
1951	51	24	13%	137	17	0.77	0.16	0.05	0.18
1963	45	18	23%	144	16	0.68	0.17	0.03	0.11
1969	44	18	24%	121	16	0.68	0.13	0.04	0.04
1975	46	19	21%	124	15	0.71	0.13	0.08	0.05
1985	43	14	26%	96	13	0.68	0.14	0.04	0.08
1991	44	13	25%	86	13	0.67	0.14	0.02	0.03
1997	41	12	30%	83	13	0.64	0.13	0.02	0.05
2005	39	11	32%	79	13	0.63	0.12	0.02	0.03
Mean	*46*	*18*	---	*121*	*15*	*0.70*	*0.14*	*0.04*	*0.07*

Table 8. Channel planform parameters measured from aerial photograph sets, Rio Chama *downstream* of El Vado Dam, New Mexico, 1935-2008.

Most of the change in width along both study reaches is associated with bar stabilization and side-channel (anabranch) abandonment, and an overall decrease in channel activity, such as bar movement, avulsions, and erosion, as well as the concomitant establishment of vegetation in these areas. Figure 7 depicts channel change between photo sets for a section of the upstream study reach below the Highway 95 bridge. The 1935 photographs display a relatively wide channel with large vegetated and unvegetated bars, often covering 65% of the channel planform width. Photographic evidence (e.g., abandoned channels, channel patterns in the floodplain, etc) suggests that the channel was relatively active prior to 1935. Between 1935 and 1954, channel avulsions occurred approximately 500 m south of the bridge and at the downstream end of the section, possibly in response to the 1942 and 1943 floods. Islands also grew and coalesced over this time period, and some erosion occurred around these stabilized bars. By 1963, some of the islands had attached to the banks and become part of the floodplain, a downstream anabranch were abandoned, and new islands were beginning to form. The trends continued through 2005, although the 1973 flood likely removed some of the established island area (upstream segment, Figure 6). In

2005, the channel exhibited a more single-thread planform pattern, appeared less active, and exhibited far fewer islands and bars (Figure 7).

A similar pattern of channel adjustment occurred along the downstream study reach, as shown in the example section adjacent to the Oaks Campground, one of the more active subreaches (Figure 8). The 1935 photos show an alternating narrow and wide channel, with bars and islands exposed in the wider subreaches. Over time, islands develop and grow together, side-channels are abandoned, and the main channel exhibits a more meandering, single-channel pattern (Figure 8).

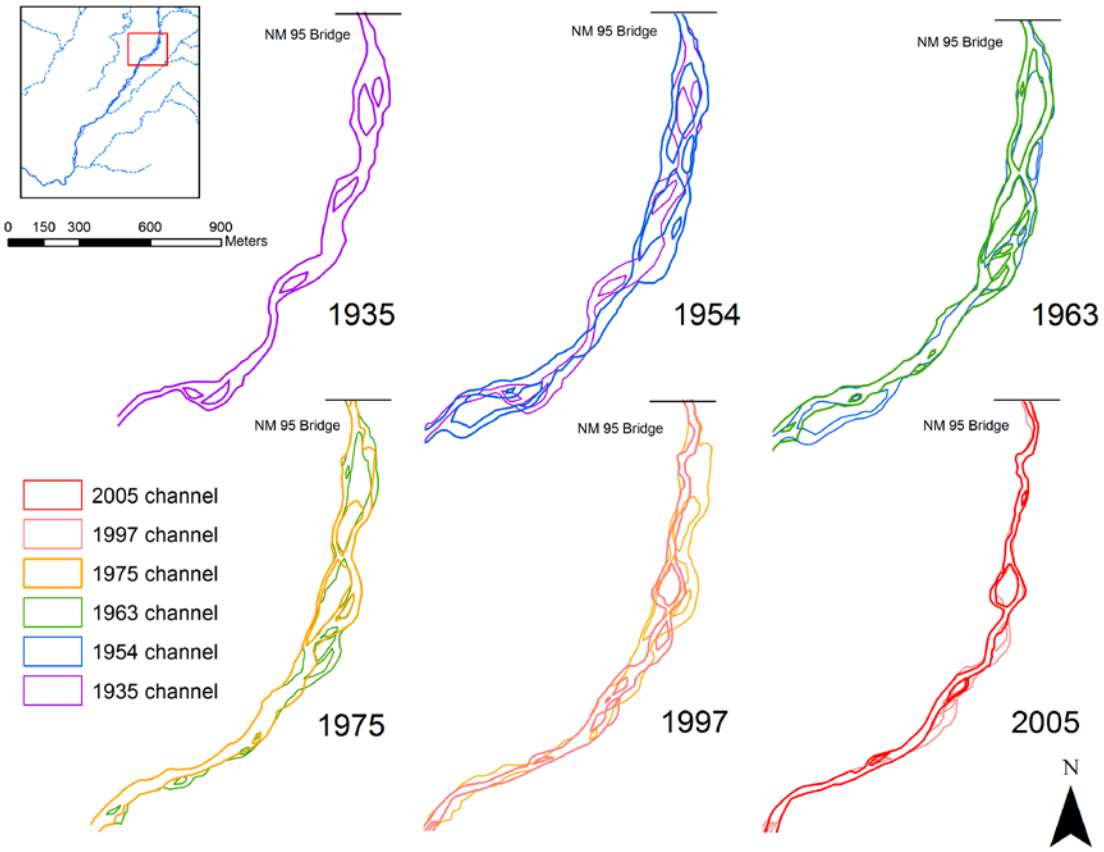

Figure 7. Channel adjustments via avulsions, anabranch abandonment, and vegetated island expansion downstream of the New Mexico State Road 95, Rio Chama upstream of El Vado Dam, 1935-2005. Insert map shows location within the study reach. Avulsions shifted channel positions and formed new side channels between 1935 and 1954, but islands formed, expanded, and coalesced throughout the study period. Channel activity (i.e., major changes in

thalweg position) decreased by 1963 and the rate of bar formation and island expansion outpaced the rate of erosion, with the result of channel narrowing and a simpler, single-thread channel.

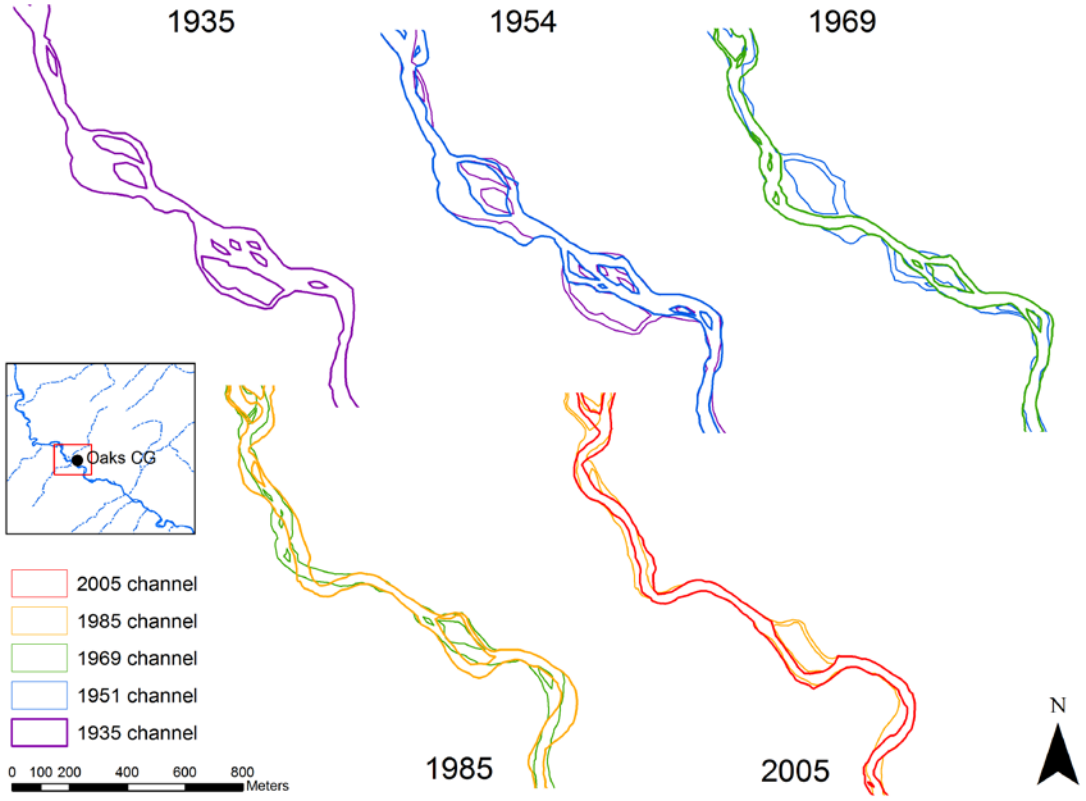

Figure 8. Channel adjustments via anabranch abandonment, and vegetated island expansion up and downstream of the National Forest Service Oaks Campground (CG), Rio Chama downstream of El Vado Dam, 1935-2005. Insert map shows location within the study reach. Vegetated islands formed, expanded, and coalesced throughout the study period. The expanding islands forced flow against banks, causing limited bank erosion However, anabranch abandonment and island expansion outpaced the rate of erosion, with the result of channel narrowing and a simpler, single-thread channel.

Because of the islands' propensity to attach to banks during narrowing periods, island area along both study reaches declines over the study period (once attached they are no longer included in the island area data). Along the upstream reach, planform island area doubled from 0.11 km^2 (± 0.04 km^2) to 0.22 km^2 (± 0.06 km^2) in 1962, and then decreased to

0.08 km^2 (± 0.02 km^2; Table 7; Figure 9). When compared to total channel area (channel and islands; Figure 9), the change in islands upstream of the dam indicates that 1935 to 1963 was a period of island expansion or production due to avulsions, with little change in total channel area. From 1963 to 1975, island area decreased while channel area remained relatively unchanged, suggesting island and bank erosion outpaced island expansion over the interval. Finally, after 1975, there was a large drop in both channel and island area corresponding to a period of bank attachment and anabranch abandonment with relative little new bar stabilization (Figure 9).

Along the downstream Rio Chama study reach, island area decreased from 0.18 km^2 (±0.03 km^2) to 0.12 km^2 (± 0.02 km^2) over the whole study period (Table 8; Figure 10). Figure 10 shows decreasing total channel area values and relatively stable island areas between 1935 and 1963. During this interval, islands establishment and growth roughly equals loss of channel area due to floodplain attachment and point bar stabilization. Between 1969 and 1975, which includes the 1973 flood, channel area increases and island area decreases, indicating a period where erosion is greater than island establishment. This interval is followed by island growth with little change in total channel area. Finally, the 1961-1969 and 1985-2005 periods are characterized by decreases in island and channel area, where established islands are attaching to the banks and little bar stabilization and island expansion occurs (Figure 10). Unlike the Rio Grande and upstream Rio Chama study reaches, a few islands in the downstream study reach have changed very little over time. They are usually located in subreaches characterized by cobble/boulder beds, multiple upstream debris-flow fans, and relatively steep slopes, such as below Arroyo de la Presa and an unnamed tributary on the opposing bank, and below Ojitos and Fuertes Arroyos.

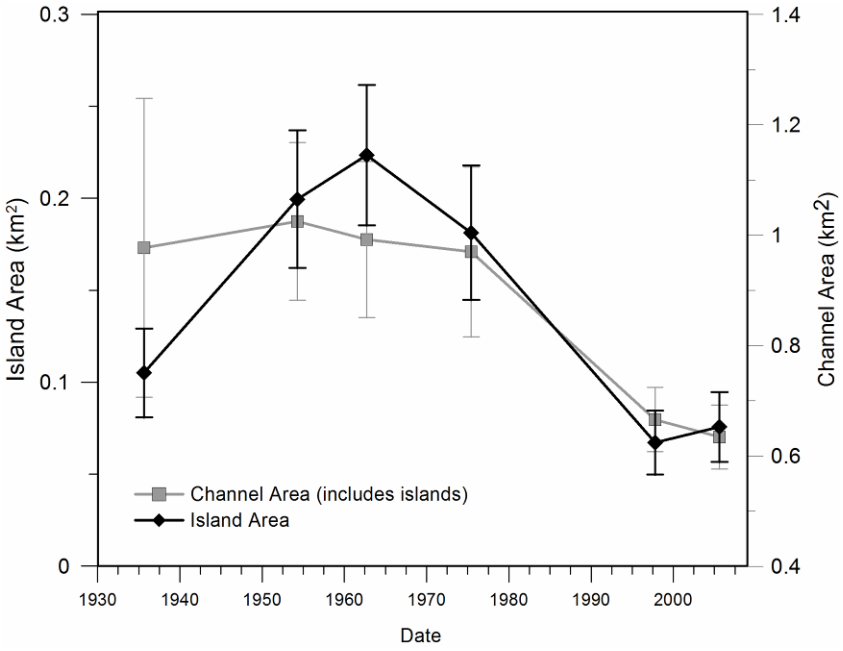

Figure 9. Change in vegetated island area and channel area along the Rio Chama upstream of El Vado Dam, 1935-2005. Vegetated island area increased through 1963 as islands formed and coalesced and then decreased as island attached to banks faster than new islands formed. Error bars represent measurement error estimated using method of Mount et al. (2003).

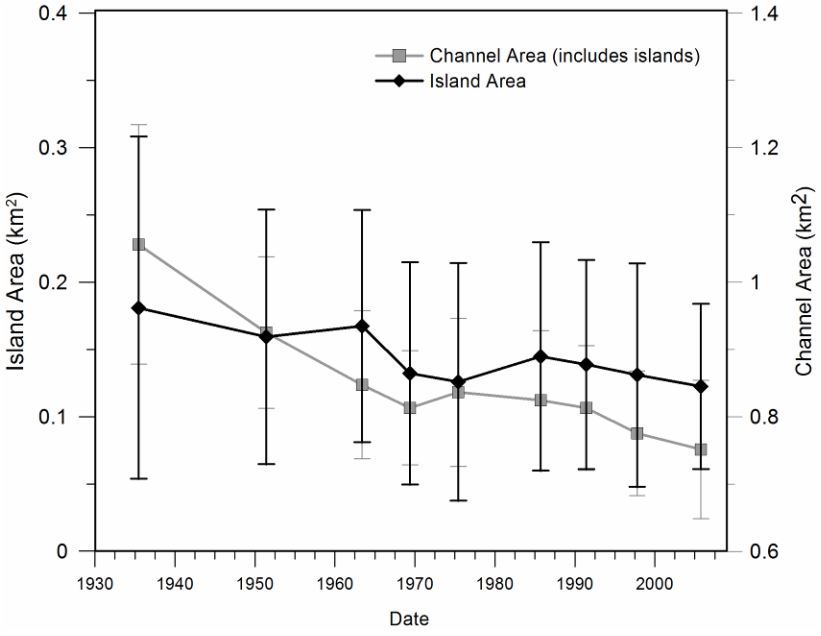

Figure 10. Change in vegetated island area and channel area along the Rio Chama downstream of El Vado Dam, 1935-2005. Vegetated island area decreased throughout the study period, as island attached to banks faster than new islands formed. Error bars represent measurement error estimated using method of Mount et al. (2003).

Semi-arid and arid rivers in the United States have experienced similar processes of narrowing over the last century. Along the Platte River, Nebraska, channels narrowed between 65% and 90% between 1938 and 1986 (~1.5%/yr), with most of the narrowing completed by the mid-1960s (Johnson, 1994). The Rio Grande below Elephant Butte Reservoir exhibited narrowing of 50-70 % between 1900 and 1970 (~1%/yr) (Everitt, 1993) and channel width along the Gila River near Stafford, AZ decreased by 90%, from 610 to 60m between 1917 and 1964. Channel widths along the well-studied Green River decreased by an average of 27% in Canyonlands National Park, Utah, between the early 1900s and the 1970s (Graf, 1978), by 19% between 1930 and 1993 near Green River, UT (Allred and Schmidt, 1999), and up to 20% downstream of Flaming Gorge Dam after it closed in 1962 (Grams and Schmidt, 2002). Van Steeter and Pitlick (1998) reported 20% narrowing along the Colorado River near Grand Junction, Colorado, between 1937 and 1993, and Hereford (1984) found narrowing of 50% of the unregulated Little Colorado, Arizona, between the 1930s and 1980s.

Comparing these width adjustment measures and their rates is difficult due to the various techniques used, the number, magnitude, and timing of impacts to the channel, channel location, bed material, and many other factors, but it is significant that all these rivers have exhibited substantial narrowing over the last century. The most important factor implicated in these studies is a reduction in peak discharges, including flow regulation at dams, irrigation withdrawals, and (or) climate. Additionally, narrowing appears to follow the general pattern described by Schumm and Lichty (1963), Burkham (1972), and Johnson (1994), characterized by (1) stalled sediment on bars or in-channel berms, (2) vegetation establishment on abandoned bars during low flow years, (3) vertical aggradation on

stabilized, vegetated bars, (4) abandonment and filling of anabranches, and (5) eventual attachment of bars to the old floodplain.

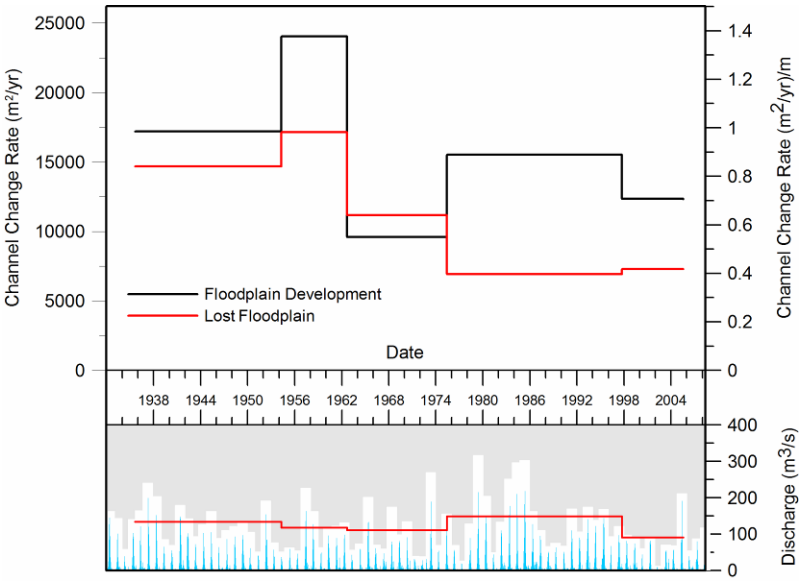

Figure 11. Erosion and deposition (floodplain stabilization) rates, Rio Chama upstream of El Vado Dam, 1935-2005. Rates of channel change are highest between 1935 and 1962 when channel activity is highest (i.e., avulsions, exposed bars, etc). Erosion rates decrease as activity slows through the rest of the study period. Floodplain formation via bar stabilization ("deposition") appears to increase during periods characterized by high peak discharge (1975-1997).

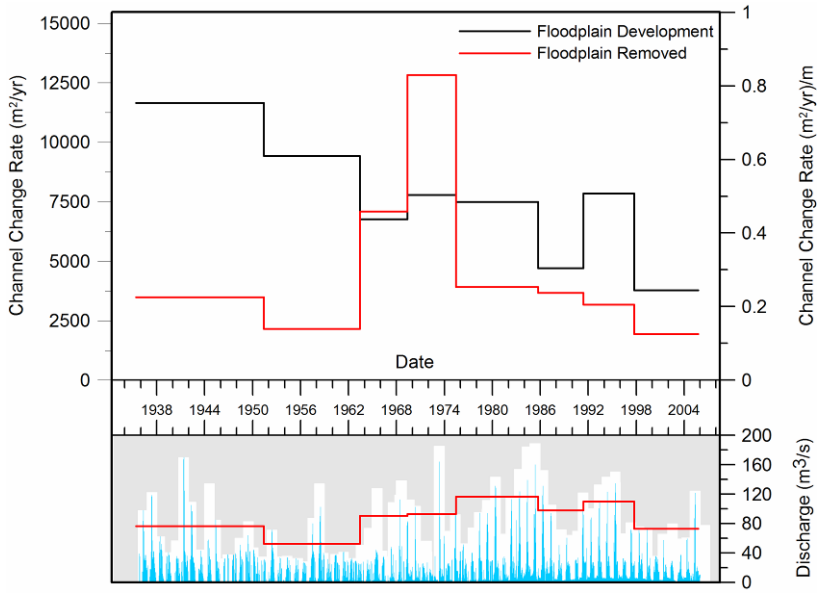

Figure 12. Erosion and deposition (floodplain stabilization) rates, Rio Chama downstream of El Vado Dam, 1935-2005. Erosion rates are highest during return of relatively high peak flows in 1960s that followed a prolonged interval of low flow starting in the early 1950s. Floodplain formation ("deposition") is highest between 1935 and 1963, after the closure of El Vado Dam (1935) and during the 1950s' low flows. After 1975, higher rates of deposition are associated with higher peak flows (e.g., 1975-1985 and 1991-1997) and erosion rates steadily decrease.

Bank erosion area along the upstream reach varied from to 0.06 km^2 to 0.28 km^2 over the 1997-2005 and 1935-1951 photo periods, respectively. On the other hand, deposition (total area of stabilized floodplain and islands) ranged from 0.34 km^2 to 0.10 km^2 over the same two photo periods. Rates of erosion for this study reach, which were elevated compared to the other, less active, study reaches due to inclusion of new channels cut by avulsions, have decreased over the entire study period, from 15,000 m^2/yr to 6,000 m^2/yr (Figure 11). Along the downstream study reach, bank erosion ranged from 0.02 km^2 over the 1997-2005 photo period to 0.08 km^2 over the 1969-1975 period. Erosion rates were relatively low prior to 1963 (~3,000 m^2/yr), especially compared to the deposition rate (~10,000 m^2/yr), but the rate increased at the end of low discharge periods following dam

closure and the 1950s drought (Figure 12). The deposition rate flattens between 1963 and 1985, when erosion is at its highest, and then alternates, as does the total channel change rate (Figure 14), with larger rates of deposition associated with larger peak flows and vice versa (Figure 12).

Over the last three decades, erosion rates along the Rio Grande through Albuquerque were similar to those along the downstream Rio Chama reach, at 0.23 m^2/yr/m of channel from 1972 to 2006 along the Rio Grande and 0.18 m^2/yr/m from 1975 to 2005 for the downstream reach. However, when the erosion rates are normalized by contributing basin area, the rates are an order of magnitude higher along the Rio Chama ($2.1x10^{-4}$ m^2/yr/km^2 vs. $1.3x10^{-3}$ m^2/yr/km^2). The Rio Chama is typically cutting into higher terraces compared to the Rio Grande banks, and likely results in a higher volume of sediment in the channel, as well. Primarily because new channels and anabranches cut during avulsions were considered "erosion," rates for the upstream Rio Chama were almost twice those for the lower reach, even before normalization.

Assuming that more floods would result in more erosion, it is unclear why bank erosion rates were low during the wettest period, 1975-1997, and higher prior to 1975. The sequence of long droughts followed by large floods may play a major role in moving sediment through the system, both in the Rio Chama basin and elsewhere in the Southwest (e.g., Schumm and Lichty, 1963, Burkham 1972). Both study reaches experienced the most erosion after long periods of reduced peak flow (Figures 11 and 12). Floods in 1956 and 1957, followed a time span where five of six annual peak flows did not exceed 70 m^3/s and may be responsible for eroding banks around expanded point bars and newly formed islands, and (or) destabilizing banks via incision. The flood of 1973 also likely caused the

realignment of some channels and stabilized bars over the 1963-1975 photo period, which was characterized by the lowest average peak discharge (Figure 11). Moderate to large floods in the 1960s and early 1970s, including the 1973 flood, likely produced similar erosion along the downstream study reach (Figure 12). These floods followed a long period of drought, where flow releases from El Vado Dam were held below 60 m^3/s in 11 of 16 years and below 100 m^3/s in all but one year. It seems likely that the channel may have narrowed during lower peak flows through 1967, becoming too constricted to carry subsequent larger floods.

The juxtaposition could also relate to the amount of material being delivered from hillslopes and tributaries. Many of the Rio Chama tributaries are intermittent, and it is possible that more sediment was being delivered to the channel during the wetter 1975-1996 period than the channel could convey, compared to relatively little sediment delivery during drier years except large, coarser inputs during occasional flash floods. Additionally, the short period of reduced peak flows between 1987 and 1991, coupled with increased moisture carried over from the mid-80s, may have allowed enough deposition and vegetation growth to allow for the balance to shift slightly from erosion to more channel narrowing.

One of the main goals of the Rio Grande study (Swanson et al., 2007; 2010 submitted), as well as the Rio Chama study, is to relate the changes in channel planform documented on historical aerial photographs to changes in the hydrology through the river reaches. However, along the Rio Chama, comparing the hydrograph to adjustment rates is complicated by the long time periods between photo sets, variability in the hydrographs, and large amounts of error associated with rates of channel change. Additionally, channels adjust

to both the water and *sediment* supply, so relying on water discharge data alone makes interpretation difficult.

Unlike the Rio Grande through Albuquerque, where periods of relatively low flows are generally associated with channel narrowing, channel adjustments do not consistently match changes in peak flow along either of the Rio Chama study reaches (Figure 13 and Figure 14). For instance, the largest narrowing (decrease in planform area) rates along the upstream reach occur during the 1954-1962 period (6,800 m^2/yr ±30,000 m^2/yr) of relatively low peak flow (mean peak flow = 108 m^3/s) and the 1975-1997 period of relatively high peak flows (148 m^3/s) including the largest discharges in the record (Figure 13). During the 1963-1975 photo period, the channel stabilized at flows similar to the 1954-1962 period, and narrowing rates during the extremely low flows in the late 1900s and early 2000s slowed from the 1975-1997 interval (Figure 13). Similarly, the highest narrowing rates along the downstream study reach occur during the 1935-1963 periods of relatively low peak flows (~7,000 m^2/yr (± 13,000 m^2/yr); mean peak flow = 60 m^3/s), especially in relation to pre-dam (1935) floods, and then the high peak flow periods between 1975 and 1985 (3,000 m^2/yr (± 15,000 m^2/yr); mean peak flow =117 m^3/s) and 1991 and 1997 (4,700 m^2/yr (± 21,000 m^2/yr); mean peak flow =110 m^3/s; Figure 14).

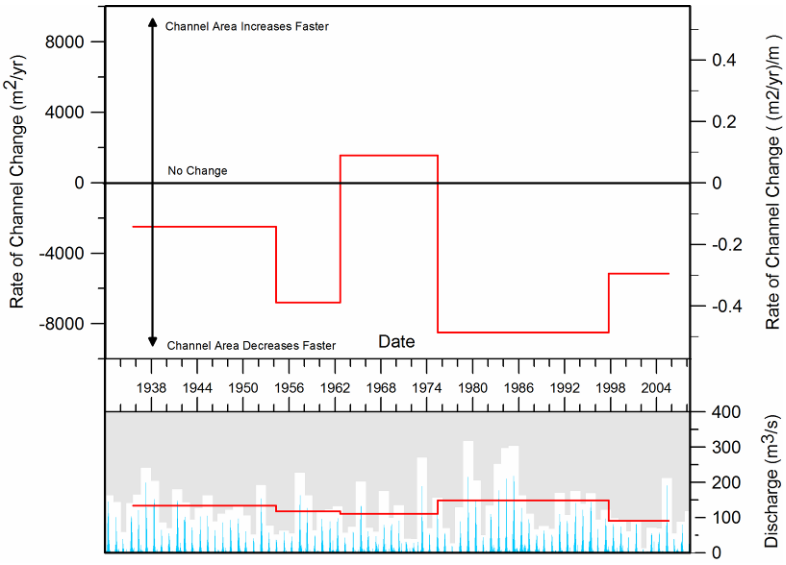

Figure 13. Rates of channel change over photograph periods, Rio Chama upstream of El Vado Dam, 1935-2005. Rates of channel change are highest (farthest from 0) between 1954 and 1962, which includes a prolonged drought period, and between 1975 and 1997, the wettest period. Little change occurs between 1962 and 1975, a period of variable peak discharge, but with the lowest average flood value.

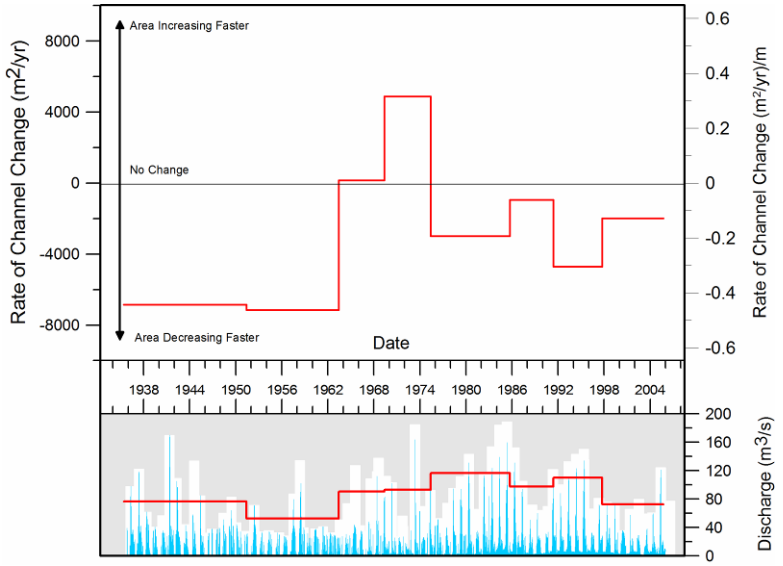

Figure 14. Rates of channel change over photograph periods, Rio Chama downstream of El Vado Dam, 1935-2005. Rates of channel change are highest (farthest from 0) between 1935 and 1963, which immediately follows El Vado Dam closure (1935) and includes a prolonged drought period. The channel widened between 1969 and 1975, presumably due to the 1973 flood. After 1975, enhanced rates of channel change (narrowing) are associated with period of relatively high peak flows (e.g., 1975-1985 and 1991-1997).

Between 1935 and 2005, both Rio Chama study reaches and the Rio Grande through Albuquerque narrowed, primarily by the processes outlined above, but the timing and magnitudes of the adjustments differed at all three sites. Width adjustment rates for the Rio Grande study reach and the Rio Chama downstream of El Vado appear similar with steep drops in width and area between 1935 and the early 1960s followed by much slower declines after 1975. The Rio Grande had been clearly narrowing prior to 1935 (Figure 15), largely related to a shift in climate and land use, but had narrowed by 63% between 1935 and 1962. Channel training and flood control measures conducted in the 1940s and 1950s and dam construction along upstream tributaries and the mainstem Rio Grande (e.g., El Vado-1935, Jemez Canyon-1953, Abiquiu-1963, Cochiti-1971) likely contributed to both the magnitude and timing of channel narrowing (Swanson et al., 2010 (submitted)).

The accelerated rate of narrowing between 1935 and 1962 along the lower Rio Chama study reach is readily attributed to flow regulation and sediment trapping at El Vado Dam, which closed in 1935. However, the apparent climatic influence on channel planform along the Rio Grande suggests that some of the change below El Vado Dam could be attributed to a similar climate shift. Upstream of El Vado Dam, the channel narrowed 12% between 1935 and 1963 and although still relatively unstable, also began to exhibit fewer shifts in channel position, whereas downstream, the channel narrowed by 23% over the same period. After 1963, the rate of change along the downstream study reach declined, but the upstream reach continued to steadily decrease in width at a slightly faster rate than over the earlier part of the study period. Upstream declines in channel planform area and width suggest that the downstream study reach may have narrowed over the 1935 to 1963 period despite the dam, but the dam definitely increases the magnitude and rate of channel

adjustment over this period, and may have counteracted any lag in adjustments due to an influx of sediment from upstream.

It is unclear what causes the apparent narrowing along the upstream reach. Although the average peak flows decrease by less than 10 m^3/s, estimated discharges for the largest floods appear higher in the decades before 1935 than for the 1935-1954 photo period. Large floods may have disrupted the system, leaving numerous anabranches and large amounts of sediment exposed for subsequent transport and island/floodplain construction. Land use might be another factor. Grazing and lumber activities in the upper Rio Chama basin peaked in the early 1900s, which may have resulted in large amounts of sediment entering the system (Figures 16-18), as seen in the exposed bars on the 1935 and 1954 photographs along both study reaches. Combined with high flows, the sediment may have stressed the system prior to, and during, the early part of the study period, resulting in the upstream channel activity and providing sediment for the narrowing that occurred downstream.

The land use pressure likely abated by the 1960s, and numerous small dams were placed on Rio Chama tributaries between 1935 and 1954, which likely attenuated sediment and water discharges at downstream confluences. Though not quantified, some changes in vegetation are also apparent in both study areas from the 1935 photographs to the 2006 photographs, suggesting changes in hydrology and (or) land use. The largest observable change is that grassy areas in the 1935 pictures support more shrubs by 1975, especially juniper, pinyon, and sagebrush on higher terraces on the canyon floor. This shift has been documented in other parts of northern New Mexico during this period as well (e.g., Gottfried et al., 1995; Wilcox et al., 1996), and the conversion from grassland to shrubland may greatly increase runoff and erosion rates on associated slopes (e.g., Wilcox et al., 1996). Much of

the narrowing planform along the upstream reach could be in response to related changes in upland water and input production. Much of the sediment transported through the fluvial system originates through hillslope erosion in the headwater reaches (Schumm, 1977), and the rates at which these headwater channels deliver sediment to downstream reaches affect downstream channel depositional processes, such as the construction of bars and floodplains, which strongly depend on sediment supply.

A large increase in sediment supply to channels with established floodplains can lead to floodplain aggradation and terrace construction (Miller and Benda, 2000). For example, logging activities in the Pacific coastal ranges initiated channel widening and aggradation, followed by narrowing when sediment supply decreased again (e.g., Roberts and Church, 1986; Madej and Ozaki, 1996). Similarly, Miller and Benda (2000) observed channel widening, braiding, and fining, followed by coarsening and anabranch and terrace formation, after multiple debris flow pulses entered a stream channel. When the related sediment had passed, they observed channel incision and associated narrowing.

The relative lack of trend in streamflow data for the upstream reach, especially compared to the Rio Grande, suggests that sediment loads likely play a large role in the observed channel adjustments along the Rio Chama, especially upstream. Although there is no direct evidence for an increased sediment supply or channel widening and aggradation along the Rio Chama prior to 1935, land use practices that accelerated hillslope and tributary erosion (e.g., arroyo cutting; Fig. 16) could have contributed to the state of the channel during the early part of the study period. Photographic evidence for a decrease in sediment delivery to the Rio Chama channel after 1935 include the construction of numerous check dams on tributaries to the upstream reach, and reduction in braiding and distributary channels

along the Rio de la Brazos and Rito de Tierra Amarilla. The timing and magnitude of potential upstream land use impacts on the downstream Rio Chama study reach is unknown, but presumably increased sand loads could have impacted the reach before dam closure, and likely would have eventually impacted the site if the dam was not built. Narrowing along the Rio Grande between 1918 and 1962 may also partly be a similar rebounding process following increased sediment supply from arroyo incision and headwater land use in the late 1800s and early 1900s, and narrowing below the Rio Chama may have resulted in less sediment supply for the Rio Grande, assuming the narrowing effect was not attenuated.

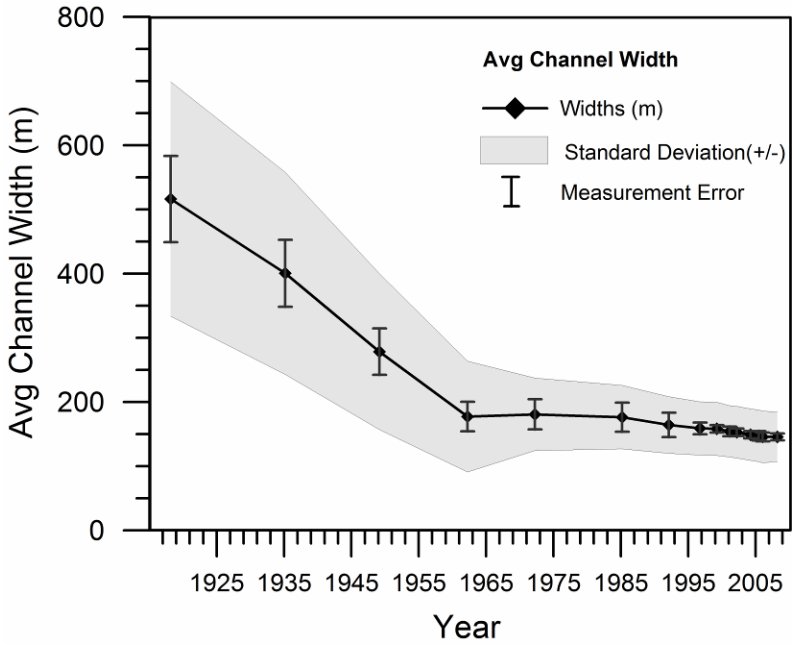

Figure 15. Change in Rio Grande average channel width through Bernalillo County (Albuquerque), New Mexico, 1918-2008. Channel widths decrease over the study period, but most of the adjustments are complete by 1962. Channel heterogeneity represented by the standard deviation in channel width (gray) also decreases. From Swanson et al., 2010.

Figure 16. Historic photograph depicting land use in the upper Rio Chama watershed from the Carson National Forest (http://www.fs.fed.us/r3/about/history/carson/). "Overgrazed range near Tierra Amarilla Grant. This range was typical of much of the range on the Carson at the time" Photo by J. T. Jardine; FS #171978; 1922)

Figure 17. Historic photograph depicting land use in the upper Rio Chama watershed from the Carson National Forest (http://www.fs.fed.us/r3/about/history/carson/). "Small lake with the burned over, overgrazed, and eroded slopes of Canjilon Mountain in the distance." Photo by R. King; FS #440695; 1946.

Figure 18. Historic photograph depicting land use in the upper Rio Chama watershed from the Carson National Forest (http://www.fs.fed.us/r3/about/history/carson/). ""Rain digging gullies and carrying away soil. The heavy, silt-laden water runs off during a heavy rain on nearly barren slopes." Photo by D. O. Todd; FS #482982; 1957.

Research on other rivers draining semi-arid drainages, including the Rio Grande through Albuquerque (Swanson et al., 2007, 2010), indicates faster rates of change are associated with drought periods (Burkham, 1972; Johnson, 1994; Allred and Schmidt, 1999). Although apparently true for the 1935 to 1963 photo periods, the periods characterized by large peak discharges, like the 1980's floods, seem to contribute to greater narrowing along both the Rio Chama study reaches. This shift in hydrologic control on channel planform processes is also likely due to sediment supply. In the early part of the study period, the volume of sediment available for transport in the channel may be too high for the reduced flows to move, especially downstream of El Vado. As the channel adjusts, some of this sediment gets trapped in stabilized bars and overbank deposits, and the smaller channel has less exposed bed sediment to move. After a time, it likely requires higher flows to deposit

sediment, especially coarser sand and small gravel, for continued island construction and filling abandoned channels, as well as providing water and seeds on new island and floodplain surfaces for vegetation generation (Allred and Schmidt, 1999). Alternatively, the channel could be cutting into the alluvium (degrading) in response to reduced sediment loads from reductions in grazing and forestry, and possible extreme floods, and along the downstream study reach, sediment trapping by El Vado Dam. Finally, it is also possible that the channels are narrowing quickly during 2 to 3 year periods of low discharge within a study period, and the large floods only maintain the channel. Under this scenario, however, longer periods of reduced peak flow should produce greater rates of narrowing.

Adjustment locations. Along the Rio Chama upstream of El Vado, relatively large width adjustments occurred along the entire study reach upstream of the Rito de la Tierra Amarilla, with large amounts of activity between the NM Highway 95 Bridge and the in-channel gravel mine downstream of Park View Village (now Los Ojos, NM) and between the village of LaPuente and the Rito de la Tierra Amarilla confluence (Figure 19). In these subreaches, widths reductions of 20-30 m between photo periods and total narrowing often greater than 50 m exceed estimates of measurement uncertainty. The channel downstream of the bridge appears to widen along some subreaches between 1935 and 1954, followed by narrowing after 1975. Downstream of LaPuente, narrowing is the dominant adjustment over the entire study period, although relatively little change occurs in the bedrock canyon at the downstream end of the study reach.

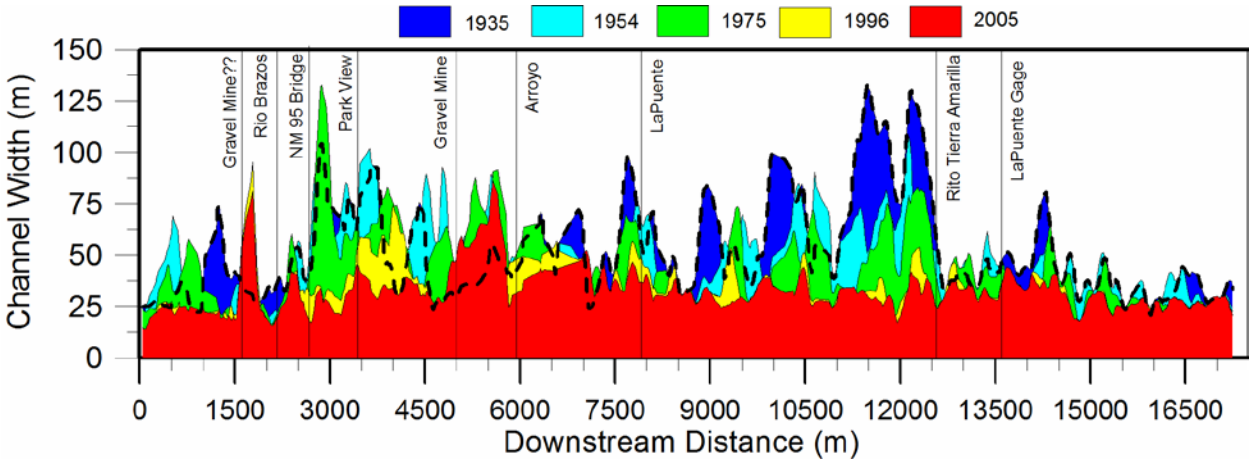

Figure 19. Change in channel width along the Rio Chama upstream of El Vado Dam, New Mexico,1935-2005. Black dashed line represents 1935 width. Channel activity (avulsions, widening, etc) is most prominent between 1935 and 1963, primarily between the NM 95 bridge and the downstream gravel mine. Major channel narrowing occurred throughout the study period along the 4 km subreach upstream of the Rito de Tierra Amarilla confluence. Relatively little planform change took place along the canyon subreach downstream of the Rito de Tierra Amarilla, and gravel mines maintained a larger active channel (exposed bed) while in operation.

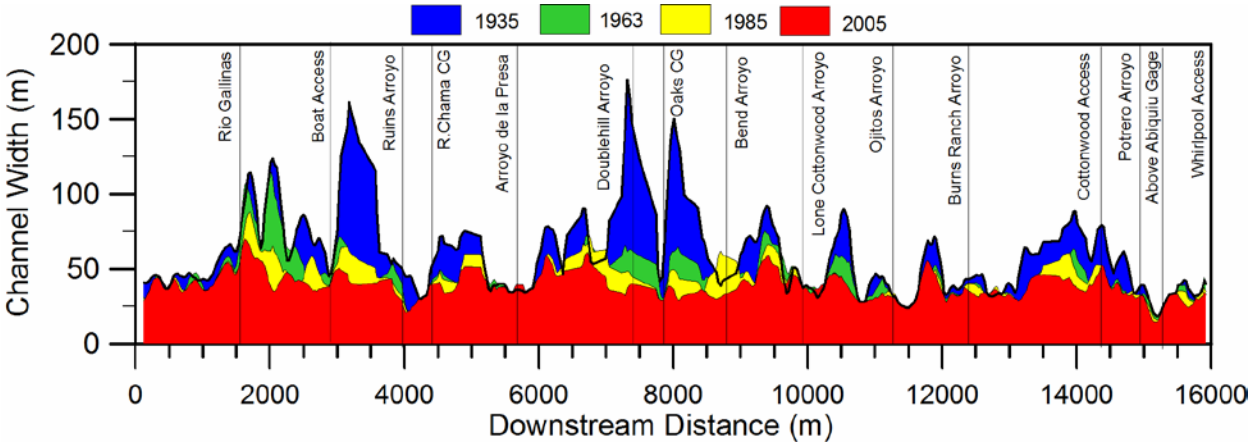

Figure 20. Change in channel width along the Rio Chama downstream of El Vado Dam, New Mexico, 1935-2005. Black solid line represents 1935 width. Channel narrowing takes place between distinct nodes of little channel change related to tributary inputs (e.g., downstream of the Rio Gallinas confluence) and floodplain and (or) valley confinement by alluvial deposits and bedrock.

Major changes in width along the downstream Rio Chama study reach appear to occur between discrete nodes (Figure 20), including the subreaches (1) between the Rio Gallinas and the Ruins Arroyo confluences with the mainstem, (2) from just below Arroyo de la Presa to just above Lone Cottonwood Arroyo (concentrated up and downstream of the Oaks Campground), and (3) the 2 km upstream of Potrero Arroyo. Adjustment in these areas appears to be related to channel confinement and tributary inputs. The narrowing at the north end of the study reach is likely associated with reduced peak flows and a large sediment influx from the Rio Gallinas. Additionally, a bottleneck for sediment transport may form where the valley pinches and the river enters a confined reach at Ruins Arroyo. Below the Arroyo de la Presa confluence, the channel is partly confined by boulders and cobbles presumably associated with late Quaternary debris-flow deposits. In this subreach (2), major narrowing occurs where the meander belt widens and the floodplain and Quaternary deposits are primarily sand. Two tributaries enter the river at Oaks Campground, which confine the channel at the confluence and appear to control width up and downstream as well. Finally, another transition from relatively wide alluvial valley to a bedrock confined valley occurs just upstream of the Potrero Arroyo confluence, which likely controls sediment storage during periods of higher sediment supply relative to discharge.

Channel response in reaches with tributary confluences is a function of the ratio of tributary to mainstem water flux, sediment flux, and sediment size (Ferguson et al., 2006), and possibly how fast vegetation can colonize exposed tributary deposits. Along the Rio Grande through Albuquerque, narrowing is greatest downstream of tributary sediment inputs where fans impinge on the channel and deposition occurs on downstream bars and side channels. This response indicates the volume of sediment entering the system is too much for

the channel to transport effectively (Swanson et al., 2010). Planform adjustments at tributaries along the Rio Chama are not as straightforward, and seem to depend on changes in the timing of sediment delivery as well as valley characteristics, especially channel confinement.

Along the upstream Rio Chama study reach, changes at the Rio de los Brazos are minimal, largely because the mainstem is confined against bedrock at the confluence. As soon as the floodplain widens again, below the Highway 95 bridge, instability followed by major narrowing characterize channel adjustments. Early images of the tributary (1935 and 1954) feature a braided system with many anabranches joining the Rio Chama at the confluence. The 2005 photographs show a much narrower channel with only two junction points, further suggesting a decrease in tributary sediment transport over the study period. Upstream of the Brazos junction, variable planform change may be associated with inputs from Cañones Creek and another unnamed tributary entering the Rio Chama just upstream of the study reach. On the other hand, the Rito de la Tierra Amarilla seems to have little downstream impact, tributary enters the Rio Chama within a narrow bedrock canyon where finer sediment might be moved more effectively. A backwater effect upstream of the confluence may contribute to narrowing in LaPuente-Rito de Tierra Amarilla subreach, but the shift from relatively wide valley to narrow canyon might produce the same effect.

Tributary controls at the Rio Gallinas and Oaks Campground along the downstream study reach have already been noted. Many of the other tributaries along the downstream Rio Chama enter in confined reaches, where sediment, especially the sand needed for bar growth, is likely transported more effectively. Changes in channel planform at these locations are relatively small, but changes in sediment supply from these sources likely

contribute to adjustments in less confined subreaches located downstream. Examples include the subreaches downstream of the Arroyo de la Presa and Ruins Arroyo confluences (Figure 20). Additionally, small tributaries such as Doublehill Arroyo and a companion arroyo on the opposing bank, as well as a small, unnamed tributary downstream of the boat access, likely contribute sand that helps fill abandoned side channels at these locations.

Cross-section adjustment. Very few data describing channel cross-section characteristics are available for the Rio Chama study reaches. Both study reaches lie within original Spanish Land Grants, so surveys across the channels in the area are not part of the General Land Survey records. Cross-sections measured at the USGS stream gage sites are not always measured in the same locations or same time of year so comparisons are difficult, and requests for data have been met with resistance. Therefore, any discussion focused on vertical changes is speculative, but should be a part of any discussion on general channel change. Along with a loss of Rio Chama planform area, a decrease in active cross-sectional area also likely occurred over the study period. Mid-channel and point bars have likely expanded via both vertical and horizontal accretion, and filled in some of the pre-dam cross-sectional area. It is also possible that some of the narrowing and loss of planform area occurred due to channel degradation related to sediment trapping by El Vado Dam and possible decreases in tributary sediment inputs. Much of the narrowing observed along the Rio Grande between Cochiti Dam and Albuquerque (Alameda Bridge) is attributed to "hungry water" releases and related incision below the dam (e.g., Leon 1998), and therefore, it seems possible that a similar response could occur below El Vado Dam. Indirect evidence to support channel degradation include inset terraces adjacent to the channel observed by the authors and documented by Persico et al. (2005), and apparent armoring observed by Dr. Tim

Ward (Civil Engineering, Univ. of New Mexico, personal communication). Additionally, the stage-discharge relationship for the AQR gage was adjusted in 1999 due to a 3 ft change in channel bed elevation relative to a fixed datum at the site (Lynn Miller, Field Chief, USGS – Albuquerque Office, personal communication). However, there are numerous local gradient controls (channel bedrock, debris-flow deposits) and sediment sources (tributaries, banks) that may help mediate channel incision this far downstream from El Vado Dam. Initial deposition and vegetation encroachment along the alluvial reaches may also promote channel degradation during later high flow events by decreasing the width-to-depth ratio. Larger flows may be contained over a smaller channel bed area, increasing shear stress over the bed which promotes more sediment transport. This process may be especially true at the outside of existing and developing meander bends. Increased degradation at the toe of outside banks may lead to greater bank destabilization and erosion.

Conclusions

In general, a historical analysis of channel change using aerial photographs produces useful information concerning channel planform over time. Measuring channel characteristics from spatially referenced photos in a geographic information system allows for the collection of quantitative data defining planform channel and bar areas. These data can then be used to locate areas of active bank erosion and channel deposition, and determine rates of change. However, the amount of error in these measurements can often be quite high, limiting final interpretations.

Study reaches located along the Rio Chama both upstream and downstream of El Vado Dam exhibit channel narrowing between 1935 and 2005. Much of the channel adjustment downstream of the dam occurred between 1935 and 1963, immediately after dam

closure and over a prolonged period of relatively low peak flows. Although some narrowing occurred upstream of the dam during this period, most of the narrowing along this study reach took place after 1975, presumably due to land use changes and associated changes in sediment supply.

The formation, expansion, and stabilization of mid-channel and point bars resulted in much of the narrowing, which took place primarily in wider sub-reaches along the more alluvial sections of the study reaches. Relationships between the hydrology and channel planform data are tenuous because of relatively large errors associated with delineating channel banks and islands.

Some of the relationships between the hydrology and channel change along the Rio Chama are contrary to expectations based on the previous Rio Grande research, such as the increase in channel widening despite continued drought through much of the 1963-1975 period, followed by the decrease in erosion and increase in narrowing over the wettest photo periods (1975-1996). Adding additional photographs for the analysis downstream of the study reach helped strengthen these relationships, and documenting changes upstream of El Vado provided additional information on historic change to the Chama system, as well as the Rio Grande.

Additionally, both the Rio Chama and Rio Grande studies indicate that tributary inputs play a major role in channel adjustment to modified sediment loads and hydrology. Along both rivers, narrowing reaches are often concentrated immediately up- and downstream from tributary confluences. In these systems, tributary and debris flow channels often deliver large amounts of sediment to the mainstem channel, commonly during summer runoff events out of phase with larger, longer duration, spring snowmelt flows. Depending

on the clast size and volume of the tributary sediment, these inputs can provide material to exacerbate tributary fan and downstream bar expansion, slow bed degradation, control local base levels, and adjust local slopes (Benda 1990; Benda et al., 2003; Ferguson et al. 2006). These impacts affect sediment routing, erosion, and storage both up- and downstream. Additional photographic analyses and field work may help define the factors that control the impact of these tributaries on channel configuration and modification.

References

Allred, TM, Schmidt, JC. 1999. Channel narrowing by vertical accretion along the Green River near Green River, Utah. *Geological Society of America Bulletin* 111: 1757-1772.

Andrews, ED. 1986. Downstream effects of Flaming Gorge Reservoir on the Green River, Colorado and Utah. *Geological Society of America Bulletin* 97: 1012-1023.

Benda, LE. 1990. The influence of debris flows on channels and valley floors of the Oregon Coast Range, U.S.A. *Earth Surface Processes and Landforms* 15: 457–466.

Benda, LE, Veldhuisen, C, Black, J. 2003. Debris flows as agents of morphological heterogeneity at low-order confluences, Olympic Mountains, Washington. *Geological Society of America Bulletin* 115. 9: 1110-1121.

Brandt, SA. 2000. Classification of geomorphological effects downstream of dams. *Catena* 40: 375–401.

Brice, JC. 1964. *Channel patterns and terraces of the Loup Rivers in Nebraska*. USGS Professional Paper 422-D. Department of the Interior, Washington, DC. 41p.

Brice, JC. 1975. *Air Photo Interpretation of the Form and Behavior of Alluvial Rivers.* Final Report to the U.S. Army Research Office, Durham, North Carolina.

Bryan, K. 1925. Date of channel trenching (arroyo cutting) in the arid southwest. *Science* 62: 339.

Burkham, DE. 1972. *Channel changes of the Gila River in Safford Valley, AZ, 1846-1970*. USGS Professional Paper, Department of the Interior, Washington, DC, 24pp.

(EPA) Environmental Protection Agency. 2004. Total Maximum Daily Loads for the Upper Rio Chama Watershed (El Vado Reservoir to Colorado Border). TMDL Report 9785. 171 pp.

Downward, SR, Gurnell, AM, Brookes, A. 1994. A methodology for quantifying river channel change using GIS. In *Variability in Stream Erosion and Sediment Transport*. Publication 224. International Association of Hydrological Sciences: 449–456.

Everitt, BL. 1993. Channel responses to declining flow on the Rio Grande between Ft. Quitman and Presidio, Texas. *Geomorphology* 6: 225-242.

Fassnacht, H, McClure, EM, Grant, GE, Klingeman, PC. 2003. Downstream Effects of the Pelton-Round Butte Hydroelectric Project on bedload transport, channel morphology, and channel-bed texture, lower Deschutes River, Oregon: Geology and Geomorphology of the Deschutes River, Oregon. *Water Science and Application*, v. 7, p. 175-207.

Ferguson, RI, Cudden, JR, Hoey, TB, Rice, SP. 2006. River system discontinuities due to lateral inputs: generic styles and controls. *Earth Surface Processes and Landforms* 31: 1149–1166.

Fogg, JL, Hanson, BL, Mottl, HT, Muller, D P, Eaton, RC. 1992. *Rio Chama Instream Flow Assessment*, Department of the Interior, Bureau of Land Management, Denver, CO, p. 133.

Gilvear, DJ, Winterbottom, SJ, Sichingbula, H. 2000. Character of meander planform change on the Luangwa River, Zambia. *Earth Surface Processes and Landforms* 16: 1-24.

Gonzalez, MA, Dethier, DP. 1991. Geomorphic and neotectonic evolution along the margin of the Colorado Plateau and Rio Grande rift, northern New Mexico, *New Mexico Bureau of Mines and Mineral Resources, Bulletin* 137, p.29-46.

Gottfried, GJ, Swetman, WT, Allen, CD, Betancourt, JL, Chung-MacCoutbrey, A. 1995. Piñon–juniper woodlands of the Middle Rio Grande Basin, New Mexico. p. 95–132. In DM Finch and JA Tainter (ed) *Ecology, diversity, and sustainability of the Middle Rio Grande Basin*. Gen Tech Rep RM-268 USDA For Serv, Fort Collins, CO.

Graf, WL. 1978. Fluvial adjustments to the spread of tamarisk in the Colorado Plateau region. *Geological Society of America Bulletin* 89: 1491–1501.

Grams, PE, Schmidt, JC. 2002. Streamflow regulation and multi-level flood plain formation: channel narrowing on the aggrading Green River in the eastern Uinta Mountains, Colorado and Utah. *Geomorphology* 44: 337-360.

Gurnell, AM. 1998. Channel change on the River Dee meanders, 1946-1992, from the analysis of air photographs. *Regulated Rivers: Research and Management* 13.1: 13-26.

Hereford, R. 1984. Climate and ephemeral-stream processes: Twentieth-century geomorphology and alluvial stratigraphy of the Little Colorado River, Arizona. *Geological Society of America Bulletin* 95: 654-668.

Hughes, ML, McDowell, PF, Marcus, WA. 2006. Accuracy assessment of georectified aerial photographs: Implications for measuring lateral channel movement in a GIS. *Geomorphology* 74: 1 –16.

Johnson, WC. 1994. Woodland expansion in the Platte River, Nebraska: Patterns and causes. *Ecological Monographs* 64: 45-84.

Lagasse, PF. 1981. Geomorphic response of the Rio Grande to dam construction. *New Mexico Geological Society, Special Publication* 10: 27–41.

Lane, EW. 1955. The importance of fluvial morphology in hydraulic engineering. *Proceedings of the American Society of Civil Engineers* 81: 1–17.

Langman, JB, Anderholm, Sk. 2004. Effects of reservoir installation San Juan-Chama Project Water , and Reservoir Operations on Stream flow and water quality in the Rio Chama and Rio Grande, Northern and Central New Mexico, 1938-2000.U.S. Geological Survey Scientific Investigations Report 2004-5188.

Leopold, LB, Bull, WB. 1979. Base level, aggradation, and grade. *American Philosophical Society Proceedings* 123: 168-202.

Lewin, J, Manton, MM. 1975. Welsh floodplain studies: the nature of floodplain geometry. *Journal of Hydrology* 25: 37-50.

Love, DW, Connell, SD. 2005. Late Neogene drainage developments on the southeastern Colorado Plateau, New Mexico: New Mexico's Ice Ages. New Mexico Museum of Natural History and Science Bulletin, v. 28, p. 151-169.

Mackin, H. 1948. Concept of the graded river. *Geologic Society of America Bulletin* 59: 463-512.

Madej, MA, Ozaki, V. 1996. Channel response to sediment wave propagation and movement, Redwood Creek, California, USA. *Earth Surface Processes and Landforms* 21: 911–927.

Makar, P, Massong, T, Bauer, T, Tashjian, P, Oliver, KJ. 2006. Channel width and flow regime changes along the Middle Rio Grande, NM. Joint 8th Federal Interagency Sedimentation Conference and 3rd Federal Interagency Hydrologic Modeling Conference, Reno, Nevada.

Manley, K, Scott, GR, Wobus, RA. 1987. Geologic map of the Aztec 1° x 2°quadrangle, northwestern New Mexico and southern Colorado. U.S. Geologic Survey, Miscellaneous Investigations Series.

Meyer, GA, Wells, SG, Jull, AJT. 1995. Fire and alluvial chronology in Yellowstone National Park: climatic and intrinsic controls on Holocene geomorphic processes. *Geological Society of America Bulletin* 107.10: 1211-1230.

Miller, D J,Benda, LE. 2000. Effects of punctuated sediment supply on valley-floor landforms and sediment transport. *Geological Society of America Bulletin* 112.2: 1814-1824.

Mount, NJ, Louis, J, Teeuw, RM, Zukowski, PM, Stott, T. 2003. Estimation of error in bankfull width comparisons from temporally sequenced raw and corrected aerial photographs. *Geomorphology* 56: 65– 77.

Mount, NJ, Louis, J. 2005. Estimation and propagation of error in measurements of river channel movement from aerial imagery. *Earth Surface Processes and Landforms* 30: 635– 643.

(MEI) Mussetter Engineering, Inc. 2003. Geomorphic and Sedimentologic Investigations of the Middle Rio Grande between Cochiti Dam and Elephant Butte Reservoir, Report prepared for New Mexico Interstate Stream Commission by Mussetter Engineering, Inc., Fort Collins, Colorado, 195p.

(MEI) Mussetter Engineering, Inc. 2006. Evaluation of Bar Morphology, Distribution and Dynamics as Indices of Fluvial Processes in the Middle Rio Grande, New Mexico. Unpublished report for the New Mexico Interstate Stream Commission by Mussetter Engineering, Inc., Fort Collins, Colorado. 156p.

Persico, L, Meyer, G, Frechette, J, New, J, and Hepler, C. 2005. Contrasts in late Pleistocene to Holocene fluvial behavior along the middle Rio Chama: New Mexico Geological Society, 56th Field conference Guidebook, Geology of the Rio Chama Basin, p. 432-433.

Petts, GE, Gurnell, AM. 2005. Dams and Geomorphology: Research progress and future directions: *Geomorphology* 71.1: 27-47.

Pohl, M. 2004. Channel bed mobility downstream from the Elwha Dams, Washington. *The Professional Geographer* 56.3: 422-431.

Poling-Kempes, L. 1997. *Valley of Shining Stone: the story of Abiquiu.* University of Arizona Press, Tucson, AZ. 272p.

Richard, G, Julien, P. 2003. Dam impacts on and restoration of an alluvial river – Rio Grande, New Mexico. *International Journal of Sediment Research* 18.2: 89-96.

Roberts, RG, Church, M. 1986. The sediment budget in severely disturbed watersheds, Queen Charlotte Ranges, British Columbia. *Canadian Journal of Forest Research* 16: 1092–1106.

Schumm, SA. 1977. *The Fluvial System*: New York, Wiley-Interscience, 338 p.

Schumm, SA, Lichty, RW. 1963. *Channel widening and floodplain construction along Cimarron River in southwestern Kansas*. United States Geological Survey Professional Paper 352-D.

Swanson, BJ, Meyer, GA, Coonrod, J. 2007. Coupling of Hydrologic/Hydraulic Models and Aerial Photos Through Time: Relating Geomorphic Change Measured from Air Photos to Hydrology. Rio Grande, NM. Unpublished report prepared for the US Army Corps of Engineers, Urban Flood Demonstration Program, May 20, 2007. 45p.

Swanson, BJ, Meyer, GA, Coonrod, J. 2008. Coupling of Hydrologic/Hydraulic Models and Aerial Photos Through Time: Relating Geomorphic Change Measured from Air Photos to Hydrology. Rio Chama, NM, 1935-2005. Unpublished report prepared for the US Army Corps of Engineers, Urban Flood Demonstration Program, May 20, 2008. 37 p.

Swanson, BJ, Meyer, GA, Coonrod, J. 2010. Magnitude and uncertainty of channel planform measurements along a regulated river using aerial photography: Rio Grande near Albuquerque, New Mexico. *Earth Surface Processes and Landforms*, submitted 1/9/2010, revised 6/9/2010).

Trimble, SW. 1983. A sediment budget for Coon Creek basin in the Driftless Area, Wisconsin, 1853-1977 *American Journal of Science* 283: 454-474.

Van Steeter, MM, Pitlick, J. 1998. Geomorphology and endangered fish habitats of the upper Colorado River, 1, Historic changes instreamflow, sediment load and channel morphology. *Water Resources Research* 34: 287–302.

Wilcox, BP, Davenport, DW, Pitlick, DW, Allen, CD. 1996. Runoff and erosion from a rapidly eroding pinyon-juniper hillslope. British Geomorphological Research Group symposium: hillslope process, Bristol, UK, 20-22 Sep 1996.

Williams, G P, and Wolman, M G. 1984. *Downstream Effects of Dams on Alluvial Rivers*. US Department of the Interior, Geological Survey, 1286.

Winterbottom, SJ. 2000. Medium and short-term channel planform changes on the Rivers Tay and Tummel, Scotland. *Geomorphology* 34: 195-208.

Chapter 3

Tributary Confluences and Discontinuities in Channel Form and Sediment Texture: Rio Chama, NM

Authors:
Benjamin J. Swanson, PhD candidate, Department of Earth and Planetary Science, University of New Mexico

Dr. Grant Meyer, Department of Earth and Planetary Science, University of New Mexico

Dr. John Pitlick, Geography Department, University of Colorado

Abstract

Numerous morphological changes can occur where two channels of distinct sediment and flow regimes meet, including abrupt shifts in channel slope, cross-sectional area, planform style, and bed sediment size along the receiving channel. Along the Rio Chama between El Vado and Abiquiu Dams, northern New Mexico, arroyo tributaries intermittently deliver sediment from erodible sandstone and shale canyon walls to the mainstem channel. Much of the tributary activity occurs in flash floods and debris flows during summer thunderstorms, which often load the channel with sand and deposit coarser material at the mainstem confluence. In contrast, mainstem channel flow is dominated by snowmelt runoff. To examine tributary controls, we systematically collected cross-section elevation and bed sediment data up and downstream of 26 tributary confluences along a 17 km reach. Data from 203 cross-sections were used to build a one-dimensional hydraulic model for comparing estimated channel parameters at bankfull and low-flow conditions at these sites As compared to intermediate reaches, confluences primarily impact gradient and bed sediment size, reducing both parameters upstream of confluences and increasing them downstream. Cross-section area is also slightly elevated above tributary confluences and reduced below.

Major shifts in slope and bed sediment size at confluences appear to drive variations in sediment entrainment and transport capacity and the relative storage of sand along the channel bed. The data were analyzed and compared to models of channel organization based on lateral inputs, such as the *Network Variance Model* (Benda et al., 2004) and the *Sediment Link Concept* (Rice and Church, 1998). At a larger scale, hillslope-channel coupling increases in the downstream third of the study reach, where the canyon narrows, resulting in steeper slopes and more continuous coarse bed material along the mainstem, and thus, limiting the contrast with tributary confluences. However, channel form and sediment characteristics are highly variable along the study reach, reflecting variations in the size and volume of sediment inputs related to the surface geology in tributary watersheds, morphology of the Rio Chama at the junction (i.e., bends, confinement), and the relative magnitude and location of past depositional events.

Introduction

Until recently, scientists and engineers have primarily viewed rivers as linear systems, characterized by gradual and progressive changes in downstream channel form and process. Between their headwaters and their mouths, channels are predicted to steadily widen and deepen, decrease their slopes, and comprise smaller substrate sizes (Figure 1; Knighton, 1998, Benda et al., 2004). This linear perspective has informed, and been informed by, ideas ranging from downstream channel geometry relationships (Leopold and Maddock, 1953; Church, 1992), roughness adjustments (Bathurst, 1993), general patterns of sediment supply and storage (Schumm, 1977; Church, 2002), and the organization of lotic biota (Vannote et al., 1980).

A linear view of rivers predicts trends in channel form and ecology through watersheds reasonably well, especially at large scales. However, spatial variations in sediment and water yield along main channels and their tributaries often complicate these trends. Local differences in watershed geology, relief, climate, and disturbance type and magnitude (e.g., land use, fires, and dams) result in differences in runoff timing and volume within drainage networks. Additionally, differing sub-watershed characteristics may cause variations in channel and hillslope sediment yield and delivery processes (e.g., in snowmelt runoff, flash floods, or debris flows). Therefore, channels that drain dissimilar subcatchments often carry flows with much different magnitudes and peak runoff periods, as well as different sediment loads and calibers. Where tributaries and mainstem channels with these distinct sediment and flow regimes meet, numerous morphological changes can occur, and ultimately disrupt the gradual downstream trends predicted by the linear model (Figure 1). This alternative perspective, termed the *Network Variance Model* (Benda et al., 2004), has important implications for geologists, geomorphologists, engineers, and stream ecologists (Rice et al., 2008), especially in viewing streams at smaller scales (1-100 km reaches).

Depending on the relative differences in discharge, sediment size, and sediment load carried by a tributary and its mainstem channel, the mainstem may react in a variety of ways, both up and downstream of confluences (Knighton, 1980; Ferguson et al., 2006). Perhaps the main focus of research on the impact of tributary inputs has been the fluctuation of bed-sediment size along the receiving channels. At the largest spatial scales, bed material progressively changes from boulders or cobbles to gravels and then to sands along many river systems (e.g., Robinson and Slingerland 1998). However, at smaller scales, researchers have observed step-like discontinuities in the downstream fining trend (Miller, 1958; Church

and Kellerhals, 1978; Knighton, 1984; Dawson, 1988; Icham and Radoane, 1990; Brewer and Lewin, 1993; Rice and Church, 1998; Davey and Lapointe, 2006). These discontinuities are characterized by large increases in bed material size at confluences, where the volume and (or) size of the sediment influx redefines the attributes of the bed material along the main channel. Between the confluences, bed sediment sizes decrease, largely due to sorting processes along these subreaches (Rice and Church, 1998). In the literature, the point or zone of sediment input is often referred to as a lateral sediment source (LSS) and the segment of grain size reduction is termed a sediment link (Rice and Church, 1998 Davey and LaPointe, 2006). Observations of bed sediment discontinuities may also occur at other sediment sources along the mainstem, such as bedrock outcrops, bank erosion sites, and landslides (Davey and LaPointe, 2006). Although rarer, step decreases in particle size have also been observed at tributaries and other sources (e.g., Knighton, 1980; Brewer and Lewin, 1993), but their permanence depends on the volume of the input, as small amounts of finer material will likely be entrained.

Previous investigations of tributary effects on mainstem channel morphology have also focused on changes in hydraulic geometry associated with differences in discharge between tributaries and their mainstems, and downstream of confluences (Miller, 1958; Mosley, 1976; Best, 1988), as well as the flow structure and morphology at confluence sites (Rice et al., 2008 and sources therein). However, relatively little field research has focused on downstream changes in width, depth, or slope, especially in relation to bed sediment discontinuities at confluences. Researchers have documented increases in channel slope accompanying abrupt changes in flow and sediment discharge at channel junctions (Rice and Church, 1998; Ferguson, et al., 2006; Hanks and Webb, 2006), and Richards (1980) observed

downstream adjustments in mainstem channel width below tributary-mainstem junctions. Benda et al. (2004) reviewed 14 studies that explored geomorphic impacts at 168 confluences in humid and semi-arid sites in the western United States. Responses included gradient adjustments, changes in substrate character, upstream sediment deposition, channel instability, and the formation and (or) presence of rapids, terraces, floodplains, side channels, midchannel bars, meanders, ponds, and log jams. Additionally, longer-term tributary controls on channel character are implied in examinations of fan impingement on mainstem channels (Russell, 1954; Grant and Swanson, 1995), and large, debris flow-related convexities in the longitudinal profile of the Colorado River (Hanks and Webb, 2006).

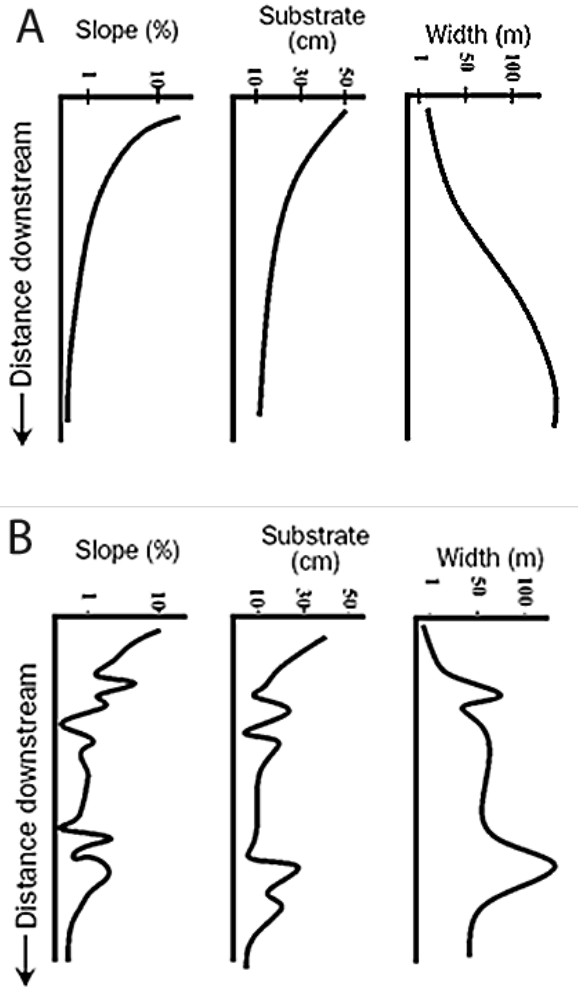

Figure 1. Linear model (A) versus network variance model (B) for predicted downstream trends for various channel characteristics (adopted from Benda et al. 2004). The linear model predicts general trends at large scales (>>10^2 km), but the network variance model includes breaks in these trends caused by disturbances along the channel, especially related to water and sediment inputs at tributary junctions.

Complex shifts in cross-sectional shape, planform, slope, and bed material along a channel are especially likely in rivers flowing through mountainous or canyon environments. Geology, relief, and other watershed characteristics are typically more heterogeneous than in lowland regions. Also, channels are more frequently and more directly connected (cf.

Harvey, 2001) to hillslopes through major pulses of erosion and sediment transport. Mountain river reaches are commonly impacted by landslides, debris flows, and flash floods, in contrast to lowland channels that receive a more consistent sediment supply (e.g., Benda and Dunne, 1997). Sediment delivered during hillslope events dominates the supply along some reaches, and associated large volumes and sediment sizes are more likely to force changes in downstream channel parameters, such as gradient, width, and clast size.

In this study, we investigated the impacts of 26 tributary channels, including debris-flow dominated tributaries, along 17 km of the lower Rio Chama Canyon in northern New Mexico. First, we describe the influence of tributary channels on mainstem Rio Chama geomorphology, including channel bed sediment, gradient, and channel geometry. We then compare these results to current models of how tributary inputs should impact the system, and expand on the models of sediment discontinuity presented by Rice and Church (1998) and Davey and Lapointe (2006). Most prior studies have concentrated only on larger tributaries or those that create larger impacts (Benda et al., 2004). However, the 26 tributary junctions covered here represent 86% of the total junctions along the river, including a wide range of tributary sizes and input types. Additionally, investigations of the sediment link concept have been focused on alpine environments in the northwestern United States and British Columbia, Canada (Rice et al., 1996; Rice and Church 1998), and along the St. Mary River in the glaciated Canadian Shield of eastern Canada (Davey and LaPointe, 2006), where links are often structured around discrete tributaries or point sources of coarse sediment. Our study was conducted in an arid environment characterized by a wide variation in channel hydrology and sediment delivery, making it well-suited to investigate multiple aspects of

tributary impacts to discontinuities in both morphology and sediment characteristics at tributary confluences.

Study Area

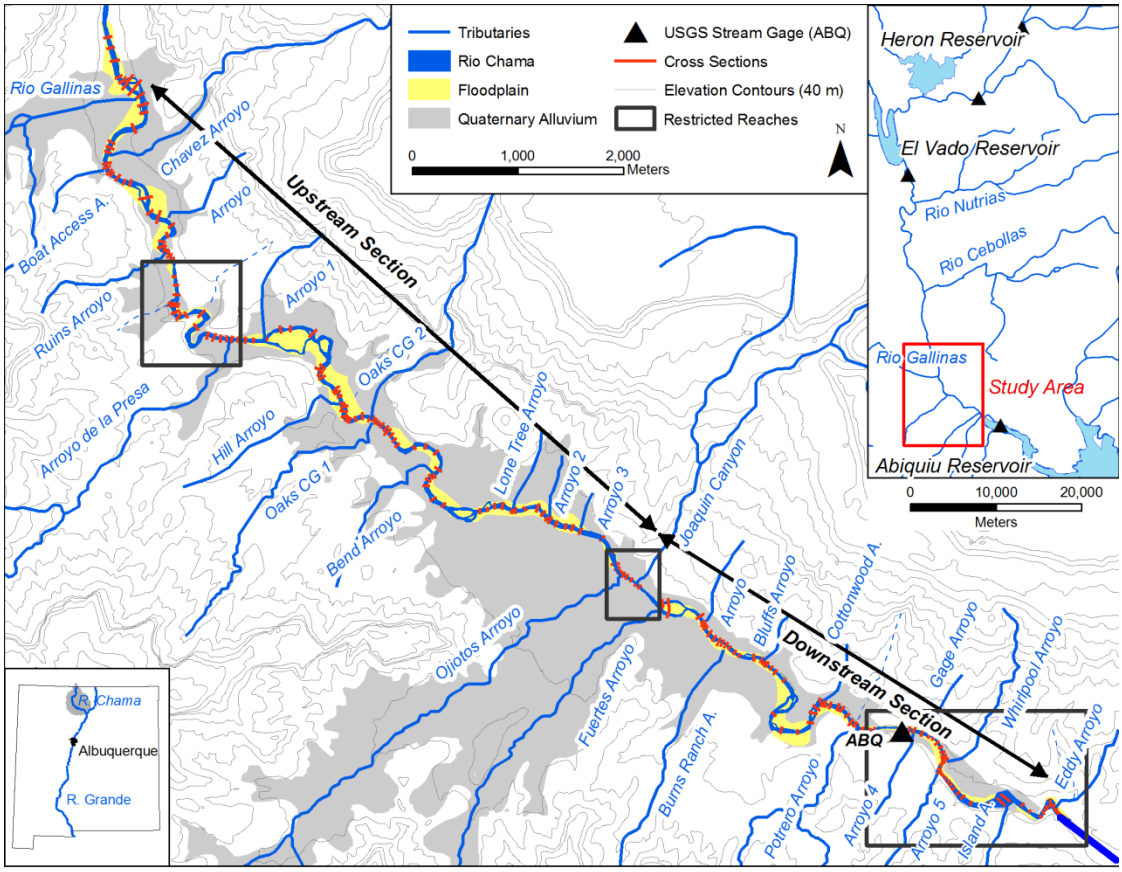

Figure 2. Rio Chama Study Area, NM, between the Rio Gallinas confluence and the upstream end of Abiquiu Reservoir. The channel flows within a relatively narrow floodplain, bordered by a variable area of Quaternary tributary alluvial fan deposits and local fluvial terraces. Black boxes indicate where the channel is at least partially semi-confined by bedrock and (or) bouldery landslide and fan deposits. The study reach is divided into an upstream and downstream section based on changes in sediment size, slope, and channel areas (see text).

Setting. The Rio Chama is the largest tributary to the Rio Grande in New Mexico, draining 8,300 km^2 above its confluence with the Rio Grande near Española, NM (Figure 2). The river is divided into upper, middle and lower sections by El Vado and Abiquiu Dams,

respectively. The middle section, between these dams, flows with the Chama Canyon, and the study reach lies at the downstream end of the canyon. Rio Chama headwater streams drain the southern San Juan Mountains, characterized by conifer forests, snowmelt-dominated hydrology, and variable but relatively resistant bedrock. The middle and lower watersheds are characterized by more erodible sedimentary rocks, sparser shrub vegetation, and summer monsoon-dominated storm hydrology of the Colorado Plateau and Rio Grande Rift (Fogg et al., 1992; Love and Connell, 2005).

The study reach includes 17 km of the middle Rio Chama downstream of El Vado Dam, between the Rio Chama – Rio Gallinas confluence and the upper end of Abiquiu Reservoir (Figure 2). The lower Chama Canyon here is formed primarily in Triassic and Jurassic mudstones and sandstones capped by Cretaceous Dakota Formation sandstone. The rocks are often exposed along cliff faces, although large landslide deposits, primarily consisting of failed Morrison formation mudstone and Dakota sandstone, cover many of the canyon slopes. Large volumes of sediment are deposited along the canyon and valley floor, including thick sand deposits (2- 5 m) presumably linked to Holocene tributary and hillslope activity (Persico et al., 2005). These deposits are larger in area on the west side of the river, and generally pin the channel to the east side of the canyon (Figure 2).

Hydrology. Average high temperatures in the semi-arid study area range between 5.6°C in the winter and 30.6°C in the summer; average lows vary from -8.6°C to 14.4°C. Average annual precipitation in the study area is approximately 28 cm (26 cm at Abiquiu Dam, NM, and 30.5 cm at Ghost Ranch, NM; wrcc.dri.edu), with over half falling during short duration, high intensity, summer thunderstorms. Higher elevations in the Rio Chama

headwaters receive up to about 100 cm of precipitation, including a greater proportion of winter snowfall.

Two USGS stream gages bracket the Rio Chama study reach (Figure 2). At the Rio Chama below El Vado Dam (EVD) gage (08285500; waterdata.usgs.gov), the record spans from 1914 through the present, with continuous daily data recorded since 1935. The Rio Chama above Abiquiu Reservoir (AQR) gage (08286500; waterdata.usgs.gov) includes data from 1961 through the present. Since 1961, EVD and AQR gages have measured similar flows (EVD= 0.93*AQR; R^2=0.98), with average daily flows of 12 and 13 m^3/s, respectively. Major differences in discharge at the two gages occur during spring snowmelt runoff or following substantial precipitation events in the middle watershed. Most of the additional flow at AQR, especially during spring runoff, likely enters the Rio Chama from larger tributaries between El Vado Dam and the study reach (i.e., Rio Cebollas and Rio Nutrias; Figure 2). The downstream section of the Rio Gallinas flows most of the year, but discharge during annual dry periods is insignificant (< 1 m^3/s). It also enters within the first kilometer of the study reach. Therefore, for this study, flow along the entire reach is assumed to equal the flow at AQR.

Mean peak flow at AQR is 96 m^3/s, with average maximum peak flows (top 10%) of 170 m^3/s and average minimum peaks (bottom 10%) of 42 m^3/s. The 2-year flood is approximately 80 m^3/s. However, El Vado Dam moderates flood flows within the study reach. Pre-dam peak flow measurements collected at EVD between 1914 and 1924 (n=7) averaged 137 m^3/s. Since 1961, the mean annual peak discharge at the Rio Chama at La Puente (LPT) gage (08284100)), upstream of the dam, is 124 m^3/s, which is 30% higher than the mean peak flow at AQR. Additionally, a regression equation based on a comparison

between daily flows at the Rio Grande at Otowi gage with discharge data at LPT, and its predecessor, the Rio Grande near Park View gage (08283500), predicts an average pre-dam peak discharge of at least 135 m^3/s, 40% higher than the post-dam average (LPT=0.48RGO-17.8; R^2=0.78). Although operations at El Vado Dam dominate channel discharge in the reach, flood peaks and therefore channel dynamics are still primarily associated with spring snowmelt from the upper watershed (Figure 3). Summer storms also increase flows. They generally occur over small areas, but may generate high magnitude, relatively short duration flood events along the mainstem. Most of the sediment movement in the tributary watersheds occurs during these storm events (Figure 3).

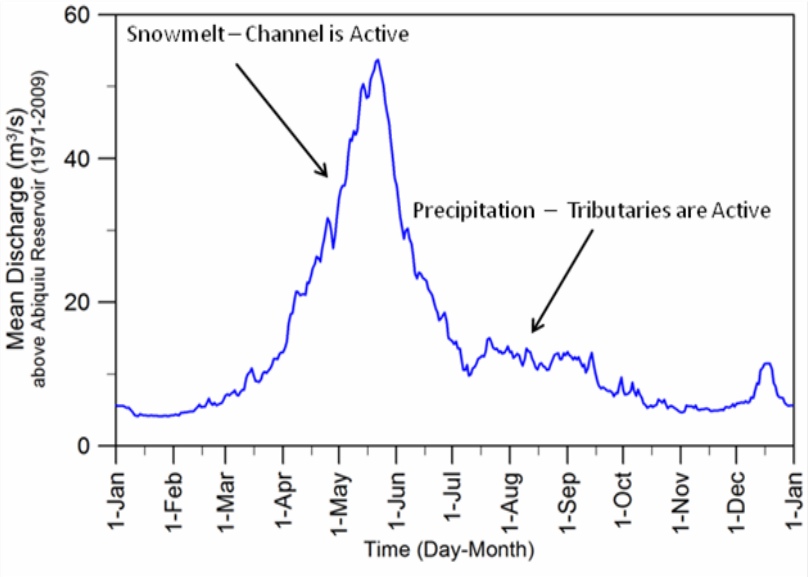

Figure 3. Average daily discharge for the Rio Chama above Abiquiu Reservoir (AQR) gage. The hydrograph shows a large peak associated with spring snowmelt runoff, followed by a period of slightly elevated flows representing short duration, high magnitude convective storms during the summer monsoon. Most of the geomorphic work in the mainstem Rio Chama occurs during the snowmelt period, whereas most of the work in the tributaries occurs during and after localized convective storms.

Channels. Within the valley, the river alternates between alluvial and semi-alluvial reaches. Channel movement is limited by boulders deposited by debris flows at some fan toes and by large Quaternary landslides on the northeast bank opposite of Potrero Arroyo and at Gage Arroyo. Bedrock confines the channel from *Ruins Arroyo to Arroyo de la Presa* and downstream of *Potrero Arroyo* (Figure 1; dark gray areas in Figures 5, 7-11). Along the study reach, channel bed material alternates between dominantly sandy subreaches and those characterized by cobbles and boulders. Since closure of El Vado Dam, the study reach has narrowed from an average width of around 55 m to 40 m, but the rate of channel change has been much slower over the past two decades. Most of the change occurred between the Rio Gallinas and Rio Chavez junctions, and in alluvial reaches further downstream (Swanson et al., 2010).

The tributaries entering the Rio Chama along the study reach drain areas ranging from 0.2 to 67.2 km^2, except for the Rio Gallinas which has a watershed area of 726 km^2. These tributaries have built alluvial fans of widely varying size and texture on the canyon floor. Tributary channels are commonly incised within the fan deposits, although some of these arroyos are discontinuous and flow becomes unconfined before reaching the river. Bed material at the downstream ends of the arroyos is primarily sand and small gravel, but a wide range of deposit textures is present (Faulconer, 2011). They are intermittent channels characterized by flash floods and (or) debris flows during intense summer thunderstorms. As such, they often carry high-volume sediment pulses with a wide range of sediment sizes. Along the Rio Chama, deposits at tributary mouths range from small, cobble and gravel debris cones, to broad sandy fans, to channel-spanning debris-flow boulder deposits and downstream bars of varying size and age (Figure 4). These deposits are generally inundated

at flows between 20% and 50% of the 2-year recurrence interval, but areas of some fans remain shallow relative to the thalweg.

Figure 4. Tributary fan and rapid formed at the mouth of Canada del Presa. Flow is from right to left. The fan comprises newly deposited sand and small gravels (2007) over debris-flow cobbles and boulders. The deposit creates an area of deeper, low-velocity flow upstream, and steeper, shallower flow downstream.

Methods

Field data. In order to examine tributary impacts on channel parameters, a series of cross sections was surveyed at 26 tributary junctions along the study reach. Sites were chosen based on air photo and field reconnaissance, and included 90% of the tributaries that, since 1935, clearly extended to the river margin before becoming unconfined, including 2 sites where the downstream terminus of the arroyos have filled in or been abandoned over that time. Gully channels that reach the river, but are clearly associated with road construction (i.e., little discernable channel upstream of the road), were not included in the total, and seem to have little current impact on the Rio Chama. At each confluence site, between 4 and 12 (mean = 6) cross sections were surveyed using Leica Total Station

equipment. At least one cross section was located in each of three subreaches: (1) directly *upstream* of the confluence, (2) along the tributary *fan* (immediately below the confluence), and (3) *downstream* of the confluence. Each cross section was placed to best represent local channel geomorphology (i.e., bed and bank material, width, depth, water surface slope). Spacing between cross-sections within each tributary site was nonetheless relatively even (20 – 40 m). Additional data were collected between tributary sites for comparison. These *intermediate* cross sections were located in riffles and runs not directly associated with any tributary inputs. All cross sections included adjacent floodplain surfaces, estimated top of bank, water surface elevations, and breaks in slope within the channel cross section. Top of bank (bankfull stage) positions were determined by locating a distinct break in bank slope and vegetation. Additionally, a longitudinal water surface profile was surveyed along the entire study reach at a discharge of 13 m^3/s. Points for the profile were spaced an average of 40 m apart and included all major breaks in slope.

At each surveyed cross-section, sediment was characterized using a modified Wolman pebble count (Wolman, 1954). Grain size diameters were measured at 0.5 ψintervals using a gravelometer every 0.2 m across the entire channel bed ($\psi = \log_2 D$). The mean number of measurements per cross section was 168, ranging from 53 to 361. The five cross sections with less than 100 samples were located along narrow channels dominated by boulder and bedrock beds. In sand-dominated subreaches, attempts were made to measure any gravel buried by less than 15 cm of sand, but the sand deposits were often deep and therefore, the number of gravel samples was often less than 100 at these cross sections. Notable grain size percentiles for each cross section (D_{16}, D_{50}, and D_{84}, where D is the clast diameter where 16%, 50%, and 84% of the sample, respectively, is finer) were determined

visually from histograms of the pebble count data. The geometric mean of the grain size (D_{am}) at each cross section was calculated as $\sqrt{D_{16} \times D_{84}}$.

Hydraulic modeling. Field surveys were conducted during low flow conditions between 2 and 8 m^3/s for cross-sections and pebble counts and 13 m^3/s for the long profile. To predict channel and hydraulic properties at given flows, such as the estimated bankfull flood, two HECRAS models were developed using the cross section data up- and downstream from Ojitos Arroyo, respectively. The models were fit to the water surface data collected during the field surveys by adjusting the Manning's roughness value over the reach. Final low-flow roughness values were 0.056 for the upstream model and 0.074 for the downstream reach, reflecting the greater degree of channel-hillslope connectivity and generally coarser bed material along the downstream section (this study). Additionally, downstream surveys were generally conducted at lower flows to reduce risk of accident in the steeper, rockier subreaches. Modeled water surface elevations compared relatively well to field measurements ($R^2 = 0.94$), with average differences between measured and modeled water surface elevations of 1 cm, standard deviation of 5 cm, and a maximum difference of 15 cm. The resulting long profile also visually compared well to the long profile surveyed in the field. For bankfull conditions, the discharge was set to 70 m^3/s (recurrence interval ~ 1.8 yrs) and roughness values were reduced to 0.028 for both models. Model output agreed relatively well with bankfull channel parameters identified in the field. Regression coefficients (R^2) for field estimations of the bankfull channel versus model outputs were 0.88 for width, and 0.85 for average depth.

Statistics. The spatial variability inherent in channel characteristics often complicates the identification of discontinuities in channel attributes at tributary junctions.

In order to delimit statistically significant changes in channel characteristics (e.g., D_{50}, slope, width, depth), all of the data from cross-sections classified as *intermediate* (those located between the tributary sites) were compared to 1) the cross-section data obtained for the *upstream*, *fan*, and *downstream* subreaches grouped for the entire study reach, and to 2) the data collected in the *fan* group at each individual site ("significant" will refer to "statistically significant" in the rest of this chapter). For the most part, the data were not normally distributed, so the analyses tested for differences in mean values using the nonparametric Mann-Whitney Rank Sum test at a significance level of 5% ($\alpha = 0.05$).

For the sediment data, we also followed the method for statistically identifying sediment links presented by Rice and Church (1998). This method detects sites having a statistically significant increase in sediment size compared to the channel just upstream. It assumes decreases in sediment size at confluences due to inputs of finer sediment are relatively short lived, because the relative coarseness of the mainstem indicates it can remove the finer material. We expand on this method by using Mann-Whitney Rank Sum U-Tests ($\alpha = 0.05$) to compare the sediment diameters at the five cross-section sites immediately upstream, which is, on average, approximately 10 channel widths. Including additional upstream cross-sections is justified because of the relatively short spacing between cross-sections in our study. This provides a better test for reach-scale impacts from tributary inputs. The practice also reduces the influence of the sand often stored upstream of debris flow fans on the analysis. The sediment link analysis differs from the comparisons between geomorphic sites by including all of the pebble count data for the individual cross-sections (not just the mean D_{50}, D_{84}, or D_g for the cross-sections in each position), and it analyzes the data at a more local scale. Analyses using the raw data and data converted to the ψ scale

($\log_2 D$) provided similar results (converted data provided in Figure 5). Finally, although the sample size is small, Mann-Whitney Rank Sum U-Tests ($\alpha = 0.05$) were also used to compare channel shape parameters at each cross-section with data from the five cross-sections immediately upstream. For these one-tailed tests, the expected difference between means was assumed to match the overall trend for the study reach. For example, slope increases downstream of the majority of the tributary junctions along the Rio Chama study reach (see Results), so for the difference in mean values between a cross-section site and the five cross-sections immediately upstream to be "significant", the change in the mean had to be positive as well as statistically valid. Similarly, depth and area were expected to decrease, and width and sediment size were expected to increase. Although the sample size is small and the data are non-normal, the statistics provide a sense of where discontinuities in channel characteristics are occurring.

Watershed analysis. In order to investigate how various tributary watershed characteristics might modify their channel impacts on the mainstem, a 30-m digital elevation model (DEM) of the study area was divided into subwatersheds in a GIS using hydrology tools provided in TauDEM (http://hydrology.usu.edu/taudem/taudem5.0/documentation.html). Within each subwatershed, grid analyses were conducted to calculate total area, stream length, and relief, as well as cell-by-cell slope, stream order, and a surrogate for stream power (contributing area x slope). The cell-by-cell values were averaged over each subwatershed and along the main, DEM-defined channel within the subwatershed. These values were then compared to reach-averaged (*fan* sites) mainstem sediment size (D_{50}, D_{84}), geometry (slope, depth, and width, and a measurement of downstream impact length based on visual air photo analysis and the channel geometry survey data. Rice (1998) performed a

similar analysis with watershed area, slopes, stream power, and other factors measured from DEMs to determine surrogates to field data for locating which tributaries might disrupt downstream sediment fining.

Results

Along the Rio Chama, local tributaries are responsible for supplying much of the current coarse bed sediment, as shown by the overwhelming prevalence of sandstone rock types from these tributary basins over quartzites and other metamorphic and volcanic lithologies that predominate in the upper Rio Chama basin. The pebble count data included far fewer metamorphic clasts than the more local sandstones (>10%), and most of those likely came from local terrace deposits. Coarse sediment is delivered by tributaries during short pulses associated with summertime convective thunderstorms. Because they occur during periods of relatively low mainstem flow, tributary water discharges likely have little impact on the channel directly; however, coarse sediment delivered to the Rio Chama along tributary channels during these storms likely impacts mainstem form and process.

Bed sediment. Bed sediment texture is quite variable along the study reach (Figure 5), with D_g ranging from sand (< 2 mm; < 1ψ) to cobbles (140 mm; 7ψ). Much of the gravel and cobbles are subangular to angular, and often embedded. Using all of the pebble count data the geometric mean (D_g) is 4.1ψ (17 mm), and the median grain size (D_{50}) of the reach is 4.6ψ (24 mm), D_{16} is 1ψ (2 mm), and D_{84} is 7.2ψ (143 mm). With the sand fraction removed from the analysis, D_g, D_{50}, D_{16}, and D_{84} are 5.8ψ, 6.1ψ, 4.1ψ, and 7.5ψ (55, 70, 17, and 176 mm), respectively. Although the channel bed is primarily gravels and cobbles, sand accounted for 33% of the sampled bed sediment, placing the Rio Chama as transitional between a gravel-bed and sand-bed river (Wilcock, 1993).

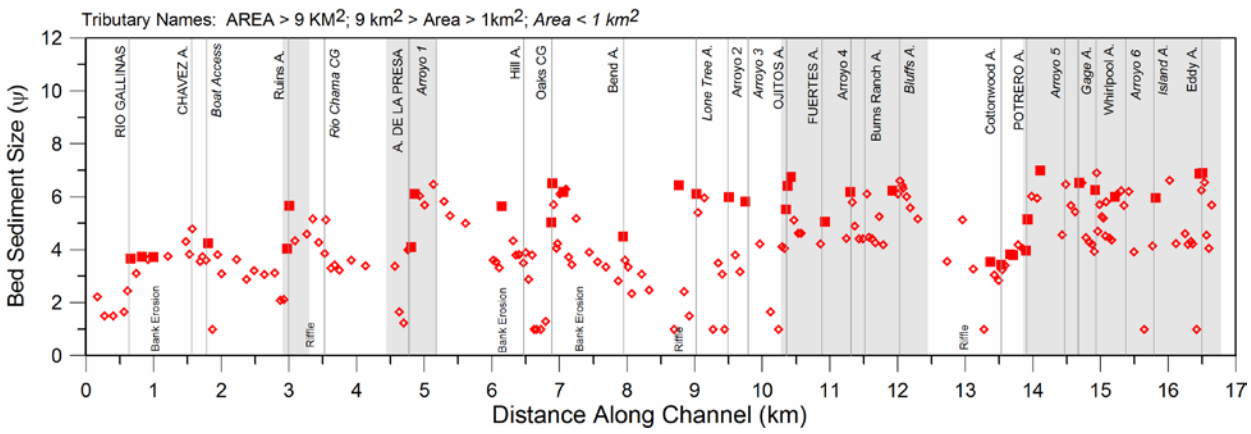

Figure 5. Grain size changes along the Rio Chama study reach. Red squares represent the 33 locations where the increase in grain size is statistically significant compared to the 5 cross sections upstream. These sites of significant change are associated with 19 of the 26 confluences. Gray areas represent reaches of river partially semi-confined by bedrock.

Much of the variability in the sediment data appears to be associated with tributary inputs. As in previous studies (Church and Kellerhals, 1978; Rice and Church, 1998, Davey and LaPointe, 2006; etc), sediment size typically increases sharply at confluences, often by 3ψ or more, and then declines until the channel encounters the next substantial sediment input. In some cases, such as confluences with *Ruins, Presa, Oaks, and Eddy Arroyos*, a sharp drop in grain size occurs just upstream of the junctions as well. The sediment data grouped by geomorphic position support this generalization (Table 1; Figure 6). Grain size data collected in the *upstream* positions have a mean of 9 mm for D_g, 3 mm for D_{16}, 7 mm for D_{50}, and 30 mm for D_{84}, compared to larger means of 17, 4, 16, and 78 mm, respectively, for the *intermediate* group (Table 1). Mean D_g, $D_{16,}$ and D_{84} for the *fan* group, however, are double the mean D_g, $D_{16,}$ and D_{84} for the *intermediate* group, and the D_{50} for the *fan* category is 2.9 times larger. Relative to the *intermediate* group, all the shifts in sediment-size

seen in the other groups are statistically significant (U-test, $\alpha = 0.05$) except the D_{16} for the *downstream* category (Table 1). With the sand fraction removed from the analysis, the relationships remain the same, except the difference between the mean D_{16} at the *upstream* and *intermediate* sites is significant, but the difference between the D_{50} particles and D_{84} particles at these two locations is not. Additionally, greater variability is associated with the bed-sediment data for the *fan* and *downstream* groups under both scenarios (Figure 6).

	D_{16}			D_{50}			D_{84}			D_g		
Geomorphic Position	mean(ψ)	mean(mm)	probability	mean(ψ)	mean(mm)	probability	mean(ψ)	mean(mm)	probability	mean(ψ)	mean(mm)	probability
intermediate	1.8	3.5	---	4.0	16.1	---	6.3	77.6	---	4.0	16.5	---
upstream	1.3	2.5	0.097	2.8	6.8	0.019	4.9	30.0	0.022	3.1	8.7	0.005
fan	3.0	7.9	<0.001	5.5	46.4	<0.001	7.2	149.4	<0.001	5.1	34.1	0.001
downstream	2.4	5.3	<0.001	5.2	36.3	0.003	7.0	130.5	<0.001	4.9	29.2	<0.001
Geomorphic Position	$D_{16\ gravel}$ mean(ψ)	mean(mm)	probability	$D_{50\ gravel}$ mean(ψ)	mean(mm)	probability	$D_{84\ gravel}$ mean(ψ)	mean(mm)	probability	**Sand %** mean(%)		probability
intermediate	4.4	20.5	---	5.8	57.2	---	6.9	118.5	---	33%		---
upstream	3.8	13.5	0.010	5.2	35.7	0.058	6.7	100.6	0.652	52%		0.001
fan	4.7	26.2	0.038	6.3	81.0	0.006	7.5	175.5	<.001	19%		0.001
downstream	5.0	31.0	0.003	6.5	91.6	0.001	7.6	199.3	<.001	26%		0.140

Table 1. Statistical analysis (Mann-Whitney Rank Sum Test) results comparing mean grain size parameters adjacent to tributary junctions to the grain sizes found in the intermediate positions. Based on $\alpha = 0.05$, most of the results indicate that significant increases in grain size occur along the fans and downstream of the junctions.

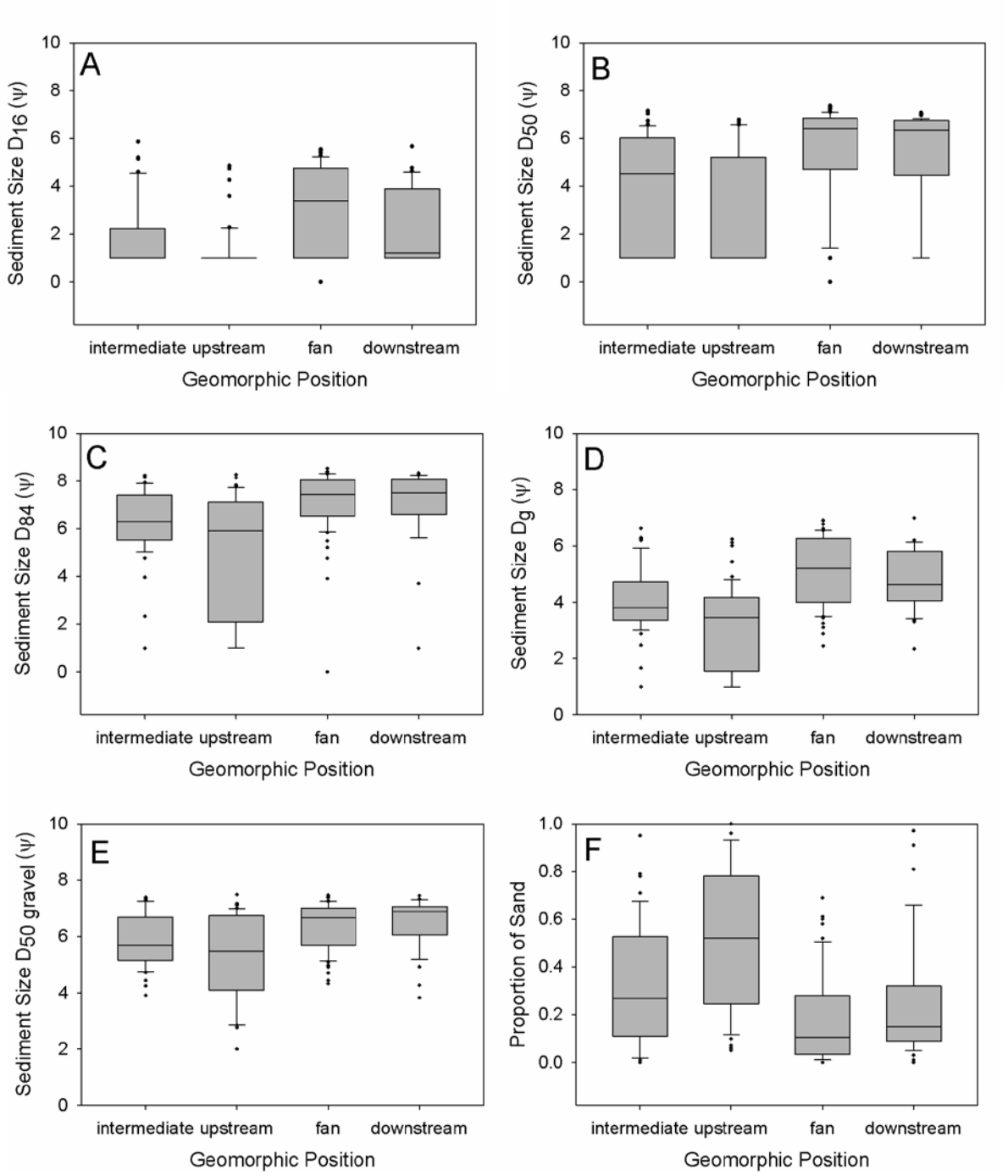

Figure 6. Comparison of sediment size data at various geomorphic positions relative to tributary confluences. In general, sediment sizes are larger and more variable at cross-sections categorized as fan or downstream sites and slightly finer at cross-sections directly upstream of junctions. Upstream sites also comprise a higher proportion of sand along the bed. A) Grain size where 16% of the sample is finer (D_{16}). B) Median grain size (D_{50}). C) Grain size where 84% of the sample is finer (D_{84}). D) Geometric mean grain size (D_g). E) Median grain size (sand removed; $D_{50\ gravel}$). F) Proportion of sand along the cross-section.

	Dgm		%sand		Slope		Width		Depth		Area	
Confluence	*mean (mm)*	*probability*	*mean (%)*	*probability*	*mean(m/m)*	*probability*	*mean(m)*	*probability*	*mean (m)*	*probability*	*mean (m^2)*	*probability*
Rio Gallinas	10	1.01E-04	54%	2.89E-07	0.0018	2.78E-01	63	2.03E-19	0.71	1.22E-15	63	3.11E-12
Chavez Arroyo	21	2.75E-01	18%	9.53E-05	0.0012	2.29E-02	41	1.95E-02	1.01	8.63E-06	42	7.51E-02
Boat Access	16	1.37E-02	34%	4.25E-01	0.0011	8.16E-03	37	3.80E-01	0.97	2.72E-07	36	4.11E-05
Ruins Arroyo	16	2.35E-02	17%	4.00E-05	0.0030	2.27E-07	21	2.77E-13	0.95	8.43E-08	21	4.47E-16
Rio Chama Campground	25	2.79E-01	37%	1.58E-01	0.0012	2.29E-02	66	2.42E-21	0.99	1.88E-06	65	7.14E-14
Arroyo de la Presa	34	5.18E-04	30%	2.50E-01	0.0035	1.24E-10	41	2.22E-02	0.92	6.24E-09	37	8.45E-05
Arroyo 1	89	6.20E-25	4%	2.34E-10	0.0052	4.52E-20	41	3.31E-02	0.69	4.56E-16	28	7.32E-11
Hill Arroyo	11	3.01E-04	37%	1.47E-01	0.0009	7.57E-04	48	6.83E-08	1.03	3.00E-05	49	2.29E-02
Oaks Campground	48	2.08E-10	24%	8.35E-03	0.0030	2.27E-07	32	6.03E-04	1.13	2.21E-02	36	6.14E-05
Bend Arroyo	18	4.81E-02	25%	1.88E-02	0.0005	2.85E-06	47	4.08E-07	1.09	1.68E-03	51	1.71E-03
Lone Tree Arroyo	56	1.04E-13	10%	3.99E-08	0.0012	2.29E-02	38	3.60E-01	1.11	5.66E-03	43	1.32E-01
Arroyo 2	64	7.91E-17	0%	6.20E-12	0.0022	1.13E-02	51	1.90E-10	1.01	8.63E-06	51	8.08E-04
Arroyo 3	57	3.42E-14	6%	1.50E-09	0.0030	2.27E-07	42	1.25E-02	1.39	1.76E-04	58	1.25E-08
Ojitos Arroyo	80	2.45E-22	7%	2.80E-09	0.0059	3.87E-23	39	2.80E-01	1.02	1.43E-05	39	4.40E-03
Fuertes Arroyo	64	8.41E-17	3%	9.35E-11	0.0103	3.39E-36	61	2.88E-18	0.72	3.34E-15	44	3.33E-01
Burns Ranch Arroyo	33	1.46E-03	19%	2.74E-04	0.0039	4.00E-13	32	5.62E-04	0.96	1.84E-07	31	3.84E-09
Bluffs Arroyo	88	1.34E-24	2%	5.07E-11	0.0035	1.24E-10	35	3.25E-02	1.09	2.30E-03	38	5.87E-04
Cottonwood Arroyo	10	1.13E-04	45%	1.22E-03	0.0010	2.60E-03	49	1.90E-08	1.36	1.33E-03	67	8.89E-15
Potrero Arroyo	39	5.72E-06	20%	6.61E-04	0.0085	8.49E-32	35	3.68E-02	0.95	8.43E-08	33	1.82E-07
Arroyo 5	89	6.39E-25	4%	2.34E-10	0.0052	4.52E-20	32	6.14E-04	1.01	8.63E-06	30	2.05E-09
Gage Arroyo	93	6.32E-26	5%	5.91E-10	0.0064	4.24E-25	27	2.29E-08	0.88	3.63E-10	24	3.67E-14
Whirlpool Arroyo	75	1.13E-20	11%	1.20E-07	0.0041	2.60E-14	33	3.39E-03	1.14	3.61E-02	38	7.72E-04
Arroyo 6	30	1.82E-02	20%	5.07E-04	0.0052	4.52E-20	37	3.89E-01	0.89	7.84E-10	32	1.45E-08
Island Arroyo	51	1.03E-11	8%	9.75E-09	0.0088	1.34E-32	37	3.48E-01	0.70	8.80E-16	26	2.59E-12
Eddy Arroyo	40	1.44E-06	17%	2.57E-05	0.0065	1.80E-25	42	5.84E-03	0.70	6.33E-16	29	1.04E-10
Intermediate	***23***		***33%***		***0.0017***		***38***		***1.22***		***45***	

Table 2. Statistical analysis comparing channel parameters in the fan reach of each site to the data for all the intermediate sites. Light shading indicates significant shifts in the means in the expected trends, and dark indicates shifts in the means in the direction opposite of the expected trend. Grain sizes, slopes, and widths were expected to increase, and cross-section area, depths and sand % were expected to decrease.

At each tributary site along the study reach, however, the fluctuations in bed-sediment sizes are more complicated than the grouped data suggest (Figure 4, Table 2). Compared to the sediment at all the cross-sections classified as *intermediate*, fans with significantly larger bed sediment occurred at 18 of the 26 tributary junctions, but clast sizes at *Gallinas, Boat Access, Hill, and Cottonwood Arroyos* were significantly smaller. The modified Rice and Church (1998) sediment link analysis found 33 cross-sections that could be classified as supply points (Figure 4). Of these 33 cross-sections, 27 are directly related to tributary fans at 19 of the 26 confluences (73%). Four additional significant points of sediment supply were identified where eroding banks included gravel deposits instead of primarily sand (i.e.,

upstream of *Hill, Lone Tree,* and *Cottonwood Arroyos,* downstream of *Oaks Campground*). The remaining two locations, upstream of *Cottonwood* and *Bluffs Arroyos*, respectively, are associated with riffles formed in bends along the channel as described in Davey and LaPointe (2006). Except for at *Hill Arroyo*, grain size increases at each of the arroyo sites at and immediately downstream of the junction.

Sand. Much of the variability in sediment size at tributary junctions relates to the amount of sand stored within the channel. The mean proportion of sand at cross-sections categorized as *upstream* of confluences was 52% versus 27% for the *intermediate* group and 9% for the *fan* group (significant at $\alpha = 0.05$). Along the channel, twenty of the 26 tributary sites were associated with statistically significant decreases in sand along the bed. Sand bed subreaches (sand fraction > 50%) form upstream of many of the junctions, especially where tributary fans constrict the channel, such as at *Presa, Oak Campground, Ojitos,* and *Eddy Arroyos* (Figures 6 and 7). The subreach between *Lone Tree Arroyo* and *Ojitos Arroyo* is primarily a sand bed channel, in part related to the large embayment in the canyon to the southwest which is characterized by voluminous sandy tributary fan deposits. The channel is also semi-confined at *Ojitos Arroyo* between the fan deposits of that drainage and a complex of coarse bouldery debris-flow deposits emanating from Joaquin Canyon just downstream (Figure 2). This constriction is associated with a major long-profile convexity and low upstream gradients (Figure 8). The proportion of sand along the bed also seems to be modified by local conditions, such as along large point bars and sandy fan complexes, and at tight bends against bedrock walls which force upstream deposition.

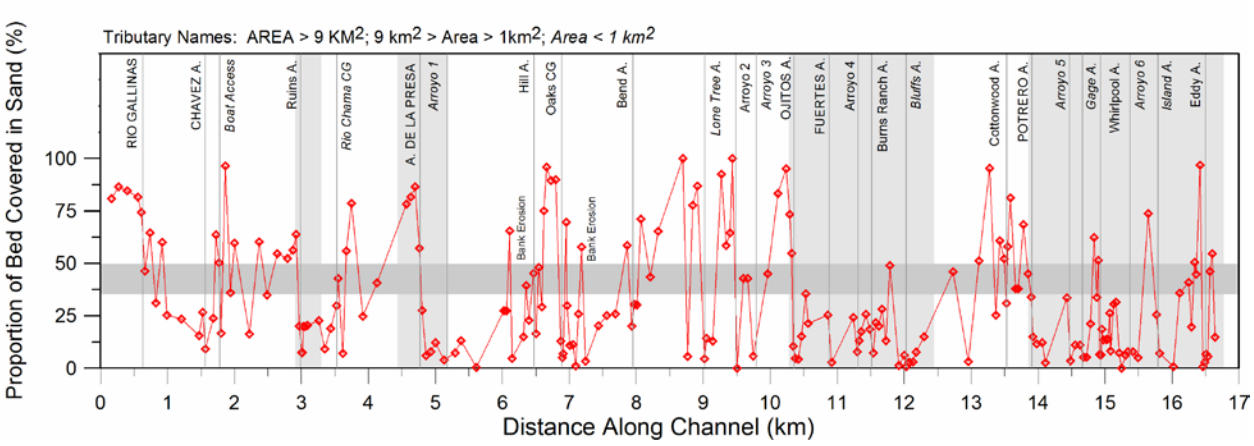

Figure 7. Proportion of sand along the channel bed within the study reach. Sand tends to accumulate upstream of many of the tributary junctions (> 70% sand at *Presa, Oaks, Lone Tree, Ojitos, Eddy*, and others), and is relatively low (< 20%) downstream of these junctions. Exceptions include the *Boat Access, Hills Arroyo,* and *Cottonwood Arroyo.* Light gray shading represents reaches of river partially semi-confined by bedrock. Dark gray horizontal shading represents transition from sand bed to gravel bed.

Channel slope. Overall, the longitudinal profile of the Rio Chama study reach is slightly convex; however, it is divided into concave segments broken by distinct inflections (Figure 8). The inflections are often associated with tributary confluences, although the largest changes in the profile, at *Arroyo de la Presa, Ojitos Arroyo, and Potrero Arroyo*, are also related to narrower valleys and Quaternary landslide and debris-flow deposits (Figure 2). The flatter reaches, from *Rio Gallinas to Ruins Arroyo*, from *Bend* to *Ojitos Arroyo*, and from *Bluffs* to *Potrero Arroyo* are less semi-confined. Below *Potrero Arroyo*, the valley narrows and the steeper channel is semi-confined by bedrock and boulders at the base of large fan deposits.

Mean friction slope, calculated in the HECRAS model, for the entire study reach is 0.0026, with average slopes of 0.0015 upstream of the Ojitos Arroyo inflection point and 0.0037 downstream. However, slope is highly variable along both reaches, and much of the

variability is associated with tributary junctions (Figure 9). Slopes increase downstream of almost every tributary site, and the largest slope values, typically between 0.01 and 0.02, occur just downstream of tributary junctions, especially between *Potrero Arroyo* and the downstream end of the study reach, and in the other more semi-confined reaches (e.g., *Arroyo de la Presa, Ojitos Arroyo*). Comparing each cross-section with the 5 cross-sections directly upstream shows 39 cross-sections with statistically significant increases in bankfull slope. Of these 39 sites, 31 are directly related to tributary fans at 17 of the 26 confluences (65%; Figure 9). At low flow, 20 of the 26 tributary sites have significantly larger slopes. Smaller tributaries and tributaries with predominantly sandy deposits rather than gravels and cobbles have less impact on the slope (e.g., *Cottonwood* and *Bend Arroyos)*. Significant increases in slope also occur where the channel erodes gravelly banks, at two sites, downstream of *Rio Gallinas* and upstream of *Lone Tree Arroyo*.

When averaged by position relative to tributaries (Figure 10A; Table 3), the mean gradients downstream of tributary confluences (*fan* and *downstream*) are twice the gradients measured at *intermediate* reaches at bankfull conditions, and almost three times greater at low flow. Slopes directly *upstream* of confluences are insignificantly less than slopes along control reaches indicating some of the tributaries force backwater conditions upstream (Tables 2 and 3).

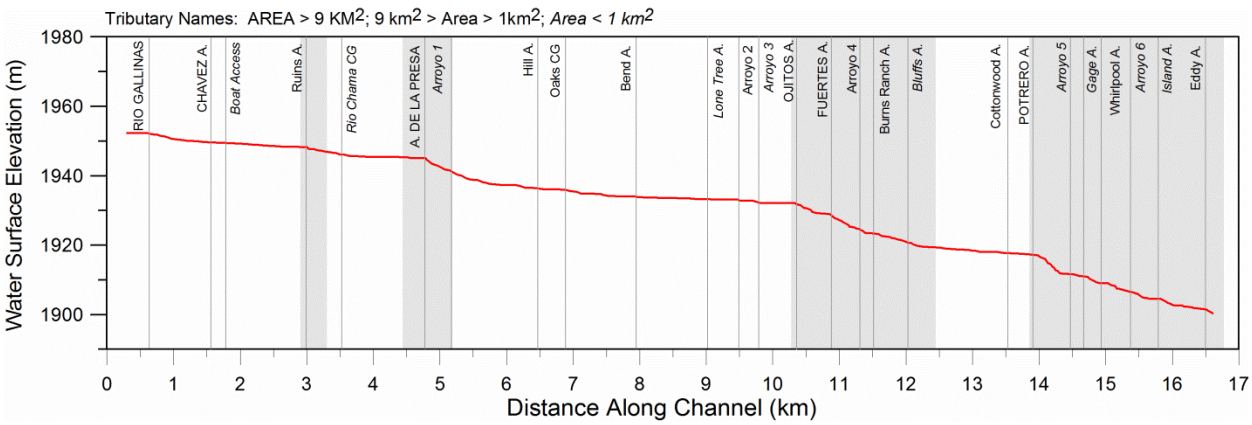

Figure 8. Longitudinal water-surface profile (at 13 m3/s) for the Rio Chama study reach. Overall, the profile is slightly convex; however, it is divided by numerous concave sections, especially at *de la Presa, Ojitos, and Potrero Arroyos*. The downstream section is divided into distinct steps, largely developed at tributary junctions. Gray areas represent reaches of river partially semi-confined by bedrock.

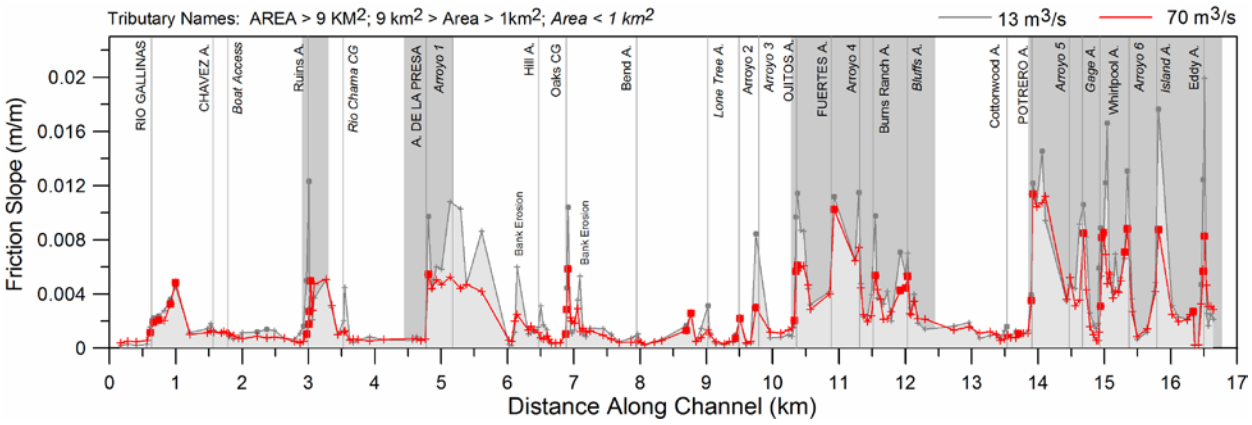

Figure 9. Downstream variations in friction slope along the Rio Chama study reach. Slope increases downstream of most of the tributaries, with larger increases during low flow periods (gray lines). Slope tends to be higher in semi-confined reaches (dark gray background) and in the downstream section, where the number of tributaries entering the system is higher (e.g., downstream of *Potrero Arroyo*). Dark gray areas represent reaches of river partially semi-confined by bedrock.

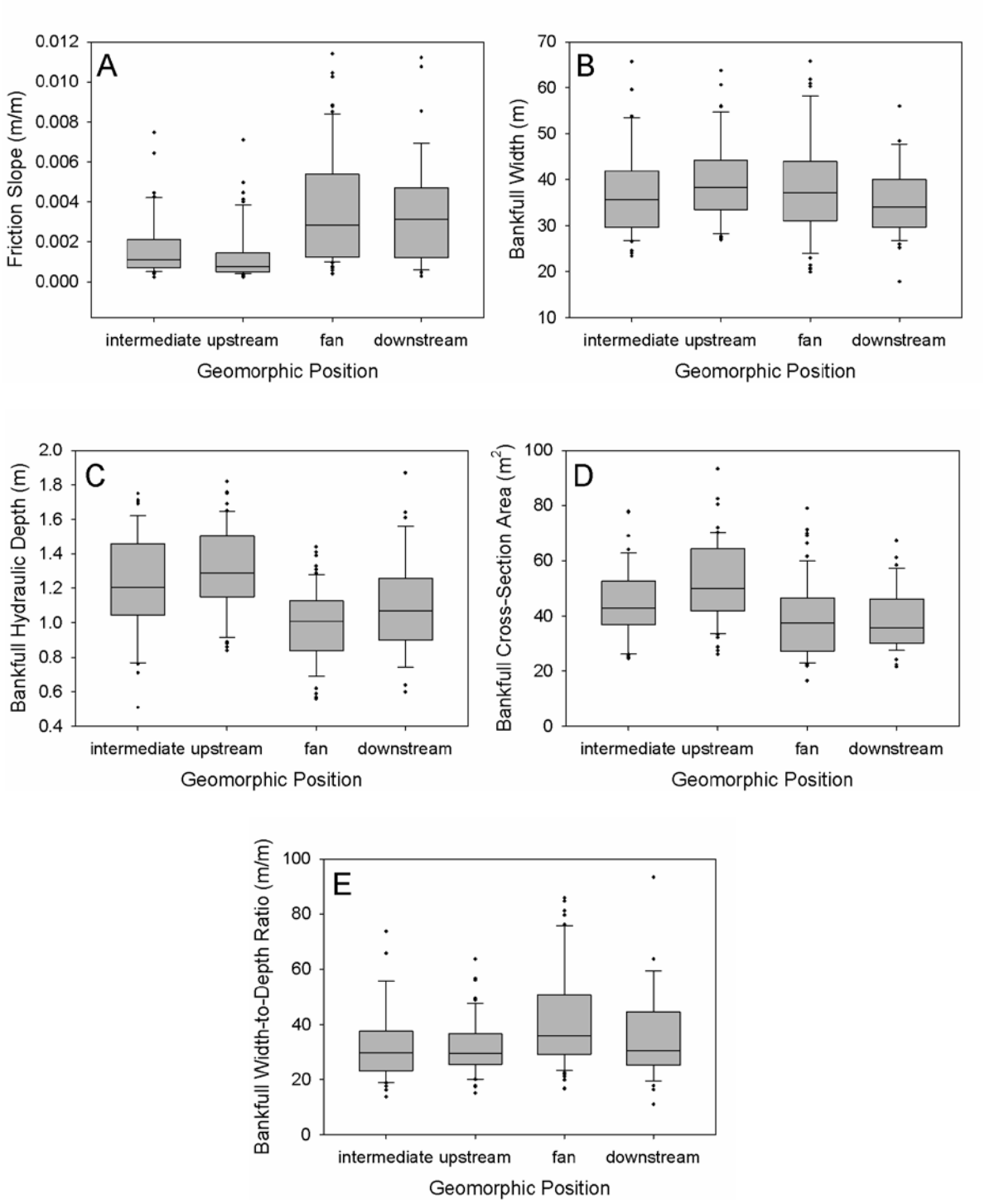

Figure 10. Comparison of bankfull channel geometry data at various geomorphic positions relative to tributary confluences (also see Table 3). A) Slope decreases slightly at *upstream* positions and increases significantly at *fan* and *downstream* positions. B) Bankfull widths increase insignificantly at *upstream* and *fan* positions. C) Average flow depths increase significantly at *upstream* geomorphic positions. D) Flow cross-section area is significantly

higher at *upstream* sites and significantly lower at *fan and downstream* positions. E) Width-to-depth ratio is significantly higher at *fan* sites.

	Slope		***Width***		***Depth***	
Geomorphic Position	*mean(m/m)*	*probability*	*mean (m)*	*probability*	*mean (m)*	*probability*
intermediate	0.0017	---	38	---	1.2	---
upstream	0.0014	0.058	40	0.121	1.3	0.160
fan	0.0037	<0.001	39	0.700	1.0	<0.001
downstream	0.0035	<0.001	36	0.534	1.1	0.042
	Area		***W:D***			
Geomorphic Position	*mean (m^2)*	*probability*	*mean (m/m)*	*probability*		
intermediate	45	---	35	---		
upstream	52	0.008	32	0.869		
fan	39	0.019	42	0.007		
downstream	38	0.012	36	0.430		

Table 3. Statistical analysis (Mann-Whitney Rank Sum Test) results comparing mean Rio Chama geometry parameters at cross-sections to geometry parameters in the intermediate positions. Based on $\alpha = 0.05$, the results indicate significant discontinuities (probability $< \alpha$) in slope, average depth, and area occur across tributary junctions, but, except for slightly wider widths upstream of junctions, shifts in top width are not significant. Width:Depth (W:D) ratios are statistically higher at *fan* positions.

Channel form. Bankfull flow widths along the study reach, as identified in the field, and low flow widths, as estimated in HECRAS, vary between 13 m and 78 m, with a mean of 38 m at bankfull and 33 m at 13 m^3/s. Comparing widths by geomorphic position (Table 3, Figure 10B) reveals that values for widths at the *fan* and *upstream* positions at flows near bankfull are larger, but the differences are statistically insignificant relative to the *intermediate* group. Despite the weak statistical evidence for a simple overall impact, it appears that some tributary confluences have important impacts on channel width, although the magnitude and direction of the changes vary among individual sites. Average channel width at all *intermediate* cross-sections is significantly larger than average widths at 7 individual *fan* sites and significantly smaller than at 11 *fan* sites (Table 2). When compared

to cross-sections directly upstream, bankfull widths are significantly greater at 29 cross-section sites. These locations are associated with 14 tributary sites (54%); however, in some cases the increases are directly upstream of the tributary input and in others, directly downstream (Table 3, Figure 11A). Relationships are not straightforward, but appear to relate to channel morphology at each site. Sites where the channel narrows downstream are generally situated in the more alluvial reaches, although the overall sediment size and volume delivered to the main channel and the confluence's location relative to channel bends also appear to influence the relative width.

Bankfull hydraulic depths (i.e., average flow depth at a cross-section) along the study reach vary between 0.5 m and 2.0 m (Figure 11B) with a mean hydraulic depth of 1.2 m. At 13 m^3/s, the mean depth is 0.6 m. The depths show a clearer pattern when comparing geomorphic position than changes in channel width. Relative to the *intermediate* group, *upstream* cross sections are slightly but insignificantly deeper, and cross-sections in the *fan* and *downstream* positions are significantly shallower (Table 3; Figure 10C). At low flows, mean hydraulic depth is significantly higher for the *upstream* data (P = 0.04) and lower for the *fan* data (P = <0.001). For individual *fan* sites, mean bankfull depth dropped significantly across all of the confluences when compared to the mean value for all of the *intermediate* reach data. The localized results show statistically significant bankfull depth decreases at 32 cross-sections, with 28 cross-sections associated with 16 of the 26 tributary sites (62%; Figure 11B). As with other parameters, depths did not decrease significantly at smaller tributary sites, or where recent fan deposition is primarily sand, such as at *Hill Arroyos*. Additionally, depths significantly decreased at sites characterized by erosion along gravelly banks (e.g., upstream of *Hill and Oak Campground Arroyos*). Bankfull hydraulic

depths also tended to increase upstream of sharp bends in the channel, often drowning out impacts to slope, depth, and sediment size downstream of tributary sites. Examples of this phenomenon include bends downstream of *Rio Chama Campsite* and *Bend Arroyos* (Figure 2).

Significant changes in slope, width, and hydraulic depth across confluences resulted in significant fluctuations in flow cross-section area as well. Mean bankfull cross-sectional area for the study reach was 43 m^2, but values ranged from 17 m^2 to 95 m^2. Overall, mean bankfull area for the *intermediate* position was 13% smaller than for the *upstream* position and 13% larger than for the *fan* position (Table 3, Figure 10D). At low flow, the differences were 30% larger for *upstream* areas and 21% smaller for *fan* areas, again indicating that backwater conditions form above the confluences (Table 3). At individual sites, 17 of the 26 tributaries were associated with significant decreases in mean area relative to the mean for all of the *intermediate* position data (Table 2). However, bankfull area increased significantly at *Rio Chama Campground, Hill Arroyo, and Arroyo 6*, all of which are associated with sandy inputs. When compared to the 5 cross-sections immediately upstream of each confluence, 37 of the cross-sections had significant decreases in cross-sectional area. Of these 37 sites, 30 are associated with 17 of the 26 tributaries (65%; Figure 11C). As with other parameters, significant decreases in channel area were also related to flow along bedrock outcrops and gravelly, eroding banks. Tributary sites associated with insignificant differences in cross-section area were often related to smaller tributaries or those with sandy inputs.

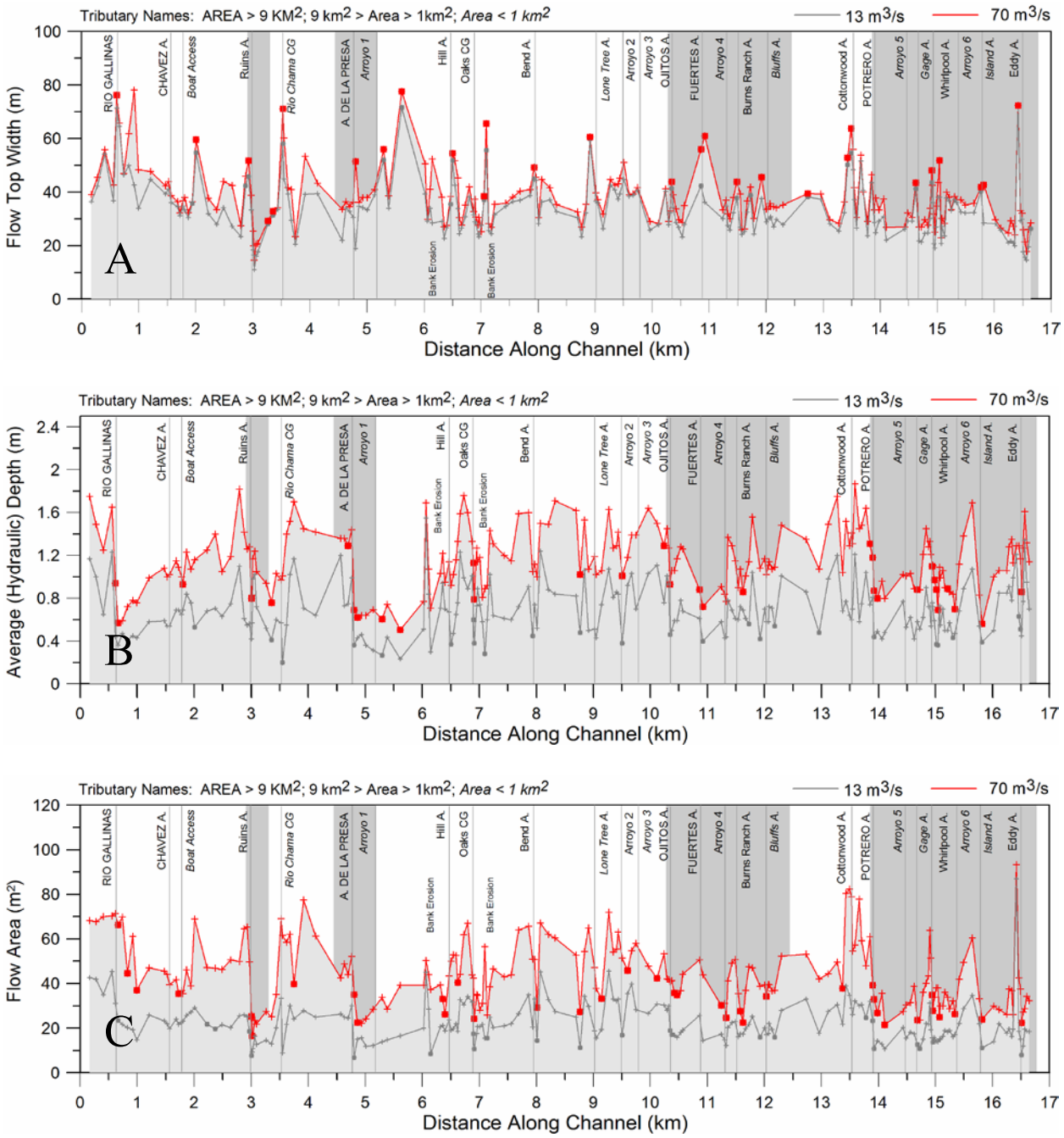
Tributary Names: AREA > 9 KM2; 9 km2 > Area > 1km2; Area < 1 km2
13 m3/s
70 m3/s
Flow Top Width (m)
Average (Hydraulic) Depth (m)
Flow Area (m2)
Distance Along Channel (km)
A
B
C
RIO GALLINAS
CHAVEZ A.
Boat Access
Ruins A.
Rio Chama CG
A. DE LA PRESA
Arroyo 1
Hill A.
Oaks CG
Bend A.
Lone Tree A.
Arroyo 2
Arroyo 3
OJITOS A.
FUERTES A.
Arroyo 4
Burns Ranch A.
Bluffs A.
Cottonwood A.
POTRERO A.
Arroyo 5
Gage A.
Whirlpool A.
Arroyo 6
Island A.
Eddy A.
Bank Erosion

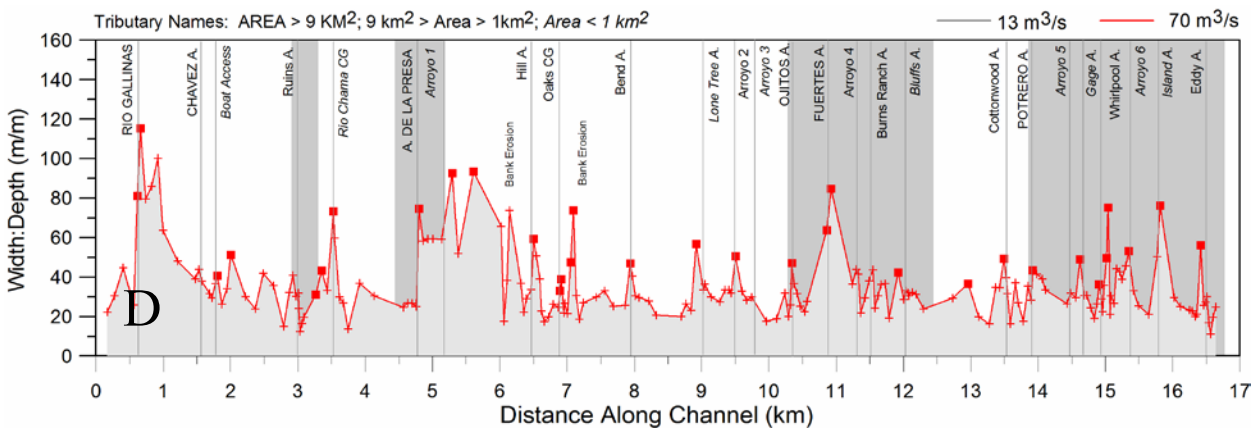

Figure 11. Changes in channel geometry along the Rio Chama study reach: A) width, B) average depth, C). area, and D) width:depth ratio). Significant changes in channel parameters, relative to the 5 sites immediately upstream, are data points shown in solid dots as opposed to crosses. 75% of the tributary sites exhibit significant changes in width, 88% of the sites exhibit significant decreases in depth, 81% of the sites exhibit significant decreases in cross-section area, and 69% of the sites exhibit increases in W:D.

Width-to-depth ratio (W:D) also varied along the study reach. Although most of the W:D values were between 20 and 40, relatively high values were usually centered on tributary junctions. Comparing widths by geomorphic position (Table 3, Figure 10B) reveals that the W:D at the *fan* positions at flows near bankfull are significantly larger relative to the *intermediate* group. When compared to cross-sections directly upstream, W:Ds are significantly greater at 29 cross-section sites. These locations are associated with 18 tributary sites (69%); however, in some cases the increases are directly upstream of the tributary input and in others, directly downstream (Table 3, Figure 11A). Like the channel width data, relationships are not straightforward, but appear to relate to channel morphology at each site.

Finally, all of the channel parameters are highly variable over the study reach, with standard deviations ranging between 30% and 40% of the means for cross section parameters, and over 100% for slope measurements. This variability is not surprising for the

Rio Chama considering the range of sediment sources and sediment history, including large Quaternary fans, landslides and debris flows, valley confinement, and other factors. Variability at tributary junctions is also likely, as pulses of sediment varying in magnitude and material sizes have likely collected at the junctions over time, sediment pulses have been redistributed and overlapped, and some tributary junctions may have shifted with the deposition of fan lobes.

Discussion

Overall, the arroyo tributaries emptying into the Rio Chama within the study reach disrupt continuity in channel geometry and sediment characteristics. Sediment size increases significantly downstream of a majority of the junctions, as does channel slope, and W:D. Over the same sections, channel depth and cross-section area decrease. There is also some indication that backwater conditions form immediately upstream of the junctions, leading to lower slopes, larger depths, and a transition from a gravel-bed channel to a sand-bed channel in many locations. On the other hand, although channel width adjustments vary from site to site, they show no overall trend. Given enough distance between confluences, the discontinuities appear to "correct" themselves to some quasi-equilibrium state before the next discontinuity occurs.

Tributary-related discontinuities observed along the Rio Chama are generally consistent with general theories of channel adjustment and with previous work describing downstream changes in bed texture. Data characterizing the changes in channel form attributed to tributary inputs help verify recently introduced conceptual models (Rice and Church, 1998; Benda et al., 2004; Davey and LaPointe, 2006) describing tributary controls on river channels. Additionally, differences in valley structure and geology provide an

opportunity to examine how these factors may modify impacts at junctions. For instance, how does the change in valley width at the downstream end of the reach alter tributary impacts? How do tributary-associated discontinuities in the semi-confined reaches differ from those in unconfined reaches?

Tributary inputs and channel change. One of the principles of fluvial geomorphology is that channels remain stable when the sediment supply and transport capacity are balanced. Lane (1955) expressed this relationship by stating that the water discharge and channel slope are proportional to the sediment flux and grain size of the sediment supply ($Q_w S \approx Q_s D_s$). A change in any one of these variables must be balanced by a change in at least one other variable in order for a channel to remain in a stable regime. For example, if the discharge increases significantly, the system should experience a reduction in slope, an increase in the volume or size of sediment it can transport, or some combination of the above. Lane's model was not originally applied to confluences, but unless the stream flow and sediment parameters in the tributary balance the flow and sediment in the receiving channel, his theory predicts an adjustment of slope and (or) grain size where the streams join. For instance, assuming similar sediment sizes, if a relatively sediment-laden tributary joins the mainstem, than the new sediment would likely overload the trunk stream unless the channel slope increases past the junction. The channel would likely aggrade at the junction in response to the impact, thus increasing the slope. Conversely, a tributary carrying significant streamflow but relatively little sediment would increase the discharge of the mainstem stream at the confluence, but not sediment load, thereby causing scour, an increase in downstream sinuosity, and (or) bed coarsening . Therefore, Lane's (1955) model predicts that changes in water discharge, sediment load, and

sediment caliber associated with tributary inputs often result in slope and grain size discontinuities along the mainstem channel. Similarly, the discontinuities and step-function changes associated with the confluence likely impose changes in channel width, depth, and other geomorphic characteristics along the channel.

Ferguson et al. (2006) used Lane's (1955) premise to assess the primary responses of mainstem geomorphology at confluences. Their one-dimensional model predicted a range of impacts at tributary junctions including aggradation, degradation, or little to no change, depending on input conditions. Very small tributaries, where relative water and sediment discharges were less than 10% of the larger channel, had little or no impact to the mainstem in the model, nor did tributaries carrying loads with grain sizes similar to the main channel. On the other hand, where the model simulated delivery of relatively coarse sediment from a relatively large tributary, the mainstem channel consistently exhibited adjustments. The modeled impacts along the receiving channel depended on the overall balance between the flow and sediment load; however, the adjustments usually included aggradation at the junction and discontinuities in main stem slope and grain size. The magnitude of the impact increased when modeled tributary loads comprised relatively large volumes of sediment with large sediment sizes, relative to the mainstem, but decreased when modeled tributary discharges approached the simulated flow in the main channel. Alternatively, degradation occurred where the secondary channel carried little to no sediment but enough flow to increase transport capacity, or if modeled sediment inputs were significantly finer than the grains that could be entrained by the primary channel. The model also predicted backwater conditions and sediment fining upstream of aggrading tributary junctions (Ferguson et al., 2006).

The ideas presented by Ferguson et al. (2006) were largely supported along the Rio Chama. Almost all of the tributaries included in the study created a discontinuity in Rio Chama bed sediment size, gradient, and (or) channel geometry. The tributaries are largely intermittent streams, but when active, the flash floods and debris flows that course down the channels can deliver large volumes of sediment, ranging from fine sands to meter-scale boulders. These pulses tend to occur when river discharge is relatively low, and therefore, the capacity is likely too low to initially sort or disperse the material, even some of the finer sediment. With respect to Lane's (1955) equation, both the sediment discharge and sediment size are often elevated by this influx of tributary sediment, whereas the discharge remains relatively unchanged. Therefore, as predicted by the Ferguson et al. (2006) model, the mainstem Rio Chama aggrades at the junctions, increasing the downstream slope. Field indicators such as entrenchment and basal scour suggest additional steepening may occur due to channel degradation at the downstream end of the impact zone at larger tributary impact areas (e.g., *Arroyo de la Presa, Potrero Arroyo, Ojitos-Fuertes Arroyos*), which further increases the slope, or the length of the impact, through the subreach.

The build-up of sediment at the junctions produces a number of discontinuities: 1) the sediment size increases at the junctions; 2) aggradation increases the downstream slope; and 3) channel depth decreases in response to the increase in slope. In fact, tributary inputs help create most of the channel heterogeneity along the Rio Chama study reach, accounting for 26 of the 37 low flow "riffles" (68 %), and all of the major pools (>1.5 x average depth). Additional sediment sources (e.g., bank erosion) accounted for 5 more riffles and the other 7 were located at constrictions and bend entrances. Changes in channel width also appear to be related to confluences, although whether the impact is upstream or downstream depends on

local conditions. Along the Rio Chama, these discontinuities are frequently accentuated by impacts upstream of the channel, which were also predicted by the Ferguson et al. (2006) model. The tributary sediment that accumulates at a confluence often obstructs flow, creating backwater or a pool upstream, which may be considered an additional discontinuity. Channel slope, depth, and sediment size often drastically decrease immediately upstream of Rio Chama junctions, such as at the *Ruins, Oaks Campground, Whirlpool,* and *Island Arroyo* sites. In some cases, as noted along the Rio Chama and the St. Mary's River (Lapointe and Davey, 2006), the pools trap significant amounts of sand, drastically changing the bed texture.

Additional point sources of sediment also help form discontinuities along the Rio Chama study reach. Bank erosion sites that contribute significant gravel and cobbles to the stream, as compared to the primarily sandy banks along most of the channel, produce discontinuities similar to the tributaries, albeit with lesser upstream impacts. Alternatively, at junctions where tributaries consistently supply large volumes of sand instead of gravel, cobbles, and boulders, the mainstem Rio Chama channel appears to widen, and the gradient and bed sediment sizes decrease. This reaction to such tributary inputs is also consistent with "Lane's balance" (Lane 1955) and Ferguson et al.'s (2006) modeling outcomes.

Similar discontinuities at tributary junctions have been well documented in the field. Much of the basic research has been performed in western Canada by Rice and colleagues, who have primarily investigated tributary impacts to bed sediment size along the Pine and Sukunka Rivers (Church and Kellerhals, 1978; Rice and Church, 1998, Rice 1998; 1999). They found only 20% of the tributaries affected mainstem grain size, with many of the tributaries carrying insufficient discharges and (or) bedload to significantly impact bed

sediment caliber. However, larger tributaries created a sawtooth pattern in sediment size similar to but with less variability than that exhibited by the Rio Chama data. Additionally, where sediment sizes increased, a steeper channel gradient was also observed. More recently, Lapointe and Davey (2006) examined changes in bed sediment size along the St. Mary's River, in eastern Canada, and found discontinuities in sediment size forced by tributary inputs. In a fluvial environment more similar to the Rio Chama, Melis et al. (1995) found that debris flows and landslides were the main suppliers of coarse sediment at 526 tributaries of the Colorado River in Grand Canyon. Arizona. Like the Rio Chama, short, but violent precipitation events producing the sediment occur out of phase with mainstem peak flows. Resulting deposition produces steep, bouldery rapids along the main river. In New Mexico, Miller (1958) examined tributary impacts along smaller streams in the northern mountains, and also found similar relationships to those documented by Ferguson et al. (2006).

Sediment link models. Rice and Church (1998) established a conceptual model for tributary-related sediment discontinuities, where the volume and (or) size of the sediment influx at lateral sediment sources (LSS, e.g., tributaries, debris flows, etc.) abruptly alter the bed material attributes along the main channel. Between the LSS, bed material size decreases, largely due to sorting processes along these subreaches. This progression creates a sawtooth pattern when plotting bed sediment size along the channel, with sharp peaks at the LSS points and troughs immediately upstream of the succeeding LSS. Each peak-to-trough unit is referred to as a "sediment link." Davey and Lapointe's (2006) work on the St.Mary's River in the Canadian Shield expanded on the sediment link concept by including longer valley sections where the main sediment supply was a non-point source of relatively coarse,

glacial-fluvial deposits. In these subreaches, the median grain size stayed relatively constant, presumably due to the contribution of similarly sized sediment from the surrounding banks and valley deposits. They suggested altering the sediment link model to include 1) lateral point sources of material, such as an eroding bank or tributary input; 2) valley-segment sediment supply associated with valley-wall deposits; and 3) the downstream fining zones ("sediment links") below the sediment sources, where new sediment supply zones are either nonexistent or provide easily transported material.

The Rio Chama bed sediment data appear to fit the revised Davey and Lapointe (2006) model, exhibiting sediment links at tributary confluences, as well as sections where sediment size remains relatively constant. The tributary and bank erosion LSS generally lead to a quick step-up in sediment size (with exceptions), generally beginning at the upstream end of a fan, some meters upstream of the actual junction. Depending on the size of the direct tributary impact, the sediment sizes will often remain high along the fan, and then decrease downstream until the next tributary resets the bed sediment or until the sediment size levels off in valley segments. Compared to the Rice and Church (1998) study, a much higher percentage of tributaries impact the main channel along the Rio Chama, presumably due to the influx of larger material associated with flash floods and debris flows in channels that might be too small to carry such large material under "normal" sediment delivery scenarios.

In addition to the three main components of the Davey and Lapointe (2006) sediment link model, the authors also noted sand bed reaches of variable length along the St.Mary's River, which were not observed along the western Canadian streams studied by Rice and Church (1998). Along the Rio Chama, sand-bed reaches are a major component of the

discontinuities seen along the channel, at least during low flow periods. They often begin abruptly 2 to 5 channel widths upstream of significant tributary inputs, forming in the backwater zones where the aggrading sediment at junctions obstructs downstream flow. The shift to sand often equates to a decrease in sediment size of at least 2 ψ, which is comparable to the increase in sediment size at many of the LSS points. Not all the sand reaches can be directly related to recent tributary activity, however. Some of the sand reaches more likely developed behind larger impacts, such as the bouldery debris-flow fan deposits emanating from the older *Joaquin Canyon* landslides. Thus, abrupt reductions in grain size may be part of the sediment link model in systems transporting enough sand to partially fill the backwater areas above tributary fan deposits, where storage may be especially large during periods of low flow. The spatial extent of the backwater effect for a given flow stage will likely depend on the ratio of the height of aggradation at the junction to the gradient of the river. The higher the obstruction and the flatter the river profile, the farther upstream the backwater effect will extend. It is also possible that over time, the backwater zones will fill in and merge with the aggradation zones, extending the impact upstream. Similar processes have been observed associated with landslide deposits along the Navarro River, California by Sutherland et al. (2002).

Ferguson et al. (1998) noted that gravel to sand transitions occur where steep sections of mountain rivers meet valley reaches characterized by much lower slopes, and therefore, lower shear stress. At these transitions, they posited that differences in the critical shear stresses to move different grain sizes become relatively greater, making sorting more likely. The finer material becomes more easily transported relative to the coarser material, but as slope continues to decrease downstream, more finer material accumulates and coarser

material is less exposed to flow (so less readily entrained). Eventually, sand patches form and finally, where slope and (or) shear stress reaches some threshold, the bed becomes primarily sand (Ferguson et al, 1998; Wilcock, 1998). Wilcock (1998) and Wilcock and Kenworthy (2002) speculated that preferential mobility of sand could trigger abrupt gravel to sand transitions, and others have shown that sudden transitions between sand and gravel beds are more likely to occur when the sediment is bimodal (Iseya and Ikeda, 1987). The more unimodal sediment along the British Columbian systems studied by Rice and Church (1998) may have prevented sand reaches from forming.

Along the Rio Chama, the proportion of sand along the bed tends to increase away from tributary inputs, where slopes are relatively high. The sand generally accumulates in pore spaces and in areas of slack water, but where the gradient decreases above new tributary inputs or where the channel bends abruptly, the bed abruptly becomes sandy. The observed trend in sand along the channel bed (Figure 7) is consistent with the process observed by Ferguson et al. (1998), but indicates that the progression can appear at smaller scales, driven in part by the framework of sediment links and network variance. Additionally, the build-up of sand along a sediment link, in this scenario, drives the decrease in grain size along the link.

One of the major differences in the Rio Chama observations relative to previous studies is that the D_g data typically "flattens" along the less impacted intermediate sections of the study reach, instead of decreasing overall, as suggested by the previously presented sediment link models. These sections, such as *Rio Gallinas to Ruins Arroyo*, *Rio Chama Campground to Arroyo del la Presa*, and much farther downstream between *Bluffs* and *Cottonwood Arroyo* had a similar minimum D_g of approximately 3.3 ψ (10mm; Figure 5).

From *Bend Arroyo* to *Lone Tree Arroyo*, bed sediment size appeared to stabilize at a smaller value, but the channel is actively eroding an 5-6m high sandy terrace at this location, and the additional sand reduces the D_g in the reach. In part, this leveling off of bed sediment size likely reflects a lag deposit of larger clasts left from the adjacent, older, fan material, along with sand and other small diameter sediment that readily moves through the system at higher flows. Along the downstream section, there is some evidence the bed sediment size levels around 4.3 ψ (20 mm), but tributaries are close together so differentiating between point sources and valley-bottom sources is difficult. However; instead of continuously decreasing, or at least staying constant relative to the upstream section, the overall sediment size appears to step up along the downstream section, downstream of *Ojitos Arroyo*.

Finally, the Rio Chama data suggests that the LSS not only impact sediment size, but they also create fluctuations in flow depth, area, and gradient that correspond to changes predicted by the network variance model (Benda et al., 2004). In similar systems, slope should increase abruptly and then decrease downstream of tributary junctions and other LSS, and depths and areas should decrease abruptly, and then gradually increase until the next LSS. These discontinuities, which are related to the tributary-associated deposits formed at confluences, may be used to better define significant sediment supply sources and associated links, as well as determine potential impacts to the mainstem channel.

Sediment link delineation. Delineating sedimentary discontinuities using the statistical methods presented in Rice and Church (1998) is a relatively straightforward process, but not all significant changes may be represented by sediment links as defined by Rice and Church (1998) and Davey and Lapointe (2006). Choosing an appropriate length threshold for delimiting a sediment link is somewhat subjective and depends on the scale and

focus of a study (e.g., salmonid habitat, benthic ecology, sediment transport, landscape development). Short discontinuities, such as the bank erosion sites and tributary sites at *Lone Tree Arroyo*, or *Gage Arroyo* (<5 channel widths) may not be of significant length in the context of the full study reach, but may be important in channel diversity, e.g. for macroinvertebrate habitat. Additionally, position along a fining segment is important. The impact of smaller tributaries and sediment sources on channel parameters depends on their location in relation to a major upstream sediment source. For example, material eroded from a bank just downstream of *Arroyo de la Presa* will likely not register as a significant sediment texture change within this very coarse link, but may be statistically significant at the sand-dominated, tail end of the link. Most of the significant, smaller impact sites along the Rio Chama lie at the downstream end of fining segments.

Figure 12 depicts the 19 delineated sediment links for the Rio Chama study site. They are based in part on the statistical analysis, but are also based on the observance of a continuous fining trend of similar slope. Significant discontinuities in channel geometry were also used to define breaks between the links, especially slope. For example, despite an association with significant increases in sediment size and top width, *Bend Arroyo* did not produce a significant increase in bankfull slope or area warranting designation as a sediment link. Delimiting significant discontinuities along the downstream section was especially difficult due to the relatively short impacts which frequently disrupt fining in the subreaches. Table 4 provides additional information about the sediment link lines fitted to the sediment and other data. The data can be roughly divided into four groups (delimited in gray; Table 4) based on the slopes of the lines fit to the sediment data. The upstream group, above *Lone Tree Arroyo,* has relatively low line-fit slopes, but in the sandy subreach, between *Lone Tree*

and *Ojitos Arroyos*, the decreases in grain size occur in shorter distances (i.e., the slope of the line fit increases). Comparable gradients also characterize the relatively rapid decreases in sediment size downstream of *Potrero Arroyo*.

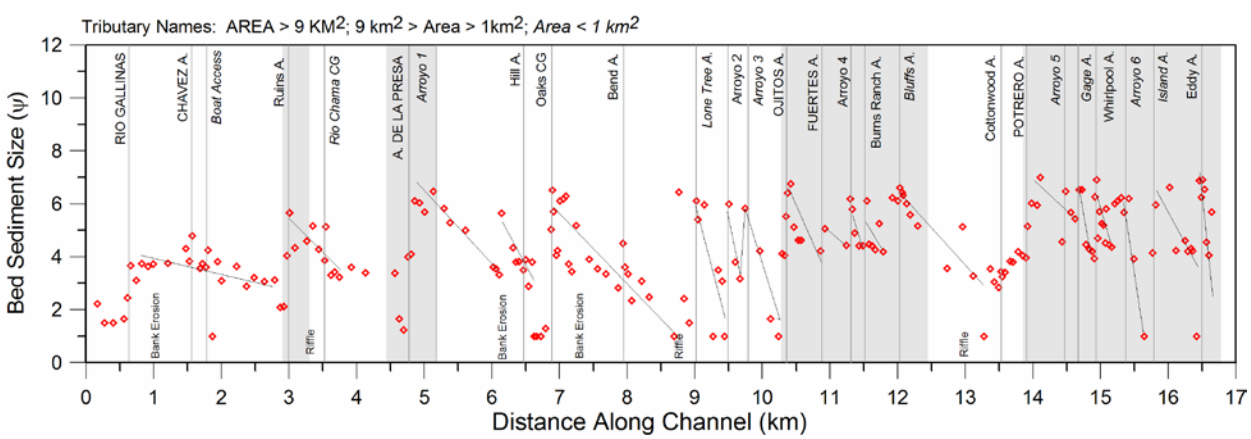

Figure 12. Sediment Links delineated for the Rio Chama Study Reach**.**

Sediment Link	***Equation***	***Slope***	***R^2***
Rio Gallinas/Chavez Arroyo	*-1.13x+5.57*	-1.1	0.15
Ruins Arroyo	*-2.72x+13.63*	-2.7	0.63
Arroyo de la Presa	*-2.62x+19.46*	-2.6	0.92
Oaks Campground	*-2.20x+20.58*	-2.2	0.58
Lone Tree Arroyo	*-11.60x+111.0*	-11.6	0.44
Arroyo 2	*-17.72x+174.21*	-17.7	0.96
Arroyo 3	*-10.95x+112.72*	-10.9	0.95
Ojitos Arroyo	*-4.67x+54.51*	-4.7	0.60
Arroyo 4	*-7.92x+95.17*	-7.9	0.75
Burns Ranch	*-3.85x+49.67*	-3.9	0.22
Bluffs Arroyo	*-2.57x+37.15*	-2.6	0.79
Potrero Arroyo	*-5.09x+78.14*	-5.1	0.72
Arroyo 5	*-7.31X+112.33*	-7.3	0.91
Gage Arroyo	*-7.21x+111.97*	-7.2	0.30
Whirlpool Arroyo	*-6.84x+108.14*	-6.8	0.41
Island Arroyo	*-3.93x+68.31*	-3.9	0.62
Eddy Arroyo	*-13.11x+222.87*	-13.1	0.32

Table 4. Parameters describing the sediment link lines fitted to Rio Chama sediment and other data. The data can be roughly divided into four groups (delimited in gray shading and no shading) based on the slopes of the lines fit to the sediment data. The upstream group,

above *Lone Tree Arroyo,* has consistently lower slopes, but in the sandy subreach between *Lone Tree and Ojitos Arroyos*, the decreases in grain size occur rapidly (i.e., the slope of the line increases). Variable but still comparable gradients characterize the relatively fast decrease in sediment size downstream of *Potrero Arroyo*.

Controls on tributary-associated discontinuities. Along the Rio Chama study reach, the overall direction of change in channel geometry and sediment data appears to counter the gradual downstream trends predicted by generalized models on larger-scale alluvial river systems (e.g., Robinson and Slingerland, 1997; Paola et al., 1992) For example, instead of an overall decrease in sediment size, the D_g and D_{50} increase downstream. Also, the channel gradient appears to increase, and bankfull area and width appear to decrease, when the opposite trends would be predicted. Although these contrary trends are noteworthy, the study reach is short with respect to the full length of the Rio Chama, and there are no large tributaries entering the reach, making comparisons to watershed-wide studies on similar sized systems somewhat problematic. Additionally, the downstream increase in bedrock exposure may also control some of the steeper slopes downstream of *Potrero Arroyo*.

The study reach can be divided into upstream and downstream sections at *Ojitos Arroyo* (Figure 2). The upstream section flows through alluvial valley fill material within a wider valley floor, whereas the downstream section is more semi-confined and often flows along rocky canyon walls mantled by bouldery landslide deposits. Tributary junctions occur more frequently in the downstream sections as well (Figure 2). Table 4 provides a comparison between geomorphic conditions in the two sections. The mean D_g and D_{50} are 190% and 410% larger along the downstream section, respectively. Channel slope is 2 times larger downstream, whereas width and area are 13 and 20% smaller, respectively.

Additionally, many of the larger fluctuations in both grain size and slope along the channel occur in the downstream section (Figures 5-11).

Channel Characteristic	Upstream Reach mean	Downstream Reach mean	Comparison probability
Slope (m/m)	0.002	0.004	<0.001
width (m)	41	36	0.001
depth (m)	1.14	1.14	0.576
area (m^2)	46	37	<0.001
D_g (mm)	22	42	<0.001
D_{50} (mm)	34	74	<0.001
$D_{50\ gravel}$ (mm)	55	110	<0.001

Table 5. Comparison of Rio Chama channel characteristics for the sections upstream and downstream of Ojitos Arroyo. The geometric mean grain size – D_g , median grain size -D_{50}, median grain size with sand removed – $D_{50\ gravel}$, and friction slope are all significantly larger along the *downstream* section, whereas bankfull top widths are smaller, and little difference exists between upstream and downstream hydraulic depths.

Much of the difference between the two segments is likely related to differences in geology and direct hillslope-channel sediment connectivity (cf. Harvey, 2001). In general, the more connected, or coupled, the two systems are, the more rapidly and directly sediment moves from the hillslopes to the main channel. Upstream of *Ojitos Arroyo*, the canyon walls are dominated by cliff exposures of friable Entrada and Morrison Formation sandstones, which produce voluminous sand, and the broader valley floor primarily features Chinle Group mudstones and large sandy Quaternary fill deposits. Downstream, exposure of the underlying resistant Chinle Group sandstones forces the valley to narrow. Also, along the downstream section, the river is pinned against the eastern canyon walls, which are often mantled by colluvium containing large boulders and cobbles in a matrix of weathered Morrison Formation mudstone material. This unstable colluvial material is prone to mobilization in debris-flow and flash flood events. Given that there is also a limited buffer

between the valley walls and the channel, the downstream tributaries are more likely to deliver large clasts to the channel. In the wider upstream valley, the source areas for larger clasts are generally farther from the main channel, and they likely get deposited and remobilized numerous times along the sandy fans and arroyos before reaching the primary channel. Only very large precipitation events, landslides, or arroyo wall failures increase the likelihood that larger clasts will be delivered to the channel in the upstream section. In some cases, such as the relatively large Chaves Arroyo, most of the finer sediment is deposited in the floodplain, and only a small sandy channel finds its way to the mainstem. In addition, there tend to more be more tributaries that reach the channel in the downstream segment, and the channel also flows through three large, bouldery, deposits, which originated off the eastern canyon walls at *Joaquin Canyon* (opposite *Ojitos Arroyo*), opposite of *Potrero Arroyo*, and at *Gage Arroyo*. These deposits contribute to the "resetting" of sediment size, slope, and depth at these locations, and the overall difference between the upstream and downstream sections. Thus, a revised sediment link model for canyon rivers like the Rio Chama should provide for long river sections that are bedrock-semi-confined and well-connected to diffuse hillslope sediment sources, thus dominated by consistently coarse bed material, but which are nonetheless impacted by more focused tributary inputs (Figure 13).

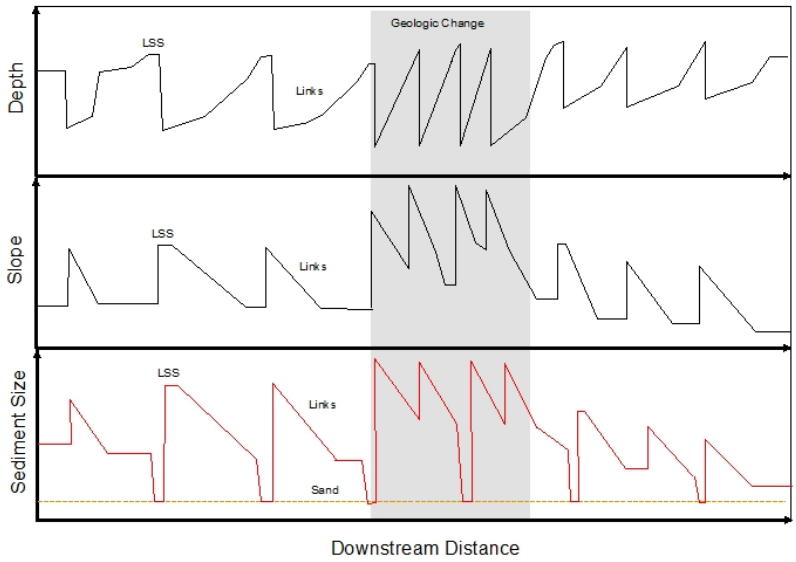

Figure 13. Revised sediment link model depicting LSS and links and their corresponding impacts on slope and depth, based on Rio Chama observations. The model includes sand bed subreaches, subreaches with consistent values of all three parameters, and a sudden increase (or decrease) in the pattern across changing geology or sediment input types.

To provide guidance as to which tributaries may produce sediment discontinuities along a channel, Rice (1998) analyzed numerous tributary watershed characteristics to determine which tributaries impact the Skunkuna and Pine Rivers. He discovered that watershed area and slope were the only two factors with significant impacts. A similar analysis was conducted for the Rio Chama study area, comparing tributary fan length and the length of mainstem impacts measured from air photos and the survey data with watershed area and watershed and tributary channel relief, lengths, slopes, slope-area product, and other metrics. With the Rio Gallinas watershed removed from the analysis, most of the observable relationships were relatively weak (R^2 from 0.31 – 0.44). Additionally, the tributary watershed parameters had little or no impact on mainstem sediment size (D_{50}, D_{84}, $D_{50\ gravel}$, $D_{84\ gravel}$), slope, or geometry at the mainstem-tributary junctions (R^2<0.15). These

comparisons reinforce the findings of Rice (1998), who suggested that sediment networks are inherently discontinuous, especially in relation to the hydrologic network. Although larger tributary watershed areas, in general, may concentrate flow or have a higher probability of experiencing a debris-flow or flash-flood event, and therefore, may be more likely to have a greater impact on the mainstem, other factors such as tributary-mainstem connectivity, debris flow magnitude, event frequency, geomorphic history, aspect, and other factors also contribute to variations in impacts at confluences (Rice, 199; Walling, 1983). This complexity may be especially relevant in arid-region systems such as those found in the southwestern United States.

The change in valley character helps create the pattern of relatively unconfined and semi-confined channel reaches observed in the study area (vertical gray shading in Figures 5-11). The juxtaposition of varying confinement, largely associated with the aforementioned differences in connectivity and watershed character, creates differences in the channel form at junctions to begin with, but it also leads to differences in how the channel changes through a tributary junction (Figure 14, Table 6). Channel slopes are higher in semi-confined reaches and channel areas and widths are generally smaller relative to the unconfined reaches. Depths are generally the same. Generally, within the semi-confined and unconfined groups, trends in the differences between geomorphic positions are similar, with exceptions. The change in width at *fan* sites versus *intermediate* sites in unconfined locations is statistically significant, whereas the significant difference in width and depth at semi-confined locations is *upstream* of the junction. Also, changes in slope through tributary junctions changes by a similar scale at fan positions (3X), but the magnitude is larger in semi-confined locations.

Confined	***Slope***		***Area***		***Width***		***Depth***	
Geomorphic Position	*mean(m/m)*	*probability*	*mean (m^2)*	*probability*	*mean (m)*	*probability*	*mean (m)*	*probability*
intermediate	0.0025	---	22	---	27	---	1.20	---
upstream	0.0021	0.082	30	0.002	35	0.003	1.17	0.843
fan	0.0080	0.001	17	0.089	28	0.803	0.96	0.037
downstream	0.0055	0.005	18	0.099	29	0.278	1.12	0.244
Unconfined	***Slope***		***Area***		***Width***		***Depth***	
Geomorphic Position	*mean(m/m)*	*probability*	*mean (m^2)*	*probability*	*mean (m)*	*probability*	*mean (m)*	*probability*
intermediate	0.0014	---	25	---	37	---	1.16	---
upstream	0.0009	0.796	29	0.003	37	0.474	1.22	0.020
fan	0.0044	<0.001	19	0.034	41	0.038	0.89	0.005
downstream	0.0032	0.021	20	0.467	31	0.118	1.08	0.782

Table 6. Comparison of Rio Chama channel characteristics for semi-confined and unconfined sections of the channel (gray shading in Figures 5-11). Channel slopes are higher in semi-confined reaches and areas and widths are generally smaller relative to the unconfined reaches. Depths are generally the same. Generally, within the semi-confined and unconfined groups, trends in the differences between geomorphic positions are similar, with exceptions. The change in width at *fan* sites versus *intermediate* sites in unconfined locations is statistically significant, whereas the significant difference in width and depth at semi-confined locations is *upstream* of the junction. Slope through tributary junctions changes by a similar scale at fan positions (3X), but the magnitude is larger in semi-confined locations.

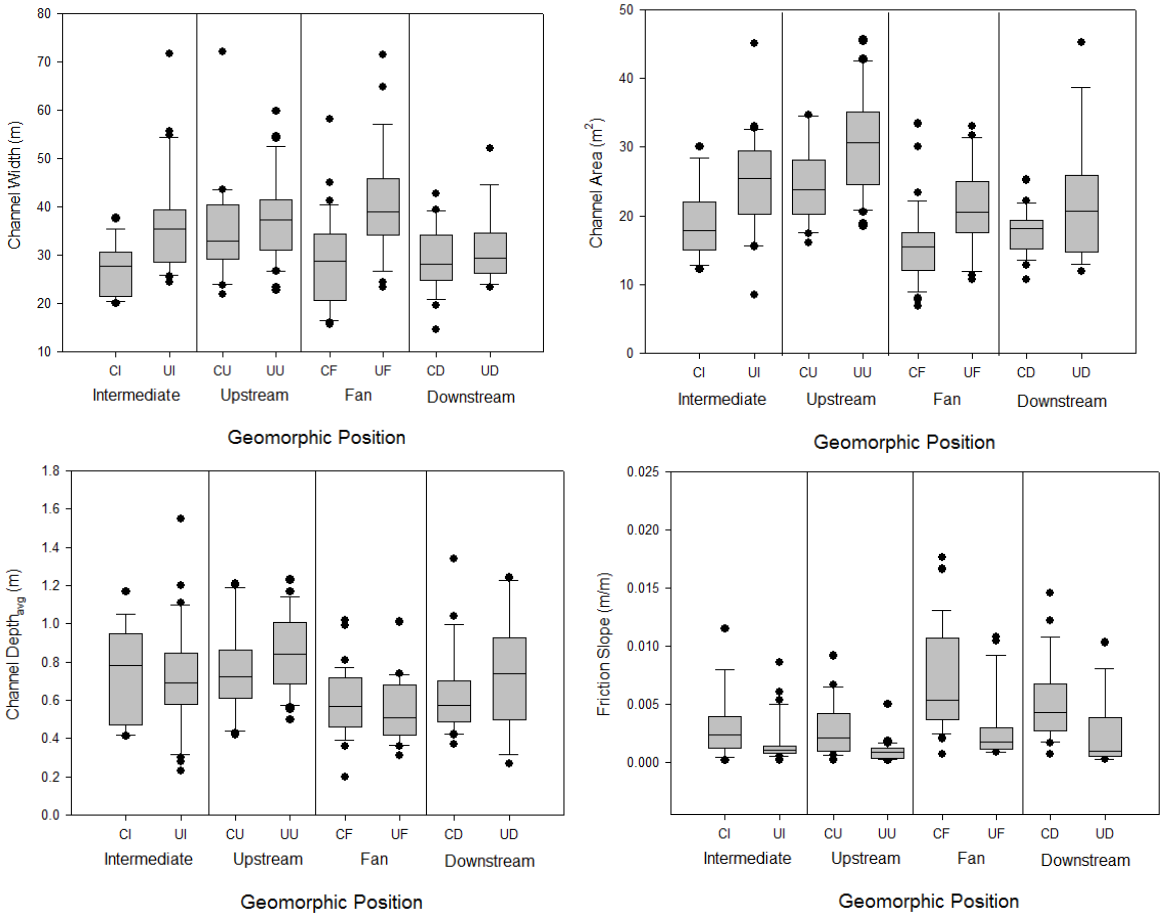

Figure 14. Comparison of Rio Chama channel characteristics for semi-confined and unconfined sections of the channel (gray shading in Figures 5-11). Channel slopes are higher in semi-confined reaches and areas and widths are generally smaller relative to the unconfined reaches. Depths are generally the same. Generally, Within the semi-confined and unconfined groups, trends in the differences between geomorphic positions are similar, with exceptions. The change in width at *fan* sites versus *intermediate* sites in unconfined locations is statistically significant, whereas the significant difference in width and depth at semi-confined locations is *upstream* of the junction. Changes in slope through tributary junctions changes by a similar scale at fan positions (3X), but the magnitude is larger in semi-confined locations.

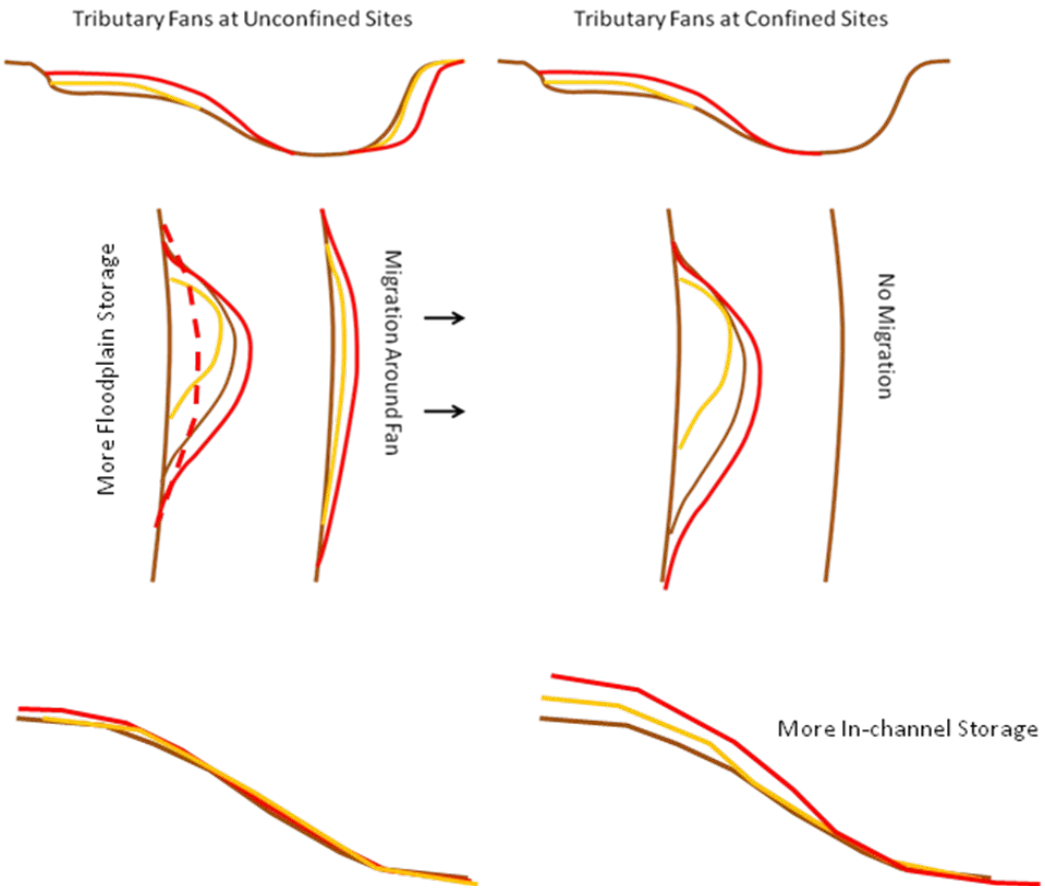

Figure 15. Channel adjustment at fans in unconfined and semi-confined sites. At unconfined sites, the channel can adjust laterally to inputs from a tributary, but at semi-confined reaches, the channel likely adjusts vertically.

Variations in how the mainstem channel adjusts to tributary impacts appear to be strongly influenced by whether lateral adjustments at the delivery points are possible. If deposition creates a debris-flow fan in an unconfined reach, the channel will not only aggrade, it will also likely widen and begin to flow around the fan, comparable to a point bar growing during punctuated pulses of sediment. Provided that the supply is more or less continuous, coarse sediment will continue to aggrade the channel at semi-confined sites, limiting upstream flow and sediment transport, and maintaining the steep, coarse subreaches downstream. Under both conditions, armoring likely develops rapidly during low-magnitude

flows. Montgomery and Brummer (2006) posited that these lag deposits can shield sediment pulses and store large volumes of sediment in mountain channels over time periods exceeding the recurrence interval of floods that can reorganize their beds. At semi-confined sites, this lag formation likely occurs repeatedly, building over past events. At unconfined sites, although an armor layer may form, the channel may be continually moving away from the preceding layer (Figure 15). Although the data indicate that wider channels form at fans in the unconfined reaches, and that fan deposits in semi-confined reaches create a greater "dam-like" impact, with greater impacts upstream of junctions, the actual relationships are problematic. There are also other major differences between the tributaries entering at both unconfined and semi-confined locations. For instance, tributaries entering the mainstem in semi-confined reaches, such as Arroyo de la Presa and Potrero Arroyo, drain larger areas than most of the tributaries entering into relatively unconfined reaches. Also, more semi-confined reaches are often associated with more connected tributaries that may deliver larger material more consistently.

In addition to watershed and valley controls, researchers have also determined that the age of the impact affects its magnitude (Grant and Swanson, 1995; Benda et al., 2003; 2004). Overall, the sediment sources along the Rio Chama are complex deposits which are variable in both time and space. This variability appears to create highly variable tributary and primary channel conditions with respect to bed sediment as well as gradient and channel planform. In many ways, past tributary-mainstem interactions provide the template for the current channel configuration in the study reach. The Rio Gallinas, Chavez Canyon, and other tributaries appear to have supplied enough sand to overwhelm the mainstem Rio Chama and force widespread aggradation around 700-500 years ago (Persico et al., 2005).

The sediment influx in these locations built the large sandy fans present in the upper section of the study reach, and forced the river away from the tributaries, creating large bends (Figure 2). Downstream of Ojitos Arroyo, the deposits emanating from *Joaquin Canyon*, opposite *Potrero Arroyo*, and at *Gage Arroyo* also create steep, coarse sections of channel that influence how sediment supplied from adjacent tributaries interacts with the mainstem. Although these deposits are undated, and are perhaps younger than the upstream sandy fan deposits, air photo analyses indicate they have not been active at the Rio Chama since 1935.

A review of historical photographs (Swanson et al., 2010b) suggests that there has been no major change at most of the tributary sites over the last half century. The *Ruins* and *Bend Arroyo* fans appear to have enlarged over that time, but at most of the sites, areal extents of the active fans remain essentially unchanged. However, a few of the tributaries have disconnected from the primary channel over this time. *Chaves Arroyo, Arroyo 3, Arroyo 6*, and an unnamed arroyo upstream of *Ruins Arroyo* have generally filled in with sediment over the past 50 years. Additionally, almost all of the affected sites included small, fresh deposits of sand and gravel at tributary mouths after major storm events. Despite evidence suggesting that large volumes of coarse sediment have not been delivered to the Rio Chama in the last several decades, elevated slopes and grain sizes have persisted at tributary junctions to the present. Even at the more active junctions, rates of sediment supply are likely low. Sediment influx magnitudes and rates have not been measured for the Rio Chama, but at the Grand Canyon, where there is much greater relief on the canyon walls, Melis et al. (1995) estimated that significant debris flows occurred about once every 10-100 years along most of the tributary channels. The longevity of poorly sorted, coarse debris flow and landslide deposits along receiving waterways has been documented by others up to

10^2 to 10^3 years (Meyer and Leidecker, 1999; Miller and Benda, 2000; Benda et al., 2003), and is often related to the formation of a lag deposit (Gran and Montgomery, 2001; Brummer and Montgomery, 2006). The resulting fining sections, therefore, have much to do with continued supply at these sites, but also how the mainstem river adjusts after their initial formation.

Finally, local relationships between fluvial geomorphology conditions, tributary size and sediment load parameters complicate the relationships between channel geometry character and tributary confluences. For instance, mainstem channels may be wider in bends to begin with, despite the tributary. On the other hand, where tributaries enter the mainstem in semi-confined reaches, such as at *Ruins Arroyo* and *Arroyo de la Presa*, channel widths are limited and *upstream* depths are often the greatest relative to other geomorphic positions (i.e., intermediate, fan, and downstream), especially at low flow. Bedrock banks also force tight bends in some locations, creating backwater conditions upstream that may affect the style and magnitude of an impact, often drowning out tributary effects. Additionally, sediment delivery at Rio *Gallinas, Hill Arroyo, and Cottonwood Arroyo*, where channel areas increase below their respective junctions, appears to be primarily sand and pebbles. Where tributaries are associated with channel narrowing, such as *Ruins, Oaks Campground, and Ojitos Arroyos*, a larger proportion of cobbles and boulders are located at the junction.

Ecological Implications

Tributary inputs that create sudden downstream changes in bed texture, channel shape, and (or) area also likely abruptly alter the form and function of closely associated lotic ecology (e.g. Rice et al., 2001; Benda et al., 2004, Davey and LaPointe, 2006). Tributary inputs may divide the river into a variety of habitat types and (or) geomorphic units, at a

variety of scales, both longitudinally and across the channel. For example, where tributaries provide an abundance of sediment, they may create upstream pools, provide downstream spawning habitat, and result in a variety of flow depths, velocities, and sediment structures across the channel (Davey and Lapointe, 2006).

Because inputs of sediment and water can influence mainstem habitat in the vicinity of confluences, Benda, et al. (2004) proposed that they may be hotspots of lotic biodiversity. Davey and Lapointe (2006) extend this idea a step further. They posit that biotic gradients, which are driven in part by changes in channel form and process, are closely associated with channel adjustments at the link scale. They introduce the link discontinuity concept (LDC), where each significant input of water and sediment to a primary channel creates an organizational framework for biologic communities as well as geomorphology. According to the LDC, "lateral sources of water and sediment are not exceptional features that temporarily reset inevitable, systematic, downstream changes in physical conditions (cf. Vannote et al. 1980); rather, by defining patterns of water and sediment flux, they are entirely responsible for moderate and large-scale variations in physical habitat along all river channels." In turn, the LDC provides a framework to evaluate how biological communities and ecological gradients respond to perturbations in river systems.

Although direct measurements of biological productivity, species richness, or other metrics were not conducted along the Rio Chama study reach, roughly 34,000 bed sediment clasts were observed in the process of size measurements during lower flow conditions. Many of these clasts were populated by macroinvertebrates, allowing some well-supported qualitative observations. At and below tributary junctions, the number of mayfly, stonefly, and caddisfly larvae greatly increased, especially where loose cobble clasts suggested higher

bed mobility. Macroinvertebrate numbers were observed to decrease as sediment size decreased and the proportion of sand on the bed increased. Thus fewer macroinvertebrates were observed in the reaches directly upstream of junction sites, especially in the sandy reaches. These numerous qualitative observations of macroinvertebrates suggest that abrupt changes in bed sediment texture and slope at tributary junctions and other sediment sources also abruptly change the types and numbers of biota.

Infrequent flash floods and debris flows are the main transport processes in the tributary channels of the Rio Chama. These generate pulses of sand and gravel that can completely alter existing mainstem habitat at confluences by burying bed structures and altering local flow patterns. At the tributary junctions, inputs of coarse, poorly sorted bed material produce steep subreaches and diverse hydraulic habitats. Varying flow directions, depths, velocities, and shear stresses along the fan and immediately downstream likely promote species diversity. Many of these tributary impact zones have short lengths (< 3 channel widths), but create habitat islands for species requiring specific lotic conditions, as opposed to resetting the ecological framework. Downstream, where the bed material becomes better sorted and more sand is stored, there is a shift toward more homogeneous flow structures and fewer habitat types. In sandy subreaches, the bed texture and flow structure becomes much more monotonous, with lower velocity flows, but with much greater bed mobility. These backwater zones often host a very different assemblage of invertebrates, usually meiofauna and microfauna, than the macroinvertebrates found in the strongly contrasting habitat type associated with the more stable, gravel-cobble substrate and faster, more turbulent flow. Additionally, the backwater areas may provide important nurseries for larval fishes.

Conclusions

Along the Rio Chama study reach, the influx of cobbles and boulders from flash floods and debris flows at ephemeral tributary confluences create marked discontinuities in channel characteristics, including bed texture, slope, depth, width, and cross-section area. Sediment texture modifications associated with these areas of sediment supply support the sediment link model proposed by Rice and Church (1998) and extended by Davey and Lapointe (2006). In strongly bimodal systems, where the bed material consists of a large proportion of sand in addition to gravel, and both are transported during moderate flow events, sand storage plays an important role in the downstream fining sequence between lateral supply inputs. Sands often accumulate in the low-velocity subreaches formed upstream of the next supply point. The results from the Rio Chama also suggest that shifts in the geomorphic and (or) geologic setting can also alter the framework in which the sediment links operate, changing the overall slope and grain sizes, as well as the spacing of significant inputs and fining zones. In similar settings, where sediment inputs to the mainstem are high relative to hydrologic inputs, the slope along the primary channel should increase downstream of the confluences, and depth and area will likely decrease. Width variations are more complex, however, and are strongly influenced by the degree of valley confinement as well as the texture of the tributary inputs.

Overall, understanding how tributary sediment inputs control sediment distributions and channel geometry along rivers has important implications for a variety of management and research activities. The ability to recognize channel discontinuities and the intervening segments can help guide sampling efforts for both geomorphic and lotic ecology studies and provide for greater understanding distributions of lotic species distributions. This framework

can also provide direction for restoration efforts and improve modeling of sediment transport and channel dynamics.

References

Bathurst, J.C. 1993. Flow resistance through the channel network. In: Beven, K., Kirkby, M.J. (Eds.), *Channel Network Hydrology*. Wiley, Chichester, pp. 69 –98.

Benda, L.E., Andras, K., Miller, D. J., and Bigelow, P. 2004. Confluence effects in rivers: interactions of basin scale, network geometry, and disturbance regimes: *Water Resources Research*, 40: W05402, doi:10.1029/2003WR002583.

Benda, L.E., Veldhuisen, C., Black, J. 2003. Debris flows as agents of morphological heterogeneity at low-order confluences, Olympic Mountains, Washington. *Geological Society of America Bulletin*, 115.9: 1110-1121.

Benda LE, and Dunne, T. 1997. Stochastic forcing of sediment routing and storage in channel networks. *Water Resources Research* 33: 2865–2880

Best, J. L. 1988. Sediment transport and bed morphology at river channel confluences. *Sedimentology* 35: 481–498. doi: 10.1111/j.1365-3091.1988.tb00999.x

Brewer, P.A., and Lewin, J. 1993. In-transport modification of alluvial sediment: field evidence and laboratory experiments. In:Puigdefabregas, C., Marzo, M. (Editors), Special Publications of the International Association of Sedimentologists, 17, pp. 23-35.

Brummer, C. J., and Montgomery, D.R. 2006. Influence of coarse lag formation on the mechanics of sediment pulse dispersion in a mountain stream, Squire Creek, North Cascades, Washington, United States. *Water Resources Research,* 42: W07412, doi:10.1029/2005WR004776.

Bull, W. 1997. Discontinuous ephemeral streams**.** *Geomorphology* 19. 3-4 227-276.

Church, M. 1992. Channel morphology and typology. In *The Rivers Handbook*. P. Carlow and G. E. Petts, eds., Blackwell Science, Malden, MA, pp. 126–143.

Church, M. 2002. Geomorphic thresholds in riverine landscapes. *Freshwater Biology*, 47: 541– 557

Church, M., and Kellerhals, R. 1978. On the statistics of grain size variation along a gravel river. *Canadian Journal of Earth Sciences*, 15: 1151-1160.

Davey, D., and Lapointe, C. 2006. Sedimentary links and the spatial organization of Atlantic salmon (*Salmo salar*) spawning habitat in a Canadian Shield river. *Geomorphology*, 83.1: 82–96.

Dawson, M. 1988. Sediment size variation in a braided reach of the Sunwapta River, Alberta, Canada. *Earth Surface Processes Landforms* 13: 599-618.

Faulcaner, J. 2011. *Sediment size variability along tributary channels to the Rio Chama, NM.* Unpublished B.S. thesis, Department of Earth and Planetary Sciences, University of New Mexico, 49pp.

Ferguson, R., Hoey, T., Wathen, S., Werritty, A. 1996. Field evidence for rapid downstream fining of river gravels through selective transport. *Geology*, 24.2: 179–182.

Ferguson, RI, Cudden, JR, Hoey, TB, and Rice, SP. 2006. River system discontinuities due to lateral inputs: generic styles and controls. *Earth Surface Processes and Landforms*, 31: 1149–1166.

Fogg, J. L., Hanson, B. L., Mottl, H. T., Muller, D. P., and Eaton, R. C. 1992. *Rio Chama Instream Flow Assessment*, Department of the Interior, Bureau of Land Management, Denver, CO, p. 133.

Gran, K. B., and Montgomery, D. R. 2005. Spatial and temporal patterns in fluvial recovery following volcanic eruptions: Channel response to basin-wide sediment loading at Mount Pinatubo, Philippines, *Geological Society of America Bulletin*, 117: 195 – 211.

Grant, G. E., and Swanson, F. J. 1995. Morphology and processes of valley floors in mountain streams, western Cascades, Oregon, In Costa, J. E., Miller, A. J., Potter, K. W., and Wilcock, P. R., eds., *Natural and Anthropogenic Influences in Fluvial Geomorphology: Geophysical Monograph*: Washington, D.C., American Geophysical Union, p. 83-101.

Hanks, T. C., and Webb, R. H. 2006. Effects of tributary debris on the longitudinal profile of the Colorado River in Grand Canyon. *Journal of Geophysical Research*, 111: 13.

Harvey, A. M. 2001. Coupling between hillslopes and channels in upland fluvial systems: implications for landscape sensitivity, illustrated from the Howgill Fells, northwest England. *Catena*, 42: 225-250.

Ichim, I., and Radoane, M. 1990. Channel sediment variability along a river: a case study of the Siret River (Romania). *Earth Surface Processes and Landforms* 15: 211-225.

Iseya, F., and Ikeda, H. 1987. Pulsations in bedload transport rates induced by a longitudinal sediment sorting: a flume study using sand and gravel mixtures. *Geografiska Annaler. Series A, Physical Geography* 69: 15-27.

Knighton, A.D. 1980. Longitudinal changes in size and sorting of stream bed material in four English Rivers. *Geol. Sot. Am. Bull.*, 91, 55-62.

Knighton, A. D. 1989. River adjustment to changes in sediment load: the effects of tin mining on the Ringarooma River, Tasmania 1875-1984. *Earth Surface Processes and Landforms* 14: 333-359.

Knighton , A. D. 1998. *Fluvial Forms and Processes: a new perspective*. Edward Arnold, London, 418 pp.

Lane, E.W. 1955. The importance of fluvial morphology in hydraulic engineering. Proceedings of the American Society of Civil Engineers 81: 1–17.

Leopold, L.B., and T. Maddock, Jr. 1953. *The Hydraulic Geometry of Stream Channels and Some Physiographic Implications,* U.S. Geological Survey Professional Paper 252.

Love, D. W., and Connell, S. D. 2005. Late Neogene drainage developments on the southeastern Colorado Plateau, New Mexico: New Mexico's Ice Ages. *New Mexico Museum of Natural History and Science Bulletin* 28: 151-169.

Melis, T.S., Webb, R.H., Griffiths , P.G., and Wise, T.W. 1995. Magnitude and Frequency Data for Historic Debris Flows in Grand Canyon National Park and Vicinity, Arizona. US Geological Survey Water-Resources Investigations Report no. 94-4214

Meyer, G.A., and Leidecker, M.E. 1999. Fluvial terraces along the Middle Fork Salmon River, Idaho, and their relation to glaciation, landslide dams, and incision rates: A preliminary analysis and river-mile guide. In Hughes SS, Thackray GD, eds. *Guidebook to the Geology of Eastern Idaho.* Pocatello (ID): Idaho Museum of Natural History: 219-235.

Miller, J.P. 1958. High mountain streams: effects of geology on channel characteristics and bed material. Memoir 4, State Bureau of Mines and Mineral Resources, New Mexico Institute of Mining and Technology, Socorro, N.M., 53 pp.

Miller, D.J., and Benda, L.E. 2000. Effects of punctuated sediment supply on valley-floor landforms and sediment transport. *Geological Society of America Bulletin*, 112.2: 1814-1824.

Mosley MP. 1976. An experimental study of channel confluences. *Journal of Geology*, 84: 535–562.

Paola, C, Parker, G, Seal, R, Sinha, S, Southard, J, and Wilcock, P.R. 1992. Downstream fining by selective deposition in a laboratory flume. *Science*, 258: 1757-1760.

Persico, L, Meyer, G, Frechette, J, New, J, and Hepler, C. 2005. Contrasts in late Pleistocene to Holocene fluvial behavior along the middle Rio Chama: New Mexico Geological Society, 56th Field conference Guidebook, Geology of the Rio Chama Basin, p. 432-433.

Rice, S., and Church, M. 1998. Grain size along two gravel-bed rivers: statistical variation, spatial pattern and sedimentary links. *Earth Surface Processes and Landforms*, 23: 345-363.

Rice, S.P. 1998. Which tributaries disrupt downstream fining along gravel-bed rivers? *Geomorphology*, 22: 39-56

Rice, S.P., Greenwood, M.T., and Joyce, C.B. 2001. Tributaries, sediment sources, and the longitudinal organization of macroinvertebrate fauna along river systems. *Canadian Journal of Fisheries and Aquatic Sciences* 58: 828–840.

Rice, S.P., Roy, A.G., Rhoads, B.L, eds. 2008. *River Confluences, Tributaries and the Fluvial Network.* John Wiley and Sons, Chichester, UK. 456p.

Robinson, R.A.J., and Slingerland, R.L. 1997. Origin of fluvial grain-size trends in a foreland basin: the Pocono Formation of the Central Appalachian Basin. *Journal of Sedimentological Research*.

Russell, R.J. 1954. Alluvial morphology of Anatolian Rivers. *Annals of the Association of American Geographers*, 44.4: 363-391.

Schumm S.A. 1977. *The Fluvial System*. Wiley-Interscience, New York, 338pp

Sutherland, D.G., Ball, M.H., Hilton, S.J., and Lisle, T.E. 2002. Evolution of a landslide-induced sediment wave in the Navarro River, California. *Geological Society of America Bulletin*, 114.8: 1036-1048.

Swanson, B.J., Meyer, G.A., and Coonrod, J. 2011. Magnitude and uncertainty of channel planform measurements along a regulated river using aerial photography: Rio Grande near Albuquerque, New Mexico. *Earth Surface Processes and Landforms*, 36.7: 885-900.

Vannote R.L., Minshall, G.W., Cummins K.W., Sedell J.R., and Cushing C.E. 1980. The river continuum concept. *Canadian Journal of Fisheries and Aquatic Sciences*, 37: 130–137.

Wilcock, P.R. 1993. Critical shear stress of natural sediments. *Journal of Hydraulic Engineerin,* 119.4: 491–505.

Wilcock, P.R., and Crowe, J.C. 2003. Surface-based transport model for mixed-size sediment. *Journal of Hydraulic Engineering* 129.2: 120–128.

Wilcock, P.R., and Kenworthy, S.T. 2002. A two-fraction model for the transport of sand/gravel mixtures. *Water Resources Research* 38.10: 1194.

Wolman, M. G. 1954. A method of sampling coarse river-bed material: *American Geophysical Union Transactions* 35: 951-956.

Chapter 4

Tributary Confluences and Discontinuities in Sediment Transport Processes: Rio Chama, NM

Authors:
Benjamin J. Swanson, PhD candidate, Department of Earth and Planetary Science, University of New Mexico

Dr. Grant Meyer, Department of Earth and Planetary Science, University of New Mexico

Dr. John Pitlick, Geography Department, University of Colorado

Abstract

Abrupt changes in channel morphology often occur where two channels of disparate sediment loads meet, including shifts in channel slope, depth, and bed sediment size along the receiving channel. In turn, these tributary-controlled differences in channel characteristics control sediment transport processes. Along the Rio Chama, between El Vado and Abiquiu Dams, northern New Mexico, arroyo tributaries intermittently deliver sediment from erodible sandstone and shale canyon walls to the mainstem channel via flash floods and debris flows during summer thunderstorms. Some of this sediment is then redistributed in the mainstem by flows associated with snowmelt runoff. To examine tributary controls on key hydraulic parameters and bedload transport, we systematically collected cross-section elevation and bed sediment data up and downstream of 26 tributary confluences along a 17 km reach. Data from 203 cross-sections were used to build a one-dimensional hydraulic model for comparing estimated channel parameters at bankfull conditions at these sites. Output from the models was then used to spatially compare parameters such as velocity, shear stress, and stream power along the channel. Additionally, the data were used to

estimate hourly bankfull and annual bedload transport rates along the channel. As compared to intermediate reaches, away from tributary junctions, confluences primarily impact gradient and bed sediment size, reducing both parameters upstream of confluences and increasing them downstream. The changes in slope likely produce statistically significant changes in velocity, shear stress, and stream along the channel as well, generally limiting these parameters upstream of confluences and increasing them downstream. Major shifts in these hydraulic parameters and bed sediment at confluences appear to drive variations in sediment entrainment and transport capacity and the relative storage of sand along the channel bed. In most cases, entrainment is limited, but bedload transport rates are slightly higher downstream of tributaries along the Rio Chama. Although the larger clasts downstream of junctions slow transport, steeper slopes likely help to pass the smaller gravel and sand. Sand especially may be flushed through these reaches via suspension. Tributary sediment inputs have had substantial influence on channel changes in response to the closure of El Vado Dam, and likely will control future changes as well.

Introduction

The predominant view of fluvial systems is that channel morphology, sediment character, and associated processes undergo gradual and steady downstream changes. Numerous studies of downstream hydraulic geometry and bed sediment changes imply that channel width and depth steadily increase, and sediment size and gradient decrease down the length of streams (e.g., Leopold and Maddock, 1953; Robinson and Slingerland, 1997, Paola et al., 1992). These generalized ideas informed and were strengthened by subsequent process-related characterizations of river systems, including further documentation of downstream changes in channel geometry (Leopold and Maddock, 1953; Church, 1992),

roughness adjustments (Bathurst, 1993), general patterns of sediment supply and storage (Schumm, 1977; Church, 2002), and ecological processes in channels (e.g., Vannote et al., 1980). Although this linear perspective duly predicts downstream channel changes at larger scales, at smaller scales, channel morphology and sediment characteristics are significantly impacted by lateral constraints and sediment sources, especially tributary inputs (e.g., Rice and Church, 1997; Davey and Lapointe, 2006; Constantine et al., 2008, Joeckel and Henebry, 2008; Swanson et al., 2012a). These studies have demonstrated substantial, often abrupt, shifts in bed material caliber, gradient, depth, width, and other characteristics at tributary confluences, as well as directly up- and downstream of these junctions.

Rivers and streams are often assumed to adjust so they may efficiently transport their sediment load through the system. However, because tributary confluences impact the primary driving and resisting forces in sediment transport (i.e., slope, discharge, and sediment size and load), they presumably have distinct local impacts on shear stress, stream power, flow velocity, and other transport related characteristics, and thus, sediment transport connectivity (cf. Harvey, 2001; Hooke, 2003). Effects are especially likely where the delivery and receiving channels are characterized by dissimilar sediment and discharge regimes. Past investigations have described discontinuities in reach-to-reach sediment connectivity, where abrupt changes in sediment capacity along a channel are associated with abrupt changes in sediment storage. In some reaches, relatively low transport capacity and higher delivery rates result in sediment accumulation on channel bars. These "sedimentation zones" (Church and Jones, 1982) are often associated with adjacent tributary or channel margin inputs of coarse sediment (Schmidt and Rubin, 1985; Martin and Church, 1995; Hooke, 2003; Hanks and Webb, 2006), and with sediment waves passing through the system

from upstream sources (Knighton, 1989; Madej and Ozaki, 1996; Miller and Benda, 2000). Adjacent reaches, however, may freely pass almost all incoming sediment, even at low flows (Church and Jones, 1982, Hooke, 2003). This juxtaposition indicates that sediment transport and storage are often localized at the reach scale, which in turn, may result in chronic channel instability at these locations (Church and Jones, 1982; Martin and Church, 1995; Brewer and Lewin, 1993; Hooke, 2003). In addition, valley geomorphology also controls sediment connectivity, where valley width, slopes, bar deposition, and other factors change the sediment transport and storage potential along a river or stream (e.g., Wathen and Hoey, 1997, Miller and Benda, 2000). If channel morphology is a strong control on in-channel deposition, then environmentally induced shifts in sediment inputs can alter the spatial and temporal connectivity from reach to reach over longer time periods.

Previous research on historical channel planform change along the Rio Grande (Swanson 2010a) and Rio Chama (Swanson et al., 2010b), New Mexico, indicated that tributary-mainstem interactions along these rivers strongly influence the styles and patterns of historical channel adjustment. These channel changes have occurred in response to droughts, channel engineering, and dam management that have altered discharge and sediment supply and changed bank erodibility. Along the Rio Grande, much channel narrowing occurred directly downstream of tributaries. Tributary-delivered sediment that could no longer be carried by the reduced peak flows downstream of Cochiti Dam collected in backwater areas and on floodplains, as well as on stalled bars and islands in these locations (Swanson et al., 2010a). Within the Rio Chama study area, 54 km downstream of El Vado Dam, width changes appeared to be restricted to reaches immediately downstream of the Rio Gallinas-Rio Chama confluence and more alluvial subreaches, away from arroyo junctions

(Swanson et al., 2010b). Such discrete pockets of channel change indicate that these systems are likely divided into reaches characterized by disparate capacities to transport sediment supplied to the system, both from upstream in the mainstem and from tributary or other local sources.

Although there are a number of studies that document adjustments in sediment size and gradient associated with tributary junctions (e.g., Miller, 1958; Knighton, 1984; Dawson, 1988; Icham and Radoane, 1990; Swanson et al., 2012a), few, if any, have quantified the impact of these adjustments to shifts in shear stress, flow velocity, and ultimately, sediment transport processes. In this study, we describe how changes in channel character related to tributary confluences alter sediment transport parameters along the Rio Chama in northern New Mexico. Tributary confluences along the study reach are associated with changes in bed-sediment size, gradient, and channel depth (Swanson et al., 2012a), which result in abrupt shifts in flow velocity and shear stress along the channel. In turn, we utilize sediment transport relationships to describe how entrainment and transport capacity vary along the channel, and how this might impact sediment routing and channel adjustment.

Study Area

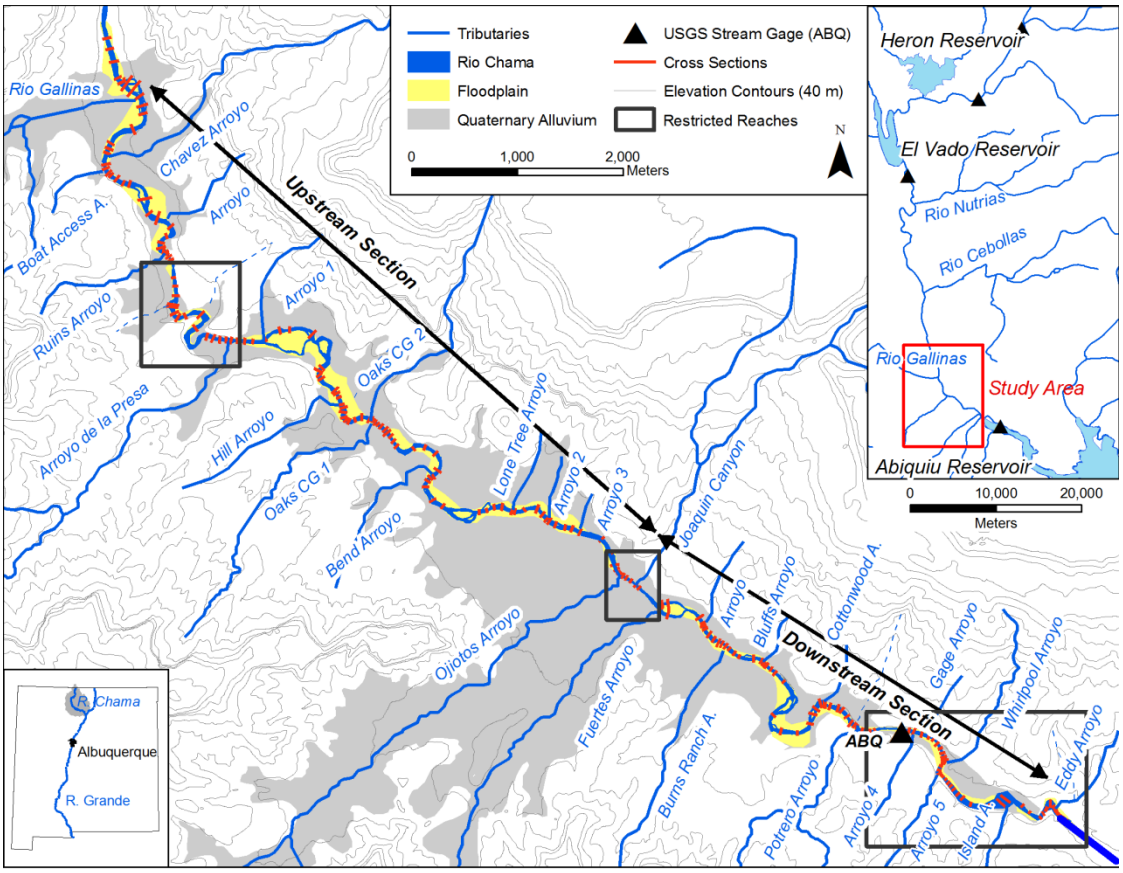

Figure 1. Rio Chama study area, NM, between the Rio Gallinas confluence and the upstream end of Abiquiu Reservoir. The channel flows within a narrow floodplain bordered by a variable area of Quaternary tributary alluvial fan deposits and local fluvial terraces. Black boxes indicate where the channel is at least partially confined by bedrock and (or) bouldery landslide and debris-flow fan deposits. The study reach is divided into an upstream and downstream section based on changes in sediment size, slope, and channel areas (see text).

The study reach includes 17 km of the middle Rio Chama canyon downstream of El Vado Dam, between the Rio Gallinas confluence and the upstream end of Abiquiu Reservoir (Figure 1; Swanson et al., 2012a). The canyon walls are formed by Mesozoic sandstones and mudstones capped by Cretaceous Dakota Sandstone. Large landslide deposits cover many of the canyon slopes. Large volumes of tributary fan sediment are stored along the valley floor.

The study reach is divided into upstream and downstream sections at *Ojitos Arroyo* (Figure 1) based on differences in sediment size, slope, and channel areas. The broader upstream valley section is formed within erodible Triassic mudstones. Sandy tributary fan deposits are often exposed in 2-5 m high cutbanks along the main channel (Persico et al., 2005), although some tributaries have also produced coarse gravel deposits up to boulder size within and adjacent to the main channel, and sandstone channel boundaries are locally present (Swanson et al., 2012a). The generally narrower downstream section is semi-confined by resistant sandstone outcrops and bouldery landslide material. Tributary junctions occur more frequently in the downstream sections as well (Figure 1).

Hydrology. Two USGS stream gages bracket the Rio Chama study reach (Figure 1). At the Rio Chama below El Vado Dam (EVD) gage (08285500; waterdata.usgs.gov), the record spans from 1914 through the present, with continuous daily data since1935. The Rio Chama above Abiquiu Reservoir (AQR) gage (08286500; waterdata.usgs.gov) includes data from 1961 through the present. Since 1961, EVD and AQR gages have measured similar flows (EVD = 0.93*ABQ; R^2=0.98), with average daily flows of 12 and 13 m^3/s, respectively. Differences in discharge at the two gages primarily occur during spring runoff and substantial precipitation events in the middle watershed. Most of the additional flow at AQR, especially during spring runoff, likely enters the Rio Chama from larger tributaries upstream of the study reach (i.e., Rio Cebollas and Rio Nutrias; Figure 1). Although the Rio Gallinas likely adds to the flow, it enters within the first 500 m of the study reach, and discharges little water except during spring runoff and after very large storms. Therefore, for this study, flow along the entire reach is assumed to equal the flow at AQR.

Mean peak flow at AQR is 96 m^3/s, with average maximum peak flows (top 10%) of 170 m^3/s and average minimum peaks (bottom 10%) of 42 m^3/s. The 2-year flood is approximately 80 m^3/s. However, El Vado Dam moderates flood flows within the study reach. Pre-dam peak flow measurements collected at EVD between 1914 and 1924 (n=7) averaged 137 m^3/s. Since 1961, the mean annual peak discharge at the Rio Chama at La Puente (LPT) gage (08284100)), upstream of the dam, is 124 m^3/s, which is 30% higher than the mean peak flow at AQR. Additionally, a regression equation based on a comparison between daily flows at the Rio Grande at Otowi gage (RGO) with discharge data at LPT (*LPT=0.48xRGO-17.8*; R^2=0.78), and its predecessor, the Rio Grande near Park View gage (08283500), predicts an average pre-dam peak discharge of at least 135 m^3/s, 40% higher than the post-dam average. Although operations at El Vado Dam dominate channel discharge in the reach, flood peaks and, therefore, channel dynamics are still primarily associated with spring snowmelt from the upper watershed (Figure 3). Summer storms also increase flows. They generally occur over small areas, but may generate high magnitude, relatively short duration flood events along the mainstem. Most of the sediment movement in the tributary watersheds occurs during these storm events (Swanson et al., 2010b; 2012a).

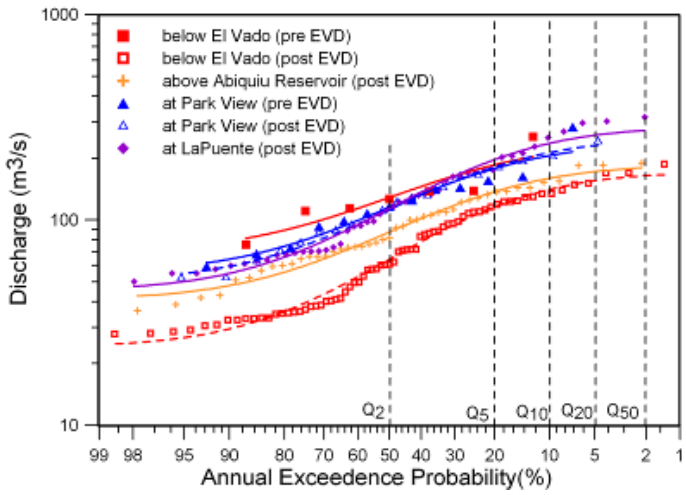

Figure 2. Exceedence probabilities for peak discharges along the Rio Chama. Post-El Vado peak flows are smaller downstream of El Vado Dam (below El Vado, above Abiquiu Reservoir) than upstream (at Park View, at LaPuente). The 2-yr flow (Q_2) at the above Abiquiu Reservoir gage, which represents the study reach, is around 76 m^3/s.

Channels. The juxtaposition of sandy, gravelly beds and banks, and confining bedrock and coarse tributary fan and hillslope material (>180 mm), creates alternating subreaches of alluvial and relatively non-alluvial channel along the Rio Chama. Within the alluvial reaches, the channel is essentially self-formed, flowing largely through mainstem channel and floodplain deposits, and thus reflecting the load and discharge of the river. In the non-alluvial reaches, the channel form and movement is limited by boulders at the toes of some tributary fans, bouldery Quaternary landslide deposits, and local bedrock banks from *Ruins Arroyo* to *Arroyo de la Presa* and downstream of *Potrero Arroyo* (Figure 1).

The tributary channels are primarily arroyos (cf. Bull, 1997) incised along lower reaches into coarse hillslope deposits and alluvial fans. They are intermittent channels carrying flash floods and (or) debris flows during violent summer thunderstorms. As such, they deliver infrequent pulses of sediment relative to "normal" perennial alluvial tributaries, but with higher volumes of material and a wider range of sediment sizes. Along the Rio

Chama, deposits at tributary mouths range from small gravel debris cones to channel-spanning debris-flow deposits of varying grain sizes and ages. These deposits are generally inundated at flows between 10% and 80% of the 2-year recurrence interval.

Methods

Field data. In order to examine tributary impacts on sediment transport, a series of cross sections was surveyed at 26 tributary junctions along the study reach. Sites were chosen based on air photo and field reconnaissance, and included 86% of the tributary confluences connected with the river since 1935. At each confluence site, between 4 and 12 (mean = 6) cross sections were surveyed using Leica Total Station equipment. At least one cross section was located in each of three subreaches: (1) directly *upstream* of the confluence, (2) along the tributary *fan* (immediately below the confluence), and (3) *downstream* of the confluence. Each cross section was placed to best represent local channel geomorphology (i.e., bed and bank material, width, depth, water surface slope). Nonetheless, spacing between cross-sections at each tributary site was relatively even (20-40 m). Additionally, data were collected between tributary sites for comparison. These *intermediate* cross sections were located in riffles and runs not directly associated with any tributary inputs. Cross sections comprised the adjacent floodplain surfaces, estimated top of bank, water surface elevations, and breaks in slope within the channel cross section. Top of bank (bankfull) positions were determined by locating a distinct break in bank slope and vegetation. Additionally, a longitudinal water surface profile was surveyed along the entire study reach. Points for the profile were spaced an average of 40 m apart and included all major breaks in slope.

At each surveyed cross-section, sediment was characterized using a modified Wolman pebble count (Wolman, 1954). Grain size diameters were measured at half ψ intervals using a gravelometer every 0.2 m across the entire channel bed. The mean number of measurements per cross section, was 168, ranging from 53 to 361. The five cross sections with less than 100 samples were located along narrow channels dominated by boulder and bedrock beds. In sand-dominated subreaches, attempts were made to measure any gravel buried by less than 10 cm of sand, but the sand deposits were often deep and the number of gravel samples was often less than 100 at these cross sections. Notable grain sizes for each cross section (D_{16}, D_{50}, D_{84}, where D is the clast size where 16%, 50%, and 84% of the sample, respectively, is finer) were determined visually from histograms of the pebble count data. The geometric mean of the grain size (D_g) at each cross section was calculated as $\sqrt{D_{16} \times D_{84}}$. Additionally, analyses were also conducted using only the gravel ($D_i > 2mm$) portion of the sampled sediment at each cross-section, where for instance, the $D_{50\ gravel}$ would be a clast with the mean diameter for just the gravel portion of the sediment at a site.

In a previous study, Swanson et al. (2012a) fit linear equations to downstream changes in D_g, D_{50}, $D_{50gravel}$, and the proportion of sand on the bed along the Rio Chama study reach in order to delimit sediment links below tributaries (Figure 3). Slope, width, and depth data were also modeled with linear equations over Rio Chama reaches. A comparison of the field data and the modeled data resulted in regression coefficients (R^2) of 0.78, 0.51, and 0.79 for D_g, D_{50}, *and* $D_{50gravel}$, respectively, 0.85 for slope, 0.69 for width, and 0.58 for depth. These modeled data were used in the sediment transport relationships described later in the document in order to reduce some of the within-reach variability, especially with regards to slope, which has a strong influence on estimates of sediment transport rate.

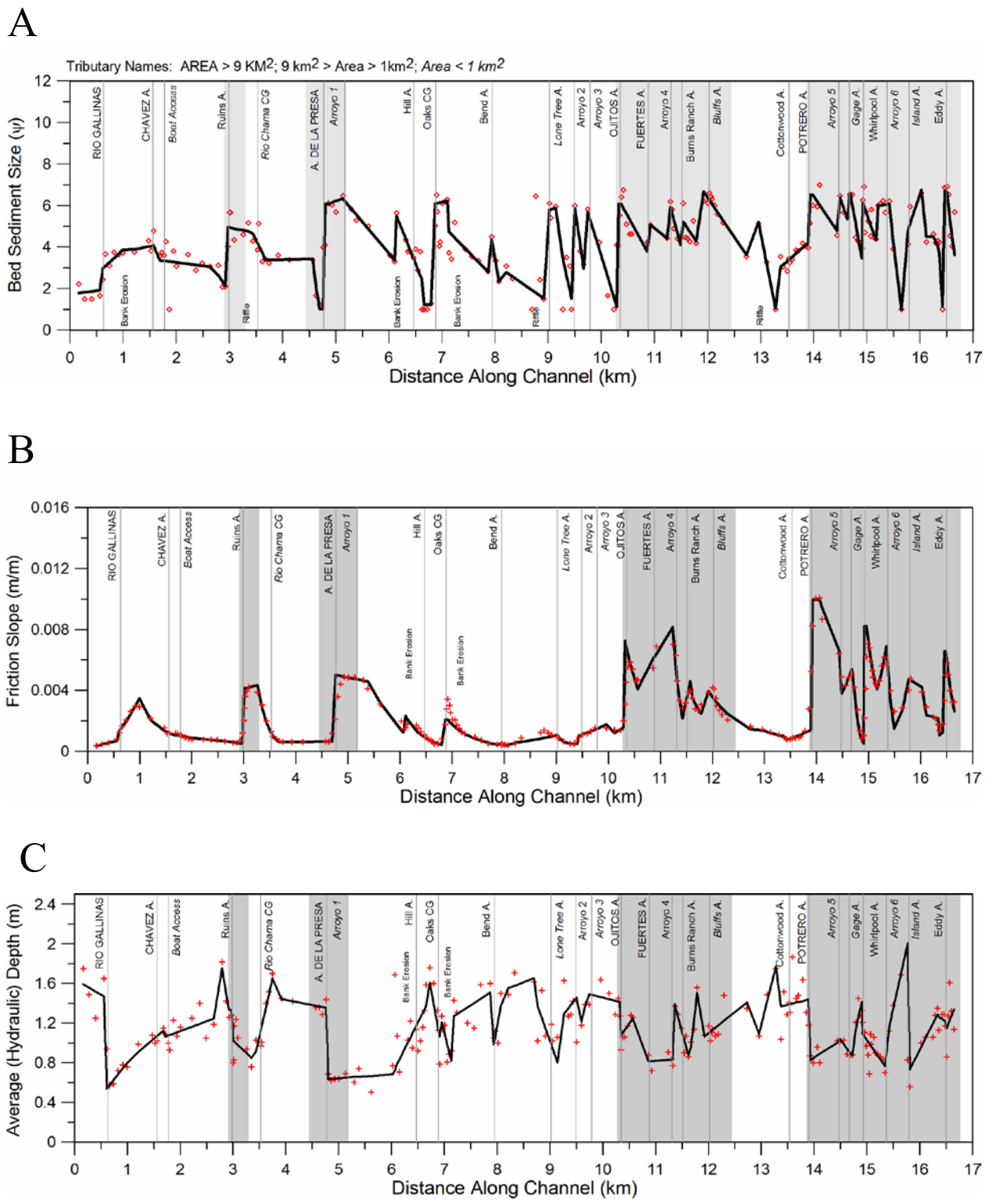

Figure 3. Linear models fit to A) sediment data (Dg), B) friction slope, and C) average depth data. Results were used in the hourly, bankfull and annual bedload transport relations.

Hydraulic modeling. Field surveys were conducted during low discharges of between 2 and 8 m^3/s for cross-sections and pebble counts, and 13 m^3/s for the long profile. To predict channel and hydraulic properties at given flows such as the estimated bankfull flood, two HECRAS models were developed using the cross section data up- and downstream from *Ojitos Arroyo*, respectively. The models were fit to the water surface data collected during the field surveys by adjusting the Manning's roughness value over the reach. Final low-flow roughness values were 0.056 for the upstream model and 0.074 for the downstream reach, reflecting the greater degree of channel-hillslope connectivity and associated coarser bed material and other factors along the downstream section (Swanson et al., 2012a). Additionally, downstream surveys were generally conducted at lower flows to reduce risk of accident in the steeper, rockier subreaches. Modeled water-surface elevations compared well to field measurements ($R^2 = 0.94$), with average differences between measured and modeled water surface elevations of 1 cm, standard deviation of 5 cm, and a maximum difference of 15 cm. The resulting long profile also visually corresponded well to the long profile surveyed in the field (Figure 4). For bankfull conditions, the discharge was set to 70 m^3/s (recurrence interval ~ 1.8 yrs) and roughness values were reduced to 0.028 for both models. Model output agreed well with bankfull channel parameters identified in the field. Regression coefficients (R^2) for field estimations of the bankfull channel versus hydraulic model outputs were 0.87 for width, 0.84 for average depth, and 0.94 for shear stress. The cross-section averaged flow velocity, shear stress, and stream power values used in the study were output from the models.

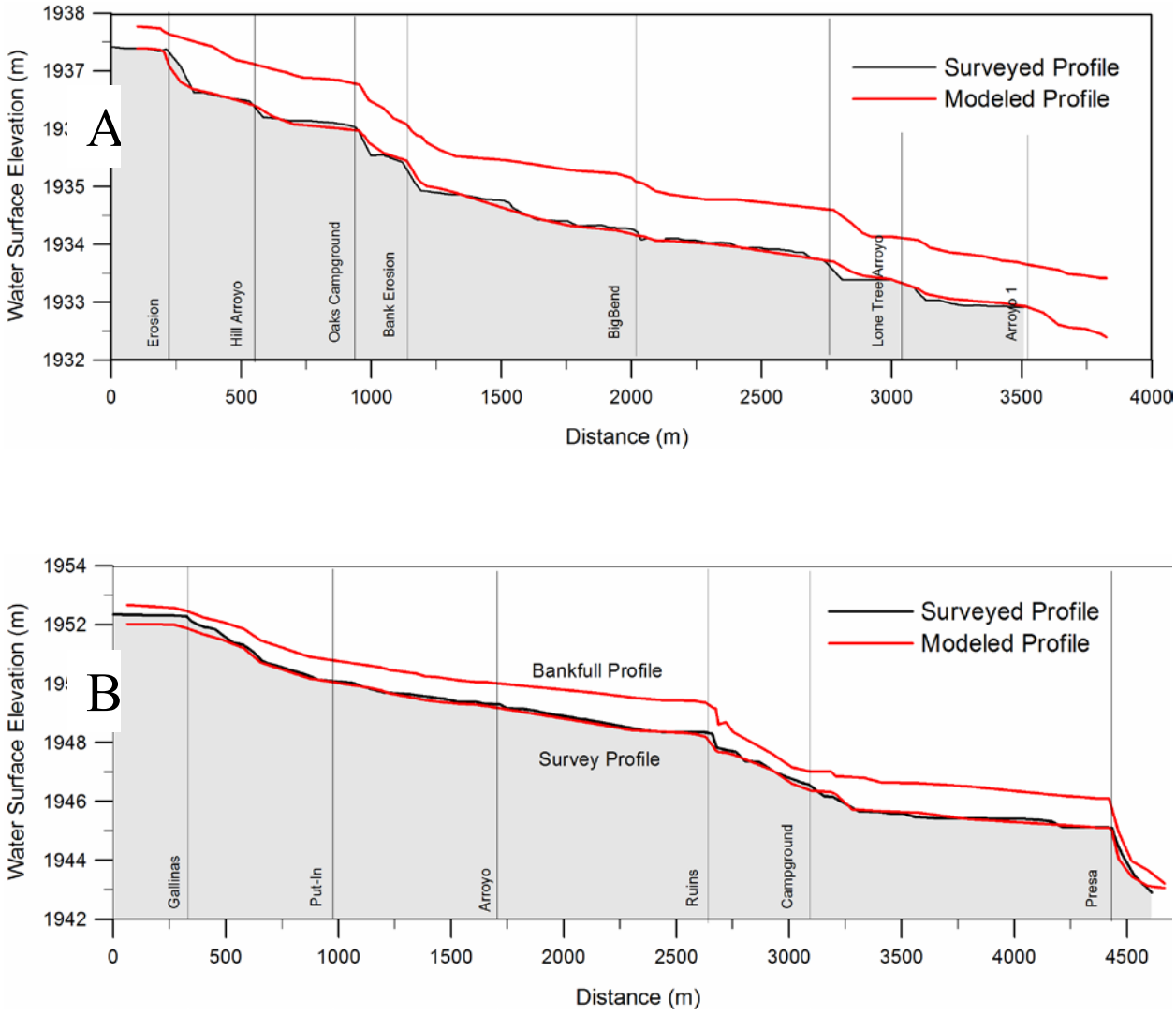

Figure 4. Comparison of surveyed water surface elevations and HECRAS output water surface elevations for (A) the upstream reach, between the Rio Gallinas and Arroyo de la Presa, and (B) the middle reach of the study area, from upstream of Hill Arroyo to Arroyo 1.

Statistics. The spatial variability inherent in channel characteristics often complicates the identification of discontinuities in channel attributes at tributary junctions. In order to delimit statistically significant changes in channel characteristics across confluences (e.g., D_{50}, slope, velocity, shear stress), the data from cross-sections classified as *intermediate* (between the tributary sites) were compared to the cross-section data obtained

for the *upstream*, *fan*, and *downstream* groups for the entire study reach. The analyses tested for a difference in means using the Mann-Whitney Rank Sum test at a significance level of 5% (alpha = 0.05).

Although sample sizes for each confluence are rather small, Mann-Whitney Rank Sum tests were used to compare channel shape and hydraulic parameters at each cross-section with data from the five cross-sections immediately upstream ($\alpha = 0.05$). For these tests, the expected difference between means was assumed to match the overall trend for the study reach. For example, slope increases downstream of the majority of the tributary junctions along the Rio Chama study reach (Swanson et al., 2012a, this study), so for the difference in the mean slope values between a cross-section site and the five cross-sections immediately upstream to be "significant", the change in the mean had to be positive as well as statistically valid. Similarly, shear stress, flow velocity, and stream power were also expected to increase below junctions, and average channel depth was expected to decrease.

Bedload entrainment. Several factors control bedload transport along river and stream channels, including water discharge, channel width, depth, and slope, as well as the grain sizes available for transport. Modeled channel parameters and field-collected sediment data were used to determine if and where channel sediment was able to move at given flows, as well as to delineate spatial differences in bedload transport capacity at the bankfull discharge. The process involves a number of steps. First, the hydraulic parameter driving sediment movement in the channel needs to be calculated, which for this analysis is average boundary shear stress:

(1) $$\tau = \rho g R S_f,$$

where τ is average boundary shear stress, ρ is the density of water, g is gravitational acceleration (9.81 m/s^2), S_f is the friction slope derived from the HECRAS model (i.e., slope back-calculated from HECRAS cross-sections and discharge outputs), and R is hydraulic radius.

To change this value to a dimensionless parameter for later comparison, average cross-sectional shear stress was converted to dimensionless shear stress:

(2) $$\tau^* = \tau/(\rho_s-\rho)gD_{50},$$

where τ^* is the dimensionless shear stress, ρ_s, the density of the sediment, which is set to the density of quartz grains, 2650 kg/m^3, and τ, ρ, and g are as in (1)

The next step calculates the dimensionless shear stress predicted to initiate movement of a particle, or the critical Shields stress (τ^*_c). Although previous studies have primarily relied on estimates of a constant τ^*_c for a representative grain size, usually between 0.03 and 0.06 for D_{50} (Buffington and Montgomery, 1997), recent studies indicate τ^*_c increases with channel slope (Mueller and Pitlick, 2005; Lamb et al., 2008). Therefore, instead of using a fixed value of τ^*_c for initial sediment motion, the empirical equation presented in Mueller et al. (2005) was utilized:

(3) $$\tau^*_r \sim \tau^*_c = 2.18S_f + 0.021,$$

where S_f is channel friction slope.

Along channel beds characterized by heterogeneous sediment sizes, τ^*_c is further modified by the effect of the grains on each other and the clasts' impact on the flow at the bed. In mixed-size sediments, larger grains often shelter smaller grains from the flow, limiting the mobility of the finer fraction. Also, while having greater weight, larger clasts may be more

easily mobilized because they are more exposed to the flow and experience a higher fluid force than if all the clasts were the same size (e.g., Profitt and Sutherland, 1983; Komar and Li, 1988; Parker, 1990). A hiding function presented by Parker and Klingeman (1982) was used to adjust τ^*_c values for varying sediment sizes at each cross-section:

(4) $$\tau^*_{ci} = \tau^*_c(D_i/D_{50})^{-b},$$

where τ^*_{ci} is the critical shear shear stress needed to estimate a particle of size fraction i, τ^*_c is the critical shear stress as estimated with the Mueller and Pitlick (2005) equation (3); D_i is the diameter of sediment fraction i; and D_{50} is the median grain size at each cross-section. For this study, b was set to 0.81, an average value taken from previous studies (see Parker 2008 (ASCE manual 110)).

For a particle of diameter D_i to be entrained, τ^* must be greater than $\tau^*_{ci.}$

Using the estimates of τ^*_{ci}, the discharge required to initiate bed material movement, Q_{ci}, can also be calculated:

(5) $$Q_{ci}=BR_{ci}\,(R_{ci}^{2/3}S_f^{1/2})/n$$

where $d_{ci}{\sim}R_{ci} = \tau_{ci}/\rho g S_f$, and B is width, d is depth, R is hydraulic radius, S_f is friction slope, and n is Manning's roughness value, set to 0.028 for bankfull discharge as explained above.

Transport capacity. In addition to evaluating whether or not a particle of median grain size can be entrained at a given flow (e.g., bankfull flow), both bankfull bedload transport capacity and annual bedload transport capacity were evaluated for the 203 cross-sections along the Rio Chama study reach.

The Rio Chama channel includes both sand and gravel bed reaches, with the majority being somewhere between. Therefore, in order to examine changes in sediment transport

capacity, we needed a transport relation designed to account for a wide range of material and associated hiding effects, and the nonlinear impact of sand content on gravel transport rates (Wilcock, 1998; Wilcock and Kenworthy, 2002; etc). The surface-based transport relation of Wilcock and Crowe (2003) meets these criteria. It is based on the full grain size distribution of the bed surface, including the sand. Their model calculates an estimated sediment transport capacity, W^*_i for a grain of size D_i per unit width of channel using the following equations:

$$W_i^* = \begin{cases} 0.002\phi^{7.5} & \phi < 1.35 \\ 14\left(1 - \frac{0.894}{\phi^{0.5}}\right)^{4.5} & \phi \geq 1.35 \end{cases} \quad (6)$$

where

$$\phi = \frac{\tau}{\tau_{r_i}}, \qquad \tau_{r_i} = \tau_{r_{50}}\left(\frac{D_i}{D_{50}}\right)^b$$

and the exponent b in the hiding function is calculated from:

$$b = \frac{0.67}{1 + \exp\left(1.5 - \frac{D_i}{D_m}\right)} \quad (7)$$

where D_m is the mean grain size of the bed surface. In this case D_g replaced D_m as per the suggestion of Parker (2008).

The dimensionless reference shear stress for D_m, τ^*_{rm}, is similar to τ^*_c, but instead of representing the stress required to initiate movement of D_m, it is the stress required to move a reference volume of D_m (i.e., $W^* = 0.002$). For D_m, τ^*_{rm} is found using the relation:

$$\tau^*_{r_m} = \frac{\tau_{r_m}}{(s-1)gD_m} \quad (8)$$

where τ^*_{rm} is calculated using an empirical function that accounts for variations in sand content:

$$\tau^*_{r_m} = 0.021 + 0.015\exp(-20F_s) \quad (9)$$

where F_s is the percent of sand on the bed surface.

Values of W^*_i are calculated for each size fraction (i) then weighted by the proportion of that size fraction on the bed surface, F_i. The instantaneous, width-integrated, bed load transport rate for each particle size (Q_{bi}) is calculated using the following equation (10) and then summed over all sizes to get the bedload transport rate for the cross-section (Q_b):

$$Q_{b_i} = \frac{W^*_i F_i B u^3_* \rho_s}{(s-1)g} \quad (10)$$

where W^*_i is calculated using (6), B is channel width, u^* is shear velocity ($(\tau/1000)^{0.5}$), and ρ, ρ_s, and g are as in (1) and (2).

The average annual transport rates were estimated by running the HECRAS models at average daily discharge increments of 7 m^3/s ranging from 3.5 to 88 m^3/s. The HECRAS results were then input into the Wilcock and Crowe (2003) transport relations to estimate annual transport rates for the central discharge in each increment (i.e., 7 m^3/s, 14 m^3/s, 21 m^3/s, …, 84 m^3/s). These results were then multiplied by the proportion of days per year each discharge increment occurred.

Results

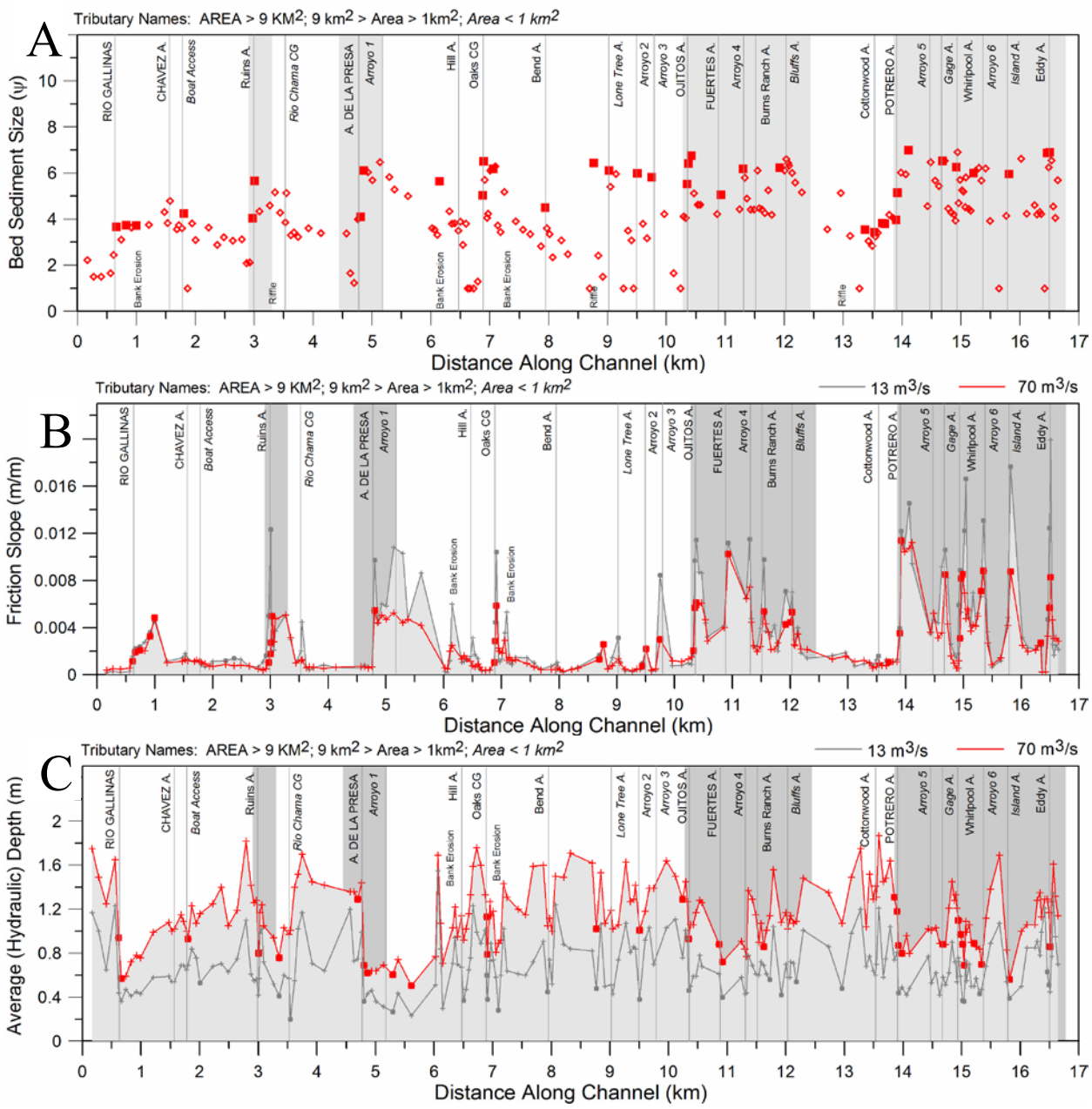

Figure 5. Changes in A) bed sediment size, B) friction slope, and C) average depth along the Rio Chama study reach channel, from Swanson et al. (2012). Significant changes in channel parameters relative to the 5 sites immediately upstream are shown in solid blocks as opposed to crosses. 73% of the tributary sites exhibit significant increases in sediment size, 65% of the sites exhibit significant increases in depth, and 62% of the sites exhibit significant decreases in cross-section area.

In an associated study, Swanson et al. (2012a) characterized geomorphic impacts on the Rio Chama study area channel related to tributary inputs, and described significant, abrupt changes in channel slope, depth, and bed sediment size at confluences. Because sediment size, slope, and flow depth data are common parameters associated with quantifying sediment entrainment and transport, the data exhibiting the longitudinal variations of these characteristics are provided in Figure 5, and a brief summary follows. Along the study reach, bed material size often increases sharply at confluences, usually by a factor of 4 to 8 (Figure 5). The sediment then tends to fine downstream, largely due to a downstream increase in the proportion of sand along the bed. Along many sections of the channel, the D_g (geometric mean diameter of the sediment) reaches a relatively constant minimum of approximately 3 ψ (~10 mm), before being sharply elevated by the next substantial sediment input. In other subreaches, especially along the downstream segment of the study reach, the gradual decrease in grain size below one tributary input is interrupted by the next input in close succession. Of the 26 tributary sites, 19 (73%) exhibited a statistically significant increase in the geometric mean sediment diameter (D_g), and at many sites the increase was more than 2.5 ψ greater (a factor of 5 in mm) than for bed sediment situated away from new sediment sources (Figure 5). Additionally, at some locations, such as *Ruins, Presa, Oaks, Whirlpool, and Eddy Arroyos*, the mainstem channel bed immediately upstream of the junctions was entirely dominated by sand.

Friction slope also increased immediately downstream of almost every tributary site, often by an order of magnitude (Figure 5). The largest slope values, typically between 0.01 and 0.02 m/m, occur just downstream of tributary junctions in more confined subreaches (e.g., *Arroyo de la Presa, Ojitos Arroyo;* Figure 5). Seventeen of the 26 confluence sites

exhibited significantly higher gradients (65%; Figure 5), and when averaged by position relative to tributaries, bankfull gradients downstream of tributary confluences (*fan* and *downstream positions*) are twice the gradients measured at *intermediate* reaches (Swanson et al, 2012a). Slopes directly *upstream* of confluences are also smaller than slopes along control reaches indicating some of the tributaries force upstream backwater conditions.

The steeper slopes are commonly associated with abrupt decreases in bankfull flow depth as well. The localized results showed statistically significant bankfull depth decreases at 16 of the 26 tributary sites (62%; Figure 5), with statistically significant decreases in *fan* and *downstream* depths and a slight, insignificant, increase in *upstream* depths. Average bankfull depth for *intermediate* sites was17% higher than the average depth measured at *fan* and *downstream* positions.

As in previous work (e.g., Werrity, 1992), the Rio Chama data also suggest that other sources of sediment supply, such as eroding gravel banks (as opposed to sand banks), may also influence channel bed sediment texture and geometry, similar to the tributary impacts, and that tributaries delivering primarily sand and fine gravel have smaller, sometimes contrary, impacts. Additionally, the downstream section of the study reach, below *Ojitos Arroyo*, is characterized by larger slopes and grain sizes, presumably due to the more confined channel receiving abundant coarse hillslope sediment (Swanson et al., 2012a).

Variations in shear stress and velocity.

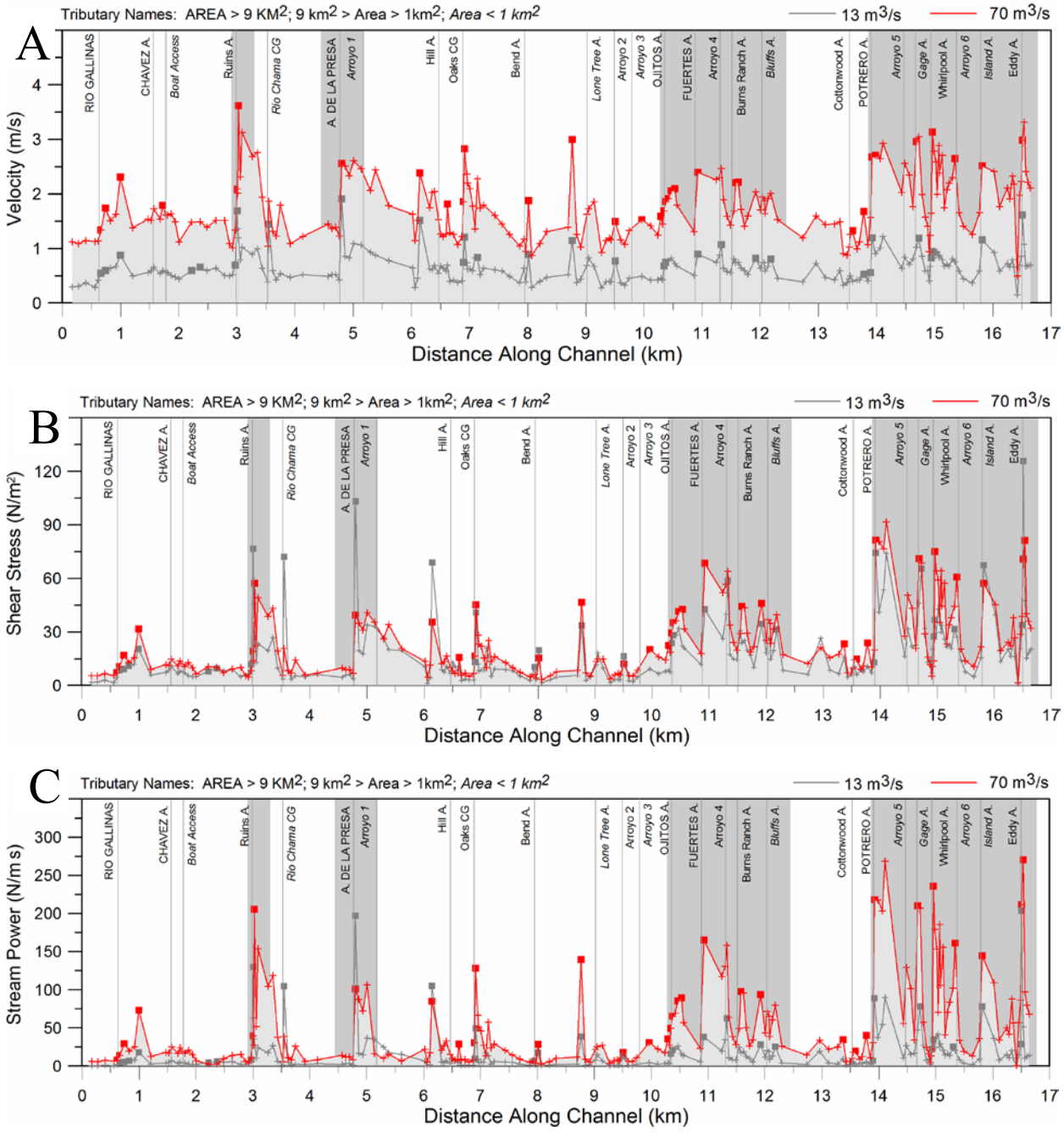

Figure 6. Downstream variation in A) average cross-section velocity, B) average cross-section shear stress, and C) average cross-section stream power along the Rio Chama study reach. Significant changes in channel parameters, relative to the 5 sites immediately

upstream, are shown in solid blocks as opposed to crosses. 54% of the tributary sites exhibit significant increases in velocity, 65% of the sites exhibit significant increases in shear stress, and 65% of the sites exhibit significant increases in stream power. Grey shading represents areas where the channel is semi-confined.

	Velocity		***Shear Stress***		***Stream Power***	
Geomorphic Position	*mean(m/s)*	*probability*	*mean (N/m^2)*	*probability*	*mean (N/m s)*	*probability*
intermediate	1.7	---	20	---	37	---
upstream	1.4	0.001	13	0.005	21	0.019
fan	2.0	0.001	31	0.014	71	0.006
downstream	2.0	0.010	31	0.001	68	0.002

Table 1. Statistical analysis (Mann-Whitney Rank Sum test) results comparing mean Rio Chama hydraulic characteristics at cross-sections adjacent to confluences with hydraulic parameters in the intermediate positions. Based on $\alpha = 0.05$, the results indicate significant discontinuities in velocity, shear stress, and stream power occur across tributary junctions (probability < α that means are the same.

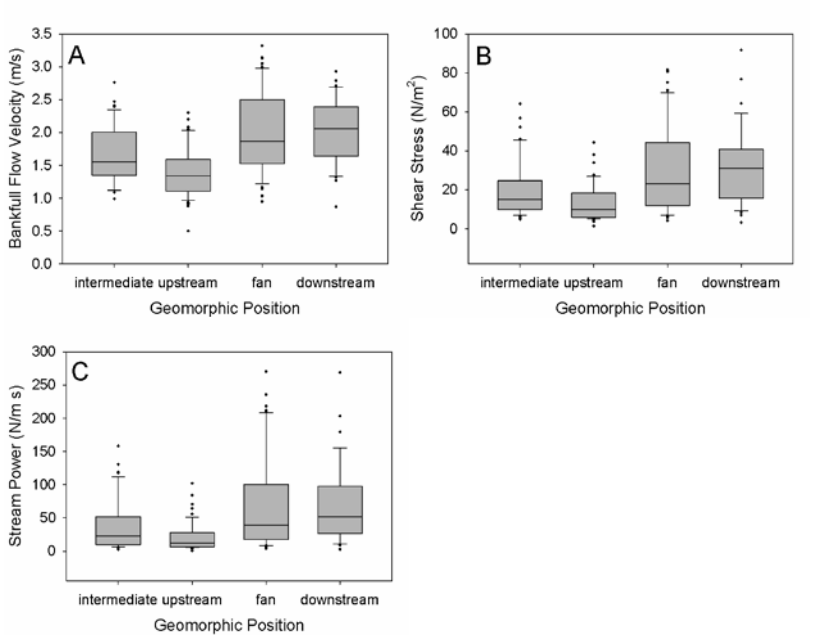

Figure 7. Comparison of hydraulic data at various geomorphic positions relative to tributary confluences: A) average cross-section velocity, B) average cross-section shear stress, C) average cross-section stream power. In general, velocities, shear stresses, and stream power are greater and more variable at cross-sections categorized as fan or downstream sites, and less at cross-sections directly upstream of junctions.

Along with discharge, the three hydraulic parameters most often used to estimate sediment transport are flow velocity (Hjulstrom, 1935; Karim and Kennedy, 1990), stream power (Bagnold, 1966; Yang, 1972), and shear stress (Meyer-Peter and Muller, 1948; Parker, 1990; Wilcock and Crowe, 2003). All three are directly related to the slope and depth of the channel, which are highly variable along the study reach (Figure 5; Swanson et al., 2012a). Accordingly, these hydraulic variables also fluctuate greatly along the Rio Chama.

Flow velocity. Mean bankfull flow velocity (averaged across each cross section) along the channel is 1.8 m/s, with velocities upstream of Ojitos Arroyo of 1.6 m/s and 1.9 m/s downstream. However, velocities are highly variable along both segments, and much of the variability is associated with tributary junctions (Figures 6 and 7). Mean flow velocities increase downstream of almost every tributary site, sometimes by a factor of 2.5, and the largest velocity values, typically around 3 m/s, occur just downstream of *Ruins, Potrero, Whirlpool, and Eddy Arroyos*. Comparing each cross-section site with the 5 cross-sections immediately upstream located 33 cross-sections where increases in bankfull flow velocity were statistically significant. Of these 33 sites, 26 are directly related to tributary fans at 16 of the 26 confluences (62%; Figure 6). At low flow, 14 of the 26 tributary sites (54%) produced higher velocities. Smaller tributaries and tributaries that appear to primarily deliver sand rather than gravels have less impact on the flow rate (e.g., *Boat Access or Hill Arroyo*). Significant increases in velocity also occur where the channel has eroded gravel banks, as opposed to sand, such as upstream of *Hill Arroyo* and downstream of *Oaks Campground Arroyo*.

When averaged by position relative to tributaries (Figure 7), bankfull velocities at the *upstream, fan, and downstream* positions are all significantly different than those categorized

as *intermediate*. Mean velocities downstream of tributary confluences (*fan and downstream positions*) are approximately 18% larger than those estimated at *intermediate* reaches, and mean velocities *upstream* of confluences are 18% less than at the *intermediate* sites (Table 1). The slower flow upstream of tributary confluences provides further evidence that aggradation at the junction creates backwater conditions upstream.

Shear stress. Bankfull shear stress is also highly variable along the channel. Over the entire reach, the cross-section averaged shear stress ranges between 1 and 97 N/m^2, with a mean of 24 N/m^2. The upstream section has an average shear stress of 15 N/m^2 and the downstream section has an average of 36 N/m^2. Like the other parameters, major fluctuations in shear stress along the channel are largely controlled by tributary inputs (Figure 6). Along the study reach, 33 cross-sections were identified as significantly different in shear stress compared to the 5 cross-sections immediately upstream. Of those, 25 cross-sections were associated with tributaries at 17 of the 26 confluence sites (65%). When averaged by position relative to the tributary junction, bankfull shear stress *upstream* of tributary junctions is about 50% less than at *intermediate* positions, which in turn, is approximately 50% less than at *fan and downstream* positions, and all three of these differences, relative to the *intermediate* sections, are significant (Table 1; Figure 7).

As with slope, grain size, and velocity, coarse bank-derived inputs also create short but significant discontinuities in shear stress along the study reach, and smaller channels and channels currently supplying finer material appear to have insignificant impacts. Importantly, shear stress at some cross-sections actually increases at lower flows, notably at the *Ruins, Rio Chama Campground, Presa, and Eddy Arroyos*, where gradients increase with decreasing downstream water levels (Figure 5).

Stream power. Variations in bankfull stream power (i.e., average cross-section shear stress x average cross-section velocity) through confluences derived from the HECRAS model are similar to the fluctuations observed in bankfull shear stress, only exaggerated (Figure 6). Values vary from 10 to 250 N/m s, but mean values for the cross sections immediately downstream of tributary junctions (*fan and downstream* positions) are nearly twice as large as the mean for *intermediate* cross sections (Table 1, Figure 7). *Upstream* cross-sections produce only 57% of the stream power of *intermediate* sections. Along the channel, local mainstem stream power significantly increases at 17 of the 26 confluences (65%), and abrupt shifts at some of these junctions can be higher than 500% (Figure 6).

Critical vs. Grain Shear Stress. The potential for entrainment of median-sized bed sediment (D_{50} *and* $D_{50\,gravel}$) sediment at bankfull flow (~70 m^3/s) along the Rio Chama study reach is shown in Figure 8. This assessment is based on a comparison of the critical dimensionless shear stress (τ^*_c, shear stress required to entrain a mean particle, D_{50}) and the dimensionless shear stress (τ^*, shear stress acting on the particle at bankfull). Where τ^*/τ^*_c is greater than 1 (i.e., $\tau^* > \tau^*_c$), the D_{50} at the individual cross-section can be entrained, whereas if τ^*/τ^*_c is less than 1 (i.e., $\tau^*_c > \tau^*$), the D_{50} likely will not be entrained. Along the study reach, τ^*_c for D_{50} at each cross-section ranges from 0.019 to 0.049, with a mean of 0.031, and estimated τ^* is between 0.005 and 0.764, with an average of 0.077. For $D_{50\,gravel}$, τ^*_c ranges from 0.001 to 0.047, with an average of 0.020, and τ^* is between 0.001 and 0.098 with a mean of 0.020. The analysis indicates that the D_{50} and finer sediment is readily entrained between tributary junctions, but immediately downstream of junctions, the D_{50} and $D_{50\,gravel}$ are often too coarse to be transported under existing bankfull conditions. The

difference between τ^*_c and τ^* is often especially large ($\tau^* > 2\tau^*_c$) in the clearly alluvial reaches, and in the sandy subreaches upstream of larger impacts (e.g., *Presa, Oaks Campground, Ojitos, Potrero, and Island Arroyos*; Figure 8). In contrast, the D_{50} is relatively immobile in the more confined, semi-alluvial reaches, indicated by the darker gray background areas in Figure 8. Consistent with these estimates, larger gravels and cobbles at most of the tributary sites were often difficult to remove from the bed during field sampling, whereas gravels less than 45 mm were often lying loose.

Exceptions to the abrupt decrease in sediment entrainment potential downstream of tributary confluences occur at the *Rio Gallinas, Chaves, Boat Access, Rio Chama Campground, and Hill Arroyo* junctions (Figure 8). At these locations, the tributaries enter the mainstem over broad sandy alluvial fans and floodplain deposits, which appear to primarily deliver sands with some small gravel (< 22 mm) to the mainstem Rio Chama. Additionally, a few bank erosion sites upstream of *Hill Arroyo* and downstream of *Oaks Campground Arroyo* appear to disrupt the entrainment potential along the channel.

In addition to examining whether bankfull flows along the Rio Chama can entrain the D_{50} *at each cross-section*, it is also useful to look at how readily the channel might pass sediment of given sizes from reach to reach. Figure 9 provides comparisons of τ^*_{ci} and τ^*_i for sediment with diameters of 2 mm (coarse sand, blue), 24 mm (D_{50} for entire reach, red), and 69 mm ($D_{50\,gravel}$ for the entire reach, yellow), respectively. Sand should be entrained at bankfull flows along the entire channel, although differences between τ^*_{ci} *and* τ^*_i are generally smaller immediately downstream of tributary confluences. As with the D_{50} at each cross section, particles of 24 mm and 69 mm are typically less likely to be entrained downstream of tributary junctions (i.e., $\tau^*_{ci} > \tau^*_i$). However, in some of the steeper reaches,

such as immediately downstream of *Potrero, Gage, and Eddy Arroyos*, the Rio Chama appears to be able to just entrain these gravels (i.e., $\tau^*_{ci} \sim \tau^*_i$). Additionally, τ^*_{ci} *and* τ^*_i are similar at many of the other confluences sites, especially downstream of *Ojitos Arroyo*, suggesting there is likely partial transport of the overall D_{50} and $D_{50\ gravel}$ material (i.e., a relatively small portion of the surface clasts may move over the duration of a transport event) at these locations during bankfull flows and higher.

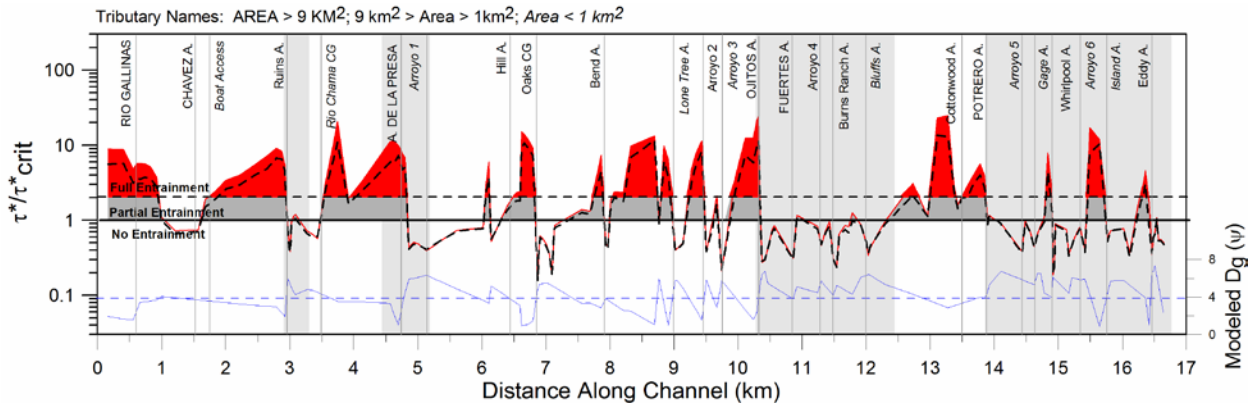

Figure 8. Downstream variations in the ratio of dimensionless shear stress (τ*) and the dimensionless Shields shear stress (τ^*_c) for the D50 at bankfull discharge for each cross-section along the Rio Chama study reach. Immediately downstream of confluences and in semi-confined reaches (gray background), the median grain size is generally immobile, whereas in the alluvial reaches, bed material is more readily entrained ($\tau^*/\tau^*_{ci} > 2$; red areas). The blue line represents a generalized model of the geometric mean grain size (D_g) along the channel. A comparison of the two lines suggests that the bed becomes mobile when the D_g is less than 12 mm.

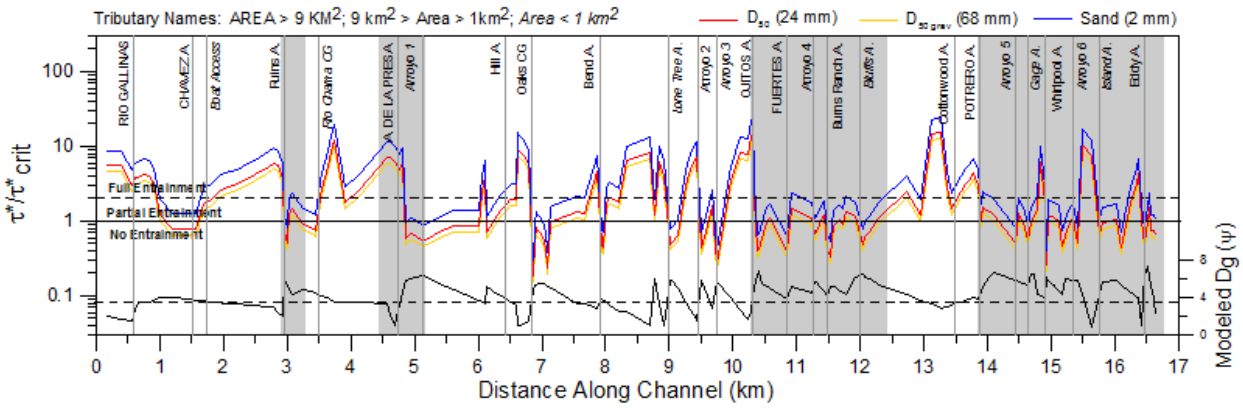

Figure 9. Downstream variations in the ratio of dimensionless shear stress (τ^*_i) and the dimensionless Shields shear stress (τ^*_{ci}) for sand and the overall D50 along the Rio Chama study reach. Sand is largely mobile along the study reach. Immediately downstream of confluences and in semi-confined reaches (gray background), the overall median grain sizes (with and without sand included in the analysis) are immobile to partially mobile, whereas in the unconfined reaches, these gravels are readily entrained ($\tau^*_i/\tau^*_{ci} > 2$).

	$\tau^*_{D50}/\tau^*_{crit\,D50}$		$\tau^*_{D50\,gravel}/\tau^*_{crit\,D50\,gravel}$		$\tau^*_2/\tau^*_{crit\,2}$	$\tau^*_{24}/\tau^*_{crit\,24}$	$\tau^*_{69}/\tau^*_{crit\,69}$	
Geomorphic Position	*mean*	*probability*	*mean*	*probability*	*mean*	*mean*	*mean*	*probability*
intermediate	4.1	---	2.7	---	5.0	3.1	2.6	---
upstream	6.1	0.079	4.0	0.114	7.2	4.5	3.7	0.163
fan	1.4	<0.001	1.1	<0.001	2.5	1.6	1.3	<0.001
downstream	1.6	<0.001	1.2	<0.001	2.4	1.5	1.2	0.002

Table 2. Statistical analysis (Mann Whitney Rank Sum tests) results comparing the entrainment potential (τ^*/τ^*_c) at cross-sections adjacent to confluences with the values in the intermediate positions. Based on $\alpha = 0.05$, the results indicate significant discontinuities in entrainment potential for all parameters, except at upstream sites for the individual grain sizes. Median-sized particles are most likely to be entrained in *upstream* positions, and less likely to be entrained downstream of junctions (*fan and downstream positions*).

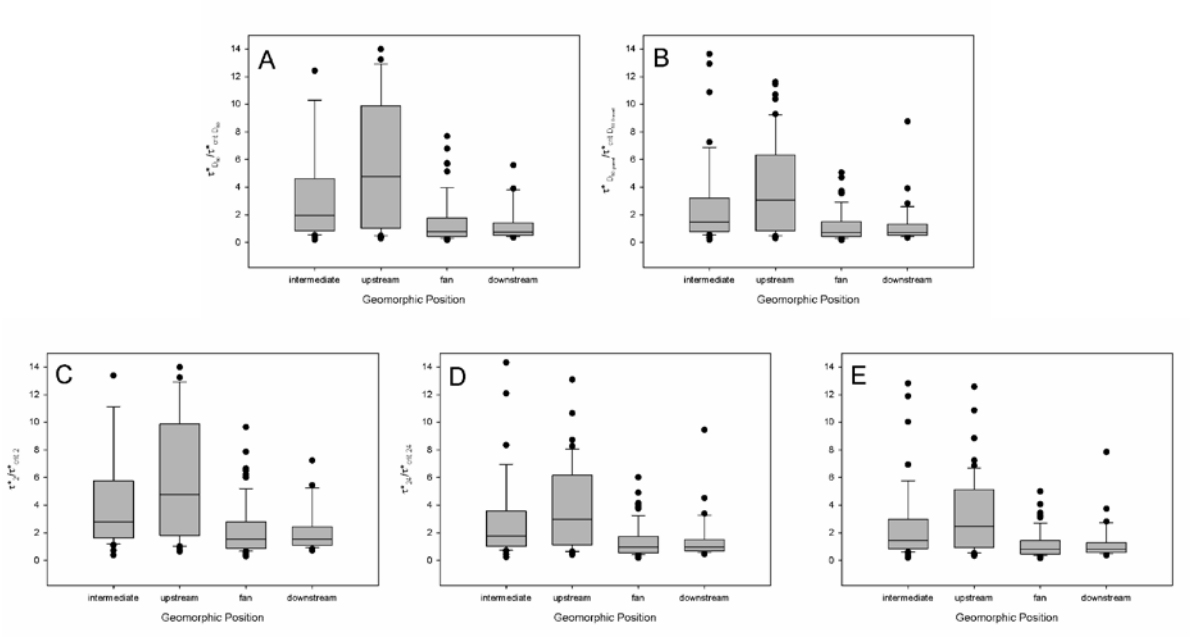

Figure 10. Comparison of entrainment potential results (τ^*/τ^*_c) at various geomorphic positions relative to tributary confluences. In general, sediment is more readily entrained in the upstream positions, and less likely to be entrained in the fan and downstream positions. A) D_{50} at each cross-section, B) $D_{50\ gravel}$ at each cross-section (sand removed from analysis) C) sand (2 mm), D) D_{50} for entire reach (24 mm), and $D_{50\ gravel}$ for the entire reach (69 mm).

Figure 10 and Table 2 provide comparison between τ^*/τ^*_c data categorized by geomorphic position relative to tributary junctions. Median-sized particles in all five cases can be entrained, with D_{50} particles in the *upstream* category (whether sand or gravel) having the largest differential between τ^* *and* τ^*_c. All differences in τ^*/τ^*_c are statistically significant, except the *upstream* position versus the *intermediate* position for entrainment of 2, 24, and 69 mm particles. The τ^*/τ^*_c at the upstream locations indicate some additional transport may occur relative to the intermediate positions, although the difference is insignificant. Downstream of confluences (*fan and downstream* categories), average τ^*/τ^*_c values suggest that entrainment of gravels is possible ($\tau^*/\tau^*_c>1$), but the differential is not large, and sediment will not move as easily as at the *intermediate and upstream* sites.

Transport capacity.

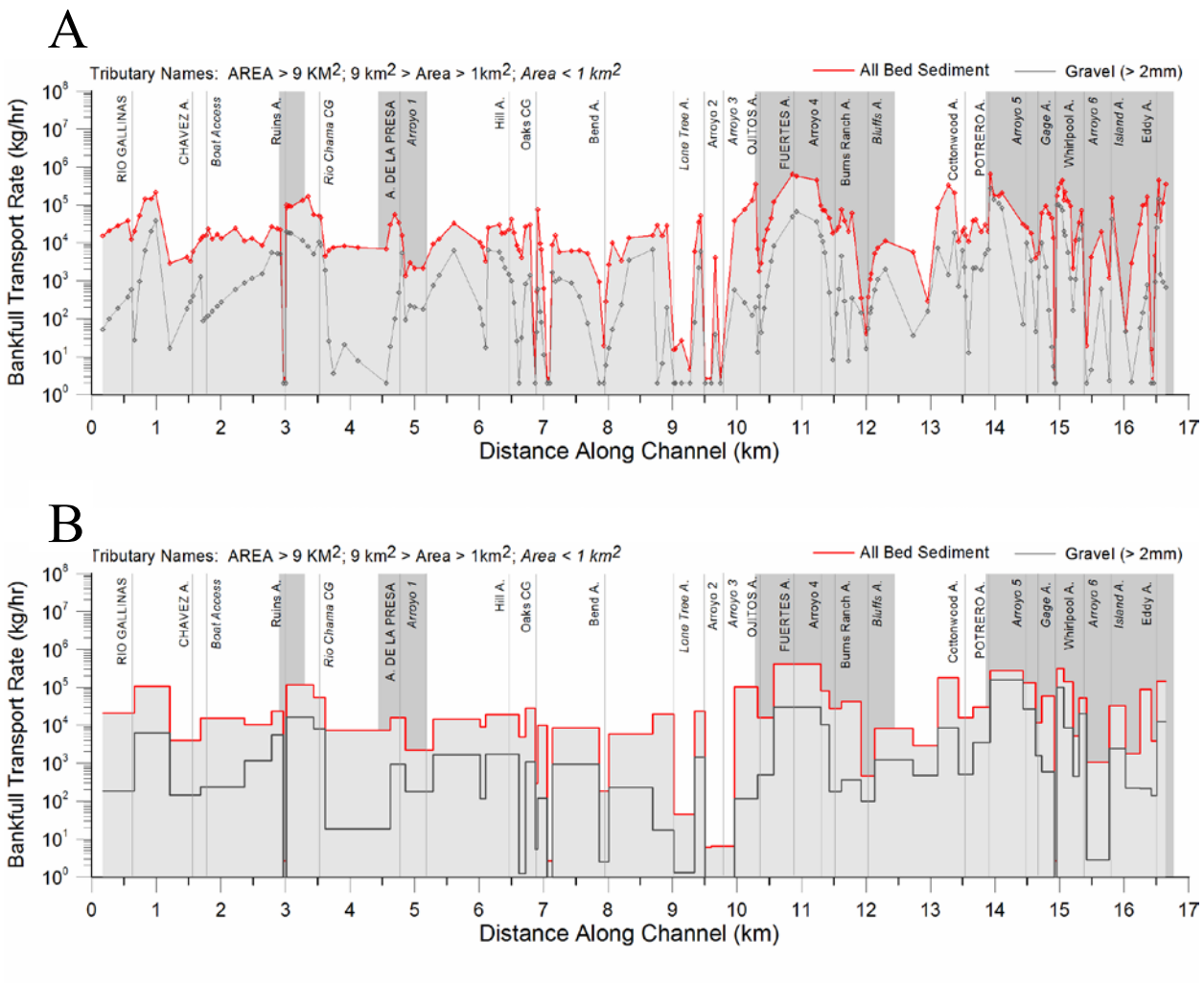

Figure 11. Downstream variations in bankfull bedload transport rate based on calculations using the Wilcock and Crowe (2003) transport relations. A) Data from individual cross-sections. B) Calculations based on reach-averaged values.

Geomorphic Position	Q_s-bankfull			Q_{gravel}-bankfull			Q_s-annual		
	log_{10}(mean)	kg/hr	probability	log_{10}(mean)	kg/hr	probability	log_{10}(mean)	t/yr	probability
intermediate	4.02	10500	---	2.74	550	---	4.82	66800	---
upstream	3.96	9200	0.19	2.11	130	0.01	4.95	89800	0.08
fan	3.64	4400	0.33	2.69	490	0.04	4.80	62600	0.09
downstream	4.15	14000	0.23	2.68	480	0.41	4.80	62600	0.15

Table 3. Statistical analysis (Mann-Whitney Rank Sum test) results comparing bankfull and annual bedload transport estimates at cross-sections adjacent to confluences with the values in the intermediate positions. The results suggest transport rates are largest along the *downstream* positions, and least at *fan* positions during bankfull flow, although none of the differences are statistically significant. For gravel (> 2 mm), transport rates at bankfull flow decrease significantly at the *upstream* of confluences. Annual rates are similar at all of the sites except for a statistically insignificant increase in annual transport at the upstream geomorphic position.

Application of the Wilcock and Crowe (2003) formula yields a wide range of bedload transport rates at bankfull discharge along the study reach (Figure 11), as expected given the large variability in channel form, shear stresses, and bed sediment size. Estimates range from around 5.5 x 10^5 to 6.5 x 10^5 kg/hr downstream of *Ruins*, *Fuertes, Potrero, and Whirlpool Arroyos,* to < 10 kg/hr upstream of *Oak Campground Arroyo, Lone Tree Arroyo to Arroyo 3*, and *Whirlpool and Eddy Arroyos*. The average bankfull transport rate is 6.0 x 10^4 kg/hr, and the average transport rate for gravel is 9.1 x 10^3 kg/hr. Figure 11B shows the same analysis, but the calculations are performed using data averaged over specific subreaches. The subreaches were delimited visually based on sediment size, slope, and shear stress based on the field data. Mean hourly, bankfull transport rates based on the reach-averaged data are 5.3 x 10^4 kg/hr (< 10 to 4.1 x 10^5 kg/hr) for sand and gravel, and 8.3 x 10^3 kg/hr (< 10 to 1.6 x 10^5 kg/hr) for gravel.

As with the other channel characteristics, tributary junctions appear to be associated with much of the variability in the bedload transport data. At many of the sites, especially in the upstream sections, above *Ojitos Arroyo*, transport rates abruptly drop upstream of the

junctions, and then increase downstream of the junctions (e.g., *Rio Gallinas, Ruins, Bend, and Oaks Campground Arroyos*). Along the downstream section, however, the impacts at confluences are more complicated. In some locations, notably *Bluff, Gage, Whirlpool, and Eddy Arroyos*, the previous relation holds, but, at other sites, such as immediately downstream of *Lone Tree, Ojitos, and Island Arroyos, and Arroyo 6*, transport rates decrease abruptly and substantially, unlike the increases in transport rates predicted at the other sites. Estimated bedload transport rates along the upstream section of the Rio Chama study reach (upstream of *Ojitos Arroyo*) are also relatively small (2.4×10^4 kg/hr) compared to the downstream section (9.5×10^4 kg/hr). Extremely low rates of transport relative to the rest of the study reach were estimated for the extended sandy segment of the river between *Lone Tree Arroyo* and *Ojitos Arroyo.*

With the exception of channel width, most Rio Chama channel geometry, bed sediment, and hydraulic characteristics have distinctive differences when compared by their position relative to tributary junctions (Figures 5 and 6; Swanson et al. 2012a). Differences in bankfull bedload transport rates categorized by these positions are not so readily discernible. (Figure 12 and Table 3). This lack of significant differences should be expected, however, if there is a long term continuity of sediment transport. Mean bankfull transport rates for the *intermediate* and *upstream* sites are similar for mixed sediment, but gravel transport is significantly reduced *upstream* of junctions. The average bankfull rates for the *fan and downstream* positions tend to be similar as well, although transport at *fan* sites is predicted to be lower and rates at the *downstream* position are higher (Table 3). Figure 12 shows that the main difference between the geomorphic positions lies in the range of bedload

transport rates predicted within the *fan* site category, with smaller rates being more common than at cross-sections in the other groups.

Figure 12 also includes categorized data for predicted annual bedload transport rates for geomorphic positions relative to tributaries. Mean log-normalized bedload transport rates for the *intermediate, fan, and downstream* groups were similar (6.2×10^4 to 6.7×10^4 t/yr), but annual transport rates at *upstream* geomorphic positions is higher (9.0×10^4 t/yr). The differences in predicted annual bedload rates between *intermediate* sites and *upstream, fan, and downstream* sites are statistically insignificant based on rank-sum tests ($P > 0.05$).

Along the study reach, predicted annual bedload transport capacity varies over five orders of magnitude (10^1-10^6), and it appears that tributary and hillslope-derived sediment deposited in the mainstem channel may affect these local fluctuations in bedload transport (Figure 13). The data exhibit an overall sawtooth pattern, where small peaks at some confluences are superimposed on general increases between more substantial impacts, such as between R*io Gallinas and Ruins-Rio Chama Campground Arroyo, De La Presa and Oaks Campground Arroyos, and Oaks Campground and Lone Tree Arroyos*. Downstream of *Lone Tree Arroyo*, substantial fluctuations occur more frequently, with less of a trend across multiple junctions (Figure 13). Although most of the peaks in annual bedload transport occur just upstream of confluences, precipitous drops in transport rate also occur there (e.g., *Whirlpool and Eddy Arroyos*), and at some junctions, rates are higher immediately downstream (e.g., *Rio Gallinas, Bend, Rio Chama Campground, and Whirlpool Arroyos*).

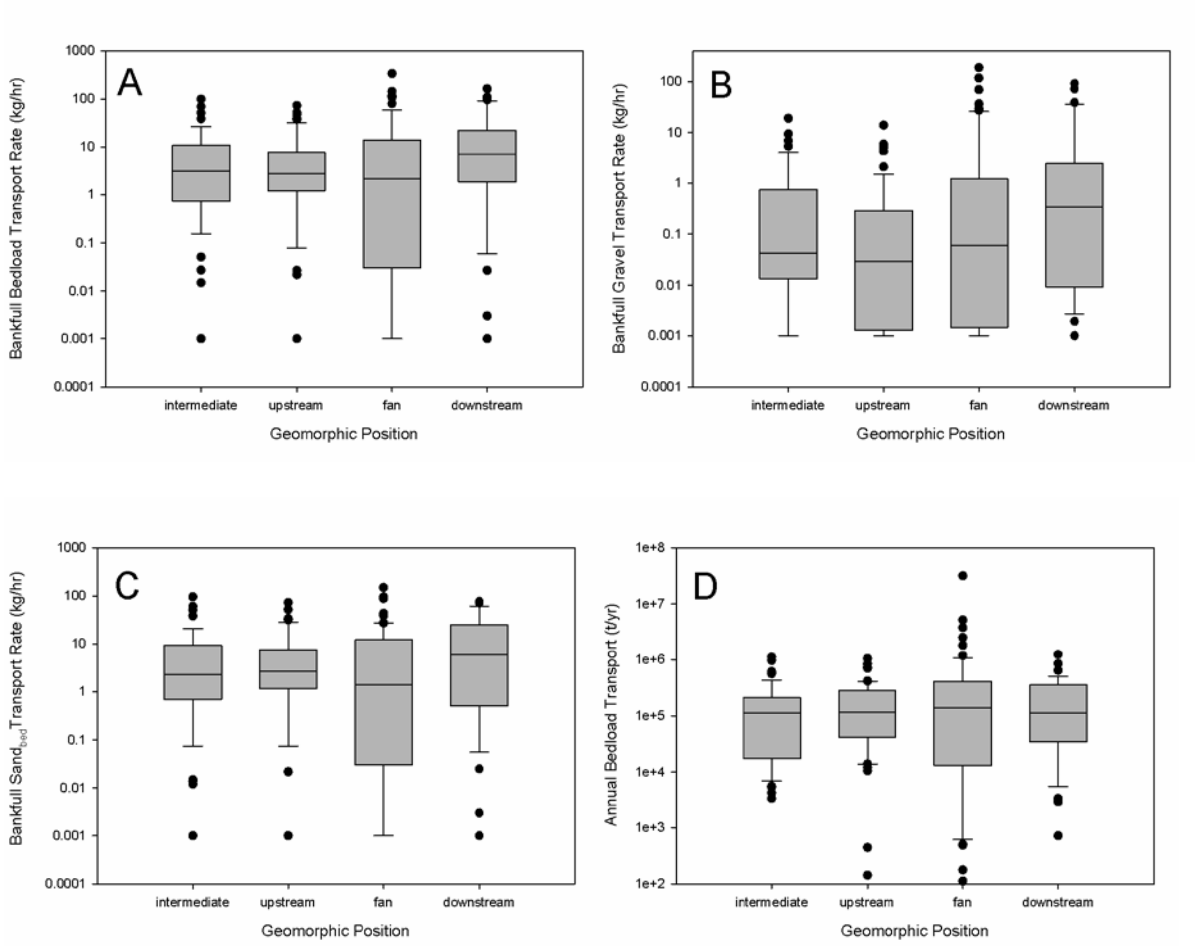

Figure 12. Comparison of bedload transport estimates at various geomorphic positions relative to tributary confluences. A) Total bankfull bedload rate, B) bedload rate for gravel, C) bedload rate for sand, and D) average annual sediment transport rate. The results suggest transport rates are largest along the *downstream* positions, and least at *fan* positions during bankfull flow, although none of the differences are statistically significant. For gravel (>2mm), transport rates at bankfull flow decrease significantly at the *upstream* of confluences. Annual rates are similar at all of the sites except for a statistically insignificant increase in annual transport at the upstream geomorphic position.

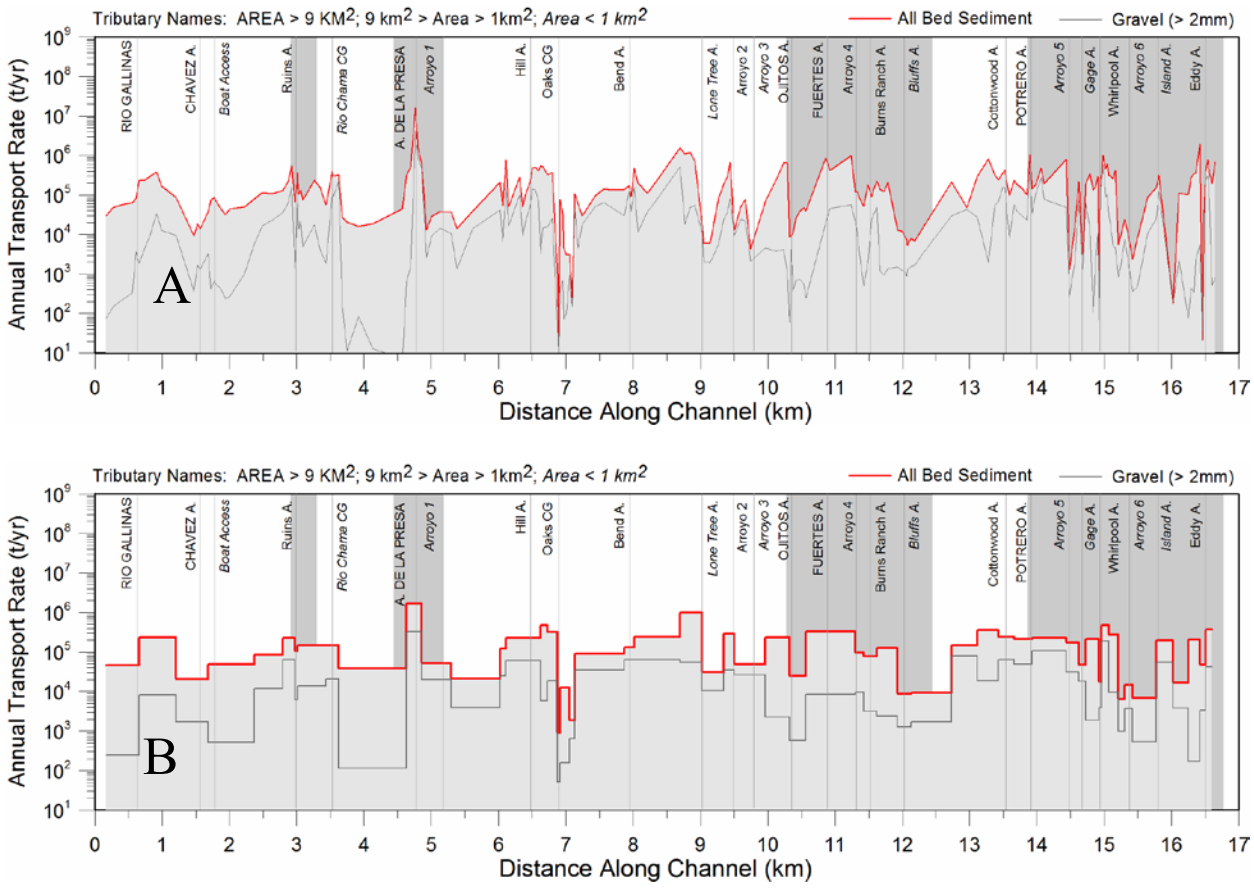

Figure 13. Downstream variations in annual bedload transport rate based on calculations using the Wilcock and Crowe (2003) transport relations. A) Data from individual cross-sections. B) Calculations based on reach-averaged values.

Discussion

When two channels of disparate sediment loads and (or) water discharges meet, the channel downstream of the confluence will typically adjust to the inputs. In cases where tributaries deliver relatively coarse sediment or large sediment loads, the mainstem channel consistently aggrades at the junction, creating discontinuities in bed sediment texture and slope up and downstream of the junction (Miller, 1958; Dawson, 1988; Rice and Church, 1997; Benda et al., 2004 (and sources therein); Davey and Lapointe, 2006; Fergusen et al., 2006; Swanson et al., 2012a). Along the Rio Chama, a majority of the tributaries (Swanson

et al., 2012a) have created discontinuities in bed sediment size, gradient, and channel depth, presumably due to aggradation of coarse material at the confluences, and possibly by subsequent selective transport and channel armoring along the depositional tributary fans (cf. Brummer and Montgomery, 2006). Because slope, depth, and grain size are primary determinants of sediment entrainment and transport capacity, it seems likely that the influx and deposition of sediment at tributary junctions impacts these processes as well.

Few if any studies have demonstrated that if the incoming sediment caliber and (or) volumes are large enough, a primary channel may exhibit abrupt changes in shear stress, stream power, and flow velocity, in addition to changes in channel geometry and sediment character. Along the Rio Chama, our results show that arroyo junctions create significant discontinuities in these hydraulic parameters (Figures 5 and 6; Table 1). Furthermore, the differences in velocity, shear stress, and (or) stream power also appear to help spatially organize entrainment processes along the channel (Figures 8-10; Table 2), and subsequently, the bedload transport processes and rates (Figures 11-13). However, effects are not always consistent from tributary to tributary (Figures 11-13), and overall differences in transport rate by geomorphic position are statistically insignificant in general (Table 4). The abrupt changes in transport rates exhibited in Figures 11 and 13 may control where along the channel adjustments are likely to occur, especially in relation to the closure of El Vado Dam in 1935.

Although much of the research on tributary effects on mainstem channels has focused on sediment size, perhaps the main channel impact is an increase in slope. In many studies of mountain streams, the increased gradient likely drives channel morphology, hydraulics, and bed sediment texture changes, as well as transport, by controlling velocity and shear

stress along the channel. Mueller and Pitlick (2005) noted that shear stress was more strongly tied to slope than depth along Halfmoon Creek, CO. Similarly, along the Rio Chama study reach, the regression coefficient (R^2) for shear stress and slope is 0.79, whereas for shear stress versus depth along the study reach, R^2 is only 0.25. The shifts in slope are largely related to punctuated sediment delivery from flash floods and debris flows that supply coarse sediment from the tributary arroyos to the Rio Chama. The pulses of sediment often contain large volumes of material and (or) material that may be too large to entrain even during high flows along the mainstem. Therefore, the mainstem aggrades, at least temporarily (cf. Lisle et al., 2001; Fergusen et al., 2006). In turn, local increases in long profile concavity immediately below tributary junctions create a pattern of bankfull shear stress and velocity that likely shapes the pattern of sediment texture observed along each subreach (Ferguson and Ashworth, 1991; Parker, 1991; Ferguson et al., 1996, Rice and Church, 1997).

Based on the relatively small hydraulic geometry exponents associated with downstream velocity changes (typically between 0.1 and 0.2; Leopold and Maddox, 1953), Davey and Lapointe, (2006) posited that tributary sediment inputs produce only small changes in velocity, especially at high flows, but they expected important shifts in shear stress as predicted at other sites characterized by discrete fining zones (e.g., Rice and Church, 1997). Along the Rio Chama, mean tributary-induced variations in bankfull flow velocity are relatively small but significant (Table 2). Local velocity changes can range from small disruptions to abrupt increases up to 2.5 times the average velocity just upstream of a junction, with even larger shifts in shear stress and stream power (Figure 6). These step changes in hydraulic parameters are partly due to tributary fans that impinge on the

mainstem, narrowing the channel, but the shifts are also due to a large increase in slope at these sites. The abrupt shifts are observable at both low and bankfull flows, despite the tendency for higher discharges to smooth water surface slopes and reduce the influence of sediment texture on roughness. The initial increase and subsequent tapering off of velocities and shear stress are often maintained over substantial lengths, mimicking the form taken by the sediment links and associated changes in channel geometry described by Swanson et al. (2012a).

Entrainment. Under equilibrium conditions, bankfull channels are often thought to maintain a bed shear stress that is large enough to transport a majority of the bed material, but not so large that the channel will unravel (Parker, 1979). The linear model of downstream changes in channel character posits that dimensionless shear stress ($\tau*$) approximates a threshold value and is generally constant with distance downstream. However, Wohl and Achyuthan (2002) suggested that longitudinal differences in bank materials, cross-sectional channel geometry, and other factors cause $\tau*$ to deviate from this constant value, and these deviations, in turn, help produce variations in bed texture along a channel.

Downstream fining below tributaries is related to this process, but it is more an interplay between relatively immobile arroyo inputs deposited at confluences, channel geometry adjustments, and associated variations in bed shear stress. Field investigations by Ferguson and his colleagues (e.g., Ferguson et al. 1996) linked downstream sediment sorting to strong profile concavity and associated decreases in bed shear stress. Others have shown the dominance of dispersion, largely related to selective transport, of large sediment pulses supplied to mainstem channels from tributaries or hillslope failures (e.g., Lisle et al., 2001;

Sutherland et al., 2002). The ability of selective sorting to produce downstream fining depends on differences in sediment mobility between fine and coarse grains.

Figure 8 exhibits the variations in τ^*/τ^*_c and a smoothed version of the sediment size (D_g) data for the Rio Chama study reach. The data indicate that downstream of many of the tributaries, where sediment sizes are decreasing quickly, bed sediment is either immobile or only weakly mobile. In these subreaches, strong fining is likely associated with size-selective transport, where finer gravels are likely transported under conditions of threshold or critical τ^* (τ^*_c), but coarser clasts are only partially mobile to immobile. Under these conditions, size selectivity allows relatively fine grains to move downstream more frequently and rapidly than coarser ones, resulting in a concentration of coarse material upstream. Aggradation along the fans may facilitate fining in the segment by promoting selective deposition of large grains during large events. As the finer materials are removed from the initial deposition, an armor layer may form, reducing access to the material (whether fine or coarse) underneath (e.g., Montgomery and Brummer, 2006)

Well downstream of the tributary sites, the geometric mean grain size diminishes very little, and (or) the percentage of sand increases in the downstream direction. Constantine et al. (2008) suggested that this reduced rate of fining is driven by a transition from size-selective transport to equal mobility of bed material. Equal mobility (i.e., the condition where all the material, both fine and coarse, can be moved at once) is not reached in natural gravel-bed streams until bed shear stress greatly exceeds the critical shear stress necessary to entrain the median-sized bed surface particle. At this point, the coarse surface layer can break apart, allowing entrainment of the underlying sediment as well (Parker and Klingeman, 1982; Parker et al., 1982; Wilcock, 1992). Constantine et al. (2008) inferred from this

observation that downstream fining is strongest in stream reaches where τ^*/τ^*_c is nearest the threshold of general motion ($\tau^* \sim \tau^*_c$; $\tau^*/\tau^*_c = 1$), and weakest where equal mobility is the dominant entrainment style ($\tau^* >> \tau^*_c$; $\tau^*/\tau^*_c > 2$) (Wilcock, 1992). However, along the Rio Chama channel, τ^*/τ^*_c often does not exceed 2 until the bed becomes dominated by sand and fine gravel, either across the whole channel or in patches, resulting in a D_g in the fine gravel range (8-16 mm; Figure 8). Values of τ^* in the more alluvial sections generally exceed the threshold value at each site (average $\tau^*_c = 0.031$) by more than 2.

On the basis of the above observations and measurements, Rio Chama tributary junctions create relatively discontinuous zones where the channel is armored and supports only size selective transport ($\tau^* < 2\tau^*_c$). In more alluvial areas, away from tributary inputs, sand and finer gravels tend to dominate the bed and transport is more nonselective ($\tau^* > 2\tau^*_c$). Constantine et al. (2008) found similar discontinuities in τ^* versus τ^*_c and downstream fining along the Consumnes River in CA. They documented downstream fining and changes in bedload mobility along discrete intervals, rather than over the whole length of their study reach. In contrast to our study, they discovered that size-selective transport and partial mobility were more likely in the alluvial reaches, and equal mobility conditions occurred in confined reaches with erosionally resistant banks. Using their guidelines, our results suggest selective transport near tributary inputs leads to a coarse and stable armored bed that is rarely disrupted, but finer tributary and upstream inputs can pass at rates controlled by size. Alternatively, equal mobility along the intermediate alluvial reaches is a function of overall finer sediment size and weak temporary armors that are readily disrupted.

The Consumnes River study reach of Constantine et al. (2008) did not include any significant inputs in tributary sediment, whereas the Rio Chama reach includes inputs of large volume and clast size. Aggradation at the junctions, especially of coarse material, should encourage downstream fining via lag formation. Also, the Rio Chama system appears to transport primarily sand, which accumulates in the tail end of downstream sections and upstream of new tributary inputs, making mobility of the surface particles more likely in these reaches.

The Rio Chama results support Constantine et al.'s (2006) suggestion that reach-selective fining has important implications for downstream fining patterns in rivers with variations in τ^*, and subsequent fluctuations in sediment mobility. Additionally, the occurrence of an immobile or only partially mobile channel bed at Rio Chama tributary junctions is consistent with other observations of selective transport and armor layer formation along steep, coarse-bedded channels (Lisle, 1995; Brummer and Montgomery, 2006). It is apparent that tributary inputs can divide a fluvial channel into discrete sections defined by different sediment transport processes and varying levels of bed stability.

Transport rates. Along the Rio Chama study reach, fluctuations in slope and sediment texture result in order-of-magnitude shifts in bedload transport rates (Figures 11 and 13), as calculated using the equations provided by Wilcock and Crowe (2003). Under "normal" fluvial conditions of more continuous water and sediment inputs at perennial tributary junctions, the expectation would be step-like increases in sediment transport rate at each new significant tributary. However, in the case of the Rio Chama, most tributaries produce an inconsistent supply of sediment, and there is no clear pattern where transport

rates respond to tributary inputs in contrasting ways upstream and downstream of the junction.

Generally, in high-gradient reaches of streams with coarse bed material, instantaneous unit bedload transport rates (load per unit width per unit time) tend to be very high; in low-gradient reaches with finer bed material, transport rates are expected to be lower. However, along the Rio Chama, the pattern of hourly bankfull rate at tributary junctions is much more complex. Many of the reaches downstream of tributaries *do* tend to have higher estimated bankfull transport rates than the reaches upstream of and between tributary sites, which are finer and less steep (Figure 11). On the other hand, downstream of *Lone Tree Arroyo*, many of the coarser sections immediately below tributary junctions exhibit a precipitous drop in predicted transport rate. At many of these locations, such as below *Presa, Ojitos, Bluffs, and Gage Arroyos* (Figure 11), the bed sediment is very coarse and very little fine material was available for transport at the time the reach was sampled. Because the Wilcock and Crowe equations (2003) include the fraction of the bed covered by each sediment interval used in the analysis, the lack of available fine material greatly reduces the estimated sediment transport rates. Additionally, the small amount of finer sediment found on the bed was efficiently sheltered behind largely immobile coarse material. Just as importantly, some of the tributary aggradation appears to create reaches that act as sediment traps at bankfull flows. Estimated bedload rates immediately upstream of *Ruins, Oak Campground, Whirlpool, and Eddy Arroyos* are close to zero (Figure 11). Backwater conditions upstream of closely spaced, sequential tributary impacts and the geomorphic impact of the bouldery debris flows emanating from Joaquin Canyon (Figure 1) also helped created the reductions in transport between *Lone Tree and Ojitos Arroyos* (Figure 11).

As previously mentioned, high-gradient reaches with coarse bed material tend to have higher *instantaneous* transport rates; however, since a relatively high discharge is required to exceed the estimated threshold Shields stress, τ^*_c, bedload transport in these reaches occurs perhaps just a few days per year. The finer, less steep reaches may have lesser erosion rates, but they also require lower shear stress (thus smaller discharges) to move the sediment on the bed. Therefore, over longer time periods, assuming a stable system that is not generally aggrading or degrading, total transport should balance from reach to reach. The coarser reaches would then be characterized by punctuated short-duration transport events at peak flows, and the finer reaches would be characterized by transport over an extended period during spring snowmelt floods, and then by smaller magnitude runoff events through the rest of the year.

The modeled annual bedload transport data for the Rio Chama support these assumptions, to a point. Many of the reaches where bankfull transport rates were low (e.g., upstream of *Ruins and Bend Arroyos*; Figure 11), have relatively higher annual rates of bedload transport compared to the other reaches (Figure 13), but the areas around tributary junctions appear to still have some overall impact on sediment transport. These apparent local controls imply that the channel is not in equilibrium; however, there may be other factors that create differences in transport rates, such as poor transport model performance associated with sensitivities to slope and sediment inputs, differences in the material stored on the fans at the time the samples were collected (e.g., fresh deposits of sand and fine gravel on the *Arroyo de la Presa* fan), and other unforeseen issues. Because bedload transport measurements were not made, the accuracy of the estimates made with the Wilcock and Crowe (2003) formulas cannot be directly evaluated. In order to fully understand erosion

and sediment transport at tributary junctions these modeled transport rates should be coupled with field measurements of bedload transport obtained over a full range of flows (Wilcock, 1992, Mueller and Pitlick, 2005), a difficult task for a river such as the Rio Chama. Uncertainties aside, the overall results suggest that the current configuration of the Rio Chama may be well adjusted to distribute the sand and small gravel inputs that tributaries provide during more frequent runoff events.

Connectivity. Along the Rio Chama, the data suggest that tributaries divide the study reach into areas where entrainment and transport vary. Aggradation at confluences appears to act like a low head dam, limiting bedload transport to finer materials which are active over longer intervals within the year. Downstream of confluences, steeper reaches with higher shear stress should have a high capacity for carrying fine to medium gravel, but the relative mobility of these sizes is reduced by the presence of very coarse gravels and cobbles on the bed surface. The larger bed material creates a "traffic jam" for coarser material, but the high slopes make passing fine material relatively easy.

Linear combinations of sediment storage and transport mechanisms through channel reaches led Hooke (2003) to describe different types of reach-to-reach connectivity. *Unconnected* reaches immediately store locally-derived sediment within the reach. *Partially connected* reaches are similar to unconnected reaches, although some coarse sediment moves downstream during moderate to extreme events. In *connected reaches*, coarse material is transported downstream during "normal" floods, and in *potentially connected* stretches of channel, the river has enough power to transport sediment, but upstream and local supply is deficient. Finally, obstructions along the reach, including both natural and artificial dams, force formerly connected reaches to be *disconnected*. Within this framework, Hooke (2004)

described potentially connected reaches of the Gila River, New Mexico, and Walnut Gulch, Arizona, attributed to coarse sediment exhaustion from upstream deposition. Hooke (2004) also described disconnected reaches at Torrealvilla, Spain. Along the Rio Chama, reaches downstream of tributary junctions tend to be *unconnected* to *partially connected* with respect to gravel, and upstream reaches maybe be *disconnected* by the aggraded fans.

Alternatively, the sand and finer material which often makes up most of the annual sediment load of many canyon rivers in the western and southwestern United States, is often transported over the relatively immobile coarse bed surfaces. This behavior has been observed in natural rivers (e.g., Kleinhans et al., 2002) and is a recognized feature of systems with a limited supply of fine sediment, such as the Colorado River (e.g., Rubin and Topping, 2001). If the channel is only transporting sand and fine gravels, its transport connectivity may depend strongly on tributary junctions, which may also control whether the finer material is transported as bedload or suspended load. Figure 14 exhibits the variations in dimensionless shear velocity along the Rio Chama and the particle sizes that will remain in suspension given these velocities (based on Dietrich, 1982). In relatively steep reaches, where no sand was observed during the sampling rounds, much of the sand and slightly coarser material (<2.8 mm) is likely transported as suspended load. However, in the less impacted subreaches, only sediment less than 1.4 mm is likely suspended. The bedload transport results (Figure 11 and 13) also delineate reaches where finer material may be slowed and stored, where it behaves more like bedload. The difference reinforces the fact that tributary junctions can divide a river into discrete fluvial environments, (cf. Benda et al., 2004; Davey and Lapointe, 2006); it also explains how bedload transport rates can be so low downstream of some of the confluence sites. If sand was not found on the bed when

sampling occurred, then it is likely flushed quickly through the fan and downstream reaches. If these passed-through fines are added to the gravel transported at these locations, then the transport values would likely become more even from reach to reach.

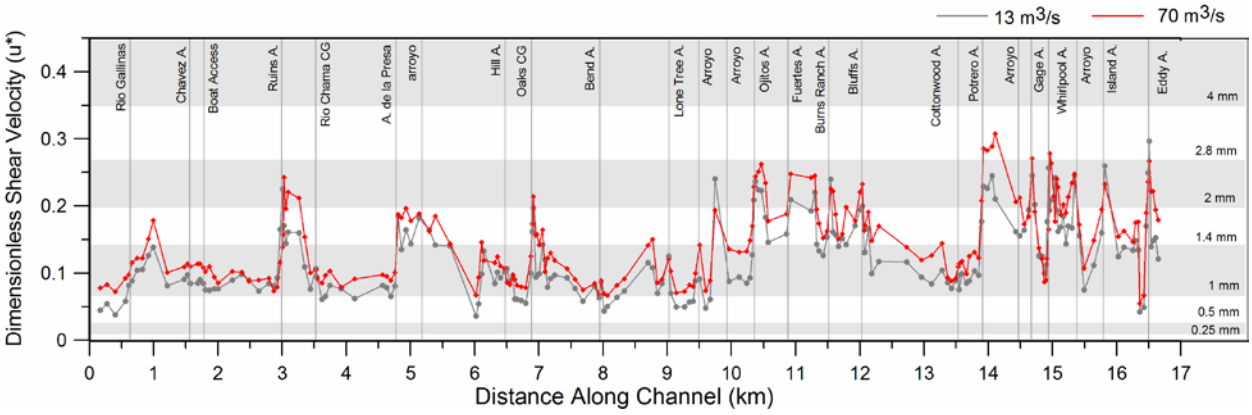

Figure 14. Downstream variations in dimensionless shear velocity based on calculations using the Dietrich (1982) relations. Along the steeper, coarser reaches downstream of tributaries, and along the more constrained reaches in the downstream section of the study reach, sands (< 2.8 mm) appear to be transported at least in part via suspension as opposed to bedload.

Transport and channel change along Rio Chama. Large rivers of the southwestern United States, such as the, Green, Colorado, Rio Grande, and San Juan Rivers all transport large annual loads of fine sediment. Like the Rio Chama, the sediment is supplied primarily by large mainstem tributaries that drain areas of erodible sedimentary rocks (Howard and Dolan, 1981; Hanks and Webb, 2006). Also like the Rio Chama, debris flows and flash floods supply pulses of coarse sediment to these channels in canyon sections (Schmidt and Rubin, 1995; Grams and Schmidt, 1999), leading to a similar pattern of coarse reaches, reaches characterized by sand patches, and sand-bed reaches. Before dam construction and operation along these rivers, large flood events occurred that were presumably capable of mobilizing the coarse fraction of the bed at the debris fans, flushing the fines and spreading

the gravels downstream (Schmidt, 1999). However, dam operations on these rivers as well as the Rio Chama have reduced flood flows, and therefore reduced the mobilization of coarse material. This reduction in mobilizing flows has likely allowed increased aggradation at junctions, and allowed large volumes of sand to be stored in the floodplain and channel. For instance, before regulation by Glen Canyon Dam in 1963, high-magnitude floods on the Colorado River reworked debris fans in the Grand Canyon by entraining all particles except large boulders. Because flow regulation has substantially decreased the river's competence, debris flows occurring after 1963 have increased the storage of less coarse-grained sediments on debris fans and in rapids (Webb et al., 1999).

Before construction of El Vado Dam in 1935, peak flows along the channel were much higher than at present. The study reach conveyed average peak flows roughly 40% higher than under post-dam conditions (135 m^3/s vs. 96 m^3/s), and post-dam maxima are roughly a third of maximum peaks estimated from the PVW, LPT, and RGO gages upstream and (or) pre-dam (see also Swanson et al., 2010b). These higher peaks would have been capable of moving much larger clasts left on the debris-flow fans, and could likely redistribute gravel and flush sand much more easily. Figure 15 suggests that along much of the study reach, and especially at tributary locations, the discharge required to entrain the overall D_{50} (24mm) and $D_{50\ gravel}$ (69mm) approximates the current maximum peaks, whereas prior to the dam, these threshold flows were closer to the 2-year recurrence interval flood. At many of the tributary junctions, such as at *Arroyo de la Presa*, *Whirlpool Arroyo,* and *Lone Tree Arroyo*, pre-dam maximums are required to move the current $D_{50\ gravel}$, and even the post-dam mean peak flow is required to entrain coarse sand (2 mm) at some locations. After closure, mainstem peak discharges able to entrain the coarser material at the

fans occur less frequently, and therefore more sediment is likely stored adjacent to the tributary junction. The reduced ability to move sediment at these locations would accentuate aggradation and associated differences in particle size, slope, depth, and other channel metrics, assuming inputs of coarse sediment have occurred over this time period.

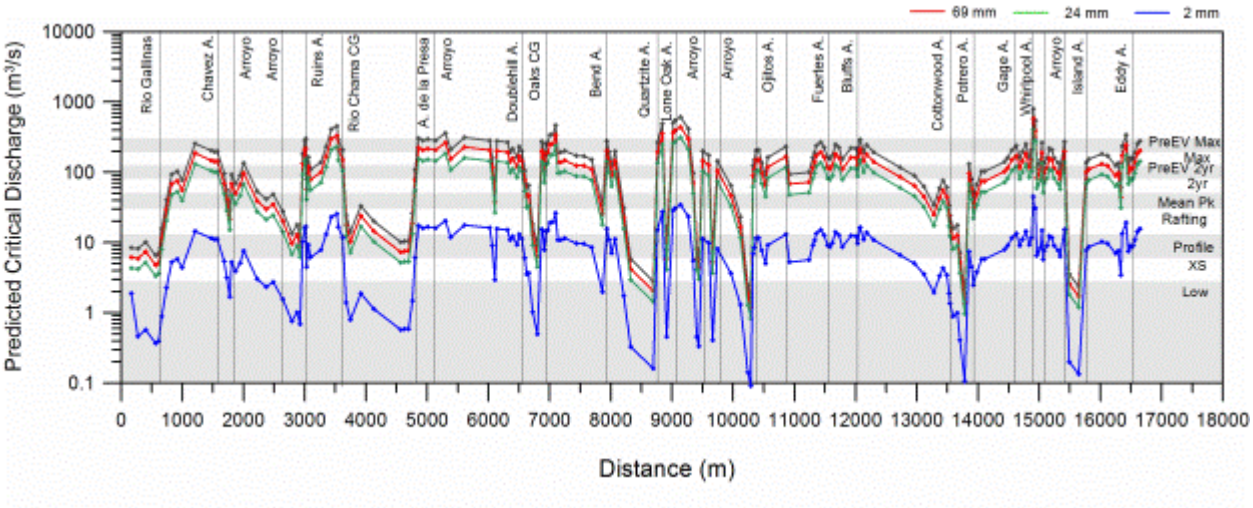

Figure 15. Critical discharge for sand and the median-sized particle for the entire reach. To entrain the overall D_{50} (24 mm), flows typically must be greater than the pre-El Vado 2-year flow, and often as high as the current maximum flows.

In response to the reduction in annual peak flows downstream of El Vado Dam, channel widths have decreased along the Rio Chama study reach, from an average of 58 m in 1935 to 39 m in 2005 (Swanson et al., 2010b). The narrowing has not occurred evenly along the study reach, however. It is primarily focused in the alluvial reaches as opposed to the semi-confined reaches (Figure 16). Additonally, tributaries appear to have some control on the changes. In general, channel narrowing is limited immediately downstream of the tributaries, despite being areas where coarse, immobile sediment presumably could enter the channel, which might promote narrowing. The main exception is the Rio Gallinas, which mostly delivers large volumes of sand that are more easily distributed. The lack of narrowing

in the semi-confined reaches may be related to the lateral confinement to begin with, where cycles of aggradation and incision might be the norm; however, as the sediment transport data suggest, it could also be related to adjustments that produce elevated transport capacity, which allows finer sediment to pass through these reaches. Currently, a full sediment budget for the reach has not been completed, but most of the observed activity on the fans includes only sand and gravel (<32 mm). This relatively small material might be easily moved to the unconfined areas where it stalled on channel flanks and bars, forming new floodplain.

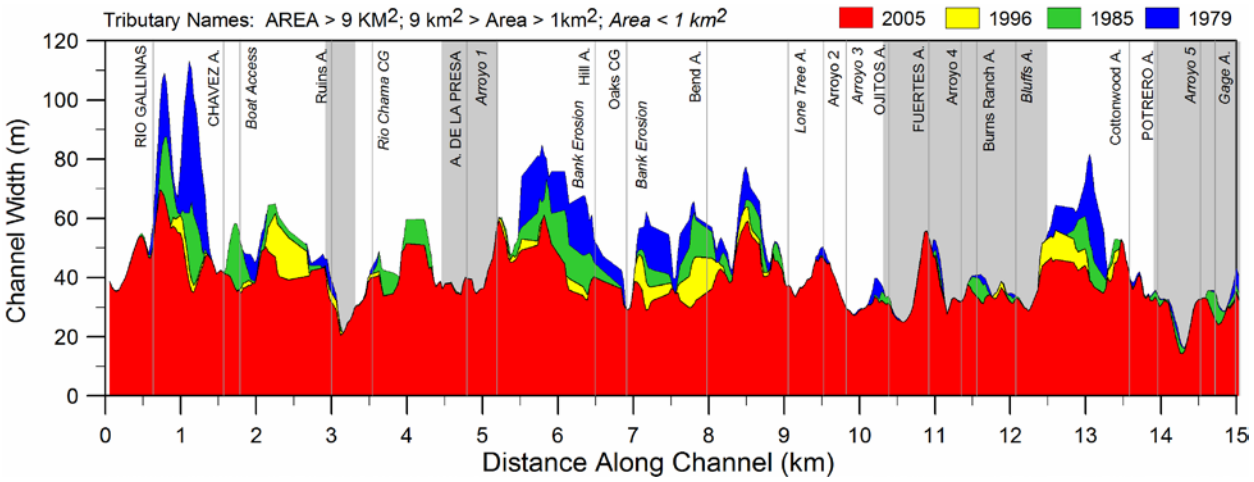

Figure 16. Reductions in channel width along the study reach between 1979 and 2005. Most of these changes are related to El Vado Dam closure and operations. The changes appear to occur only in the alluvial, unconfined areas.

Conclusions

Tributary inputs of sediment and water have been shown to cause local, abrupt shifts in channel cross-section geometry, planform, and gradients, but few researchers have documented how these shifts impact sediment transport along rivers. Along the Rio Chama, abrupt changes in gradient lead to significant changes in the hydraulic parameters often associated with driving sediment transport. Flow velocities, shear stress, and stream power

all increase downstream of tributary junctions, and are all limited upstream of confluences relative to subreaches located away from tributary junctions. The along-channel variability in shear stress and other characteristics, along with shifts in bed sediment texture, in turn lead to abrupt changes in sediment transport processes as well. The entrainment and bedload transport data presented for the Rio Chama suggest that tributary junctions have the ability to divide the channel into sections where the bed moves by size-selective transport in the steep, coarser sections below tributary junctions, or by equal mobility in the more alluvial sections between tributaries. Finer material tends to be flushed through the steeper reaches, and behaves more like bedload in the flatter areas.

Much of the sediment transport analysis was completed using equations presented by Wilcock and Crowe (2003). As with all sediment transport equations, the Wilcock and Crowe (2003) relations are highly sensitive to bed sediment size and slope. Because no field measurements of transport have been conducted, it is difficult to verify the results of the model. It also predicts bedload transport, not total transport which might be more appropriate for the Rio Chama. Future sediment transport studies along the reach should include collecting bedload samples at a variety of flows. Additional modeling should also be conducted utilizing a variety of sediment transport equations for mixed sediment.

Overall, it is apparent that when two channels of different sediment and (or) flow character come together at a confluence, downstream changes to channel form are also associated with downstream adjustments to process. Combined, these often abrupt changes lead to very different channel characteristics over short distances. These complexities in stream conditions may create challenges to sediment, water quality, and biological sampling, but also may produce heterogeneity beneficial to river ecosystems as well as recreation.

References

Bagnold, R.A. 1966. *An Approach to the Sediment Transport Problem from General Physics,* U.S. Geological Survey Professional Paper, 422-425.

Bathurst, J.C. 1993. Flow resistance through the channel network. In: Beven, K., Kirkby, M.J. (Eds.), *Channel Network Hydrology*. Wiley, Chichester, pp. 69 –98.

Benda, L.E., Andras, K., Miller, D. J., and Bigelow, P. 2004. Confluence effects in rivers: interactions of basin scale, network geometry, and disturbance regimes: *Water Resources Research*, 40: W05402, doi:10.1029/2003WR002583.

Benda, L.E., Veldhuisen, C., Black, J. 2003. Debris flows as agents of morphological heterogeneity at low-order confluences, Olympic Mountains, Washington. *Geological Society of America Bulletin*, 115.9: 1110-1121.

Brewer, P.A., and Lewin, J. 1993. In-transport modification of alluvial sediment: field evidence and laboratory experiments. In:Puigdefabregas, C., Marzo, M. (Editors), Special Publications of the International Association of Sedimentologists, 17, pp. 23-35.

Brummer, C. J., and Montgomery, D.R. 2006. Influence of coarse lag formation on the mechanics of sediment pulse dispersion in a mountain stream, Squire Creek, North Cascades, Washington, United States. *Water Resources Research,* 42: W07412, doi:10.1029/2005WR004776.

Buffington, J.M., and Montgomery, D.R. 1997. A systematic analysis of eight decades of incipient motion studies, with special reference to gravel-bedded rivers. *Water Resources Research*, 33.8: 1993–2029.

Bull, W. 1997. Discontinuous ephemeral streams**.** Geomorphology 19. 3-4 227-276.

Church, M. 1992. Channel morphology and typology. In *The Rivers Handbook*. P. Carlow and G. E. Petts, eds., Blackwell Science, Malden, MA, pp. 126–143.

Church, M. 2002. Geomorphic thresholds in riverine landscapes. *Freshwater Biology*, 47: 541– 557

Church, M., and Kellerhals, R. 1978. On the statistics of grain size variation along a gravel river. *Canadian Journal of Earth Sciences*, 15: 1151-1160.

Church, M., and Jones, D. 1982. Channel bars in gravel-bed rivers. In *Gravel-Bed Rivers*. Hey, R. D., Bathurst, J. C., and Thorne, C. R., eds. Chichester, U.K., Wiley, p. 291-338.

Constantine, C.R., Mount, J.F., and Florsheim, J.L. 2003. The effects of longitudinal differences in gravel mobility on the downstream fining pattern in the Cosumnes River, California. *Journal of Geology*, 111: 233–241

Dietrich, E.W. 1982. Settling velocity of natural particles. *Water Resources Research*, 18 (6), 1626–1982.

Dietrich, W.E., and Whiting, P. 1989. Boundary shear stress and sediment transport in river meanders of sand and gravel. In *River Meandering. Water Resources Monograph,* vol. 12. S. Ikeda, and G. Parker, Eds. American Geophysical Union, Washington DC, pp. 1–50.

Davey, D., and Lapointe, C. 2006. Sedimentary links and the spatial organization of Atlantic salmon (*Salmo salar*) spawning habitat in a Canadian Shield river. *Geomorphology*, 83.1: 82–96.

Ferguson, R., Hoey, T., Wathen, S., Werritty, A. 1996. Field evidence for rapid downstream fining of river gravels through selective transport. *Geology*, 24.2: 179–182.

Ferguson, RI, Cudden, JR, Hoey, TB, and Rice, SP. 2006. River system discontinuities due to lateral inputs: generic styles and controls. *Earth Surface Processes and Landforms*, 31: 1149–1166.

Ferguson, R., and Ashworth, P. 1991. Slope-induced changes in channel character along a gravel-bed stream: the Allt Dubhaig, Scotland. *Earth Surface Processes and Landforms*, 16: 65–82.

Grams, P.E., and Schmidt, J.C. 2002. Streamflow regulation and multi-level flood plain formation: channel narrowing on the aggrading Green River in the eastern Uinta Mountains, Colorado and Utah. *Geomorphology*, 44: 337-360.

Gran, K. B., and Montgomery, D. R. 2005. Spatial and temporal patterns in fluvial recovery following volcanic eruptions: Channel response to basin-wide sediment loading at Mount Pinatubo, Philippines, *Geological Society of America Bulletin*, 117: 195 – 211.

Hanks, T. C., and Webb, R. H. 2006. Effects of tributary debris on the longitudinal profile of the Colorado River in Grand Canyon. *Journal of Geophysical Research*, 111: 13.

Harvey, A. M. 2001. Coupling between hillslopes and channels in upland fluvial systems: implications for landscape sensitivity, illustrated from the Howgill Fells, northwest England. *Catena*, 42: 225-250.

Hjulstrom, F. 1935. The morphological activity of rivers as illustrated by River Fyris. *Bulletin of the Geological Institute,* Uppsala vol. 25, ch. 3.

Hoey, T.B., Ferguson, R. 1994. Numerical simulation of downstream fining by selective transport in gravel bed rivers: model development and illustration. *Water Resources Research*, 30: 2251-2260.

Hooke, J. 2003. Coarse sediment connectivity in river channel systems: a conceptual framework and methodology. *Geomorphology*, 56: 79-94.

Hooke, J. 2004. Analysis of coarse sediment connectivity in semiarid river channels, *in* Sediment Tranfer through the Fluvial System, IAHS conference, Moscow, Russia, p. 269-275.

Howard , A., and Dolan, R. 1981. Geomorphology of the Colorado River in the Grand Canyon. *Journal of Geology*, 89.3: 269-298.

Joeckel, RM, Henebry, GM. 2008. Channel and island change in the lower Platte River, Eastern Nebraska, USA: 1855–2005. *Geomorphology*, 102: 407-418.

Karim, M.F., and J.F. Kennedy. 1990. Means of coupled velocity and sediment-discharge relationships for rivers. *Journal of Hydraulic Engineering,* ASCE vol. 1 16.8: 973-996.

Kirchner, J.W., Dietrich, W.E., Iseya, F., and Ikeda, H. 1990. The variability of critical shear stress, friction angle, and grain protrusion in water worked sediments. *Sedimentology*, 37: 647–672.

Kleinhans, M.G., Wilbers, A.W.E., De Swaaf, A., Van den Berg, J.H. 2002. Sediment supply-limited bedforms in sand–gravel-bed rivers. *Journal of Sedimentary Research*, 27.5: 629–640.

Knighton, A. D. 1989. River adjustment to changes in sediment load: the effects of tin mining on the Ringarooma River, Tasmania 1875-1984. Earth Surface Processes and Landforms 14: 333-359.

Komar P.D., and Li, Z. 1988. Applications of grain pivoting and sliding analyses to selectiveentrainment of gravel and to flow competence evaluations. *Sedimentology*, 35: 681–95

Lamb, M.P., Dietrich, W.E., and Venditti, J.G. 2008. Is the critical Shields stress for incipient sediment motion dependent on channel-bed slope? *Journal of Geophysical Research*, 113 20pp. doi: 10.1029/2007JF000831.

Lane, EW. 1955. The importance of fluvial morphology in hydraulic engineering. Proceedings of the American Society of Civil Engineers, 81: 1–17.

Leopold, L.B., and T. Maddock, Jr. 1953. *The Hydraulic Geometry of Stream Channels and Some Physiographic Implications,* U.S. Geological Survey Professional Paper 252.

Lisle, T. E. 1995. Particle size variations between bed load and bed material in natural gravel bed channels, *Water Resources Research*, 31.4: 1107–1118.

Lisle, T.E., Cui, Y., Parker, P., Pizzuto, J.E., and Dodd, A.M. 2001. The dominance of dispersion in the evolution of bed material waves in gravel-bed rivers. *Earth Surface Processes and Landforms*, 26.13: 1409-1420.

Madej, MA, Ozaki, V. 1996, Channel response to sediment wave propagation and movement, Redwood Creek, California, USA. *Earth Surface Processes and Landforms*, 21: 911–927

Martin, Y. and Church, M. 1995. Bed-material transport estimated from channel surveys: Vedder River, British Columbia. *Earth Surface Processes and Landforms*, 20: 347–361. doi: 10.1002/esp.3290200405

Meyer-Peter, E., and R. Muller. 1948. Formulas for Bedload Transport. *Proceedings,* the Second Meeting of the International Association for Hydraulic Structures Research, Stockholm.

Miller, J.P. 1958. High mountain streams: effects of geology on channel characteristics and bed material. Memoir 4, State Bureau of Mines and Mineral Resources, New Mexico Institute of Mining and Technology, Socorro, N.M., 53 pp.

Miller, D.J., and Benda, L.E. 2000. Effects of punctuated sediment supply on valley-floor landforms and sediment transport. *Geological Society of America Bulletin*, 112.2: 1814-1824.

Mueller, E.R., and Pitlick, J. 2005. Morphologically based model of bed load transport capacity in a headwater stream. *Journal of Geophysical Research,* 110: doi:10.1029/2003JF000117. 14 pp.

Mueller, E.R., Pitlick, J., Nelson, J.M. 2005. Variation in the reference Shields stress for bed load transport in gravel-bed streams and rivers. *Water Resources Research,* 41:W04006. doi: 10.1029/2004WR003692.

Parker, G. 1990. Surface-Based Bedload Transport Relation for Gravel Rivers. *Journal of Hydraulics Research*, 28.4: 501-518.

Parker, G. 2008. Transport of gravel and sediment mixtures, chapter 3. In, *Sedimentation Engineering Processes, Measurements, Modeling, and Practice.* M.H. Garcia, ed. American Society of Civil Engineers. Chapter 3, 165-243.

Paola, C, Parker, G, Seal, R, Sinha, S, Southard, J, and Wilcock, P.R. 1992. Downstream fining by selective deposition in a laboratory flume. *Science*, 258: 1757-1760.

Parker, G. 1979. Hydraulic geometry of active gravel rivers. *Journal of Hydraulic Engineering Division*, ASCE 105: 1185-1201.

Parker, G. 1991. Selective sorting and abrasion of river gravel II. Applications. *Journal of Hydraulic Engineering*, ASCE 117: 150-171.

Parker and Klingeman, PC. 1982. On why gravel bed streams are paved. *Water Resources Research*, 18: 1409-1423.

Persico, L, Meyer, G, Frechette, J, New, J, and Hepler, C. 2005. Contrasts in late Pleistocene to Holocene fluvial behavior along the middle Rio Chama: New Mexico Geological Society, 56th Field conference Guidebook, Geology of the Rio Chama Basin, p. 432-433.

Proffitt, G.T., and Sutherland, A.J. 1983. Transport of non-uniform sediments. *Journal of Hyrdraulic Research*, 21.1: 33-43.

Rice, S., and Church, M. 1998. Grain size along two gravel-bed rivers: statistical variation, spatial pattern and sedimentary links. *Earth Surface Processes and Landforms*, 23: 345-363.

Robinson, R.A.J., and Slingerland, R.L. 1997. Origin of fluvial grain-size trends in a foreland basin: the Pocono Formation of the Central Appalachian Basin. *Journal of Sedimentological Research*.

Rubin, D.M., and Topping, D.J. 2001. Quantifying the relative importance of flow regulation and grain size regulation on suspended sediment transport α and tracking changes in grain size of bed sediment β. *Water Resources Research*, 37.1: 133-146.

Sambrook Smith, G.H., and Ferguson, R.I. 1995. The gravel-sand transition along river channels. *Journal of Sedimentological Research*, A65: 423- 430.

Schmidt, J. C., and Rubin, D. C. 1995. Regulated streamflow, fine-grained deposits, and effective discharge in canyons with abundant debris fans, In *Natural and Anthropogenic Influences in Fluvial Geomorphology*: The Wolman Volume: Geophysical Monograph. Costa, J. E., Miller, A. J., Potter, K. W., and Wilcock, P. R., eds. Washington D.C., American Geophysical Union, p. 83-101.

Schmidt, J. C. 1999. Summary and synthesis of geomorphic studies conducted during the 1996 controlled flood in Grand Canyon. In: The Controlled Flood in Grand Canyon. R. H. Webb, J. C.Schmidt, G. R. Marzolf, and R. A. Valdez, eds. American Geophysical Union Geophysical Monograph 110, Washington, D.C.,USA. p.329–341.

Schumm S.A. 1977. *The Fluvial System*. Wiley-Interscience, New York, 338pp

Swanson, B.J., Meyer, G.A., and Coonrod, J. 2011. Magnitude and uncertainty of channel planform measurements along a regulated river using aerial photography: Rio Grande near Albuquerque, New Mexico. *Earth Surface Processes and Landforms*, 36.7: 885-900.

Swanson, B.J., Meyer, G.A., and Coonrod, J. 2010b. Coupling of hydrologic/hydraulic models and aerial photos through time: fluvial geomorphologic changes along the Rio Chama, NM, 1935-2005. Unpublished report to USACE, Urban Flood Demonstration Program, July 10, 2010. 66pp.

Swanson, B.J., Meyer, G.A., and Pitlick, J. 2012. In preparation. Tributary Confluences and Discontinuities in Channel Form and Sediment Texture: Rio Chama, NM. *Geological Society of America Bulletin*, July 9, 2012.

Vannote R.L., Minshall, G.W., Cummins K.W., Sedell J.R., and Cushing C.E. 1980. The river continuum concept. *Canadian Journal of Fisheries and Aquatic Sciences*, 37: 130–137.

Walling, D.E. 1983. The sediment delivery problem. Journal of Hydrology.65: 209-237.

Wathen, S. J., and Hoey, T. B. 1998. Morphological controls on the downstream passage of a sediment wave in a gravel-bed stream. *Earth Surface Processes and Landforms*, 23: 715-730.

Webb, R. H., Melis, T. S., and Griffiths, P. G. 1999. Reworking of aggraded debris fans. in The Controlled Flood in Grand Canyon, Geophysical Monograph. Series, vol. 110, edited by A. B. Jones, pp. 37 – 51, AGU, Washington, D. C.

Werritty, A. 1992. Downstream fining in a gravel bed river in Southern Poland: Lithological controls and the role of abrasion. In *Dynamics of Gravel Bed Rivers*. Billi, P., Hey, R.D., Thome, C.R., Tacconi, P., Eds. John Wiley and Sons, Chichester, pp. 333-346.

Wilcock, P.R. 1998. Two-fraction model of initial sediment motion in gravelbed rivers. *Science*, 280: 410–412.

Wilcock, P.R., and Crowe, J.C. 2003. Surface-based transport model for mixed-size sediment. *Journal of Hydraulic Engineering*, 129.2: 120–128.

Wilcock, P.R., and Kenworthy, S.T. 2002. A two-fraction model for the transport of sand/gravel mixtures. *Water Resources Research*, 38.10: 1194.

Williams, G P, and Wolman, M G. 1984. Downstream Effects of Dams on Alluvial Rivers. US Department of the Interior, Geological Survey, 1286.

Wohl, E, Achyuthan, H. 2002. Substrate influences on incised-channel morphology. *Journal of Geology*, 110: 115-120.